Synthetic strategies in the design and construction of saccharide selective fluorescent sensors

Phillips, Marcus Damian

Award date:
2005

Awarding institution:
University of Bath

Synthetic Strategies in the Design and Construction of Saccharide Selective Fluorescent Sensors

Marcus Damian Phillips

A thesis submitted for the degree of Doctor of Philosophy

University of Bath

Department of Chemistry

June 2005

ProQuest LLC
789 East Eisenhower Parkway
P.O. Box 1346
Ann Arbor, MI 48106-1346

There is so much to do. You can wander off in space or in time, set out for Tierra del Fuego or for King Midas's court... You can build castles in Spain, steal the Golden Fleece, discover Atlantis, realise your childhood dreams and adult ambitions.

Jean-Dominique Bauby

The Diving-bell and the Butterfly

Abstract

The ability to monitor the presence of analytes within physiological, environmental and industrial systems is of crucial importance. However, due to the scale that recognition events occur at on the molecular level, gathering this information poses a non-trivial challenge. It is therefore the case that robust chemical molecular sensors with the capacity to detect chosen molecules selectively and signal this presence by altering their optical signature have attracted considerable attention over recent years.

Of particular interest is the real-time monitoring of saccharides in aqueous systems, such as D-glucose in blood. To this end the covalent pair-wise interaction between boronic acids and saccharides has been exploited.

This thesis documents research into generally applicable synthetic strategies both in the design and in the construction of novel boronic acid based fluorescent sensors with selectivity for saccharides.

All of the fluorescent sensors reported utilise boronic acid groups for the recognition of saccharides and have been designed such that photoinduced electron transfer can be mediated *via* a tertiary amine group. The use of photoinduced electron transfer directly controls the fluorescence emission intensity and as such induces a clear "off-on" response to the binding of saccharides.

The synthetic strategy established was developed during the synthesis of three distinct sets of compounds and should provide an effective route to any researcher wishing to generate a molecule containing the *N*-methyl-*o*-(aminomethyl)phenylboronic acid fragment. Furthermore the synthesis of forty compounds is reported herein including: the complete parallel synthesis of five monoboronic acid reference compounds, a refined route for five diboronic acid sensors and the complete synthesis of a novel pair of diboronic acid tipped molecular tweezers.

Contents

Acknowledgements

I owe a great deal of thanks to a rather large group of people without whose expertise, encouragement and tenacious ability to smile at any time of the day or night I would have been driven to insanity long ago.

First of all I would like to thank my supervisor Tony James for his guidance, friendship and support. Thanks also go to the members of the Tony James research group who've put up with me since I first arrived in the group as an undergraduate project student back in 1999: Yu Bai, Chris Cooper, Jim Hartley, Chris Ward, Susumu Arimori, Karine Frimat, Suvi Koskela, Giuseppe Consiglio, Laurence Bosch, Jianzhang Zhao, Sukhdeep Kaur, Vijay Kumar, Yolanda Pérez-Fuertes, Mike Thatcher, Rachel Green, Sonia Lozano Yeste and Andrew Kelly.

The past there years have been particularly busy, as well as the research documented within this thesis I have been involved in a number of projects most of which have now been handed over to others, shelved or simply never got off the ground. Within the department I would like to thank Matthew Davidson and Tom Hibbert for letting me pour allsorts of potential guest species into their lovingly hand-crafted boronic acid calixeranes. Further afield I would like to thank the Japan Society for the Promotion of Science (JSPS) for the award of a Fellowship on their 2003 summer programme and Miwa Shimura at the British Council, Tokyo, for her organisation and fantastic Thai green curries.

I am most grateful to Associate Professor Yuji Kubo at the University of Saitama for watching over me during my two month placement working on isothiouronium dyads. I would also like to extend particularly heartfelt thanks to various members of the University of Saitama's, Department of Applied Chemistry who made me feel so welcome in the face of a string of "challenging" results, the coldest Japanese summer in a decade, occasional earthquakes and the destructive force of typhoon Etau: Atsushi Kobayashi, Uchida Sayaka, Amiya Keiko, Naito Masahiro, Kato Masakazu, Yoshihiro Misawa, Yoshizawa Toshiharu, Sugiura Yuki and Ishii Yusuke.

Thanks go to all of the support staff whose work in the department converts research from mere pipe dreams into reality. In particular I would like to take this opportunity to thank John Lowe, Mark Russell, Sheila Apps, Sarah Elkins and Jane Heywood. Thanks also go to the Engineering and Physical Sciences Research Council (EPSRC) who provided the financial backing for this research.

Special thanks must go to all of the members of the Chemistry Department past and present who have made my time here so enjoyable. In particular I would highlight the "Lunch Club": Steve le Fleur, Stav, Suvi, Mike G, Chappers, Kelly, Mike E, Pervy Perkins, Di, Duncan, Gan, Fran, Helen, Stephen, Dino, Irish Gareth, Gem, Nathan, Roly, Rob T, Sarah and Sy, as well as Ana, Angie, Carly, Claudia, Dave, Dawn, Fletch, Fred, Gareth, Gary, Jay, Luke, Matt, Piers, Phil the Axe and our visiting professor Tom Fyles.

I am also indebted to everyone who took the time to proof read this thesis, especially Gareth, Ronald and Chris. In and around Bath thanks go to triathletes, housemates and friends: Phil, Nikki, James, Pam, Maz, Matt, Amy, Rebecca, Dave, Amanda, Jen, Ali, Adam and Liz.

Over the course of the past three years I have received a great deal of encouragement from "Up North". To: Bill, Pat, Jane, Danny, Brenda, Rodney and Helen's Nana; ta very much.

To: Mum, Nick, Dad, Hazel, Fay, Dave, Will and the family at large, as ever, thank you for the love, encouragement and support that has helped me through this research. I would especially like to highlight the significant financial loan that I have relied on so heavily over the past few months. Mum and Nick without your regular cash injections, the reality is that this little venture would not have been possible.

Finally to Helen, for your love, absolute faith and unerring support, thank you.

Abbreviations

Å	Ångström
AIBN	2,2'-azobisisobutyronitrile
Alloc	allyloxycarbonyl
app	apparent
Ar	aryl
BINOL	1,1'-bi-2-naphthol
bp	boiling point
br	broad
Boc	*tert*-butoxycarbonyl
Boc_2O	di-*tert*-butyl dicarbonate
°C	degree Celsius
Cbz	benzyloxycarbonyl
$CDCl_3$	deuterated chloroform
CI	chemical ionisation
cm^3	cubic centimetre
cm^{-1}	wavenumbers
COSY	correlated spectroscopy
[2.2.2]-cryptand	4,7,13,16,21,24-hexaoxa-1,10-diazabicyclo[8.8.8]-hexacosane
δ	chemical shift in parts per million
Δ	heat
2D	two dimensional
D	deuterium (^2H)
d	doublet
Da	Dalton
D-A	donor-acceptor
D-B-A	donor-bridge-acceptor
dd	doublet of doublets
ddd	doublet of doublets of doublets
dddd	doublet of doublets of doublets of doublets
dt	doublet of triplets
dec	decomposition
DCM	dichloromethane
dm^3	cubic decimetre

DMSO	dimethyl sulfoxide
e^-	electron
E. coli	*Escherichia coli*
EI	electron impact
ERI_B	electrophilic reactivity index for boron
ES+	positive phase electrospray ionisation
ES-	negative phase electrospray ionisation
Et	ethyl
EtOAc	ethyl acetate
EtOH	ethanol
ET	electron transfer
eq.	equivalent
FAB	fast atom bombardment
g	gram
GOx	glucose oxidase
h	hours
$h\nu$	incident light
HEPES	*N*-(2-hydroxyethyl)-piperazine-*N*'-2-ethanesulfonic acid
HMBC	heteronuclear multiple bond connectivity
HMQC	heteronuclear multiple quantum coherence
HPLC	high performance liquid chromatography
HRMS	high resolution mass spectrometry
I	fluorescence intensity
I/I_0	relative fluorescence intensity
ICT	internal charge transfer
J	coupling constant
k	rate constant
K	stability constant
K_a	acidity constant
K_a'	acidity constant of complexed boronic acid
K_{obs}	observed stability constant
K_{tet}	ligand – tetrahedral boronate anion stability constant
K_{trig}	ligand – trigonal boronic acid stability constant
kJ	kilojoules
λ	wavelength

λ_{em}	emission wavelength
λ_{ex}	excitation wavelength
L	Litre
LE	locally excited
lit	literature
LRMS	low resolution mass spectrometry
μM	micromolar
μm	micrometre
μmol	micromole
μL	microlitre
m	*meta*
m	unresolved multiplet / minutes
M	molar (moles per cubic decimetre) / mega
M^{-1}	cubic decimetres per mole
$[M]^+$	parent molecular ion
Me	methyl
MeOD	deuterated D4 methanol
MeOH	methanol
mg	milligram
MHz	megahertz
mm	millimetre
mM	millimolar
mmol	millimole
mol	mole
mp	melting point
mV	millivolt
m/z	mass-to-charge ratio
ν	infrared
NBA	*meta*-nitrobenzyl alcohol
NBS	*N*-bromosuccinimide
nm	nanometre
nmol	nanomole
NMR	nuclear magnetic resonance
ns	nanosecond
o	*ortho*

p	*para*
PENDANT	polarisation that is nurtured during attached nucleus testing
PET	photoinduced electron transfer
pK_a	- log K_a
pK_{aH}	pK_a of the conjugate acid
ppm	parts per million
q	quartet
qFM	quantum yield
quin	quintet
r^2	coefficient of determination
rel	relative values
ref	reference compound
R_f	retardance factor
rm	reaction mixture
rt	room temperature
σ_p	*para*-substituent parameter
s	singlet / second
S_0	singlet electronic ground state
S_1	first singlet electronic excited state
S_2	second singlet electronic excited state
sm	starting material
t	triplet
T_1	first triplet electronic excited state
TFA	trifluoroacetic acid
THF	tetrahydrofuran
TICT	twisted internal charge transfer
TLC	thin layer chromatography
TMS	tetramethylsilane
tt	triplet of triplets
p-TsOH	*p*-toluenesulfonic acid
UV	ultraviolet
wt%	weight percent

CHAPTER ONE:
Introduction

Imagine a day when blood concentrations of important analytes are determined not in a batch mode, but rather through the use of a fiber-optic bundle inserted into an artery. Each fiber is equipped with a different chemosensor, such that the real-time concentrations of several dozen analytes are provided on a monitor at the patient's bedside.

Anthony W. Czarnik

Fluorescent Chemosensors for Ion and Molecule Recognition (1993)

1 Introduction

1.1 Overview of Introduction

The recognition of a target molecule by a synthetically prepared receptor has captured the imagination of supramolecular chemists. Since its inception, research in this area has been instrumental in elucidating the mode of action of a great many biological events concerning recognition and catalysis.[1] The importance of this work was underlined with the award of the Nobel Prize in Chemistry to Cram, Lehn and Peterson in 1987 "for their development and use of molecules with structure-specific interactions of high selectivity."[2] Since then the diversity of compounds studied under the umbrella of supramolecular chemistry has grown significantly. Of particular interest are chemical molecular sensors, single molecules with the ability to both recognise and signal analytes in real time.[3,4]

The development of coherent strategies for the selective binding of target molecules, by rationally designed synthetic receptors, remains one of chemistry's most sought after goals. The research conducted to this end is driven by a fundamental inquisitiveness and need to monitor compounds of industrial, environmental and biological significance.

Within our research group we have exploited the interaction between boronic acids and diols.[5] The primary interaction of a boronic acid with a diol is covalent and involves the rapid and reversible formation of a cyclic boronate ester. The array of hydroxyl groups present on saccharides provides an ideal scaffold for these interactions and has led to the development of boronic acid based fluorescent sensors for saccharides.

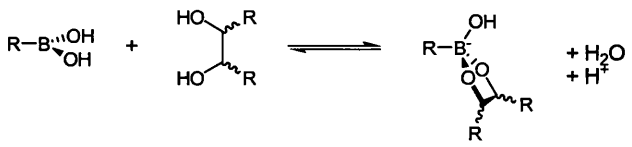

Scheme 1. *The rapid and reversible formation of a cyclic boronate ester.*

Many synthetic receptors developed for neutral guests have relied on non-covalent interactions, such as hydrogen bonding, for recognition. It is the case, however, that in aqueous systems neutral guests may become heavily solvated. Whilst biological systems

have the capacity to expel water from their binding pockets and sequester analytes wholly, using non-covalent interactions, synthetic monomeric receptors have not yet been designed where hydrogen bonding has been able to compete with bulk water for low concentrations of monosaccharides.[6]

The capacity of boronic acid receptors to function effectively in water is reflected by the number of published sensory systems designed around them. The most popular class of the fluorescent boronic acid based sensors utilise an amine group proximal to boron. The Lewis acid – Lewis base interaction between the boronic acid and the neighbouring tertiary amine has a dual role. First, it enables molecular recognition to occur at neutral pH. Second, it can be used to communicate binding by modulating the intensity of fluorescence emission through photoinduced electron transfer (PET), introducing an "off-on" optical response to the sensor.

Whilst these systems are known to function effectively and reliably a number of questions remain unanswered regarding the actual processes involved in binding and signalling. The quality of the research in this area, particularly in the past few years, has led to a significant advance in the understanding of the basic science behind the generic mode of action of this class of sensor. *This introduction will therefore bring together and critique the contemporary scientific understanding of the fundamental processes involved in the molecular recognition of saccharides by fluorescent photoinduced electron transfer (PET), boronic acid based sensors.* It should be noted that a comprehensive overview of this nature has not been previously reported in the scientific literature. *A literature review will then investigate the application of these sensory systems.* Although this review cannot be exhaustive, it is our intention to illustrate the current state of play in the field.

1.2 THE MOLECULAR RECOGNITION OF SACCHARIDES

1.2.1 Molecular Recognition

Molecular recognition lies at the very heart of sensor chemistry. The process itself involves the interaction between two substances, often termed: a host and a guest, a lock and a key or a receptor and a substrate. Importantly, recognition is not just defined as a binding event but requires selectivity between the host and the guest.

Selectivity between host and guest is a premise of compatibility. It arises between compounds with carefully matched electronic, geometric and polar elements. For synthetic receptors the potential therefore exists to engineer receptors for any chosen analyte through judicious structural design and functional group complementarity. The power of this concept is illustrated within Nature. Biological systems have evolved with exquisitely constructed active binding sites, sequestering guest molecules with near perfect selectivity.

Nevertheless, for the recognition event at a receptor to be of practical use, a further element is required. A channel of communication must be established between the receptor and the outside world. This additional quality converts a receptor into a sensor.

For a sensor to function it must therefore permit selective binding to occur between host and guest and also report these binding events by generating a tangible signal. By performing these two fundamental tasks sensors have the potential to relay information on the presence and location of important species in a quantifiable manner, bridging the gap between events occurring at the molecular level and our own.

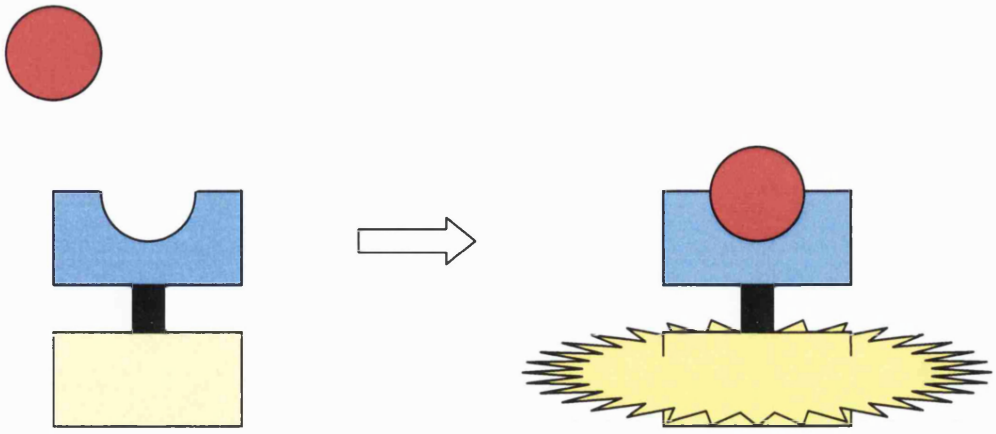

Scheme 2. *The complementary interaction between a guest analyte and a host binding pocket, illustrated here by a red guest and blue host, allows selective binding to occur between two elements. Incorporation of a unit capable of generating a physical signal in response to this binding event, converts the receptor into a sensor. In this cartoon an optical "off-on" response is depicted from an appended fluorophore, illustrated in yellow, typical of the systems developed within this thesis.*

Chemical sensors can be broadly categorised as either biosensors, or synthetic sensors. Biosensors make use of existing biological elements for recognition. Many of the physiologically important analytes already have corresponding biological receptors with intrinsically high selectivity and if these receptors can be connected to a signal transducer a biosensor can be developed.[7]

Synthetic sensors incorporate a synthetically prepared element for recognition. Whilst biomimetic receptors have been prepared, with synthetic receptors mimicking the active sites in naturally occurring biological molecules, synthetic receptors can, and often are, designed entirely from first principles.[8-10]

1.2.2 The Importance of Saccharides

Saccharides and Carbohydrates

In keeping with convention the term saccharide is used within this thesis to refer broadly to polyhydroxylated carbohydrates.[11] The product of photosynthesis, carbohydrates single-handedly account for the most prolific class of organic compounds that can be found on the surface of the Earth. Within biology they are of fundamental significance. In their most ubiquitous roles they endow Nature with structural rigidity,

in the form of cellulose, and function as the energy store that sustains life, in the forms of starch and glycogen.[12]

Not only are these compounds abundant they are also incredibly versatile. Oligo-saccharides are involved in protein targeting and folding, as well as controlling the cell recognition events for infection, inflammation and immunity.[13] From a medicinal perspective the monitoring of D-glucose has proved of particular importance. D-glucose provides the metabolic energy for most cells of higher organisms. In humans a breakdown in the transport pathways of D-glucose has been linked to conditions such as cancer,[14] cystic fibrosis[15] and renal glycosuria,[16,17] but by far the most prevalent condition resulting from ineffective D-glucose transport is diabetes mellitus.[18]

Diabetes Mellitus

Diabetes presents one of the largest health challenges to face us in the 21st century. Current reports indicate that diabetes affects 5% of the global population.[19] In the UK the increase in obesity, population age and a progressively more sedentary lifestyle has seen the prevalence of Type 1 diabetes double every 20 years since 1945.[20] Diabetes is associated with chronic ill health, disability and premature mortality. From a physiological perspective the debilitating long-term complications include heart disease,[21] blindness,[22] kidney failure,[23] stroke[24] and nerve damage leading to amputation.[25]

At an economic level the repercussions are also serious. Within the UK 5% of the National Health Service's budget is spent on treating diabetes and its complications.[26] This equates to £3.5 billion per year or £9.6 million per day. Following extensive and widespread trials, unequivocal evidence exists that monitoring and adjusting diabetic blood-sugar levels to maintain them within tight boundaries* dramatically reduces the health risks faced by diabetics.[28-30]

Structure of Saccharides

The detection of saccharides presents a curious challenge. Bristling with linked arrays of hydroxyl groups, saccharides are structurally complex. The linear form of D-glucose,

* Non-diabetic blood glucose concentrations are usually in the range 4 mM to 7 mM.[27]

for example, contains four stereocentres. Considering just its immediate family, the aldohexoses, this presents us with sixteen stereoisomers.

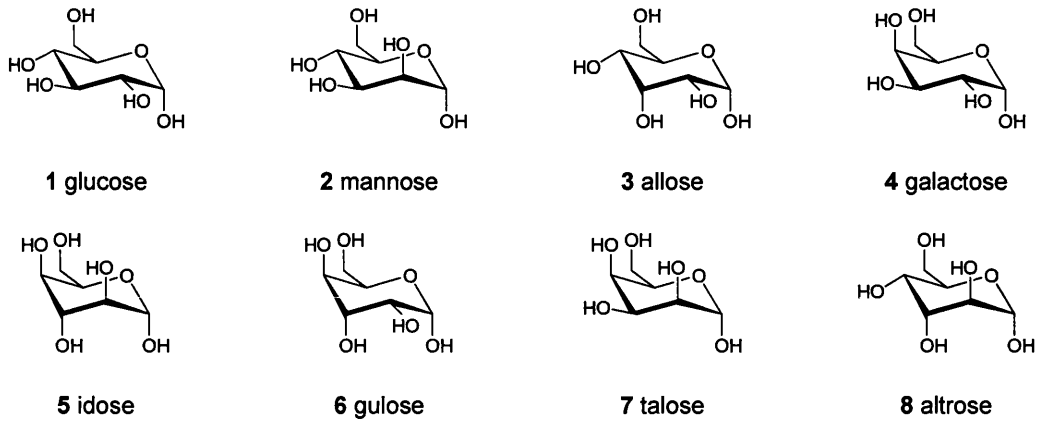

Figure 1. *The α-D-pyranose forms of the aldohexoses in their $^4C_1$ conformations.[31] Glucose is displayed on the top row with (from left to right) its 2-, 3- and 4-epimers. Idose is displayed on the bottom row with (from left to right) its 2-, 3- and 4-epimers. From the structures the similarity between these monosaccharides, their affinity for water and the complexity derived from their numerous stereogenic centres is apparent.*

In aqueous solution this complexity is further compounded by mutorotation. Cleavage of the hemiacetal ring causes interconversion between the pyranose and furanose ring forms, *via* an acyclic intermediate, with inversion of configuration at the anomeric centre equilibrating the α and β anomers thus altering the optical rotation of the solution. These properties make saccharides difficult to differentiate from each other. Furthermore in water receptors for saccharides may be heavily solvated, differentiation between water and hydroxyl groups presenting a formidable challenge in its own right.

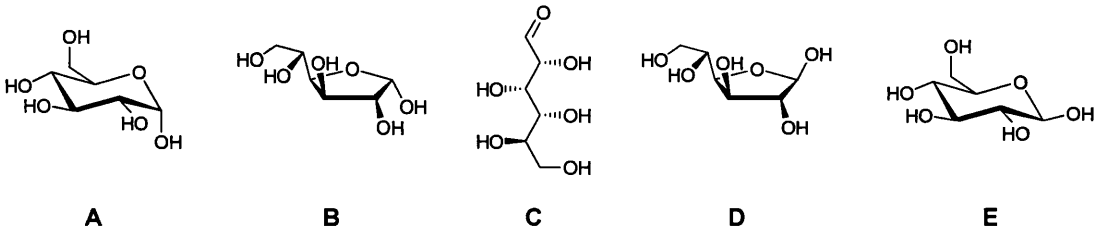

Figure 2. *D-Glucose **1** in its various configurations and the percentage composition at equilibrium of each form of the sugar in D_2O at 27 °C: (**A**) α-pyranose, 38.8%; (**B**) α-furanose, 0.14%; (**C**) acyclic form, 0.0024% (equilibrated at 37 °C); (**D**) β-furanose, 0.15%; (**E**) β-pyranose, 60.9%.[32]*

This point can be illustrated by considering the protein family, lectins. Aside from antibodies, lectins are largely responsible for carbohydrate recognition within biological

systems. Lectin – oligosaccharide binding constants are, by biological standards, unusually small, commonly in the range $10^3 - 10^4$ M^{-1}.

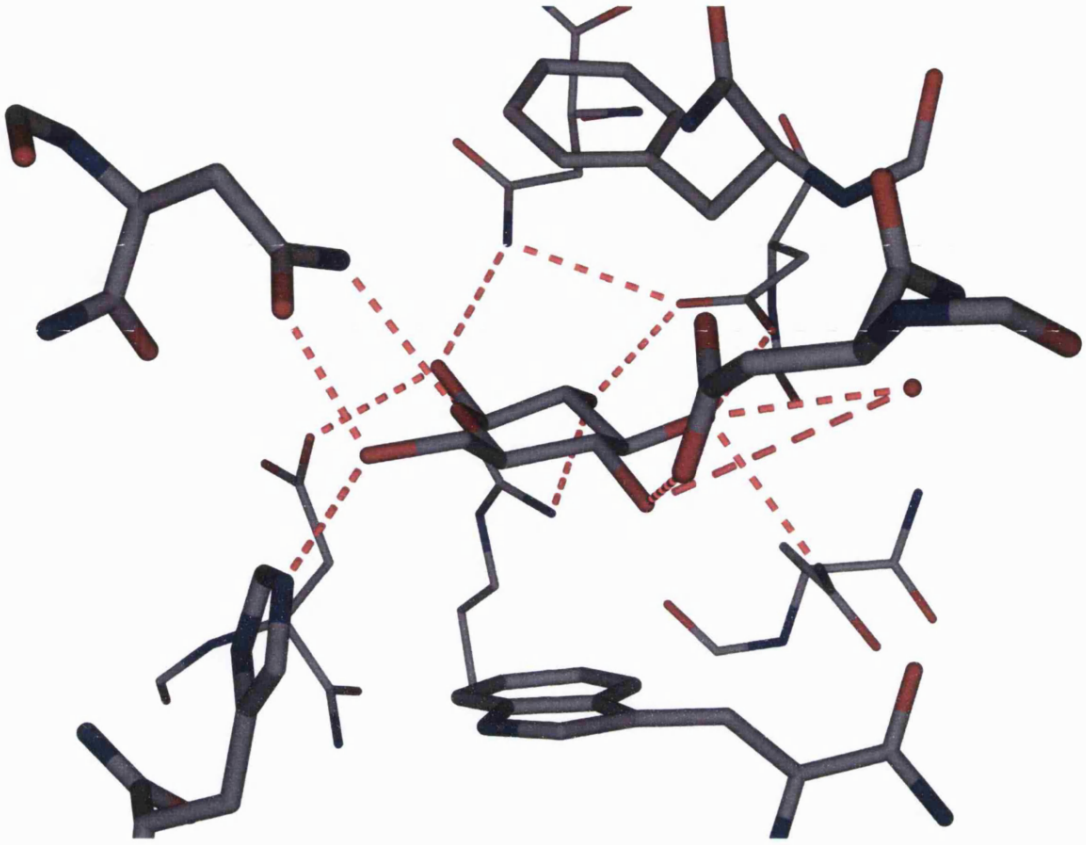

Figure 3. *Crystal structure of the E. coli glucose/galactose binding protein with β-D-glucose in situ.[33] For clarity all of the amino acids bar those involved in direct interactions with the saccharide have been stripped away. Atoms marked in red represent oxygen, blue nitrogen and grey carbon, hydrogen atoms are not displayed. The dashed red lines represent hydrogen bonds. Within the active site the monosaccharide is intercalated between two apolar residues. Axially, below the guest, the indole ring of tryptophan is visible, with the phenyl ring of phenylalanine above. Equatorially an array of thirteen hydrogen bonds provide a cooperative network from carbonyl groups, primary amides, a guanidinium, an imidazole amine and one favourably coordinated water molecule. The allosteric approach used within this active site displays the degree of sophistication and elegance Nature uses to achieve binding.*

The crystal structure of the *Escherichia coli* galactose binding protein with a bound molecule of β-D-glucose was obtained.[33] From the structure it can be observed that recognition is achieved by sequestering the monosaccharide entirely beneath the protein surface and expelling bulk water from the active site. This not only fosters a favourable entropic stabilisation but also allows the surrounding amino acid residues unfettered access to the substrate. In the binding site of the molecule β-D-glucose is sandwiched between two apolar phenylalanine and tryptophan residues axial to the ring. Equatorially an array of thirteen different complementary hydrogen bonding

interactions are provided by one advantageously sited water molecule and eight individual amino acid residues, all ideally located.

Home Blood Glucose Monitoring

Commercially the preferred tools for sensing complex molecular species have relied on the high specificity exhibited by antibodies and enzymes. Most clinical systems currently available for measuring blood glucose levels rely on the glucose oxidase enzyme (GOx, also commonly abbreviated to GOD or GO).

The majority of these home blood glucose monitoring tools rely on the invasive withdrawal of blood, typically from a pricked finger, followed by application of the sample to an amperometric enzymatic test strip allowing GOx to catalyse the oxidation of glucose to gluconic acid.[27,34]

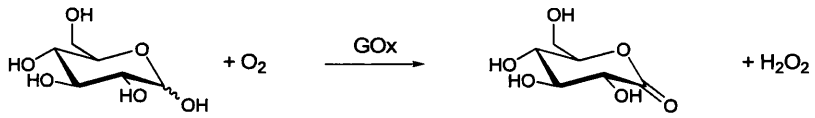

Scheme 3. *The oxidation of D-glucose to D-gluconolactone (the ring closed form of D-gluconic acid).*

Early glucose monitors measured the production of hydrogen peroxide by oxidation at a single working electrode, as in Equation 1. At a constant voltage the current generated across the cell is proportional to the concentration of hydrogen peroxide, which is in turn proportional to the glucose concentration in the sample under investigation.

$$H_2O_2 \rightarrow O_2 + 2H^+ + 2e^- \qquad \text{Equation 1.}$$

As this method of monitoring glucose is heavily dependent on the oxygen concentration a dimethylferrocene mediator was developed. At a set potential of + 160 mV glucose is oxidised with concurrent reduction of the dimethylferricinium cation; the applied potential serving to oxidise and thus recycle the resulting dimethylferrocene back to the dimethylferricinium cation.[35,36]

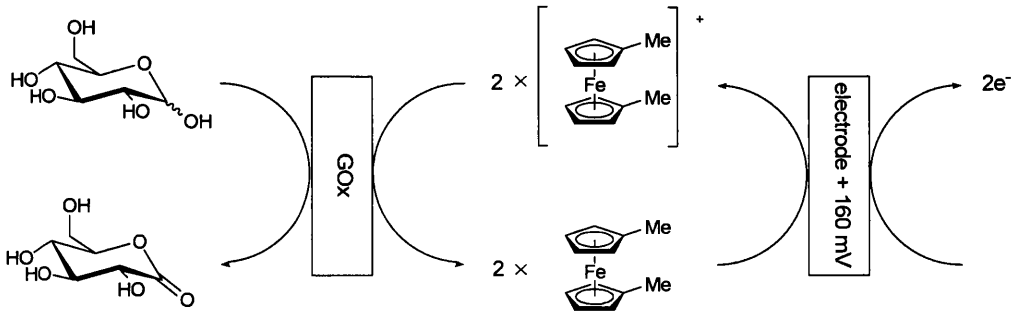

Scheme 4. *The oxidation of glucose with concurrent reduction of the dimethylferricinium cation mediator.*

There can be no question that the availability of affordable home blood glucose monitoring has revolutionised the quality of life experienced by diabetics. However, there are some inherent limitations with an enzymatic approach. The systems have to be stored appropriately, they are specific only for a few saccharides and in most cases they become unstable under harsh conditions. For this reason much work has been focused on the development of synthetic sensors with the capacity to monitor saccharides under a broad range of environmental conditions and thus allow access to a wider spread of diagnostic applications.

1.2.3 Non-Boronic Acid Appended Synthetic Sensors for Saccharides

A great amount of attention is currently devoted to the development of synthetic molecular receptors with the ability to recognise saccharides. This thesis is primarily concerned with the role of boronic acids in that recognition process, although many systems have been developed which use non-covalent interactions for recognition. A few examples are given below to provide a brief illustration of research in this area: for a more comprehensive insight the reader is directed to several recently published reviews.[6,8,9,37]

The first synthetic saccharide receptor **9** was documented in 1988 by Aoyama *et al.*[38] The calixarene framework is not large enough to actually permit the encapsulation of a saccharide within the central annulus of the bowl, but it does permit "face-to-face" recognition to occur between the calixarene's upper rim hydroxyls and those of the saccharide.

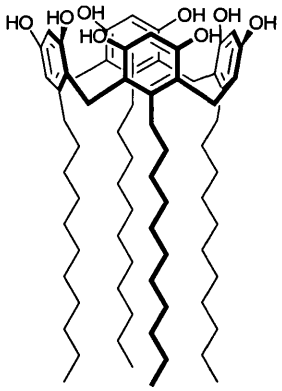

9

Inspired by the structure of the saccharide binding proteins such as the active site of the *Escherichia coli* galactose binding protein, illustrated in Figure 3 (page 8), Davis and Wareham developed the octa-amide **10**.[39] The sophisticated architecture mimics Nature in that the binding pocket is designed so as to completely encapsulate a host saccharide. The planar hydrophobic surfaces of the dual diphenyl groups provide internal apolar contacts above and below the aliphatic ring. Located equatorially to the saccharide host an array of secondary amides induces favourable hydrogen bonding interactions, anchoring the hydroxyls on the saccharide ring.

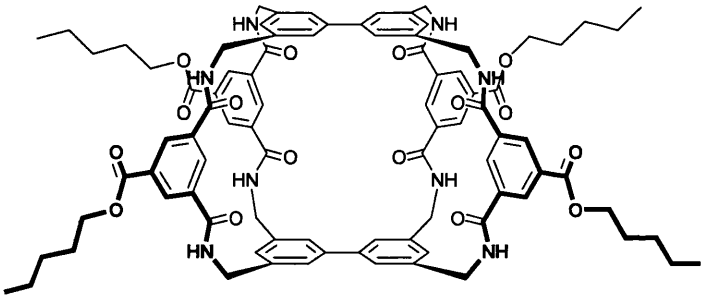

10

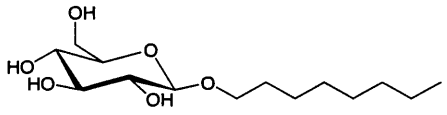

11

Even with such elegant design the reported stability constants (K_a) for sensor **10** in deuterated chloroform are reduced significantly on addition of competitive co-solvents. In the presence of octyl-β-D-glucoside **11** a ~ 300 fold reduction was witnessed in the stability constant (K_a) of sensor **10** on addition of 8% deuterated methanol to the system.[†] The stability constants (K_a) for sensor **10** with octyl-β-D-glucopyranoside **11**

[†] Unless specified otherwise all of the deuterated solvents referred to in this thesis are fully deuterated.

were 300 000 M^{-1} in deuterated chloroform and ~ 1 000 M^{-1} in 92:8 deuterated chloroform/deuterated methanol.

As well as developing recognition sites through careful structural pre-organisation, non-covalent interactions of increased strength have also been studied. Manipulation of anionic centres has proved successful as functional groups such as phosphates, phosphonates and carboxylates can be powerful hydrogen bond acceptors. Whilst the pre-organisation can be reduced, it has been found that these anionic centres provide a degree of structure in their own right. Flexible sensors with multiple anionic groups will conform to the tendency of the charged groups to repel each other so as to minimise electrostatic repulsions.

Das and Hamilton have employed phosphonate moieties in sensors such as the rigid chiral spirobifluorene **12**.[40] The racemate was used directly and although the exact nature of the hydrogen bonding motif could not be determined excellent binding was observed with octylglucosides in organic solvents. The enantioselectivity was also determined and reported as ~ 5.1:1, the greatest value reported for saccharide enantioselective discrimination by non-covalent interactions.[9] The binding constant (K_a) for sensor **12** with octyl-β-D-glucopyranoside **11** was 47 000 M^{-1} in deuterated acetonitrile.

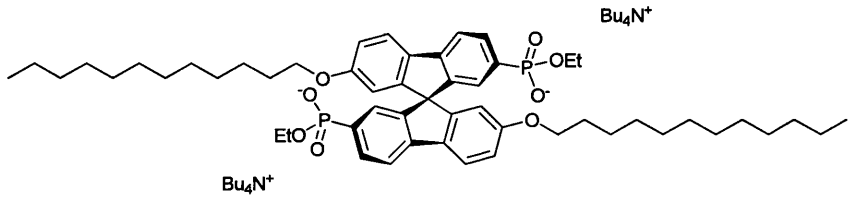

12

Diederich and co-workers have made use of binaphthalene derived macrocycles appended with internal phosphate groups to provide a ring of hydrogen bonding sites within a central recognition cavity.[41-43] One of the first of these, sensors **13**, was shown to have good selectivity for suitably sized saccharides such as the octyl-D-β-glucopyranoside **11**, the calculated inter phosphate distance of 7.2 Å being designed so as to accommodate monosaccharides exclusively. A stability constant (K_a) of 5 200 M^{-1}

was reported for the complexation of sensor **13** and octyl-D-β-glucopyranoside **11** in 98:2 deuterated acetonitrile/deuterated methanol.[43]

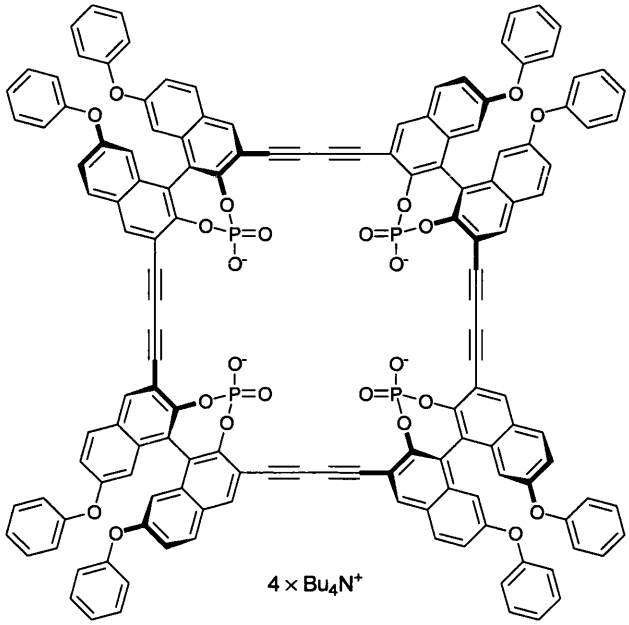

13

The major obstacle faced by all of the synthetic receptors above, which are wholly reliant on non-covalent interactions, is that of solvent competition. In aqueous systems neutral guests may become heavily solvated and are therefore unable to monitor glucose in media of specific interest to analysts such as blood, urine, tear fluid, beverages, food stuffs and so forth. No synthetically designed, hydrogen bonding, monomeric receptor has as yet been able to compete with bulk water for low concentrations of monosaccharides.[6] In overcoming this hurdle the covalent interaction between boronic acids and saccharides has proved hugely advantageous.

1.3 Complexation of Boronic Acids with Saccharides

1.3.1 A Brief History

Early Work

Boronic acid chemistry has its roots in the work of Frankland, who in 1860 documented the preparation of ethylboronic acid, with the first synthetic publication on organoboron chemistry.[44] In 1880 Michaelis and Becker reacted borontrichloride and diphenyl mercury to form dichlorophenylborane. This in turn was added to water and recrystalised as white needles in the first synthesis of phenylboronic acid.[45,46] The route was refined by 1909 and the classical synthesis of boronic acids from Grinard reagents and trialkyl borates established.[47]

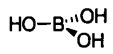

14

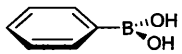

15

Figure 4. *The planar structures of boric acid **14** and phenylboronic acid **15**.*

In a pioneering series of papers spanning 29 years, from 1911 to 1940, Böeseken and co-workers elucidated the absolute structural configuration of a panoply of saccharides and other hydroxyl containing compounds.[48] The configurations were determined, in large part, from the known ability of boric acid to complex diols. As boric acid complexes formed in solution, with hydroxyl groups in favourable 1,2- and sometimes 1,3- configurations, a rise was observed in both acidity and conductivity. By tracking the changes in conductivity of boric acid solutions as saccharides were added, the relative configurations of the hydroxyl groups could be inferred. This method was employed in 1913 to conclusively determine the structure of the pyranose and furanose forms of D-glucose. Changes in conductivity revealed the relative *cis*- and *trans*-orientations of the vicinal C1 and C2 hydroxyl groups, thus permitting the absolute structural configuration of the α- and β- pyranose and furanose anomers to be attributed.[49]

Figure 5. *The pyranose anomers of D-glucose **1**: (**A**) α-D-glucopyranose and (**B**) β-D-glucopyranose. The relative cis- and trans- orientations of the vicinal C1 and C2 hydroxyl groups were inferred by tracking the changes in conductivity of boric acid solutions as these saccharides were added, permitting the absolute structural configuration of the α- and β-anomers to be attributed.*[49]

Boronic Acid – Diol Complexation

Given the significance of boric acid in the determination of saccharide configurations, it is perhaps surprising that the same properties were not observed in boronic acids until 1954.[50] During a course of investigations into aromatic boronic acids, Kuivila and co-workers observed a new compound being formed on addition of phenylboronic acid to a solution of saturated mannitol, correctly postulating the formation of a cyclic boronic ester analogous to the one known to form between boric acid and polyols.

A number of publications followed examining the properties and synthesis of boronic acids,[51-53] with the first quantitative investigation into the interactions between boronic acids and polyols in 1959.[54] In a study to clarify the disputed structure of the phenylboronate anion, Lorand and Edwards added a range of polyols to solutions of phenylboronic acid. The pH of the solutions was adjusted such that there was an equal speciation of phenylboronic acid in its neutral and anionic forms; the pH matching the pK_a. As diol was added the pH of the systems decreased, allowing binding constants to be determined through the technique of pH depression.

From these experiments Lorand and Edwards concluded that the conjugate base of phenylboronic acid has a tetrahedral, rather than trigonal structure. The dissociation of a hydrogen ion from phenylboronic acid occurs from the interaction of the boron atom with a molecule of water. As the phenylboronic acid and water react a hydrated proton is liberated, thereby defining the acidity constant K_a, see Hartley, Phillips and James.[55,‡] This is depicted in Scheme 5 by considering an explicit water molecule associated with the Lewis acidic boron. The reported pK_as of phenylboronic acid fluctuate between ~ 8.7 and 8.9,[56-61] with a recent in-depth potentiometric titration study refining this value to 8.70 in water at 25 °C.[62]

‡ J. H. Hartley, M. D. Phillips, and T. D. James, *New J. Chem.*, 2002, **26**, 1228-1237.

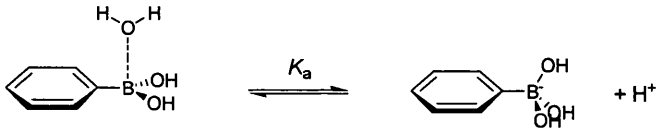

Scheme 5. *The acid - conjugate base equilibrium for phenylboronic acid in water. The dissociation of the hydrogen ion from phenylboronic acid occurs from the interaction of the boron atom with a molecule of water. Here we consider an explicit water molecule associated with the Lewis acidic boron.[55] As the phenylboronic acid and water react a solvated hydrogen ion is liberated, thereby defining the acidity constant K_a, where pK_a = 8.70 in water at 25 °C.[62]*

Whilst one explicitly associated molecule is shown in a number of illustrative schemes for clarity, water should be considered to be in rapid exchange on the Lewis acidic boron in much the same way that hydrated Lewis acidic metal ions exchange bound water. A pertinent comparison can be found with the ionisation of Zn^{2+} in water, the reaction $Zn–OH_2 \rightarrow Zn–OH + H^+$ having a pK_a of 8.8.[63]

Boronic acids have been reported to rapidly and reversibly[64] interact with dicarboxylic acids,[65,66] α-hydroxy carboxylic acids[60,66-68] and diols[54] to form esters in aqueous media.[69] The most common interaction is with 1,2 and 1,3 diols to form five- and six-membered rings respectively. From experimental observations it is well known that the kinetics of this interconversion are fastest in aqueous basic media where the boron is present in its tetrahedral anionic form.[70] Typically differences in rate of 10^4 are observed between boron in its trigonal and tetrahedral forms.[69]

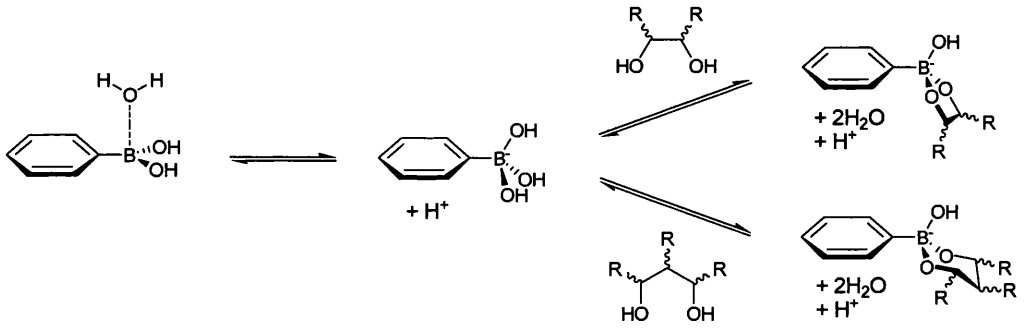

Scheme 6. *Interaction of the phenylboronate anion with 1,2 and 1,3 diols to form diol - phenylboronate complexes with five and six membered rings, respectively. From experimental observations it is well known that the kinetics of this interconversion are fastest in aqueous basic media (by a factor of 10^4) where the boron is present in its tetrahedral anionic form.[70]*

Whilst the boronate anion does account for the strongest binding of diols in aqueous media the interaction between diols and the neutral boronic acid should not be ignored.

In considering these interactions the equilibria in Scheme 6 can be readily expanded to form a thermodynamic cycle, as illustrated in Scheme 7.

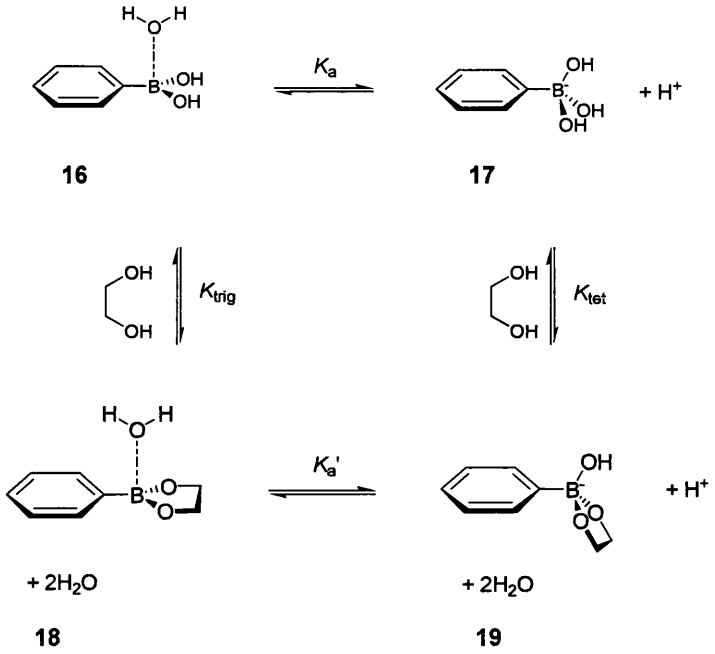

Scheme 7. *The equilibria for boronate ester formation couple to generate a thermodynamic cycle. The formation of the diol boronate anion complex is defined as K_{tet} and the formation of the diol boronic acid complex is defined as K_{trig}, where it is observed that $K_{tet} > K_{trig}$. The acidity constant of the unbound complex is defined as K_a and the acidity constant of the bound complex is defined as K_a', where it is observed that $pK_a > pK_a'$.*

Considering Scheme 7 we define the formation of the diol boronate anion complex as K_{tet} and the formation of the diol boronic acid complex as K_{trig}, where it is observed that $K_{tet} > K_{trig}$. For instance the logarithm of these constants for phenylboronic acid binding fructose in 0.5 M NaCl water is: log K_{tet} = 3.8 whereas log K_{trig} < -1.4. This difference in the value of the binding constant between K_{tet} and K_{trig} is typical, with differences of up to ~ five orders of magnitude being commonplace.[62] It is also known that the neutral boronic acid becomes more acidic upon binding. The acidity constant of the bound complex is defined by K_a', where it is observed that pK_a > pK_a'. For instance the pK_a of phenylboronic acid = 9.0 in 0.1 M NaCl 1:2 (v/v) methanol/water, under the same conditions the pK_a' of phenylboronic acid bound to fructose = 5.2; in other words the boronic ester is more acidic than the boronic acid.[62]

These phenomena were known and employed in analyte recognition for many years prior to an understanding of the mechanistic rationale behind the observed results. Although there are still various points of contention, a great deal of work has been

conducted during the last few years which has helped elucidate the cause of these empirical results. Some of these points are worthy of further scrutiny here.

1.3.2 Acidity and the O-B-O Bond Angle

O-B-O Bond Angle Contraction

The first is the change in acidity at the boron centre on binding. This change in acidity is often ascribed to the contraction of the oxygen-boron-oxygen (O-B-O) bond angle on complexation and is crucially important to the development of sensory systems containing boronic acid recognition sites as this change in acidity forms the basis of many of the signalling mechanisms used.

In unbound phenylboronic acid the molecule is trigonal planar with sp^2 hybridisation about the boron centre and an expected O-B-O bond angle of ~ 120°. Unfortunately the reported data pertaining to the structure of phenylboronic acid from x-ray crystallography has not proved effective at refining this value. The crystal structure of phenylboronic acid was reported in 1977,[71] the crystallisation process producing cyclic, nearly planar, hydrogen bonded dimers, see Scheme 8.

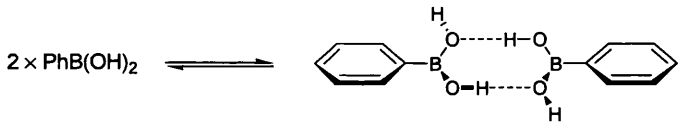

Scheme 8. *Boronic acids exhibit a predisposition to associate as cyclic hydrogen bonded dimers upon crystallisation.*

The phenylboronic acid molecules participate in linear intermolecular hydrogen bonding interactions, a binding motif comparable to the one observed in dimeric carboxylic acids. These interactions distort the O-B-O atoms from ideal geometries (O-B-O bond angles of ~ 116.3° were reported) and void a meaningful comparison between the structure of the crystals examined and the structures that one might expect for the molecules in solution. This dimerisation is commonplace in the crystallisation of arylboronic acids, with similar compressions of the O-B-O bond angles occurring in other compounds.[72] This characteristic has actually found applications in template directed supramolecular synthesis.[73,74]

In avoiding the structural distortions observed for crystalline phenylboronic acid, the extended crystal lattice formed by boric acid can be considered as an example of a boron species with no deviation from the expected 120° O-B-O bond angle. As hydrogen bonding interactions link all the hydroxyl groups, regular patterns of trigonal and tetrahedral boric acids are fashioned. A recent communication documented the single-crystal x-ray structure of boric acid with C_3 symmetry and an O-B-O bond angle of 120.0 (9)°, as in Figure 6.[75]

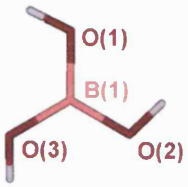

Figure 6. *The single-crystal x-ray structure of boric acid with trigonal symmetry. Atoms marked in red represent oxygen, pink boron and white hydrogen. An O-B-O bond angle of 120.0 (9)° was reported.*

On binding, this bond angle is substantially reduced and in so doing places considerable strain on the newly formed ring. Lorand and Edwards estimated that in a five-membered ring an angle of approximately 108° would be obtained. The bond angle is of course heavily dependent on the substrate bound but a good example is the single-crystal x-ray structure of the diphenylboronic acid - fructose complex obtained by Fallon and co-workers in 2004 from a 2 to 1 ratio of boronic acid and D-fructose under non-basic conditions and in the absence of Lewis basic components. From the structure it is observed that five-membered cyclic boronates have formed at the 2,3- and 4,5 positions of β-D-fructopyranose. In the absence of any Lewis basic components the structure demonstrates little deviation from planarity at the boron centre. Within the plane O-B-O bond angles of just over 113° are observed.[76]

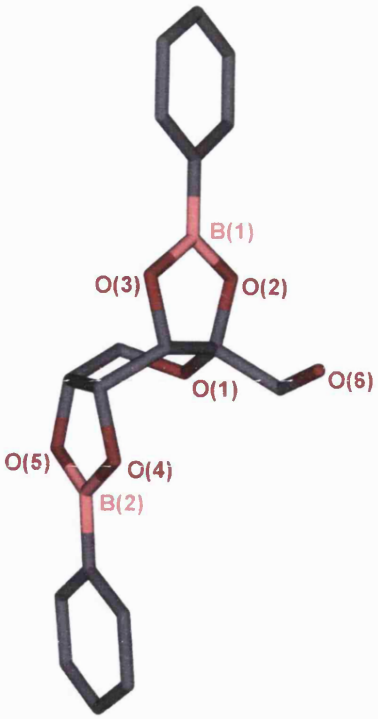

Figure 7. *The single-crystal x-ray structure of the diphenylboronic acid - fructose complex obtained by Fallon and co-workers from a 2 to 1 ratio of phenylboronic acid and D-fructose under non-basic conditions and in the absence of Lewis basic components. Atoms marked in red represent oxygen, pink boron and grey carbon. For clarity hydrogen atoms are not displayed. From the structure it can be observed that the O-B-O bond angles are reduced, in this instance, to ~ 113° from ~ 120°, whilst the structure remains almost entirely planar about the boron centres [O(2)-B(1)-O(3) = 113.31(18)° and O(5)-B(2)-O(4) = 113.65(18)°].*[76]

sp^3 hybridised orbitals are tetrahedral in nature, with an ideal bond angle of 109.5°.[77] The contraction of the O-B-O bond angle means that in the bound instance the geometry of sp^3 hybridised orbitals actually provides a closer topographic match to the complex than the geometry of sp^2 hybridised orbitals.

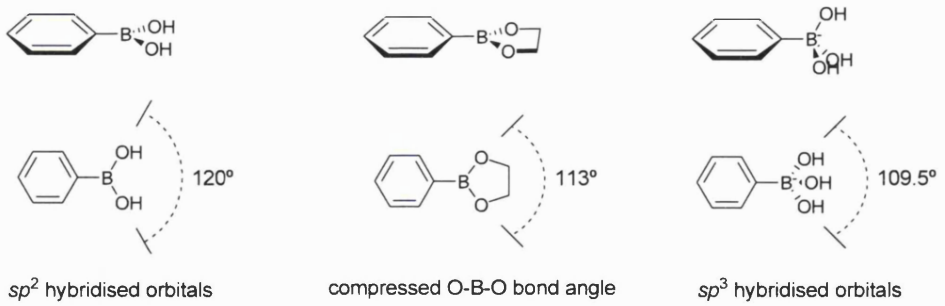

Figure 8. *The compressed O-B-O bond angle of the diphenylboronic acid – D-fructose complex*[76] *is found to be between the bond angles expected for sp^2 and sp^3 geometry. sp^3 geometry provides the closest match to the bound complex, meaning that formation of the tetrahedral boronate diol complex reduces ring strain and lowers the energy of the bound species. This results in a shift of the dynamic equilibrium between the neutral boronic acid diol complex* ***18*** *and the boronate anion diol complex* ***19****, causing the observed increase in the value of the acidity constant, K_a'.*

Rehybridisation of an sp^2 boron complex to form the sp^3 tetrahedral boronate species will therefore reduce the ring strain and lower the energy of the system. As a result it is thought that the dynamic equilibrium illustrated in Scheme 7 (page 17, and redrawn in Scheme 9 below for clarity) between the neutral boronic acid diol complex **18** and the boronate anion diol complex **19** will shift to the right, causing the observed increase in the value of the acidity constant, K_a'.[78]

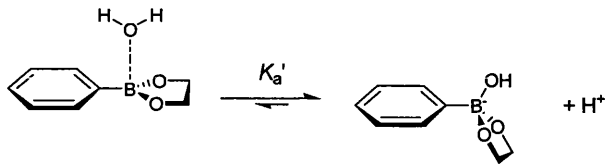

18 **19**

Scheme 9. *The acidity constant of the bound complex is defined as K_a', where it is observed that $pK_a > pK_a'$.*

Orbital Interpretation

The increase in the value of the acidity constant can be predicted somewhat more quantitatively by interpreting the hybridisation of boron's orbitals. In the case of unbound boronic acid, boron has an sp^2 trigonal planar geometry with an empty p orbital perpendicular to the plane of the molecule. It is with this unoccupied p orbital on boron that the nucleophilic oxygen lone pair on the approaching water molecule will mix. As the boron-oxygen interaction strengthens, concomitant proton dissociation occurs. By definition the ease with which this proton is dissociated determines the value of the acidity constant.

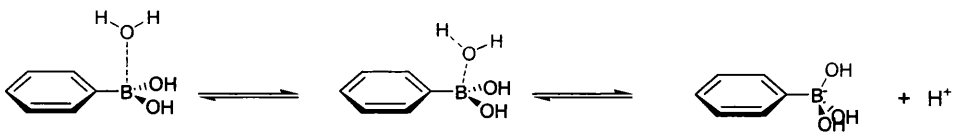

Scheme 10. *To conform to the constraints enforced upon it on complexation, boron adopts geometric characteristics between sp^2 and sp^3 hybridised orbitals, causing the vacant p orbital to develop some s character. This has the effect of deshielding the nucleus and in turn increasing the Lewis acidity at boron. The net effect is to increase the acidity of the labile hydrogen thus making the system more acidic.*

Following complexation to a diol the geometry of the orbitals at the neutral boron centre are altered. To conform to the constraints enforced upon the boron complex generated, the geometry of the boron orbitals adopt characteristics between sp^2 and sp^3 hybridised

orbitals, the empty *p* orbital therefore develops some *s* character. It is known that *s* orbitals are held closer to the nucleus than *p* orbitals. In the case of filled orbitals this means electrons within *s* orbitals are lower in energy and more effective at shielding the positive charge of the nucleus than those in *p* orbitals. In the case of boron the unhybridised *p* orbital is empty, the development of *s* character therefore has the effect of deshielding the nucleus, increasing the Lewis acidity at boron. With the Lewis acidity of the boron increased the Lewis acid – Lewis base interaction between boron and the oxygen within the approaching water molecule is augmented, weakening the adjoining O-H bond and increasing the lability of the acidic hydrogen.

Computational Analysis

Over the period 2003-2004 the relationship between boronic acid diol complexation and acidity was studied computationally. Bock and co-workers modelled the complexation of methanol,[79] 1,2-ethanediol[80] and D-glucose[81] with boronic acids. This approach allowed a quantitative evaluation of the relationship to be undertaken.

The results calculated have been found to broadly match the published experimental data on boronic acid complexation. The value of the O-B-O bond angle calculated for the five-membered ring formed on complexation of a 1,2-diol with dihydroxyborane was 113.8°.[80] A value in good agreement with the O-B-O bond angles observed in the single-crystal x-ray structure subsequently obtained, where values of 113.3° and 113.7° were reported (Figure 7, page 20).[76]

The electrophilic reactivity index for the boron atom (ERI_B) of 4-[4-(dimethylamino)[phenylazo]benzeneboronic acid was used to provide a measure of acidity.[81] Examining this ERI_B in a number of bound complexes, the computational results indicated that acidity generally increases on complex formation. Analysis of the two independent boronic acid complexes formed at the 1,2- and 4,6-positions of separate α-D-glucopyranose molecules, revealed a comparative increase in the ERI_B values (relative to the unbound boronic acid) of around 64% for the five-membered ester formed through binding at the 1,2-positions and of around 19% for the six-membered ester formed through binding at the 4,6-positions.

The computational results appear to suggest that considering a proportional relationship between O-B-O bond angle contraction and the acidity of boronic acid when complexed

to substrates such as saccharides is somewhat of a simplification. When quantified the measure of boron's acidity was found to be influenced by a number of environmental features such as through space interactions with proximal saccharide oxygen atoms. Nevertheless, in the vast majority of cases the theoretical calculations overwhelmingly agreed with the experimental observations; on complexation of a boronic acid with a poly-hydroxyl ligand the O-B-O bond angle decreases and the acidity of the boronic acid increases.

1.3.3 Complex Formation and Dependence on pH

Empirical Data

From empirical data it has long been clear that pH dominates the reaction kinetics of boronic acid – diol complexation.[70] As discussed above, a step change in the binding constants, of some five orders of magnitude, is apparent at a pH threshold where the pH of the system becomes greater than the boronic acid's pK_a.[62] The kinetics of boronic acid – diol complexation mirror this with an increase in rate of three to four orders of magnitude, when boron is present in its tetrahedral anionic form, rather than as the neutral trigonal species.[82]

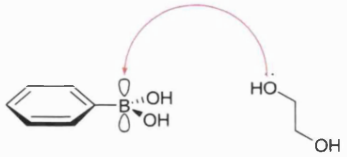

Scheme 11. *The expected attack of a diol oxygen lone pair on boron's vacant p orbital does not provide a mechanistic rationale for the four fold acceleration in rate when the boron centre develops a negative charge and the p orbital becomes occupied.*

When explaining these observations from a mechanistic, arrow pushing perspective the results may appear somewhat counter intuitive. Mechanistically one could quite reasonably envisage the first step as the attack of a diol oxygen lone pair on boron's vacant *p* orbital,[83] Scheme 11. Yet experimental data clearly indicates that this reaction is much faster when the *p* orbital is occupied and the boron centre is carrying a negative charge.

The value of rate and stability constants are not only dependent on pH; there is also a clear dependence on the acidity of the reacting ligand.[68] Whilst the binding of diols by

trigonal boronic acids can be considered to be almost negligible, this is not the case when boronic acids complex with more acidic poly-hydroxyl species such as 1,2-diphenols,[68] α-hydroxy carboxylic acids[60,66-68] and dicarboxylic acids.[65-67,84]

Unfortunately direct analysis of the reaction parameters of tetrahedral boronates with these acidic ligands is complicated by the presence of reaction pathways which are kinetically indistinguishable due to proton ambiguity.[69] Therefore, the bias of the literature towards examining the complexation of ligands with neutral boronic acids necessitates that we discuss this first in order to develop a rounded perspective of the mechanism.

Proton Transfer

In work which has been ongoing since the late 1960s, Pizer and co-workers extensively examined the physical properties of trigonal boron acid§ – ligand complexation.[67,82] From initial studies it was observed that the overall reaction proceeded with a change in geometry at boron, from trigonal to tetrahedral, on complexation.

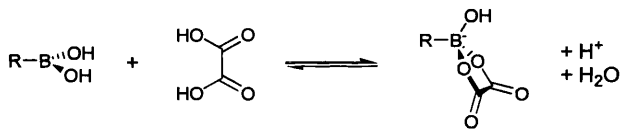

Scheme 12. *Whilst the binding of diols by trigonal boronic acids can be considered almost negligible, this is not the case when boronic acids complex with more acidic poly-hydroxyl species. Here the complexation of trigonal phenylboronic acid with oxalic acid proceeds with a rate constant $k_{COOHCOOH}$ of 2000 M^{-1} s^{-1}.[65] With trigonal boron acids complexation is generally discussed in terms of the overall reaction proceeding with a change in geometry from trigonal to tetrahedral at boron on complexation.*

It was also noted that the rates of these reactions were dependent on a number of features, in particular on the protonation of the ligand. For the complexation of phenylboronic acid with oxalic acid the rate constant was $k_{COOHCOOH} = 2000\ M^{-1}\ s^{-1}$, for the monobasic form the rate dropped to $k_{COOHCOO^-} = 330\ M^{-1}\ s^{-1}$, with a rate for the dibasic form of $k_{COO-COO^-} \leq 0.1\ M^{-1}\ s^{-1}$.[65] These results were unusual for a nucleophilic

§In keeping with contemporary terminology the term "boron acid" is used within this thesis as an extension of the nomenclature suggested by Branch *et al.*, where a differentiation is purposely not made between boronic acid and boric acid species.[85,86]

substitution process in that the highly nucleophilic dianionic species was almost entirely unreactive, whilst the most protonated attacking species reacted the most rapidly.

The observations were rationalised on the basis of the leaving group expelled and the minimisation of charge repulsion.[65] In the case where a fully protonated ligand was complexed, the more acidic proton would be transferred from the ligand to the hydroxyl on boron to allow the elimination of water.[68] One proton is therefore an absolute pre-requisite for the reaction. Experimental results indicated that the more acidic proton was involved in proton transfer with a precise correlation between rate and its pK_a. It was postulated that the dependence of reaction rates on the presence of the second, less acidic, proton could be argued on the basis of charge minimisation between the incoming anionic ligand oxygen and the leaving hydroxyl group.

Mechanistically the pathway was interpreted as a substitution reaction at boron initiated by nucleophilic attack of the ligand on the empty *p* orbital of boron.[65] Pizer proposed a transition state for the reaction of trigonal boron acids with fully protonated ligands. The transition state was discussed in terms of being associative and the intermediate complex being tetrahedral. In this transition state it was suggested that proton transfer from the entering ligand to the leaving hydroxyl could be rate-determining, as in Scheme 13.

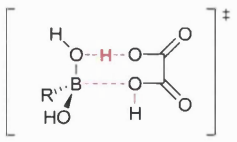

Key: ---- denotes developing/cleaving covalent bonds

Scheme 13. *The transition state proposed by Pizer was considered associative with the intermediate complex being tetrahedral. In this transition state it was suggested that proton transfer from the entering ligand (here, the oxalic acid on the right) to the leaving hydroxyl (the proton acceptor) could be rate-determining (for clarity the mobile proton is indicated in bold red).*[68] *One caveat for the proposed transition state was that the interconversion between trigonal and tetrahedral geometries should be rapid, as in the addition of* OH^- *to* $B(OH)_3$ *which had been previously assumed to be diffusion controlled.*[82]

To better understand the dependence between rate, pH and pK_a, the series of complexes formed from the ligands and trigonal boron acid species depicted in Figure 9 and Figure 10 were examined to establish trends in the stability and rate constant data.[68]

Effect of Altering the Ligand

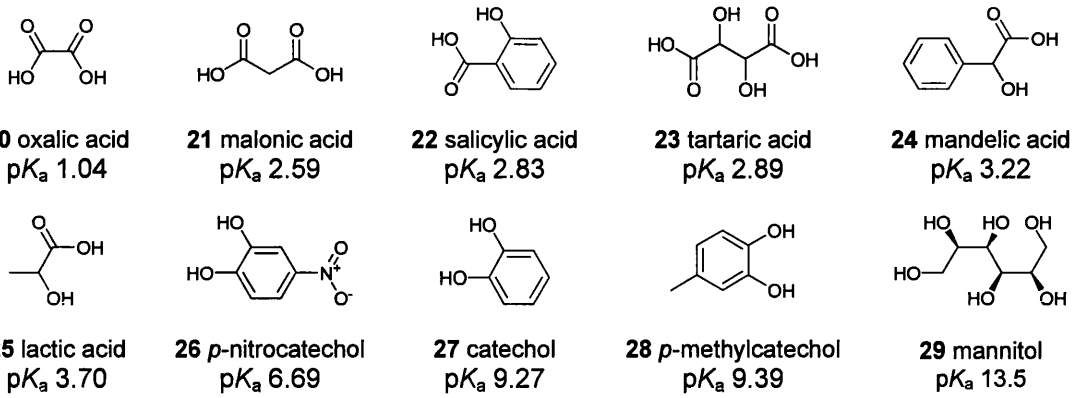

Figure 9. *The series of ligands, with their respective pK_as, as documented by Pizer.[68] It was found that for a given boron acid the stability constants for complex formation increased with increasing ligand acidity.*

Across the series of ligands examined in Figure 9 (complexing with the same boron acid) the stability constants for complex formation increased with increasing ligand acidity. This effect was brought about by an increase in the forward rate constant and a decrease in the reverse rate constant for complexation. An observation consistent with the operation of a proton transfer mechanism.

In the forward direction the proton is transferred from the ligand to the hydroxide on boron. In the reverse direction it is transferred from the entering water molecule to the leaving ligand. Therefore, increasing the acidity of the labile proton facilitates the forward proton transfer mechanism, increasing the forward rate of reaction, and impedes the reverse proton transfer mechanism, decreasing the reverse rate of reaction.

Effect of Altering the Boron Acid

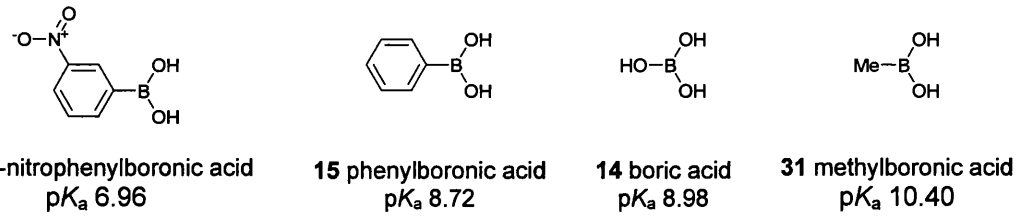

Figure 10. *The series of boron acids, with their respective pK_as, as documented by Pizer.[68] It was found that for a given ligand the stability constants for complex formation increased with increasing boron acid acidity.*

Across the series of boron acids examined in Figure 10 (complexing with the same ligand) the stability constants for complex formation increased with increasing boron acid acidity. This trend is not a function of proton transfer; instead it reflects a general enhancement in the stability of the product and transition state, a stability which increased with increasingly electronegative substituents. Where acidity was derived from the presence of an electron withdrawing substituent, the substituent had the effect of delocalising the developing negative charge on boron in the reaction. This stabilised both the transition state and the final anionic product, increasing the stability constant.

Although this accounted for the observed changes qualitatively, in instances where the acidity of the trigonal boron acid was derived in part from the stabilising effect of mixing adjacent π orbitals with the vacant p orbital on boron the trend was non-linear. It was the case that conjugative stabilisation was lost in systems such as phenylboronic acid as soon as the complex became tetrahedral: this change in geometry therefore destabilised the transition state and final ionic product relative to the starting material.

Deuterium isotope effect

More recently a number of other groups have become involved in examining the kinetics of these systems.[87-90] Studies by Funahashi, Ishihara and co-workers examined various factors, such as deuterium isotope effects on the rate of reaction and the reaction activation parameters.[87] There is general concurrence that the first step in the complexation mechanism with trigonal boron acids, the formation of the monoester, is associative and is rate limiting.[82,88-90] The fact that tetrahedral $RB(OH)_3^-$ reacts much faster than trigonal $RB(OH)_2$ supports the idea that the ring closure should not be rate limiting if a tetrahedral intermediate is formed. Both research groups agree that proton transfer is significant. However, there are differences in the interpretation of the transition state and rate-determining step.

Funahashi and Ishihara used deuterated reactants to explore complexation and observed a reduction in rate constants of 20-30%.[87] As $k_H/k_D < 2$ this result is in keeping with a secondary kinetic isotope effect, that is to say that whilst important, it is possible that proton transfer is not the slowest component of the reaction pathway.[90]

From monitoring the reaction in non-aqueous solvents Funahashi and Ishihara proposed that the interconversion from trigonal to tetrahedral geometry at boron was slow, the

formation of the initial B-O bond, not proton transfer, therefore being rate-determining. The proposed plot of reaction coordinate *versus* free energy is illustrated in Scheme 14.[89]

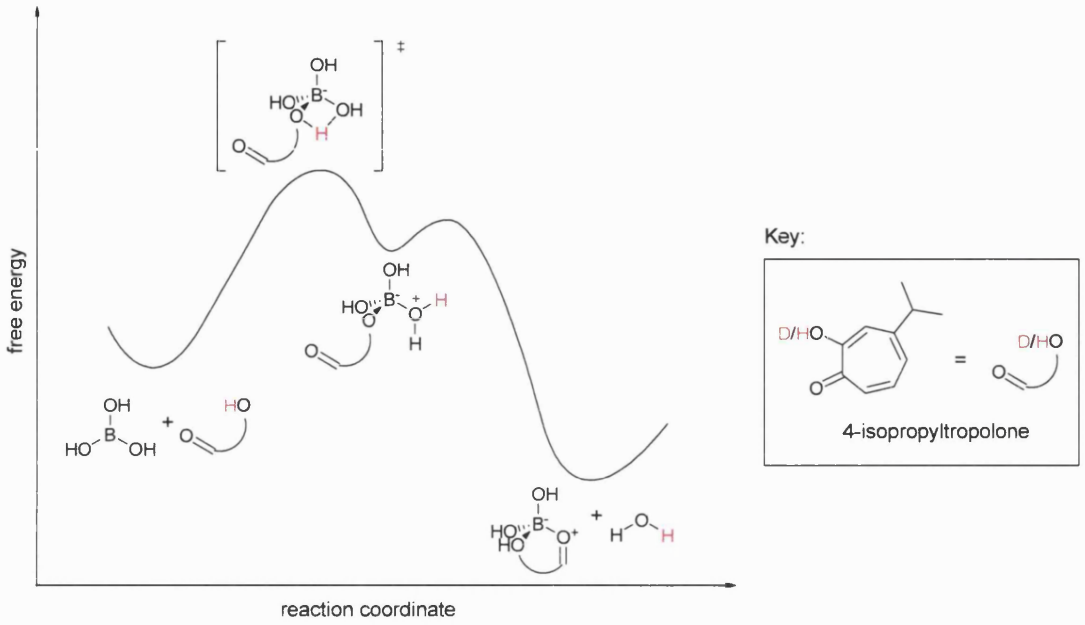

Scheme 14. *Reaction pathway for the complexation of boric acid with 4-isopropyltropolone, based on Funahashi and Ishihara's proposal.[89] This pathway is derived from the results of the deuterium isotope effects as well as the effects of conducting the reaction in non-aqueous solvents and represents the most plausible reaction pathway. In the first step the hydroxyl group of the entering ligand binds to boric acid inducing a change in geometry and forming a tetrahedral intermediate. The hydroxyl proton of the ligand may interact with a hydroxyl group on boron via hydrogen bonding in the transition state to generate the second intermediate with a coordinated water molecule attached. The second step, intramolecular ring closure with dissociation of water, proceeds rapidly.[89] For clarity the hydrogen/deuterium atom under consideration is highlighted in red.*

Computational Analysis

To further the mechanistic understanding, computational studies have been conducted by Bock and co-workers, who analysed a range of possible transition states in the formation of the B-O bond. In these studies the reaction was studied on the basis that a molecule of water was eliminated in each step, trigonal geometry was therefore restored to boron in each step. The binding of methanol,[79] 1,2-ethanediol[80] and D-glucose[81] at boron were examined. Where the reactions were simulated *in vacuo* or in acetonitrile the activation barriers were significant. On the other hand if water, ammonia or NaOH were used in the capacity of weak Lewis bases the activation barriers were substantially lowered, catalysing the reaction.

The studies ascertained that the initial dehydration step provided the greatest activation barrier, with the proton transfer aspect of the dehydration process being a dominant feature in the transition state.

In vacuo or acetonitrile boron acids reacted *via* strained four-membered transition states, with high activation barriers. In the presence of water, ammonia or NaOH, however, the most stable transition states developed were comprised of six-membered rings, this was achieved by directly utilising a solvent molecule. If water is considered, incorporating an oxygen and a hydrogen atom into the ring, one of boron's hydroxyl oxygen atoms accepts a proton shuttled from a solvent water, whilst water in turn accepts a proton shuttled from one of the ligand oxygens.

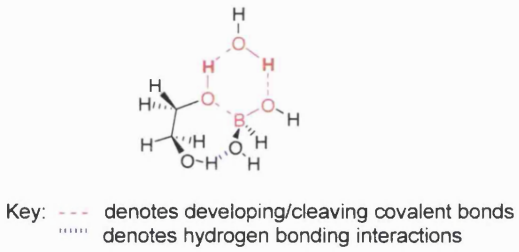

Scheme 15. *Bock's computational simulation of the lowest energy transition state for 1,2-ethanediol complexing to dihydroxy borane in the presence of water.*[81] *In water, ammonia and NaOH the most stable transition states developed were comprised of six-membered rings. This was achieved by directly utilising a solvent molecule, allowing a proton to be shuttled via the solvent molecule. Within the cyclic six-membered transition state a tetrahedral geometry was developed at boron, which was required for the transition state to occur with favourable geometry. In the computational system, the rate of proton transfer dramatically increased with the increasing Lewis basicity of the solvent molecules. Also of note is the stabilising hydrogen bond between the lower ligand oxygen and the lower boron hydroxyl depicted in the scheme.*

For the transition state to occur with favourable geometry within the cyclic six-membered transition state a tetrahedral geometry was developed at boron, an O-B-O angle of 107.3° being reported in the presence of water. Whilst the intermediate is tetrahedral, water is eliminated in this step and the system reverts to trigonal geometry with the formation of a covalent bond between the diol oxygen and boron.

In the computational system, the rate of proton transfer dramatically increased with the increasing Lewis basicity of the solvent molecules. Also of note is a secondary interaction, a stabilising hydrogen bond between the ligand oxygen and the boron hydroxyl that are not actively participating in the bond developing/cleaving aspect of the reaction.

Therefore, whilst the detailed mechanism by which trigonal boron acid – ligand complexation proceeds has not been fully elucidated, there is general agreement in the literature on a number of salient points.

The reaction proceeds in two distinct steps. The first is bimolecular and is rate-limiting. Nucleophilic attack of a ligand oxygen on the electron deficient trigonal boron forms a complex with tetrahedral geometry.[90] Within this complex a covalent boron-oxygen bond will form, but for this step to proceed a labile proton must be present on the incoming ligand to allow proton transfer to occur.[87] This proton transfer is kinetically significant, occurring either directly or through a solvent chain. The second step is a unimolecular elimination. It is initiated by intramolecular nucleophilic attack at boron by the untethered ligand oxygen. This step closes the ring to form the cyclic diester and eliminate water.

Reactions with Tetrahedral Borates

Unfortunately the evaluation of rate constants for the substitution reactions of tetrahedral borates with acidic ligands is complicated by reaction pathways which are kinetically indistinguishable due to proton ambiguity. There is therefore a comparative paucity of data for complexation with the tetrahedral boronate anions when compared to their neutral trigonal equivalents. As the rates of complexation for tetrahedral borates are much higher than the rates of complexation for trigonal boron acids the only ligands for which the kinetics of tetrahedral borate complexation have been studied are diols (ligands whose protons are not considered acidic in this context), preventing generic trends from being established.

In an effort to circumvent this problem it is possible to consider studies which have been conducted into the binding of boric acid with bidentate ligands in a 1:2 complex.[88,91] By considering the change from a 1:1 (ligand/boric acid) tetrahedral borate complex to a 2:1 (ligand/boric acid) tetrahedral borate complex the effect of pH on complexation can been studied with no structural change at boron occurring when the pH matches the pK_a.

Where chromotropic acid was studied an increase in acidity of the solution resulted in an increase in the forward and reverse rate constants.[88] Both the forward and reverse reaction rates of reaction were found to be first order with respect to the hydrogen ion

concentration. Given the first order dependence on hydrogen ion concentration Yoshimura and co-workers postulated a plausible reaction mechanism for the 1:2 complex formation of boric acid and chromotropic acid, Scheme 16.

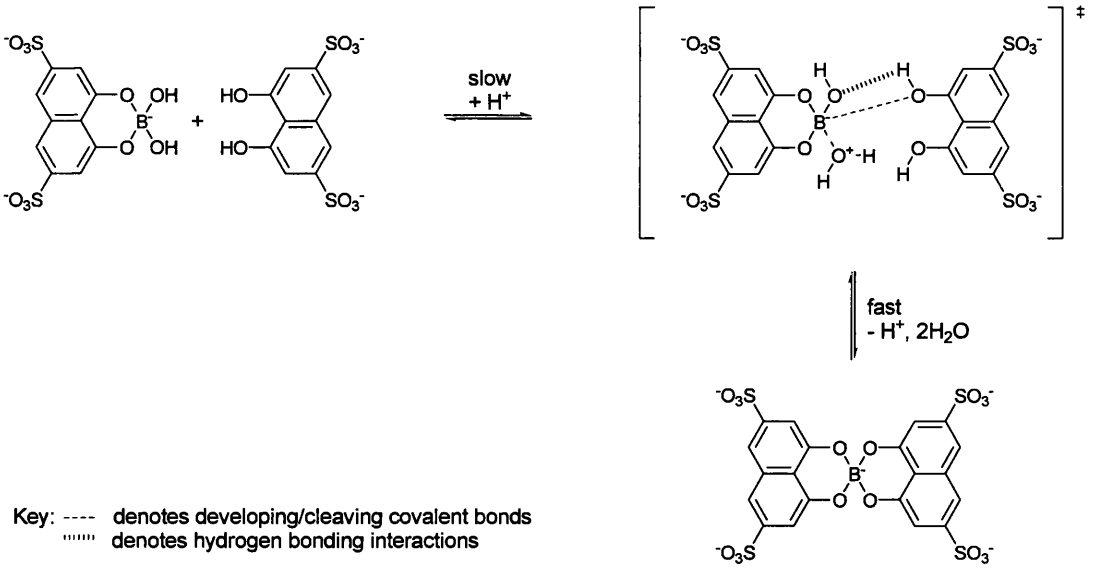

Scheme 16. *As the reaction kinetics of tetrahedral borates with most ligands cannot be followed due to the problems associated with kinetically indistinguishable pathways and proton ambiguity, studies have examined the binding of boric acid with bidentate ligands in a 1:2 complex. By considering the change from a 1:1 to a 1:2 complex a tetrahedral structure is enforced at boron. This allows parallels to be made with the complexation of other tetrahedral boronate anions. Yoshimura's proposed transition state is depicted here, illustrating the complexation of boric acid with chromotropic acid.*[88]

Yoshimura's proposed transition state was almost analogous to the one proposed by Pizer for trigonal boron species (page 25) but in the first step the solution protonates a leaving hydroxyl on boron. As the S_N2 reaction proceeds a covalent B-O bond begins to develop, forming a pentavalent boron complex in the transition state. This complex could be stabilised by the formation of a ligand – hydroxyl hydrogen bond (it would also be quite plausible for a proton transfer mechanism to occur *via* a solvent chain with concurrent hydrogen bonding stabilisation, in the manner detailed by Bock). Water would then be eliminated to restore tetrahedral geometry. Nucleophilic attack at boron from the untethered ligand oxygen would re-establish a pentavalent complex, before elimination of water closed the ring and completed the reaction.

Pentavalent Coordination at Boron

A number of transition states with pentavalent coordination at boron have been reported.[92] For example the reaction of the [BH_3-CO] complex with NMe_3[93,94] or the hydrolysis of BH_4^-.[95,96] In two instances the hypervalent boron compounds have been

found to be stable enough to synthesise and isolate,[97] with Yamashita *et al.* having recently reported the first single-crystal x-ray structure of a pentavalent boron compound, unequivocally confirming the existence of these hypervalent boron species.[98]

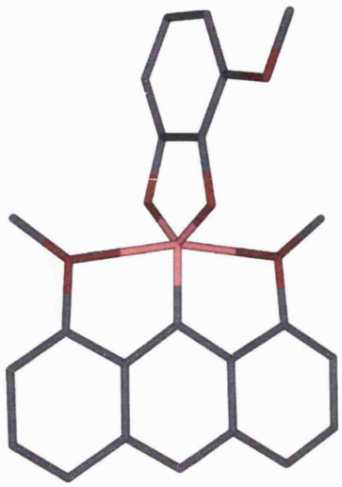

Figure 11. *A transition state with pentavalent coordination at boron would be required for the complexation of a ligand with a tetrahedral boronate anion. Yamashita et al. have recently reported the first single-crystal x-ray structure of a pentavalent boron compound, unequivocally confirming the existence of these hypervalent boron species.[98] Atoms marked in red represent oxygen, pink boron and grey carbon. For clarity hydrogen atoms are not displayed.*

Complex Formation and B-O Bond Length Dependence

Whilst unknowns still remain, Pizer has developed a plausible explanation for the observed increase in rate with tetrahedral borates over trigonal boron acids.[69] In tetrahedral borates the hydroxyls on boron are likely to be considerably more basic than their trigonal boron acid counterparts. For a good match between trigonal and tetrahedral species it is worthwhile considering the structures of $B(OH)_3$ and $B(OH)_4^-$. Between $B(OH)_3$ and $B(OH)_4^-$ there is a substantial difference in the boron-oxygen bond length, with respective values of 1.37 Å and 1.48 Å being reported.[75,99]

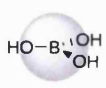

B-O bond length = 1.37 Å

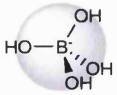

B-O bond length = 1.48 Å

Figure 12. *Rehybridisation of boron from sp^2 to sp^3 is coupled with an increase in the B-O bond length of ~ 0.1 Å. It is postulated that the increased basicity that would accompany such a change would favourably promote the proton transfer process leading to the observed rises in stability and rate constants.*

By augmenting the length and therefore decreasing the strength of the boron-oxygen bond, the hydroxyl on boron becomes more basic, becoming a better proton acceptor and thus facilitating the forward proton transfer mechanism, a mechanism with significant influence on the rates of reaction. Whilst this hypothesis has not been experimentally confirmed or disproved it does provide a reasonable explanation for the induced step change in reactivity observed when boron acids undergo a change in geometry from sp^2 to sp^3 hybridisation.

B-O Bond Length and Acidification

In reviewing the above systems for this thesis, it was postulated that the contraction of the O-B-O bond angle on saccharide binding could induce a change in the B-O bond length. It is quite plausible that if a change in the B-O bond length were to occur on binding this may lead to a change in the observed acidity of the system, see Section 1.3.2 (page18).

It would be expected that as the O-B-O bond angle contracted the B-O bond length would increase so as to minimise the effects of any interactions between the two converging hydroxyl groups. An increase in the B-O bond length would, however, induce an increase in the observed basicity of the system; the weaker B-O bond increasing the basicity of the oxygen atom, raising the pK_a.

This notwithstanding, an examination of the single-crystal x-ray structures of the dimeric phenylboronic acid (see Scheme 8, page 18)[71] and phenylboronic acid – fructose complex (Figure 7, page 20)[76] reveals that there is no change in B-O bond length. In the case of the dimeric phenylboronic acid the O-B-O bond angle is ~ 116.3°, this diminishes to ~ 113.5° in the phenylboronic acid – fructose complex, however, for both compounds the average of the B-O bond lengths reported is the same within experimental error, 1.371 Å. Therefore where trigonal to tetrahedral interconversion is absent, the B-O bond length is not observed to change on complexation for these two reported structures. This allows us to eliminate a change in the B-O bond length as a likely cause of the change in acidity at boron on boronic acid – ligand complexation.

1.3.4 Binding Constants and the Influence of Lewis Bases

The final point to be considered in boronic acid – saccharide binding is the predisposition of boronic acids to interact with different kinds of diols. The stability constants (*K*) between various polyols and boronic acids were first quantified by Lorand and Edwards and it is the case that the trends established now appear inherent in all monoboronic acids.[54]

It is well known that boronic acids readily form five-membered rings with vicinal *cis*-diols in basic aqueous media. It is also the case that six-membered rings can be formed with trans-1,3-diol groups, although the stability of these cyclic diesters is somewhat lower than their five-membered counterparts.[70,100-103]

Table 1. The binding constants calculated by Lorand and Edwards for phenylboronic acid in water at 25 °C.[54] The four monosaccharides most routinely used in the evaluation of sensors for saccharides are highlighted in red.

polyol	K / mol^{-1}
1,3-propanediol	0.88
ethylene glycol	2.80
propylene glycol	3.80
3-methoxy-1,2-propanediol	8.50
D-glucose	110
D-mannose	170
D-galactose	280
pentaerythritol	650
mannitol	2 300
D-fructose	4 400
catechol	18 000

These trends have been heavily utilised in the design of new sensors and it has been found that the apparent values determined for monoboronic acid sensors concur with the trends of the equilibrium constants reported in Table 1. Apparent values depend heavily on the environments in which the sensors have been studied and are influenced by factors such as: pH, buffer, solvent composition, the concentration of the reactants and the presence of any Lewis basic components.

In response to the growing demand for an accurate interpretation of the complex multi-component equilibria involved in these systems, an extensive investigation was conducted using the potentiometric titration technique.[62] The refined values for the acidity and binding constants displayed a good match with previously published data. Nevertheless, it became clear from the results that the thermodynamic cycle in Scheme 7 (page 17) is somewhat of a simplification. Stable complexes were found to form readily between boronic acids and Lewis bases. This represents a significant finding in sensor design as Lewis bases such as the conjugate bases of phosphate, citrate and imidazole are commonly used to buffer the pH of solutions during the spectrophotometric evaluation of sensors, adding a new degree of sophistication to the understanding of the species present in solution.

It was shown that in buffered solutions binary (boronate - Lewis base) complexes as well as ternary (boronate - Lewis base - saccharide) complexes will be formed. Under acidic conditions these ternary complexes are significant and under certain stoichiometric conditions can become the dominant components in solution.

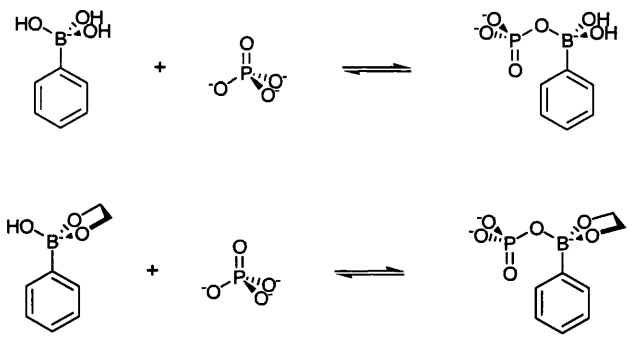

Scheme 17. *In addition to the pair-wise interaction of boronic acids with polyhydroxyl species discussed, boronic acids also form stable complexes with buffer conjugate bases. These complexes can be formed between both the free boronate anion and Lewis bases as well as between saccharide boronate complexes and Lewis bases. Not recognised until 2004, these species persist into acidic solution and under certain stoichiometric conditions can become the dominant component in the solution. The two modes of interaction between the phenylboronate anion and phosphate are illustrated here.*

When conducting fluorescence experiments in solutions buffered with a Lewis basic component there is therefore a "medium dependence" related to the formation of Lewis base adducts.[104] These complexes reduce the free boronate and boronic acid concentrations, diminishing the observed stability constants (K_{obs}).

From an experimental perspective this characteristic means that strongly Lewis basic components should be avoided by researchers in the future study of boronic acid appended systems. With care buffers can be chosen so as not to overwhelm the system being investigated. For example, phosphate buffer (pH 7.5) was found not to make a significant contribution to the observed fluorescence intensity or alter significantly the binding constants of the excited state complex under investigation.

Therefore, so long as one is aware of the conditions observed stability constants (K_{obs}) have been determined under and the effect that is induced by Lewis basic components in solution, these spectrophotometrically determined constants do provide an accessible, useful and valid measure in the development of boronic acid based sensory systems.

1.4 Boronic Acids in the Design of Fluorescent Sensors for Saccharides

1.4.1 The Application of Fluorescence in Sensing

The use of light to transfer information on events occurring between molecules is particularly advantageous; it provides researchers with a natural interface between events occurring at the molecular level and the macroscopic one. As optical signals convey information through space, fluorescent sensors can be absorbed into dynamic systems such as living tissue and relay information remotely. Sub-millisecond response times are typical, allowing information to be communicated in real-time and, if targeted correctly, fluorophores can be located with sub-nanometre accuracy, in effect permitting real-space monitoring.[105] Fluorescence also demonstrates an exceptionally high sensitivity of detection; under controlled conditions modern instrumentation has allowed analysts to detect responses from single fluorescent molecules[106-108] and in the case of fluorescent sensors, from single guest molecules.[109]

As fluorescent sensors are capable of reporting on a wealth of physical information at low concentrations (micromolar concentrations are typical), they can operate with the minimum of disturbance to the system being investigated. From an analytical perspective these characteristics are attractive and commercially the parsimonious quantities of compound required can be used to offset synthetic costs.

Fluorescent sensors can be found in many recent analytical advances, such as the continuous monitoring systems developed by immobilising fluorescent sensors onto fibre optic sensing arrays,[110] or the live imaging of analytes within cells through confocal microscopy.[111] Commercial examples of the use of fluorescent sensors include clinical tools such as the blood gas analyzers that are now commonplace within hospital high-dependency wards and ambulances allowing point-of-care diagnostic monitoring,[112-115] or the glucose responsive contact lenses currently being pioneered by the Lakowicz research group.[116] These examples highlight the robust and versatile nature of fluorescent sensors, which in turn permit rapid and accurate analyte diagnosis by portable devices.

The use of boronic acids in the development of fluorescent sensors for saccharides is a comparatively young area of research. The first publication on the subject was made by Czarnik in 1992.[117] D-Glucose selectivity was achieved two years later in 1994 by James[118] within Shinkai's industrious research group, who followed this up with enantioselective saccharide recognition a year later.[119] In the intervening decade the field has blossomed, hundreds of publications on boronic acid - saccharide recognition now embellish the scientific press, with the three articles above having been cited in more than three hundred and eighty separate publications.**

Across the diverse range of boronic acid based fluorescent sensors developed, two distinct design principles predominate in the scientific literature: internal charge transfer (ICT) and photoinduced electron transfer (PET). In both cases successful signalling of the binding event arises from alternative low energy pathways being discretely offered to either the bound or unbound sensors, these processes affecting defined spectral changes in the emission band.

1.4.2 Photoexcitation and Subsequent Relaxation

Electronic excitation of a fluorophore in its singlet ground state (S_0), by an incident photon of sufficient energy, promotes one of the fluorophore's electrons into a level of higher energy. The excited energy level initially populated will be a singlet state (such as S_1, S_2 or higher), where excitation into a vibrational level within the singlet state is commonplace.[120]

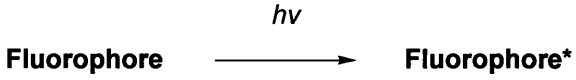

For most molecules in solution the subsequent relaxation of the molecule's energy will be rapid. Vibrational energy is swiftly lost through collisional deactivation with solvent molecules and irrespective of the singlet state initially populated, the majority of compounds will follow Kasha's rule;[121] internal conversion rapidly reducing the energy of the molecule non-radiatively until it reaches the lowest excited state available to it,

** Source: *ISI Web of Knowledge*, February 2005

the first singlet excited state (S_1). From this S_1 state (external factors permitting) fluorophores will often dissipate their remaining energy as light. The emission of a photon from this locally excited (LE) state will result in an emission wavelength corresponding to the difference in energy between the initial and final electronic and vibrational energy levels occupied.

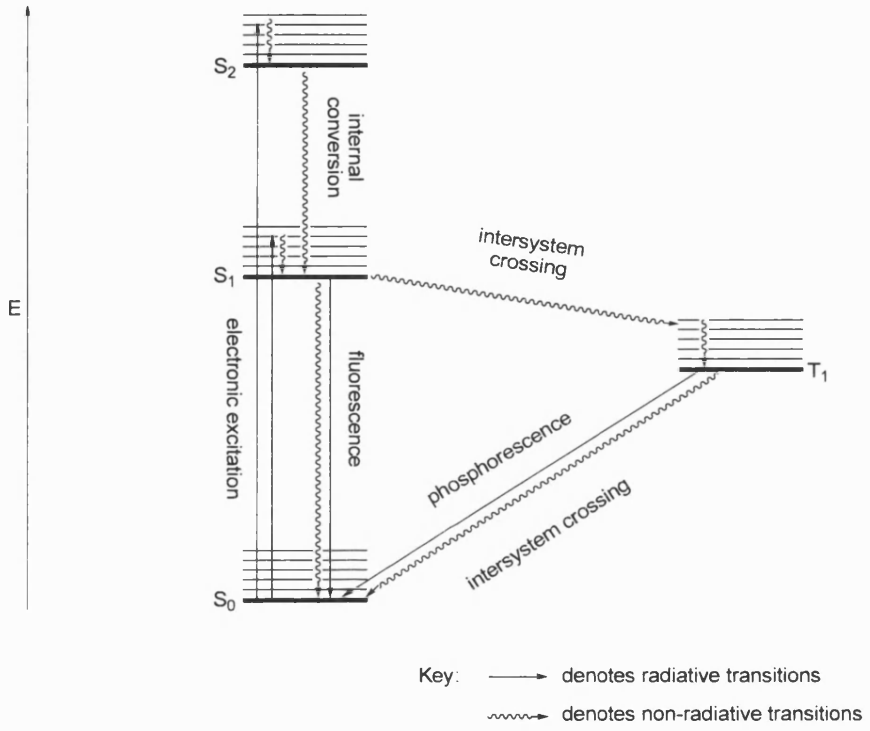

Scheme 18. *A Jabłoński diagram typical of a fluorophore in a LE state with a single emission band. Possible intersystem crossing leading to phosphorescence from the first triplet state (T_1) is illustrated for completeness.*

In considering sensor design the time dependency of these processes is not insignificant. Typical fluorescence excited state life times are of the order of 10 ns (1×10^{-8} s).[120] The absorption of light is rapid, electronic excitation occurring in around 10^{-15} s, subsequent internal conversion to the S_1 state is also rapid, occurring in around 10^{-12} s.[120] It is the lifetime of the S_1 state that is comparatively long, accounting for the ~ 10 ns excited state lifetimes and it is therefore here that many of the processes responsible for molecular signalling begin.

1.4.3 Excited State Internal Charge Transfer (ICT)

Solvent Relaxation

The characteristic Stoke's shift, or tendency of fluorophores to emit light at a longer wavelength than that absorbed, is readily understood by considering the loss of energy due to the internal relaxation processes such as those described in the Jabłoński diagram above, Scheme 18. Not only do the surrounding solvent molecules provide a convenient interface through which to dissipate a fluorophore's excess energy to the bulk system but they can also play a key role in lowering the energy of the S_1 state itself.

If a fluorophore with a dipole moment in the ground state is promoted to an electronically excited state, it is generally the case that the strength of the electronic dipole moment will grow.[120] In solutions where polar solvent molecules are free to re-orientate themselves and maximise favourable dipole-dipole interactions, the energy of the excited state can be lowered. For solvents at room temperature solvent relaxation typically occurs in 10^{-11} s.[120] This is too long a time for solvent relaxation to influence the energetics of electronic excitation and the corresponding absorption spectra. Nevertheless, solvent relaxation occurs well within the lifetime of the S_1 state. In instances where this relaxation mechanism is feasible, the energy of the S_1 excited state will be lowered and the energy of the S_0 ground state will be raised, as illustrated in Scheme 19. The net effect of this process is therefore to red shift the emission band of the fluorophore.

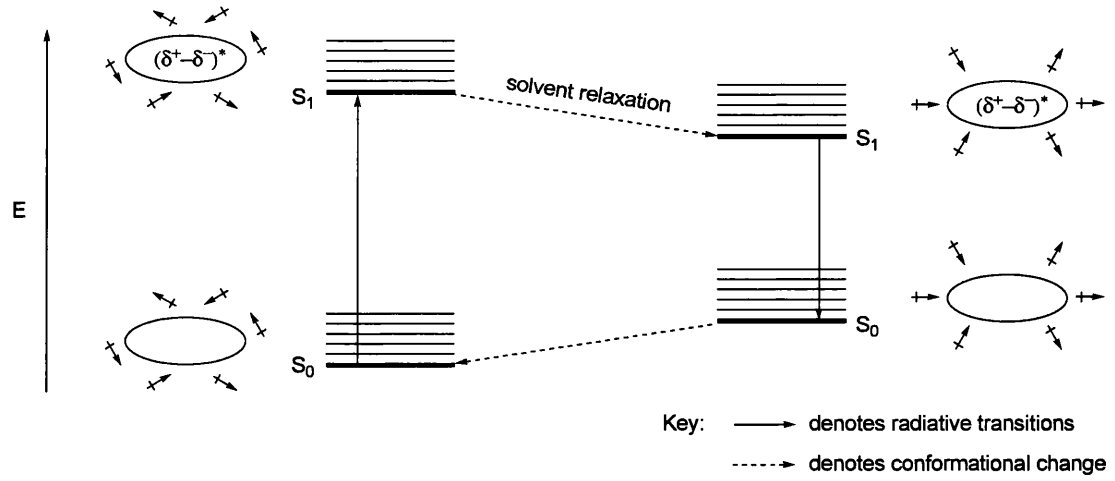

Scheme 19. *The reorganisation of polar solvent molecules around the enlarged dipole a fluorophore in its LE state permits dipole-dipole interactions to lower the energy of the S_1 state, raising that of the S_0 ground state. The stabilising solvent relaxation illustrated will red-shift the single emission band of the LE fluorophore.*

Dual Fluorescence

In many respects the stabilisation ICT imparts can be considered as an extension of the solvent relaxation mechanism. In systems where heteroatoms or strongly inductive functional groups are in contact, an imbalance in the electron density can be induced across the excited state of the molecule. This reversible charge separation creates an enlarged dipole moment, enhancing the favourable dipole-dipole interaction of the fluorophore with the surrounding solvent shell. This environmentally dependent stabilisation of the S_1 state is a process which can lead to dramatic changes in the wavelength of the emission band and as such has found great application in the field of sensing.

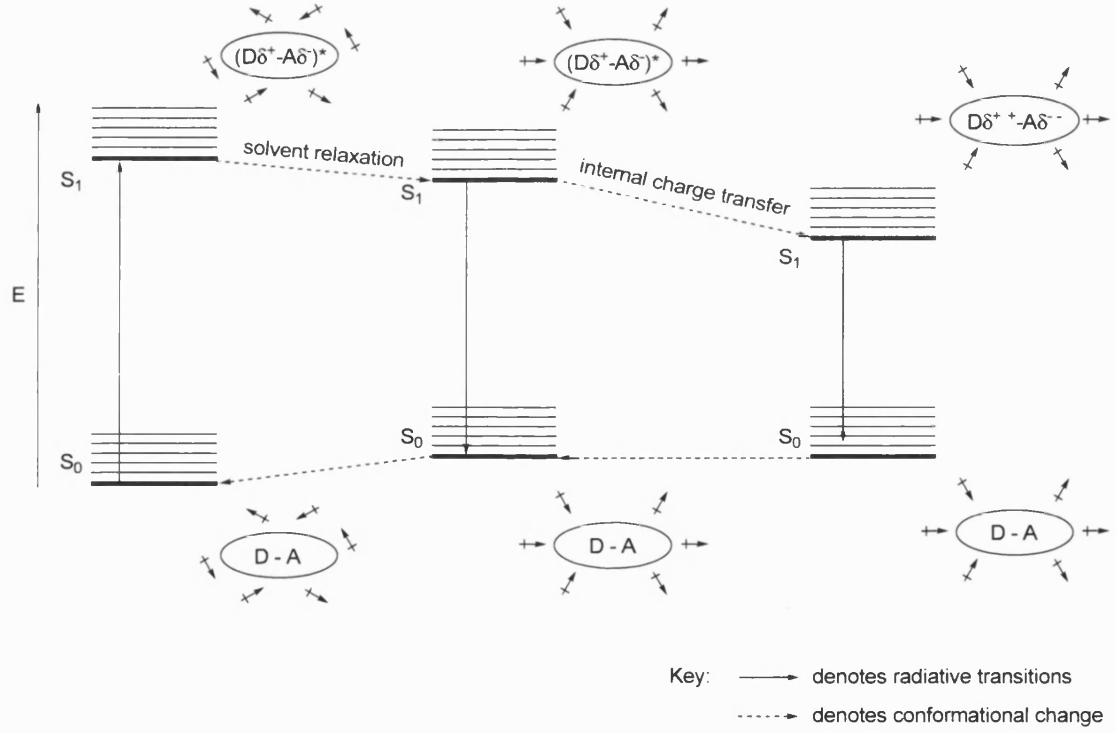

Scheme 20. *The dual emission band of an ICT fluorophore is illustrated. Whilst emission from the LE state may be modestly red shifted, the ICT will affect a dramatic shift in wavelength, environmental conditions allowing. D-A denotes a molecule containing electron donor and electron acceptor moieties.*

One of the best examples of an ICT system remains the first compound to be clearly identified as altering its fluorescence properties through ICT, *p*-(*N*,*N*-dimethylamino)-benzonitrile **32**.[122] In non-polar solvents the benzonitrile **32** was observed to display a "normal" fluorescence response, i.e. that characteristic of a benzene derivative in its LE state. In polar solvents, a second emission band of longer wavelength emerged. The

relative intensity of the long-wavelength ICT band was seen to grow with decreasing intensity of the short-wavelength LE band as a function of the increasing polarity of the medium; the dual fluorescence being strongly dependent on solvent polarity and temperature.[123]

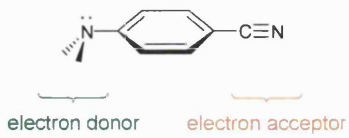

32

The structure of the benzonitrile **32** is quite typical of ICT systems which are now described in terms of incorporating an electron "donor" group and an electron "acceptor" group in close proximity or linked through a conjugated π-system.[124]

Excited State Twisted Internal Charge Transfer (TICT)

Benzonitrile **32** provides a particularly useful example as it illustrates a further process which can occur in ICT systems. Lippert *et al.* determined the value of the dipole moment in the excited ICT state of benzonitrile **32**.[123] In keeping with the discussion above, it was found to be significantly larger than that for the LE state, this finding initially led researchers to believe that the ICT state must resemble a structure approaching the highly dipolar quinoid structure, Scheme 21 (**B**).[125]

Scheme 21. *(**A**) Expected ground state structure of benzonitrile **32**. (**B**) The highly dipolar quinoid structure initially expected for the excited ICT state of benzonitrile **32**.*

A reinvestigation of the anomalous properties of benzonitrile **32** by Grabowski and co-workers revealed that this was not sufficient to account for all the experimental data obtained. The properties of the structural derivatives of benzonitrile **32** with methyl ring substituents *meta*- and *ortho*- to the amine group were examined, compounds **33** and **34** respectively.[126,127] It was found that in the same solvent system, compounds **33** and **34** behaved very differently. The *meta*-derivative **33** displayed dual fluorescence with a

dominant band from the LE state, whilst the *ortho*-derivative **34** displayed fluorescence almost exclusively from the ICT state.

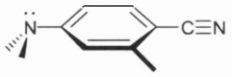

33

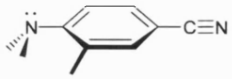

34

This finding was tentatively attributed to a steric effect, with the LE state being assigned to a coplanar (quinoid-like) structure and the ICT state being assigned to a structure in which the dimethylamino group was perpendicular to the benzene ring. In such a conformation the orbitals of the amino lone pair and the delocalised π-system of the benzene ring will be orthogonally aligned and no overlap will occur between them. The system can therefore be considered orbitally decoupled and while this situation holds a full electron transfer can occur.

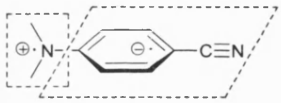

Figure 13. *The dimethylamino group is highly twisted in the CT excited state conformation, possibly perpendicular to the aromatic ring.[125] This concept is illustrated here with the radical ions of compound* ***32*** *in the TICT excited state mutually orthogonally aligned and linked by a single bond.*

This phenomenon was found to occur in a number of analogous species, the twisted conformation generally representing the most favourable species. This explanation held for over a decade and as such led to the name of excited state twisted internal charge transfer (TICT).[128] In the early 1970s new experimental evidence revealed that the TICT model failed to provide a consistent interpretation for empirical data in certain cases, nevertheless the concept of a twisted state still provides a valuable model. For a discussion on the range of hypotheses subsequently postulated regarding the structure of the ICT state and the mechanism and time scale of its formation (the exact mechanistic details still remain a point of contention after thirty years focused research) the interested reader is directed to the extensive review recently published by Grabowski, Rotkiewicz and Rettig.[125]

Structure of Fluorescent ICT Sensors

In the case of boronic acid appended fluorescent ICT sensors the design must consist of a receptor and a fluorophore. Crucially they must be integrated such that there is significant overlap between the two fragments, as illustrated in Figure 14.

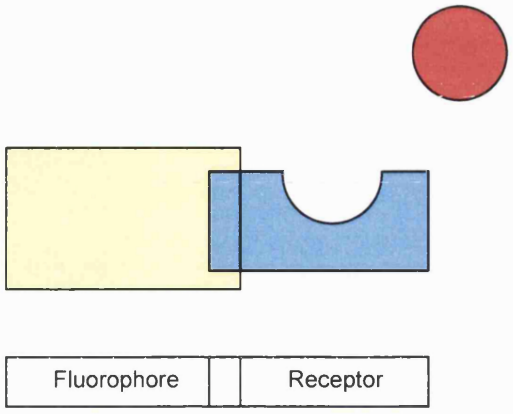

Figure 14. *Schematic representation of the overlapped Fluorophore-Receptor design assembly for fluorescent internal charge transfer (ICT) sensory systems.*

This design generally permits guest molecules to influence the electronic properties of donor or acceptor groups within ICT molecules, or otherwise invoke a conformational restraint in the rotation of key TICT bonds. Although changes in the emission intensity are often observed in parallel with changes in the emission wavelength, the principal designed mode of action for an ICT sensor is to signal substrate binding *via* a shift in the emission wavelength.

Early fluorescent sensors for saccharides

The first fluorescent sensor for saccharides was reported by Czarnik in 1992.[117] The sensor (**35**) was comprised of a boronic acid fragment directly attached to anthracene. On addition of saccharide it was noted that the intensity of the fluorescence emission for the 2-anthrylboronic acid **35** was reduced by ~ 30%. This change in fluorescence emission intensity is ascribed to the change in electronics that accompanies rehybridisation at boron. For boronic acid **35** (below its pK_a) the neutral sp^2 hybridised boronic acid displayed a strong fluorescence emission, (above its pK_a) the anionic sp^3 boronate displayed a reduction in the intensity of fluorescence emission.

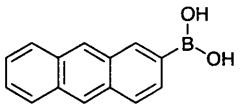

35

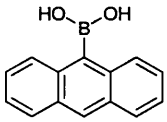

36

Figure 15. *The first fluorescent sensor for saccharides: 2-anthrylboronic acid **35**, as well as its isomer 9-anthrylboronic acid **36**. Recognition of saccharides was mediated by an apparent decrease in fluorescence intensity, due to the formation of the boronate anion.*

As discussed in Section 1.3.2 (page 18) the formation of a boronic acid – saccharide complex acidifies the boron atom, making the resultant boronic ester more acidic than the initial uncomplexed boronic acid. In this instance a pK_a of 8.8 was reported for the neutral 2-anthrylboronic acid and a pK_a' of 5.9 was reported for the 2-anthrylboronic acid complex formed in saturated fructose solution. Exploiting this phenomenon the system was buffered to a pH of 7.4, a value between the corresponding pK_a and pK_a' values reported. With this constraint in place, a high fluorescence emission intensity was observed from the uncomplexed boronic acid (pH < pK_a). However, under these buffered conditions, addition of a saccharide to the solution formed the boronic ester, lowering the acidity of the boronic species below the pH of the solution (pK_a' < pH). As a direct result the boronate anion was generated inducing the decrease in fluorescence observed on addition of saccharide.

The corresponding isomer 9-anthrylboronic **36**, was also examined but displayed smaller changes in fluorescence emission, a feature attributed to the unfavourable *peri*-interactions that would be expected at the 9-position.[129] The observed stability constant (K_{obs}) for boronic acid **35** was 270 M^{-1} with D-fructose in 1:99 (v/v) DMSO/water at pH 7.4 (phosphate buffer).[††]

[††]In instances where the stability constants documented in the source publications are dependent on the spectroscopic properties of the evaluated species in solution they are presented here as observed stability constants (K_{obs}) to denote apparent values. Where the stability of the complexes formed was reported in the form of dissociation constants or logarithmically, the values have been converted to (observed) stability constants (K or K_{obs}) within this thesis to provide consistent and comparable results.[130] To avoid the introduction of mathematical errors through rounding, the values are reported to two significant figures (where appropriate) to match the general level of accuracy found for these values within the scientific literature.

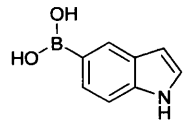

37

The research group of Aoyama investigated the fluorescence properties of 5-indolylboronic acid **37** with mono-, di- and higher saccharides.[131] It was found that the stability constants of the monosaccharides mirrored the qualitative trend established by Lorand and Edwards for phenylboronic acid.[54] When disaccharides were introduced however, a great deal of further information was gleaned, the longer chained saccharides being comparatively more stable when bound to 5-indolylboronic acid **37** than to phenylboronic acid **15**.

It was postulated that the increased stabilisation imparted to complexes with the longer chained saccharides could be derived from secondary effects such as advantageous hydrophobic interactions with the extended aromatic π-system or from CH-π interactions.

In keeping with the documented results for other arylboronic acids[100,102,103] it was observed that the reducing sugars examined had far higher observed stability constants (K_{obs}) than the non-reducing sugars examined (devoid of a hydroxyl group on the anomeric carbon). The non-reducing sugars displayed observed stability constants (K_{obs}) values with indole **37** which were either low or zero.

Further, more subtle trends were also documented. Between linkage isomers it was noticed that there was a selectivity for the 1,6 linked disaccharides over those that were 1,4 linked. More discrete still, was the selectivity between different anomers, a preference being observed for glucose appended disaccharides with an α configuration over those with a β configuration.

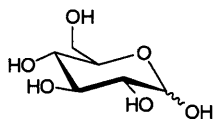

1 D-glucose

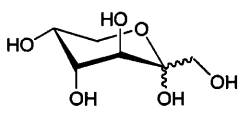

38 D-fructose

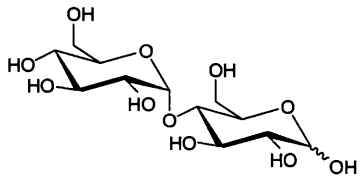

39 maltose
α-D-glucopyranosyl-(1→4)-D-glucose

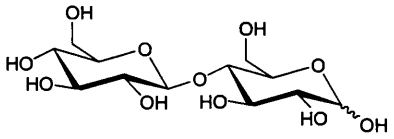

40 cellobiose
β-D-glucopyranosyl-(1→4)-D-glucose

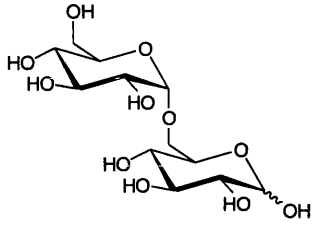

41 isomaltose
α-D-glucopyranosyl-(1→6)-D-glucose

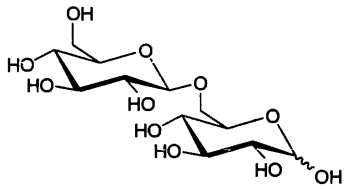

42 gentiobiose
β-D-glucopyranosyl-(1→6)-D-glucose

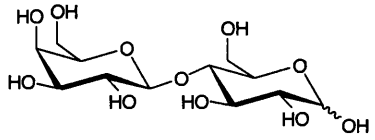

43 lactose
β-D-galactopyranosyl-(1→4)-D-glucose

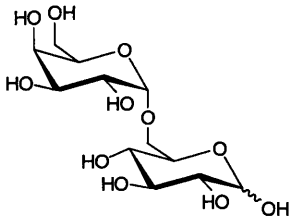

44 melibiose
α-D-galactopyranosyl-(1→6)-D-glucose

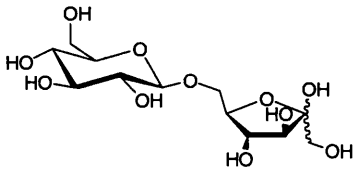

45 palatinose
β-D-galactopyranosyl-(1→6)-D-fructose

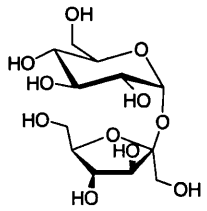

46 sucrose
β-D-fructofuranosyl-(2↔1)-α-D-glucopyranoside

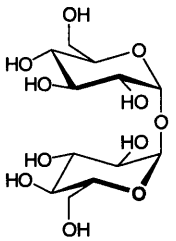

47 trehalose
α-D-glucopyranosyl-(1↔1)-α-D-glucopyranoside

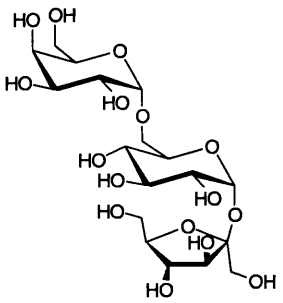

48 raffinose
α-D-galactopyranosyl-(1→6)-α-D-glucopyranosyl-
(1↔2)-β-D-fructofuranoside

The observed stability constants (K_{obs}) for indole **37** were 71 M^{-1} with D-glucose **1**, 6 300 M^{-1} with D-fructose **38**, 72 M^{-1} with maltose **39**, 30 M^{-1} with cellobiose **40**, 310 M^{-1} with isomaltose **41**, 250 M^{-1} with gentiobiose **42**, 90 M^{-1} with lactose **43**, 580 M^{-1} with melibiose **44**, 3 400 M^{-1} with palatinose **45**, ca. 0 M^{-1} with sucrose **46**, ca. 0 M^{-1} with trehalose **47**, 290 M^{-1} with maltotriose [α-D-glucopyranosyl-(1→4)-α-D-glucopyranosyl-(1→4)-D-glucose], 670 M^{-1} with maltotetrose [α-D-glucopyranosyl-(1→4)-α-D-glucopyranosyl-(1→4)-α-D-glucopyranosyl-(1→4)-D-glucose], 930 M^{-1} with maltopentose [α-D-glucopyranosyl-(1→4)-α-D-glucopyranosyl-(1→4)-α-D-glucopyranosyl-(1→4)-α-D-glucopyranosyl-(1→4)-D-glucose] and ca. 0 M^{-1} with raffinose **48** in water.

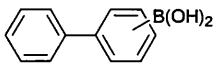

49: 2-$B(OH)_2$,
50: 3-$B(OH)_2$,
51: 4-$B(OH)_2$

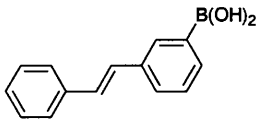

52

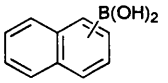

53: 1-$B(OH)_2$,
54: 2-$B(OH)_2$

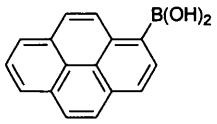

55

These systems were further investigated by Shinkai and co-workers who examined sensors **35**, and **49** - **55**. The compounds were evaluated against D-fructose and it was found that sensors **50** and **54** functioned particularly effectively. The sensors displayed strong fluorescence emission coupled with far greater fluorescence quenching on saccharide binding than previously observed (reductions in fluorescence emission of 70% and 82% were observed for sensors **50** and **54** respectively). Additionally a large induced change in the acidity of the boron species was observed on complex formation. These three characteristics made sensors **50** and **54** particularly good candidates for saccharide sensors. Indeed a strong fluorescence emission, large fluorescence response and large induced shift in the acidity of the boron species are now considered essential for the efficiency of many contemporary boronic acid appended fluorescent sensors.

Expanding on the work of Shinkai and co-workers,[132] DiCesare and Lakowicz examined a range of stilbene boronic acid derivatives to further understand the simple boronic acid – fluorophore systems discussed above.[133,134] It was initially believed that fluorescence quenching from the boronate anion, through PET caused the fluorescence response of sensors **35 - 55**. A more reasonable explanation was provided by examining the electronic properties of the boronic acid stilbene derivatives with electron withdrawing and electron donating groups introduced at the 4' position.

The interpretation of these results indicates that changes in electronic properties of the boron group, not PET, influence the spectral changes of the fluorophores, accordingly the systems are now generally discussed as ICT sensors and are treated as such within this thesis.[9]

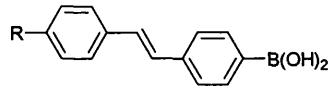

56: R = H,
57: R = OMe
58: R = $N(Me)_2$
59: R = CN

It was demonstrated that the neutral sp^2 hybridised boronic acid had acceptor group properties and the anionic sp^3 hybridised boronic acid could act as a donor group. In instances when the moiety at the 4' position and the hybridisation at boron conspired to produce a system with a donor and an acceptor linked through the conjugated stilbene scaffold, ICT was found to occur, lowering the energy of the excited state. This influence was elegantly exemplified by the examination of two diametrically opposed systems.

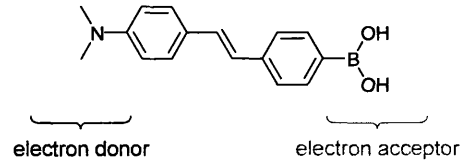

58

In the first case, 4'-(dimethylamino)stilbene-4-boronic acid **58**, the electron donating dimethylamino moiety is the donor group. When boron is sp^2 hybridised, and therefore

an acceptor, excited state ICT can occur between the amino donor and boron acceptor, red shifting the emission wavelength of the sp^2 species.

On rehybridisation of boron to sp^3 its acceptor properties are lost. This leads to a loss of the ICT effect in the excited state of the sp^3 species and shifts the emission wavelength of the fluorophore to higher energy. The inability of the sp^3 hybridised species to lower the energy of its excited state by a mechanism available to the sp^2 hybridised species causes a dramatic change in the properties of the emission band. On sp^2 to sp^3 interconversion a 45 nm blue shift is induced in the emission wavelength coupled with an increase in the emission intensity.

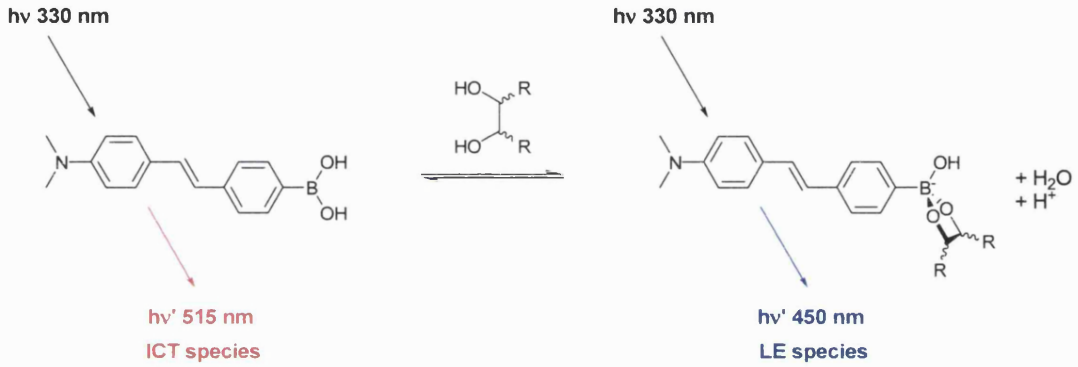

Scheme 22. *On addition of saccharide (or an increase in pH) the overall emission wavelength of sensor* ***58*** *blue shifts due to disruption of the ICT state. Colours are used to depict relative red and blue shifts in the emission wavelength rather than the actual colour of the emitted light.*

The fluorescent response to the loss of the electron withdrawing properties of boron on conversion from sp^2 to sp^3 hybridisation was verified by increasing the pH of a solution of sensor **58** (from 6.0 to 12.0) and by the addition of saccharide to a solution of sensor **58** buffered at pH 8.0 (pK_a' = 6.61, pH = 8.0, pK_a = 9.14), both titrations yielding the same results.

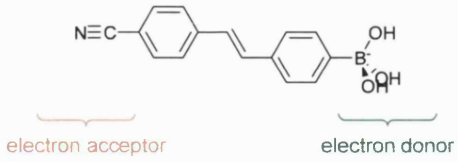

59

Conversely, in 4'-cyanostilbene-4-boronic acid **59**, the electron withdrawing cyano moiety is the acceptor group. When boron is sp^2 hybridised and therefore also an acceptor, no excited state ICT is feasible. On rehybridisation of boron to its sp^3 form, the boron becomes a donor group, allowing ICT to occur between the boron donor and cyano acceptor, red shifting the emission wavelength of the sp^3 species.

Reversing the roles of the donor and acceptor groups for the boronic acid and 4' moiety yielded values for the changes in emission wavelength and intensity for sensor **59** that were similar in magnitude to sensor **58** but occurred towards opposite ends of the electromagnetic spectrum. On sp^2 to sp^3 interconversion a 40 nm red shift was induced in the emission wavelength coupled with a decrease in the emission intensity.

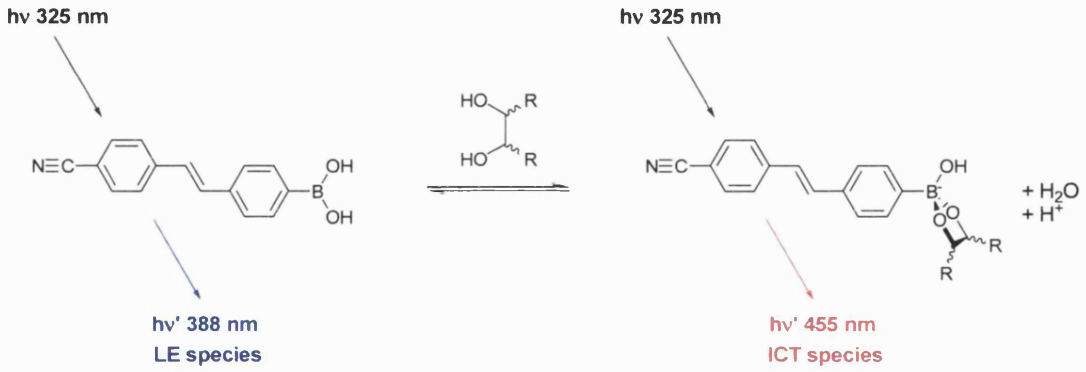

Scheme 23. *On addition of saccharide (or an increase in pH) the overall emission wavelength of sensor **59** blue shifts due to disruption of the ICT state. Colours are used to depict relative red and blue shifts in the emission wavelength rather than the actual colour of the emitted light.*

The fluorescence response to the revival of the electron donating properties of boron on conversion from sp^2 to sp^3 hybridisation was again verified by increasing the pH of a solution of sensor **59** (from 6.0 to 12.0) and by the addition of saccharide to a solution of sensor **59** buffered at pH 8.0 (pK_a' = 5.84, pH = 8.0, pK_a = 8.17), both titrations yielding the same results.

The observed stability constants (K_{obs}) for sensor **56** were 290 M^{-1} with D-fructose and 91 M^{-1} with D-glucose, for sensor **57** they were 1 000 M^{-1} with D-fructose and 23 M^{-1} with D-glucose, for sensor **58** they were 400 M^{-1} with D-fructose and 10 M^{-1} with D-glucose and for sensor **59** they were 1 500 M^{-1} with D-fructose and 55 M^{-1} with D-glucose in 2:1 (v/v) methanol/water at pH 8.0 (phosphate buffer).[133,134]

Fluorescent Internal Charge Transfer (ICT) Sensors Incorporating the *ortho*-(Aminomethyl)phenylboronic Acid Fragment

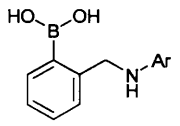

Figure 16. *o-(Aminomethyl)phenylboronic acid derivatives.*

The sensors developed within this thesis are all fluorescent PET sensors incorporating *N*-methyl-o-(aminomethyl)phenylboronic acid fragments. Given the importance of this receptor unit it seems pertinent to extend the examination of ICT sensors to include those with *o*-(aminomethyl)phenylboronic acid receptors directly coupled to fluorophores.

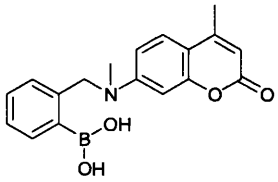

60

The first concerted effort to couple donor and acceptor fragments to produce an ICT sensor for saccharides was by Sandanayake, sensor **60**.[135] In this case coumarin was used as the fluorophore, which led to the red shifting of the emission wavelength and a decrease in the emission intensity on saccharide binding. Unfortunately these changes were rather modest with an observed stability constant (K_{obs}) of 27 M^{-1} for D-fructose in 1:1 (v/v) methanol/water.

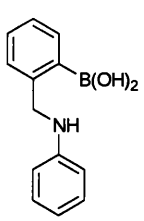

61

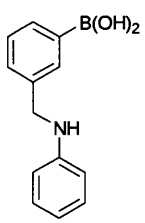

62

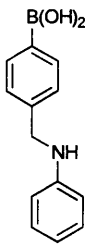

63

Bosch *et al.* prepared the aniline based sensors **61** - **63**.[136,137] On saccharide binding the emission wavelength of sensor **61** was significantly altered. In an aqueous solution buffered at pH = 8.21 the emission maxima of sensor **61** was blue shifted by 42 nm on addition of D-fructose. This observed dual fluorescence was ascribed to TICT in the case of neutral boronic acid **61** and LE states in the case of anionic boronate **61**.

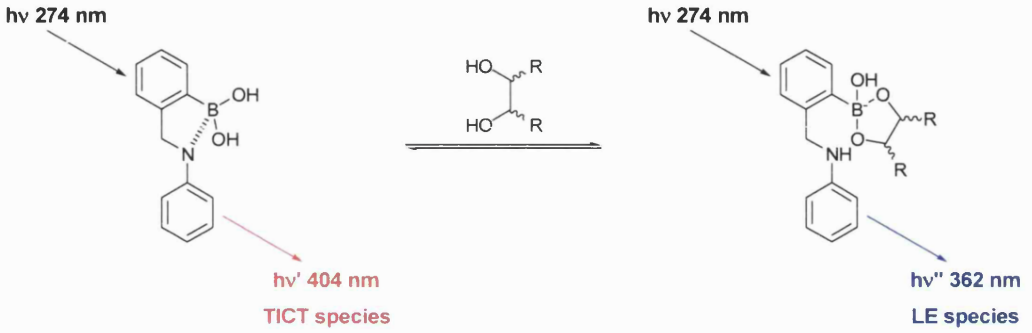

Scheme 24. *Red shifted fluorescence emission due to Twisted Internal Charge Transfer (TICT) of the neutral sp^2 hybridised form of sensor **61** and blue shifted emission due to the Locally Excited (LE) sp^3 species, in this case the boronate anion is formed due to saccharide complexation. Colours are used to depict relative red and blue shifts in the emission wavelength rather than the colour of the emitted light.*

TICT arises in the neutral boronic acid **61** due to the uncomplexed structure containing a nitrogen-boron (N-B) bond. This covalent interaction has been confirmed by x-ray crystallography, the nitrogen lone pair coordinating to the boron with the N-B bond perpendicular to the anilino π-system. This stabilisation of the excited state is lost as soon as the boronic acid is converted to the anionic boronate, either through the pair-wise complexation of a saccharide guest or through an increase in the pH of the solution.

Evaluation of sensors **62** and **63** revealed that due to the increased N-B distance associated with the *meta-* and *para-* substituted boronic acids no N-B bonds were possible, excluding stabilisation from occurring *via* TICT. The observed stability constants (K_{obs}) for sensors **61**, **62** and **63** were 79 M^{-1}, 212 M^{-1} and 129 M^{-1}, respectively, with D-fructose and 6 M^{-1}, 8 M^{-1} and 6 M^{-1}, respectively, with D-glucose in 52.1wt% methanol in aqueous phosphate buffer at pH 8.21.

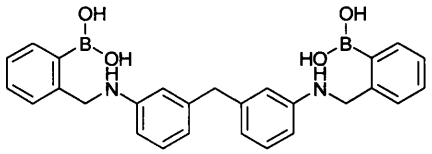

64

This design was extended to produce sensor **64**, a sensor with D-glucose selectivity induced through the introduction of a second, correctly placed, boronic acid recognition site. As we shall discuss later the careful orientation of two boronic acid units is pivotal in the design of sensors with selectivity for specific saccharides. In this instance the observed stability constants (K_{obs}) for sensor **64** were 55 M^{-1} with D-fructose and 140 M^{-1} with D-glucose in 52.1wt% methanol in aqueous phosphate buffer at pH 8.21.

1.4.4 Excited State Photoinduced Electron Transfer (PET)

Electron Transfer (ET)

Electron transfer (ET) plays a central role in the physical, chemical and biological sciences. Providing the key steps in photosynthetic and respiratory pathways, as well as many chemical reactions, ET has been extensively studied.[138,139]

Marking the first step in photosynthesis, photoinduced electron transfer (PET) is fast, extremely efficient and can occur over long distances within biological systems; in bacteriochlorophyll the first electron transfer occurs in 3 ps, with 100% quantum yield and over a distance of 17 Å.[140] Extensive biomimetic syntheses have been conducted to further understand these properties and have led to a range of compounds which can actively model this behaviour. To function, the compounds must incorporate proximal electron donating and electron accepting groups that are suitably insulated from one another.[141]

In supramolecular compounds a saturated hydrocarbon bridge has proved effective at insulating the resulting charge-separated species giving rise to a general Donor-Bridge-Acceptor (D-B-A) construction assembly.[138] The length of the bridge is significant, within these systems it is generally the case that the longer the bridge the less favourable the intramolecular ET process becomes.[142] Whilst long range intramolecular ET has been elegantly illustrated in numerous elongated, structurally rigid organic

molecules such as compound **65**,[143] these molecules represent the upper bounds of donor-acceptor separation within synthetic intramolecular ET systems.[144]

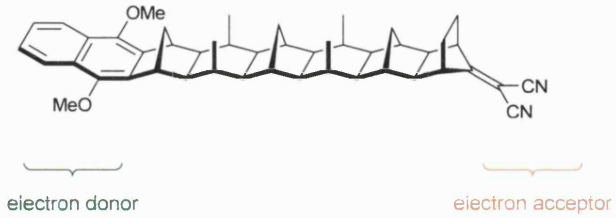

65

In the field of fluorescence the effect of quenching by ET has long been known.[120] Possibly the most efficient fluorescence quenchers to operate *via* known ET mechanisms are amines.[120] Amines efficiently inhibit fluorescence emission of most unsubstituted aromatic systems, a good example being the quenching of anthracene's fluorescence by diethylanaline,[145] Scheme 25.

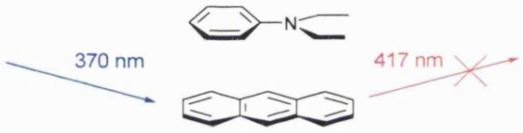

Scheme 25. *Amines quench the fluorescence of most unsubstituted aromatic systems. Blue and red are used to depict the relative Stoke's shift in wavelength rather than the observed colour.*

The efficiency of quenching in the above system (Scheme 25) was found to be a function of the solvent polarity (the intermediate radical ion pair benefiting from increased solvent polarity) and the distance between the donor and acceptor (a maximum encounter distance of ~ 7 Å being reported). From the viewpoint of designing intramolecular ET into supramolecular compounds the importance of reduced distances between donor and acceptor fragments makes an sp^3 hybridised methylene bridge ideal for ET; the bridge being suitably small, yet capable of effectively insulating the charge-separated species.

This knowledge has been adapted to allow molecular switches to be designed into fluorescent sensors through the use of amine donor groups proximal to suitable fluorophore acceptor groups, separated by methylene bridges. This design principle was first applied to a sensory system by de Silva *et al.* who reported the pH sensor **66**.[146]

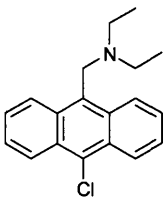

66

The pK_a of the tertiary amino group in sensor **66** is 7.7 in 8:2 water/methanol. Above this pK_a, where the amine is predominantly present as its free base, the amine lone pair can participate in ET and a highly efficient quenching of the fluorescence emission is observed. When the pH is lowered below the pK_a of the amine, so as to protonate it, the lone pair becomes involved in a bonding interaction, disrupting ET and resulting in a complete fluorescence revival.

This molecular construct has been found to function for a large array of systems.[3] The compounds relay information on whether the receptor's binding site is occupied or not by effecting a marked change in the intensity of the fluorescence emission, inducing so called "on" (high fluorescence) or "off" (low fluorescence) emission states of the fluorophore, whilst retaining many of the intrinsic properties of the receptor and fluorophore moieties.

The Mechanistic Interpretation of PET

Following electronic excitation of the fluorophore and the subsequent relaxation processes that lead to the lowest vibrational level of the S_1 excited state (see Section 1.4.2, page 38), systems in the S_1 D-B-A* state can rapidly lower their energy by undergoing a radiationless‡‡ intramolecular ET, see Scheme 26.[3,150,151]

‡‡ It is well known that an accelerating charged particle will generate electromagnetic radiation.[147] The emission of radiation at radiofrequency (tetrahertz) wavelengths during intramolecular ET has recently been documented and applied in the measurement of charge transfer rate constants. ET is not therefore a non-radiative process in the strictest sense, however, no emission will be observed in or near visible wavelengths, nor does this radiation play a significant role in the dissipation of the system's energy.[148,149]

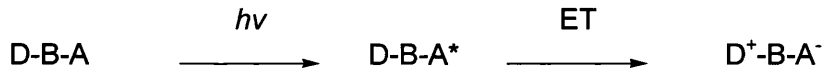

Scheme 26. *Following excitation by an incident photon donor-bridge-acceptor systems can rapidly lower their energy via electron transfer.*

Given the importance of ET this step has been comprehensively studied and a number of sophisticated theories developed to model it.[138,139] Most hinge on the seminal work by Marcus, which was recognised in 1992 with the award of the Nobel prize in chemistry.[152]

As no bond breaking or forming occurs, Marcus theory permits a simple description of the reaction coordinates in terms of the known properties of the reactants and products.[150] The energy of the charge-separated species in the S_1 D^+-B-A^- state can therefore be considered as lowered by an amount dependent on the stabilisation derived from the internal rearrangement of bond angles and lengths as well as the rearrangement of the surrounding solvent shell. In compounds where PET can occur the prerequisite is that the energy of the intermediate S_1 D^+-B-A^- state is such that it bridges the S_1 D-B-A* and S_0 D-B-A states; the interdigitated vibrational levels allowing internal conversion to occur from the lowest vibrational level of one electronic state to the hot (upper) vibrational levels of the next.[148,150]

The back ET[§§] geminate recombination from the newly formed S_1 D^+-B-A^- charge-separated species to the S_0 D-B-A ground state occurs as an internal conversion process. This rapidly neutralises the potentially damaging imbalance of charge across the compound and restores the molecule to its lowest energy ground state, thus providing the highly efficient mechanism for PET to quench fluorescence, Scheme 27.[148,150,155]

[§§] In the nomenclature used within this thesis "back ET" (also commonly called charge recombination[142,153]) denotes the thermal recombination of charge from the S_1 D^+-B-A^- state to the S_0 D-B-A state, so as to restore the donor and acceptor to their original ground state oxidation levels.[154] When examining the scientific press the reader is advised that back ET can been used to denote other ET mechanisms such as the potential S_1 D^+-B-A^- to S_1 D-B-A* pathway.[142]

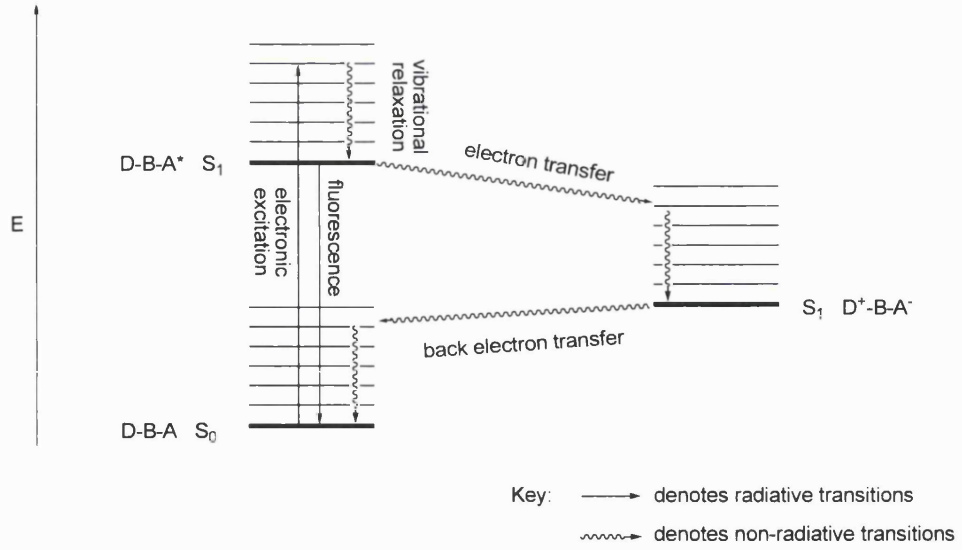

Scheme 27. *Jabłoński diagram depicting the non-radiative pathway available to compounds which undergo internal PET.*

For further information and alternative mechanistic interpretations of PET the reader is directed to several pathways that have been lucidly described within the literature.[3,148,150,151]

1.4.5 Photoinduced Electron Transfer (PET) Sensory Systems

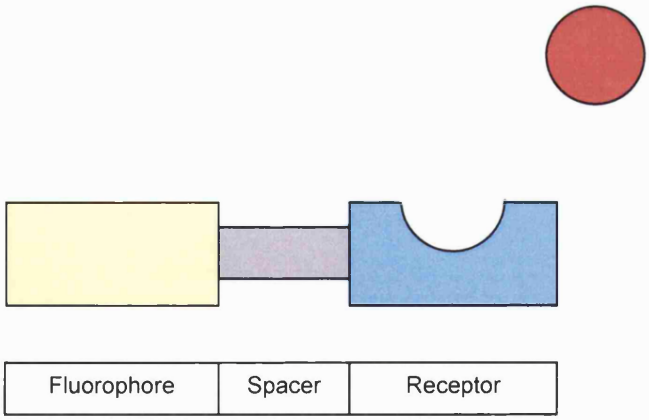

Figure 17. *Schematic representation of the Fluorophore-Spacer-Receptor design assembly for fluorescent PET sensory systems.*

In the case of fluorescent PET sensors the design is often discussed in terms of a receptor and a fluorophore separated by a spacer so as to match the Donor-Bridge-

Acceptor motif. To permit the recognition of saccharides *via* boronic acid complexation, the interaction between *o*-methylphenylboronic acids (Lewis acids) and proximal tertiary amines (Lewis bases) has been exploited, Figure 18.

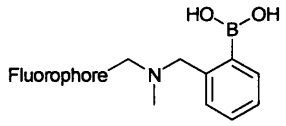

Figure 18. *The generic design of fluorescent PET sensors with the N-methyl-o-(aminomethyl)phenyl-boronic acid recognition unit.*

Whilst elucidating the precise nature of the amine base - boronic acid (N-B) interaction is currently a topic of debate and ongoing research, it is clear that an interaction does exist and it provides two distinct advantages.

The first, proposed by Wulff,[156] is that the interaction between a boronic acid and proximal amine lowers the pK_a of the boronic acid. This effect is sufficient so as to allow binding to occur at neutral, i.e. physiological, pH.

The second, relates to the contraction of the O-B-O bond angle of a boronic acid on complexation with a saccharide and the associated increase in acidity at the boron centre (discussed in Section 1.3.2, page 18). This increase in acidity of the already Lewis acidic boron augments the N-B interaction and in turn disrupts PET. The reduction in pK_a at boron on saccharide binding therefore has the net effect of modulating fluorescence emission intensity, *via* the amine group, and introducing a digital "off-on" response from the fluorophore, indicative of the boronic acid receptor being unbound or bound, respectively (see Section 1.4.6, page 68, for further discussion).

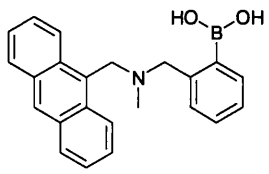

67

Figure 19. *The first fluorescent PET sensor for saccharides to have been rationally designed. In this illustration the Fluorophore-Spacer-Receptor construction is readily apparent; anthracene represents the fluorophore, methylene the spacer and N-methyl-o-(aminomethyl)phenylboronic acid the receptor.*

The first fluorescent PET sensor for saccharides to employ the *N*-methyl-o-(aminomethyl)phenylboronic acid fragment was reported by James *et al.* in 1994.[157,158] Illustrated in Figure 19, sensor **67** functioned remarkably well, a large increase in fluorescence on addition of saccharide was observed, as well as the capacity to function over a broad range of pH. Noticeably the monoboronic acid **67** displayed the same inherent trend in selectivity for saccharides as had been documented by Lorand and Edwards for phenylboronic acid 35 years earlier, a trend which appears to be inherent to all monoboronic acid receptors of this type. Qualitatively, binding constants (*K*) with monoboronic acids increase in the order: D-glucose < D-galactose < D-fructose.[54]

Diboronic Acid Sensory Systems with Selectivity for Specific Saccharides

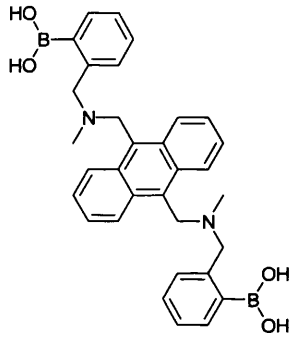

68

Figure 20. *The first rationally designed boronic acid based fluorescent PET sensor to display selectivity for D-glucose. The Receptor-Spacer-Fluorophore-Spacer-Receptor assembly requires binding to occur at both receptors in order to restore fluorescence.*

The D-fructose selective monoboronic acid based sensor **67** was enhanced with the introduction of a second boronic acid group to form the diboronic acid sensor **68**.[118,158] This Receptor-Spacer-Fluorophore-Spacer-Receptor system retained the advantage of utilising PET to modulate an "off-on" response to saccharides whilst introducing an advanced recognition site. The co-operative action of two boronic acid receptors permitted a number of possible binding modes to occur with saccharides. However, for fluorescence to be restored both boronic acid moieties must be complexed which requires either an acyclic 2:1 or cyclic 1:1 (saccharide/sensor) complex to form.

The modification proved successful and fortuitously the spacing of the two boronic acid groups provided an effective binding pocket for D-glucose. D-Glucose complexation occurred with a 1:1 stoichiometry with the saccharide binding to form a macro-cyclic

ring. Whilst the inherent selectivity of monoboronic acids is for D-fructose, in this compound the stabilisation derived from the rigid macro-cyclic ring produces a D-glucose selective system, allowing diboronic acid systems to be tuned for saccharides. The observed stability constants (K_{obs}) for sensor **68** were 320 M^{-1} with D-fructose, 4 000 M^{-1} with D-glucose and 160 M^{-1} with D-galactose in 33wt% methanol in aqueous buffer at pH 7.77.

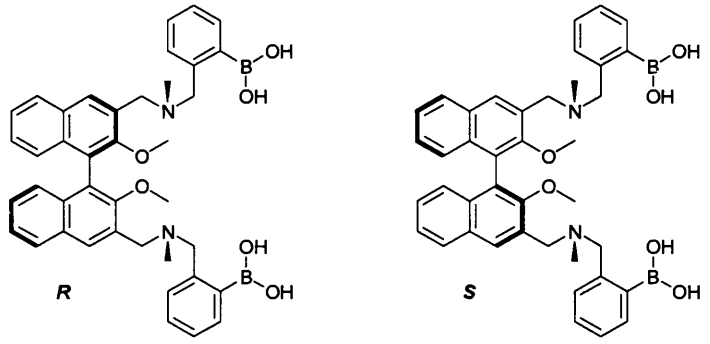

69

Extending the design parameters of sensor **68**, James and co-workers developed the chirally selective sensors *R*- and *S*-**69**.[119,159] Based on the intramolecular fluorescence quenching of 1-1'binaphthyls, sensors *R*- and *S*-**69** demonstrated that selectivity of a diboronic acid appended sensor could be tuned not only towards specific ligands, such as monosaccharides, but also towards the specific enantiomers of these ligands.

First documented in 1995, the role of sensors *R*- and *S*-**69** as tools for the chiral discrimination of monosaccharides yielded observed stability constants (K_{obs}) of (for sensors *R*-**69** and *S*-**69** respectively) 10 000 M^{-1} and 5 000 M^{-1} with D-fructose, 3 200 M^{-1} and 10 000 M^{-1} with L-fructose, 2 000 M^{-1} and 2 500 M^{-1} with D-glucose and 1 300 M^{-1} and 3 200 M^{-1} with L-glucose in 33.3wt% methanol in aqueous buffer at pH 7.77.[119]

Following observations by Houston and Gray[160] that the racemate of sensor **69** bound sugar acids such as tartaric acid with a comparable strength to the monosaccharides [an observed stability constant (K_{obs}) for tartaric acid of 1 400 M^{-1} in 33% methanol/water at pH 7.77 (HEPES buffer) was reported] the chiral complexation of these ligands was investigated.[159]

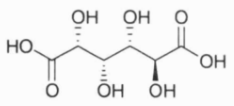

70 D-glucaric acid

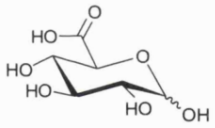

71 D-glucuronic acid

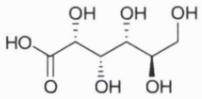

72 D-gluconic acid

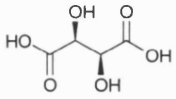

73 D-tartaric acid

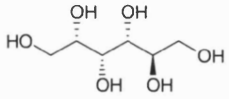

74 D-sorbitol

It was found that the recognition of D- and L-tartaric acid by sensors *R* and *S*-**69** was strongly pH dependent. At pH 8.3 the fluorescence enhancements behaved as expected. For sensor *R*-**69** with D-tartaric acid and sensor *S*-**69** with L-tartaric acid the fluorescence enhancements were large, conversely for sensor *S*-**69** with D-tartaric acid and sensor *R*-**69** with L-tartaric acid the fluorescence enhancements were small, see Scheme 28.

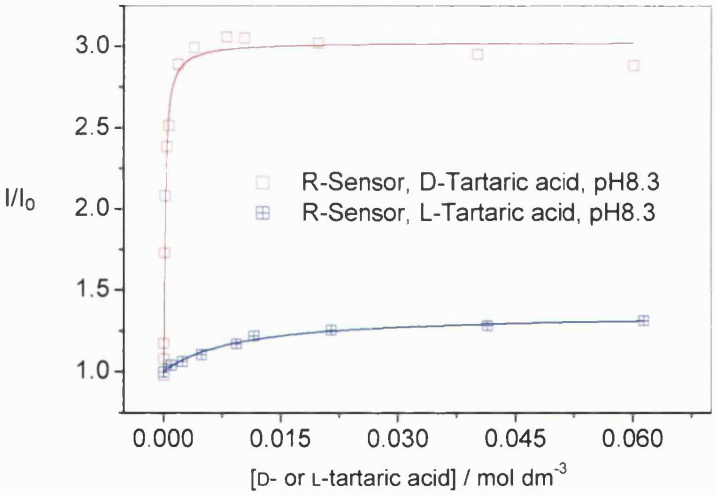

Scheme 28. *D-tartaric acid (plotted in red) and L-tartaric acid (plotted in blue) binding isotherm with sensor R-***69** *at pH 8.3. [R-***69***] = 5.0×10^{-6} mol dm^{-3}, at pH 8.3 in 0.05 M NaCl (52.1% methanol), [Tartaric acid] = 0 - 0.06 mol dm^{-3}, λ_{ex} at 289 nm, λ_{em} at 358 nm, 22 °C.*

Accordingly when the acidity was adjusted to pH 5.6 the fluorescence of sensor *R*-**69** with D-tartaric acid displayed an increase in fluorescence intensity. Quite astonishingly however, the use of tartaric acid's L-enantiomer with sensor *R*-**69** produced a decrease in the fluorescence intensity. The same relationship was observed with the mirror image host-guest complexes. Sensor *S*-**69** and L-tartaric acid displayed a fluorescence increase while sensor *S*-**69** and D-tartaric acid displayed a fluorescence decrease. These results

signify that sensors *R*- and *S*-**69** have the unusual property of allowing the fluorescence intensity of the reporting signal to be enantioselectively diminished or enhanced, relative to the fluorescence emission of the unbound species, see Scheme 29.

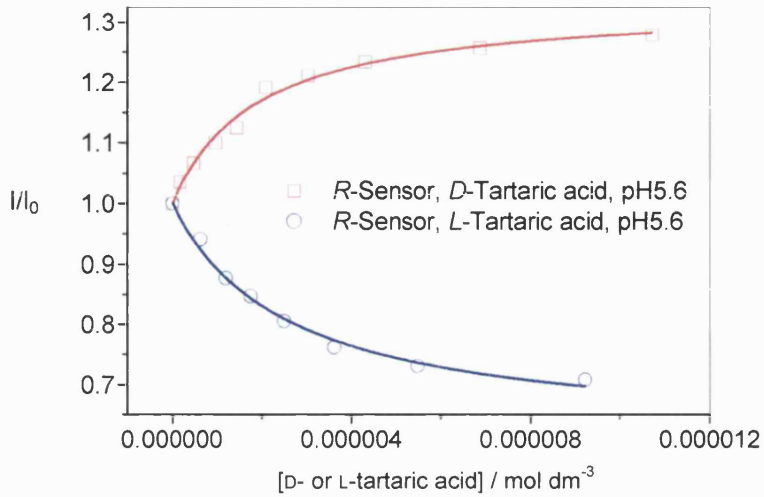

Scheme 29. *D-tartaric acid (plotted in red) and L-tartaric acid (plotted in blue) binding isotherm with sensor R-***69** *at pH 5.6. [R-***69***] = 5.0x10^{-6} mol dm^{-3}, at pH 5.6 in 0.05 M NaCl (52.1% methanol), λ_{ex} at 289 nm, λ_{em} at 358 nm, 22 °C.*

Evaluation of sensors *R*- and *S*-**69** with D-gluconic acid produced a similar enantioselective diminution or enhancement in the fluorescence intensity, curiously this was not the case with D-glucaric acid, D-glucuronic acid or D-sorbitol. It is understood that on complexation of an asymmetric guest to sensors *R*- and *S*-**69**, the orientations of the two receptor units relative to the fluorescent BINOL core are locked in an asymmetrically distorted conformation. These results imply that in all probability the normal PET quenching that mediates fluorescence intensity must be susceptible to the induced geometrical changes that occur between receptors and fluorophores within individual host-guest complexes; the degree of geometric strain varying on a case-by - case basis.

Considering the effect of geometry on both the stability of the complexes formed and the fluorescence enhancements generated, the two properties appear to be independent. For changes in geometry the observed stability constants (K_{obs}) increased up to ~ 25 fold, whilst fluorescence intensity increased only up to ~ 3 fold. The geometry of the receptor therefore has a far greater influence on substrate recognition than it does on fluorescence.

The observed stability constants (K_{obs}) for (sensors *R*-**69** and *S*-**69** respectively) were 520 000 M^{-1} and 260 000 M^{-1} with D-tartaric acid, 390 000 M^{-1} and 280 000 M^{-1} with L-tartaric acid in 52.1wt% methanol in water at pH 5.6.

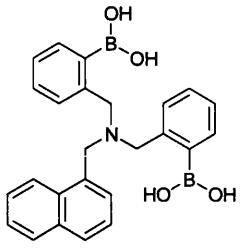

75

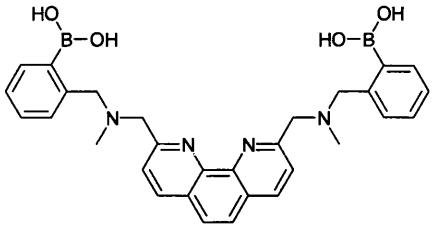

76

Figure 21. *Diboronic acid based fluorescent PET sensors with varied inter-boronic acid distance. Sensor **75** demonstrated enhanced selectivity for D-sorbitol, whilst sensor **76** displayed neither selectivity nor sensitivity towards monosaccharides.*

A number of diboronic acid fluorescent sensors were subsequently synthesised with significantly modified structures. The inter-boronic acid distance, responsible for defining the dimensions of the binding cleft proved particularly important. Where a reduced distance between the boronic acids was chosen as with sensor **75**, the sensor was found to differentiate between monosaccharides based on the number and proximity of the diol groups the saccharide contained. Ligands such as propane-1,3-diol, with only one binding site, and D-glucose, where the two diol groups were separated by one or more carbons, were entirely excluded from the binding pocket whereas smaller monosaccharides with dual adjacent diol groups such as D-sorbitol, complexed strongly. The observed stability constants (K_{obs}) for sensor **75** were 350 M^{-1} with D-sorbitol and 330 M^{-1} with D-fructose in 300:1 (v/v) water/methanol at pH 8.0, whilst the fluorescence changes for D-glucose and propane-1,3-diol were so small that observed stability constants (K_{obs}) could not be determined.

Conversely a gross increase in the inter-boronic acid distance, with a rigid spacer such as with sensor **76**, displayed a significant loss in selectivity and sensitivity. The observed stability constants (K_{obs}) for sensor **76** were 170 M^{-1} with D-fructose, 91 M^{-1} with D-glucose and 72 M^{-1} with D-galactose in 33wt% methanol in aqueous buffer at pH 7.77.

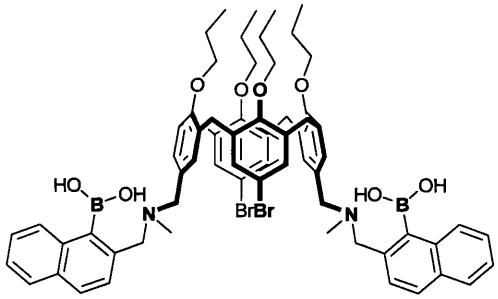

77

In an effort to develop sensors with dual boronic acid receptors favourably located so as to enhance D-glucose selectivity, boronic acid receptor groups were mounted onto a calixerane scaffold to generate sensor **77**. This elegant approach had the potential to allow a diverse range of synthetic functionality to be designed into the sensors, unfortunately the sensor displayed a poor affinity for monosaccharides. The observed stability constants (K_{obs}) were 115 M^{-1} for D-fructose (forming an acyclic 2:1 saccharide/sensor complex) and 24 M^{-1} for D-glucose (forming a cyclic 1:1 saccharide/sensor complex) in 33wt% methanol in water at neutral pH.

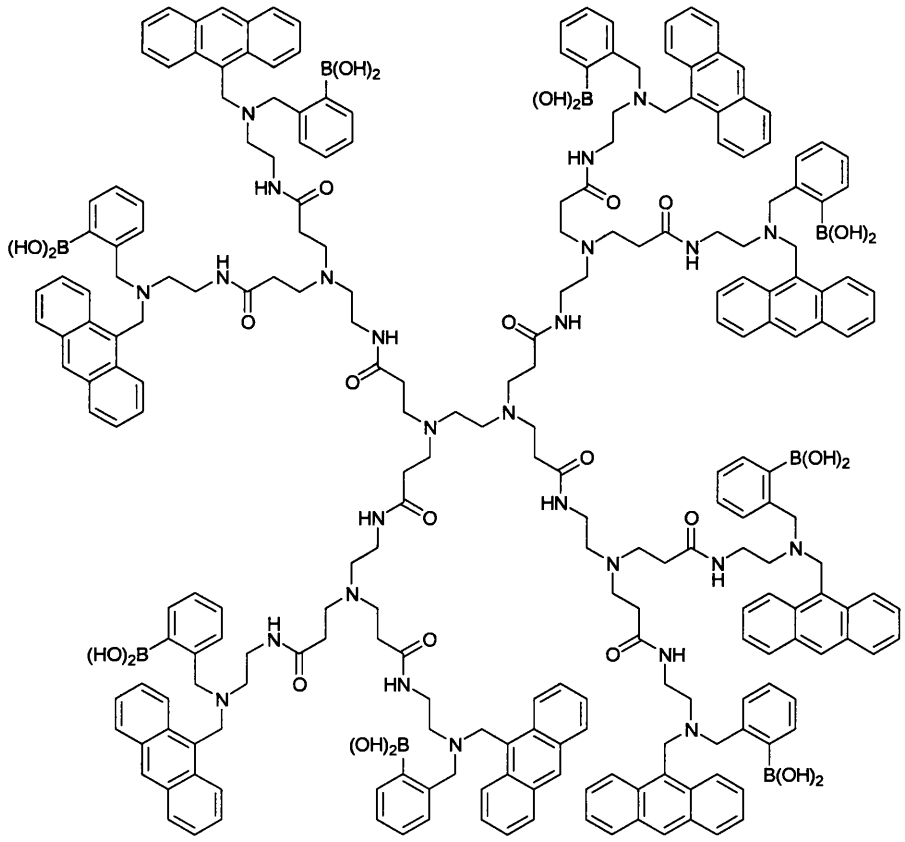

78

The boronic acid based starburst dendrimer **78** displayed an enhanced sensitivity for all of the monosaccharides it was examined against.[161] In essence the dendrimer functioned as a saccharide "sponge". Whilst the dendritic boronic acid is highly flexible and one could therefore expect little pre-organisation within the binding pocket, the boronic acid – saccharide complex was surprisingly stable. To determine the binding motifs used within this compound a number of deoxy-, deoxymethyl- and partially protected saccharide derivatives were examined. The results supported the view that even within such a flexible sensor the cooperative action of the boronic acids to form 2:1 (boronic acid group/saccharide) complexes led to an enhanced binding ability. Moreover, the results indicated that binding to D-galactose must occur primarily through the hydroxyls on the 1 and 2 positions. This is apparent from the observed stability constants (K_{obs}) reported for dendrimer **78** which were 27 000 M^{-1} with D-galactose, 16 900 M^{-1} with D-fructose and 740 M^{-1} with D-glucose in pure methanol.[161]

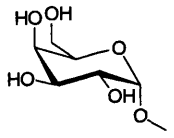

79

When the hydroxyl group on the anomeric centre was substituted for a methoxy group, as in 1-methyl-α-D-galactopyranoside **79**, the observed stability constant (K_{obs}) diminished to 40 M^{-1}, a six hundred and seventy five fold reduction in the observed stability constant (K_{obs}).

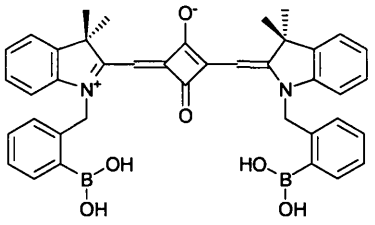

80

On addition of saccharide the diboronic acid squaraine **80** produced a fluorescence response with an emission maxima at 645 nm and a shoulder at 695 nm.[162] This

emission occurs at the blue end of the near-infrared optical window (600 - 1 300 nm) for human skin.[163]

The biomedical interest in the near-infrared section of the electromagnetic spectrum is derived from the comparatively high absorption and scattering of light by living tissues observed outside of these wavelengths.[164] Moreover, signal reduction is coupled with increased signal to noise ratios generated from the autofluorescence of mammalian vital organs and bodily fluids when subject to wavelengths below ~ 600 nm.[165] Whilst interference from these properties can be readily overcome in routine analysis, the development of fluorescent sensors with excitation and emission wavelengths inside the near-infrared band permits the biomedical imaging of sensors within bulk tissue as well as the potential transdermal monitoring of analytes *in vivo*.[165]

D-Fructose produced a 25% increase in fluorescence intensity on addition to the sensor in an ethanol/water (50 mM carbonate buffer) solution at pH 10. Unfortunately D-glucose, D-galactose and D-mannose only produced an observed change in the fluorescence intensity of 8%.

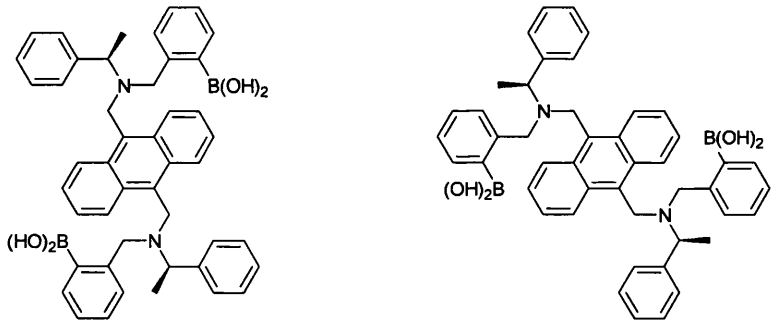

R,R *S,S*

81

The design assembly employed in these sensory systems appears to have come full circle. The recently reported chiral boronic acid based sensors *R,R*- and *S,S*-**81** are direct structural derivatives of the original D-glucose selective sensor **68** (page 60).[166]

The pH titrations demonstrated that sensors *R,R*- and *S,S*-**81** were highly selective for sugar acids such as tartaric, glucaric, gluconic and glucuronic acid (see page 62 for structures); with chemoselectivity of up to 11 000:1 (pH 5.6) being reported between species and enantioselectivity between the D- and L- forms of the ligands of up to 500:1

(pH 7.0) being reported with sensors *R,R*- and *S,S*-**81**. The same titrations were performed with monoboronic acid analogues, these analogues displayed no enantioselective discrimination between D- and L- tartaric acid indicating that for enantioselectivity a 1:1 cyclic complex must be formed.

The observed stability constants (K_{obs}) for (*R,R*-**81** and *S,S*-**81** respectively) were 830 000 M^{-1} and 10 000 M^{-1} with D-tartaric acid, 8 500 M^{-1} and 580 000 M^{-1} with L-tartaric acid in 52.1wt% methanol in water at pH 5.6.

Of particular interest to the understanding of the fundamental processes involved in PET signalling interactions is the x-ray crystal structures of sensors *R,R*- and *S,S*-**81** which were obtained both with (*S,S*-**81**) and without (*R,R*-**81**) a guest complexed in the active site. The structure permits a rare insight into the, so far undetermined, possible mode of action of the N-B interaction.

1.4.6 Amine - Boron (N-B) Interactions

The so-called coordinative or dative, nitrogen to boron (N-B or alternatively N→B) bonds have been studied for more than 100 years. The strength of N-B bonds depend greatly on the substituents at both atoms; electron withdrawing groups increase the Lewis acidity of boron, whilst electron donating groups increase the Lewis basicity at nitrogen. In considering the bond strength it is necessary to balance these electronic factors against the counteracting steric requirements of these same substituents. An investigation of 144 compounds with coordinative N-B bonds concluded that steric interactions as well as ring strain (in the case of cyclic diesters) weaken and elongate the N-B bond, which occurs with a concurrent reduction in the tetrahedral geometry of the boron centre.[167]

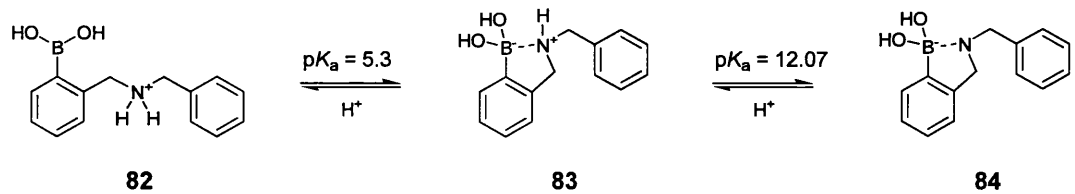

82 **83** **84**

Scheme 30. *Protonation of N-methyl-o-(phenylboronic acid)-N-benzylamine. Introduction of a neighbouring amine lowers the pK_a of the boronic acid.*

In the case of *N*-methyl-*o*-(phenylboronic acid)-*N*-benzylamine and its derivatives (Scheme 30) the extent of the N-B interaction and its precise nature has not been unequivocally determined.[62] To the extent that it does occur, it can be considered as a dehydration between the amine and the boronate anion or a Lewis base – Lewis acid interaction between the amine and the neutral boronic acid. This system has been investigated separately by Wulff, Anslyn and within the T. D. James research group.[62,156,168] ^{11}B NMR experiments demonstrate that the benzylamine derivative **83** is tetrahedral at boron.[168] This implies that there is a substantial interaction at boron, nonetheless, whilst empirical results indicate that the interacting form is favoured, the degree of interaction is unknown. A caveat is required and it is perhaps best to delineate the possible limits of this interaction.

Scheme 31 depicts a general model where, at one extreme, the acyclic forms (**85** and **86**) illustrate no N-B interaction and at the other, the cyclic forms (**88** and **89**) illustrate a full N-B interaction; the species existing in equilibrium. Species **87** involves a protonated nitrogen, therefore the ammonium cation precludes any N-B interaction.

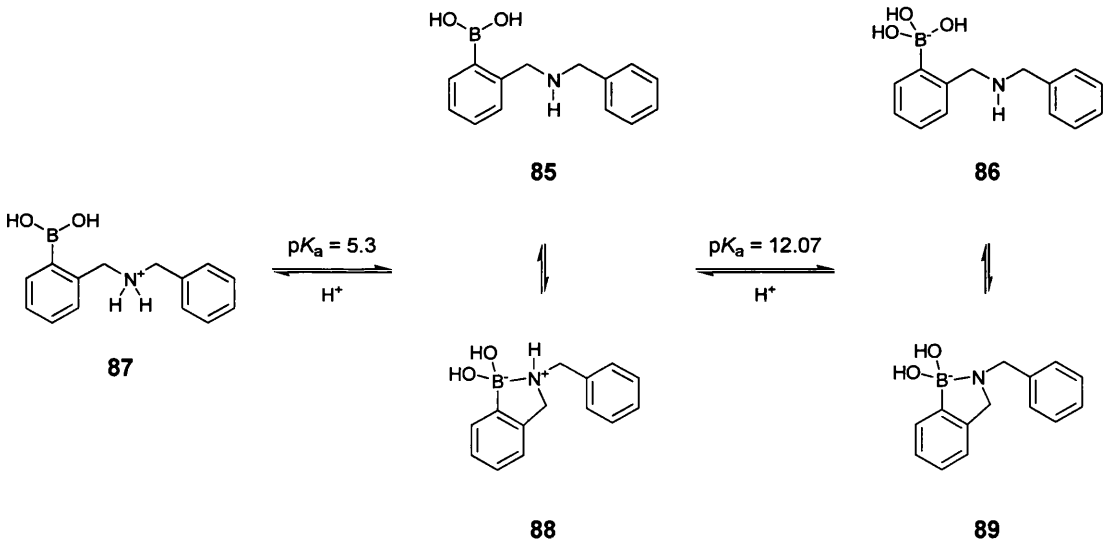

Scheme 31. *The extent of the interaction between nitrogen and boron is illustrated within the upper and lower bounds of possible contact depicted as the cyclic and acyclic forms.*[62]

The energy of the N-B interaction has been calculated from the stepwise formation constants of potentiometric titrations. Based on the relative stabilities of ternary phosphate complexes it was calculated that the upper and lower limits of the N-B interaction must be bound between approximately 15 and 25 kJ mol^{-1} in *N*-methyl-*o*-

(phenylboronic acid)-*N*-benzylamine.[62] This value is in good agreement with computational data which estimated the N-B interaction to be 13 kJ mol^{-1} or less in the absence of solvent.[104] To qualify this in terms of familiar bonding motifs the energy of the N-B interaction is about the same as that of a hydrogen bond.

As we have discussed, the strength of this interaction is a central feature in many fluorescent PET sensors, where the N-B interaction plays a pivotal role in signalling the binding event. If the interaction were much stronger, then the binding of a diol would not be able to disrupt the N-B interaction sufficiently so as to modulate a change in fluorescence. By the same token, if the interaction were much weaker then there would be no significant intramolecular N-B interaction to disrupt in the first place.

For some time the formation of a direct bond between nitrogen and boron was assumed to be responsible for the fluorescence enhancement seen when boronic acids bound diols. This interpretation does, however, raise certain questions.

The fluorescence revival in these systems functions as a digital "off-on" response. Fluorescence emission returns to the same maximal value regardless of the observed stability constant (K_{obs}) of the ligand or the pK_a' of the resulting boronate ester. It is known that the acidity of boron in other systems directly influences the strength of N-B bond. Therefore if a direct N-B bond did modulate PET we might necessarily expect the fluorescence response to vary as a function of the degree of acidity or strength of complexation, this is not the case.[169] Moreover, the numerical values reported over the past year do not agree with the interpretation of a direct N-B bond.[62,104]

The recent evaluation of sensor **81**, the first fluorescent diboronic acid sensor to be reported as a single-crystal x-ray structure both in its bound and unbound state, has recently been published.[166] In the case of the unbound receptor the geometry at boron is trigonal planar. This is important as the absence of deviation from planarity implies that there is no direct N-B Lewis base – Lewis acid bond at boron.

When bound to tartaric acid, the complex was crystallised from a methanol and dichloromethane solution. In the tartrate complex two molecules of methanol, one at each boron centre are bound through their oxygen atoms to their respective boron centres. Whilst the hydrogen atoms of methanol were not directly located it is not unreasonable to infer from the geometry that each oxygen atom will concurrently bind

to the boron centre and hydrogen bond to the adjacent nitrogen atom. Oxygen to nitrogen bond distances of around 2.7 Å were reported in this case, Figure 22.

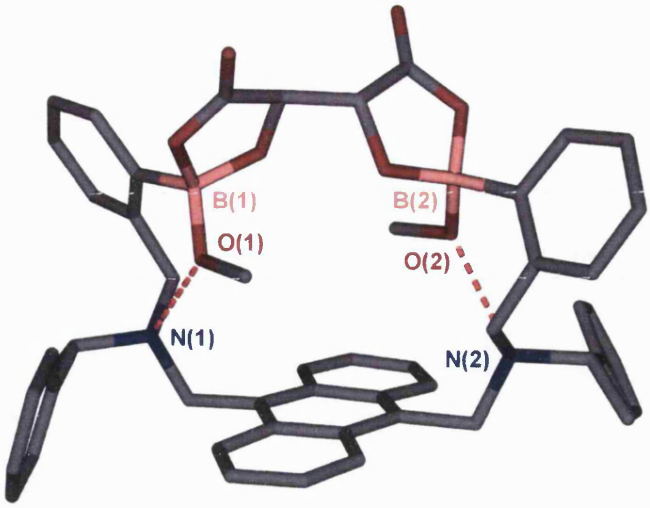

Figure 22. *The single-crystal x-ray structure of the S,S-diboronic acid (S,S-**81**) – L-tartaric acid complex isolated by James and co-workers.[166] Whilst the hydrogen atoms of methanol were not directly located it can be inferred that the geometry between the bound and unbound receptors will be similar, each oxygen atom will therefore concurrently bind to the boron centre and hydrogen bond to the nitrogen atom. Oxygen to nitrogen bond distances of around 2.7 Å were reported [N(1) O(1) = 2.655 Å and N(2) O(2) = 2.693 Å]. Atoms marked in red represent oxygen, pink boron, grey carbon and blue nitrogen. For clarity hydrogen atoms are not displayed. The red dotted lines represent hydrogen bonds.*

Whilst speculative this structural interpretation of the interaction between boronic acid and the proximal tertiary amine through a bound protic solvent molecule corresponds well with contemporary computational and potentiometric titration data, in which the formation of intramolecular seven-membered rings should not be ignored.[62,104,170,171] The values for the bond length (from the x-ray crystal structure) and for the bond strength (from the potentiometric titrations) are those that would be expected for a hydrogen bonding interaction manifested through a bound solvent molecule at the boron centre.

The idea postulated is by no means a new one. An infrared study into the interaction between nitrogen and boron in a similar system came to a similar "tentative conclusion" in 1964.[172] The experimental rationale was based on comparing two emergent peaks in infrared spectra to similar peaks in known model systems. The results indicated that in carbon tetrachloride the interaction between the nitrogen and boron of 8-quinolineboronic acid could be modulated by either water or phenol bound to the boron centre at oxygen.

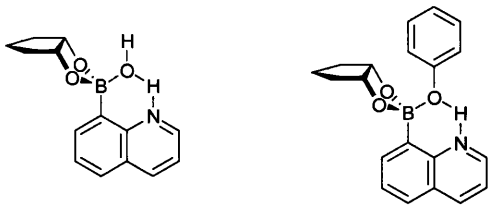

90 91

Figure 23. *Morrison's proposed complexes of the cis-1,2-cyclopentanediol ester of 8-quinolineboronic acid with solvent water and phenol molecules bridging the nitrogen and boron centres.[172] Blue bonds are used to represent dative bonding.*

It should be noted that current data on the N-B interaction (in these systems) is not sufficient to unambiguously support or dispel any given hypothesis. Current work, from a number of groups, indicates that a hydrogen bonding interaction mediated through a bound solvent molecule may provide one plausible mode of action. From recent experimental and computational work the interaction has around the same strength as a hydrogen bond and appears to causes no deviation from planarity at the boron centre of unbound sensory systems.

From a design perspective, even though the mechanism responsible for conferring binding information from boron to nitrogen remains elusive, what can be said with certainty is that this recognition unit effectively controls PET and can continue to be incorporated into sensory systems.

1.4.7 The Importance of Pyranose to Furanose Interconversion

Pyranose to Furanose Interconversion as a Function of Time and Water

In refining the selectivity of boronic acid sensors for saccharides the structure of the guest species must be addressed. Although there is a long history of research into the structural character of boronic acid – saccharide complexes, the rapid isomerisation of monosaccharides in water precludes the description of a simple generic binding motif. As we have mentioned above (page 7) the hemiacetal ring of a monosaccharide is readily cleaved in water, often reforming rings of different sizes and anomeric configurations. The equilibrium between linear, pyranose and furanose configurations as well as the α and β anomers of the pyranose and furanose rings, substantially increases the number of possible structures that may be formed on complexation.

Sensor **68** provided the first structural elucidation of a diboronic acid sensor with D-glucose complexed within the binding site. The ^{1}H NMR spectrum of this complex indicated that in deuterated methanol the D-glucose was bound in the α-pyranose form at the 1,2 and 4,6 positions, as in Figure 24.[158]

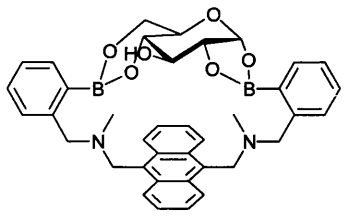

Figure 24. *The initial 1,2:4,6 complex formed between sensor **68** and D-glucose in MeOD.*[158]

A re-examination of this work was conducted by Norrild and Eggert.[173] Employing ^{13}C-1 and ^{13}C-6 labelled D-glucose the $^1J_{C1\text{-}C2}$ and $^1J_{C5\text{-}C6}$ coupling constants were monitored. Exploiting the observed reduction in the $^1J_{CC}$ value upon formation of a five-membered boronic ester,[174] the analysis determined that the previous ^{1}H NMR assignment was correct, but that the interpretation was only valid as the initial complex formed under anhydrous conditions. With time the α-D-glucopyranose isomerised to the α-D-glucofuranose form. In deuterated methanol this process was slow, twenty hours elapsed before the emergence of new NMR peaks became clear, with a complete disappearance of the original α-D-glucopyranose signals occurring after eight days. However, if water was introduced to the system, isomerisation was accelerated dramatically and after ten minutes in a 1:2 water/methanol solution isomerisation had gone to completion.

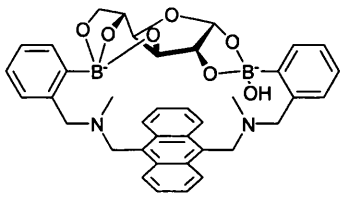

Figure 25. *The thermodynamically stable 1,2:3,5,6 complex observed to form between sensor **68** and D-glucose in basic aqueous media (given the current understanding of N-B interactions the boron bound at the 1,2 position is illustrated as a tetrahedral boronate).*[173]

In the case of sensor **68** it was concluded that once formed the complex in Figure 24 rearranges to the thermodynamically more stable 1,2:3,5,6 bound α-D-glucofuranose complex, Figure 25, as a function of time and the water content of the medium. This

binding pattern is comparable with that of other known structures, such as the commercially available diacetone-D-glucose **92**.

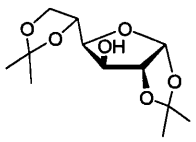

92

Indeed the furanose form of the ring is the one that might be intuitively expected. For an O-B-O fragment to bridge the gap between conformationally locked synclinal (axial and equatorial) hydroxyl groups on a pyranose ring, a substantial degree of torsional strain would be induced across the newly formed cyclic diester. In an effort to understand the significance of this torsional strain Nicholls and Paul undertook the molecular modelling of a series of boronic acid - cyclic saccharide complexes to determine the structure of the thermodynamically stable boronate esters formed.[175] It was found that the vicinal diols involved in complexation must posses, or at least be able to adopt, a syn-periplanar arrangement.

Anti-periplanar hydroxyl groups therefore fail to form boronic acid – diol complexes. Synclinal hydroxyl groups can adopt syn-periplanar geometry in instances when the energy lost due to induced distortions in the saccharide ring are outweighed by the energetic stability gained from complexation. But generally the most stable boronic acid – diol complexes occur between boronic acids and the conformationally locked syn-periplanar hydroxyl groups on furanose rings.[175]

Scheme 32. *The conformationally locked C1,C2-synperiplanar diol group of the α-D-glucofuranose ring provides an ideal binding site for boronic acids.*[175]

This relationship is consistent with previously reported observed stability constants (K_{obs}) and was illustrated by Norrild and Eggert in a study of the complexation of *p*-tolylboronic acid with D-glucose. The study provided convincing evidence of a clear preference for the furanose form of the hemiacetal ring at a stoichiometric ratio of 2:1

(boronic acid/D-glucose).[174] The extent of the thermodynamic stability of this complex becomes apparent if one recalls that α-D-glucofuranose accounts for a mere 0.14% of the total speciation of equilibrated D-glucose in water yet becomes the dominant species in solution when complexed to monoboronic acids.[32]

The Preference of Monoboronic Acids for D-Fructose.

Drawing these observations together we indicate that the apparent dependence of the stability constants (*K*) of monoboronic acids on the ability of the vicinal diols of saccharides to conform to a syn-periplanar arrangement could be used to explain the heightened stability of D-fructose over other monosaccharides, see Lorand and Edwards' results in Table 1 (page 34).

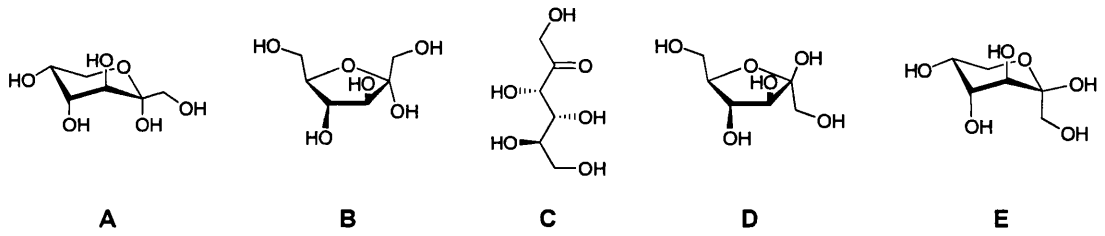

Figure 26. *D-fructose **38** in its various configurations and the percentage composition at equilibrium of each form of the sugar in D_2O at 31 °C (**A**) α-pyranose, 2.5%; (**B**) α-furanose, 6.5%; (**C**) acyclic form, 0.8%; (**D**) β-furanose, 25%; (**E**) β-pyranose, 65%.*[176]

The furanose form of D-fructose with an available syn-periplanar anomeric hydroxyl pair (C2-C3) is β-D-fructofuranose, Figure 26 (**D**). At equilibrium this species accounts for an enormous 25% of the total speciation of D-fructose in deuterated water at 31 °C.[176] This value can be contrasted with that of the furanose form of D-glucose with an available syn-periplanar anomeric hydroxyl pair, α-D-glucofuranose, which accounts for 0.14% of the equilibrated forms of D-glucose in deuterated water at 27 °C.[32] In the presence of phenylboronic acid, the stability constants (*K*) reported by Lorand and Edwards were 4 400 M^{-1} with D-fructose and 110 M^{-1} with D-glucose.[54]

From a simplistic viewpoint we indicated that a very general statistical trend appears to exist between the natural speciation of saccharide forms containing the syn-periplanar anomeric hydroxyl pair arrangement (a premise of the form's stability) and the qualitative trend observed for their stability constants (*K*) with monoboronic acids, Table 2.

Table 2. Saccharide structures containing a syn-periplanar anomeric hydroxyl pair, equilibrated percentages in D_2O and stability constants with phenylboronic acid are tabulated for a selection of saccharides.

saccharide (furanose form with syn-periplanar arrangement of the anomeric hydroxyl pair)	**structure**	**relative percentage** (of the total composition in D_2O) / %	K_{obs} (with phenylboronic acid)[54] / $dm^3\ mol^{-1}$
D-glucose (α-D-glucofuranose)	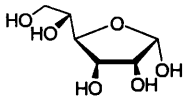	0.14[a]	110
D-mannose (β-D-mannofuranose)	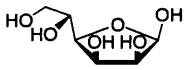	0.3[b]	170
D-galactose (α-D-galactofuranose)	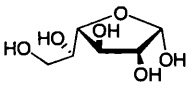	2.5[b]	280
D-arabinose (β-D-arabinofuranose)	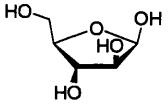	~ 2[b]	340
D-fructose (β-D-fructofuranose)	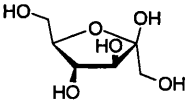	25[b]	4 400

[a] Following equilibration in D_2O at 27 °C.[32]
[b] Following equilibration in D_2O at 31 °C.[176]

Unfortunately the complexity and extensive number of possible binding motifs precludes such a simplistic approach from providing anything other than a statistical rule-of-thumb guide.

The furanose form of a saccharide may not necessarily always be the one favoured for binding. For example NMR data suggests that D-mannose may be preferentially complexed by monoboronic acids in a pyranose twist conformation, Scheme 33.[175]

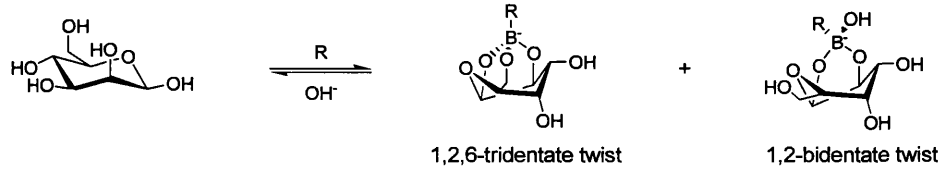

Scheme 33. *The probable twist isomers of the β-D-mannopyranose boronate esters, where R = m-nitro phenylboronic acid.*[175]

Furthermore, bidentate and tridentate complexation is known to occur, with *endo*- and *exo*-orientations of the substituents affecting the thermodynamic stability of the bidentate species, Figure 27.

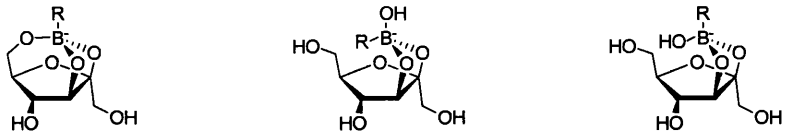

Figure 27. *The structures assigned to D-fructose at a 1:1 (p-tolylboronic acid/D-fructose) ratio.*[177]

This was illustrated in an examination into the complexation of *p*-tolylboronic acid with D-fructose.[177] From these two compounds, in aqueous alkaline solution, seven different complexes were afforded. Notably, the abundance of the major species within the system fluctuated as a function of solvent, pH and boronic acid concentration.

Disaccharides

The influence of pyranose to furanose interconversion on the observed stability constants (K_{obs}) of boronic acid complexes can be effectively demonstrated in the fluorescence response of boronic acid appended sensors with disaccharides. In examining the stabilities of disaccharides with the 5-indolylboronic acid **37** (page 46), Aoyama and co-workers noted that for non-reducing sugars the observed stability constants (K_{obs}) were significantly reduced or zero. This phenomenon was ascribed to the lack of an anomeric hydroxyl, which inhibited the formation of a strong boronic acid complex with the anomeric hydroxyl and its vicinal neighbour.[131]

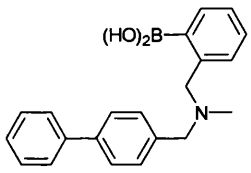

93

James and co-workers extended this investigation by evaluating compound **93** against a range of mono- and di-saccharides.[178] For D-glucose and its disaccharide derivatives melibiose and maltose, strong fluorescence responses were only observed with D-glucose and melibiose (saccharides which can interconvert between their pyranose and furanose forms). Conversely a weak fluorescence response was observed with maltose, which is covalently bound through its 4-position and as such cannot isomerise to adopt a furanose ring structure (but does posses a free C1,C2-diol functional group).

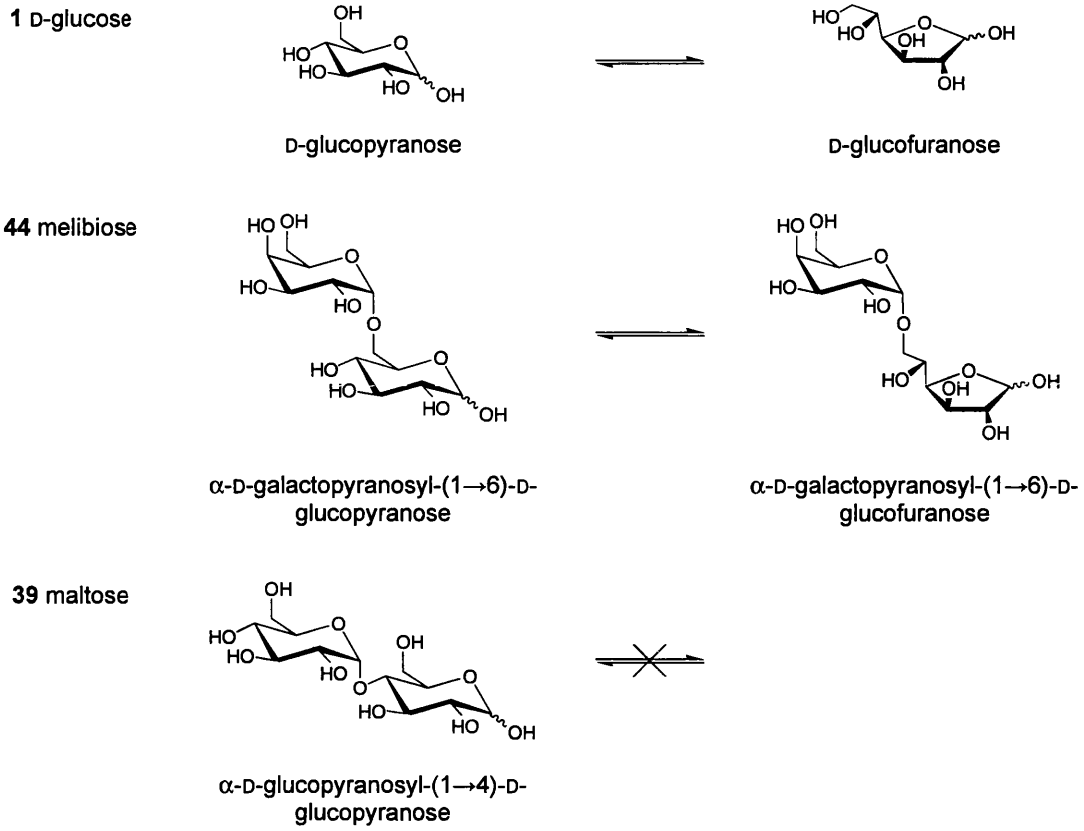

Scheme 34. *D-glucose and its disaccharide derivatives melibiose and maltose.*[178]

The same trend was observed for D-fructose and its disaccharide derivatives lactulose and leucrose. Strong fluorescence responses were observed with D-fructose and lactulose (saccharides which can interconvert between their pyranose and furanose forms). Conversely only a weak fluorescence response was observed with leucrose, which is covalently bound at the 5-position (the fourth carbon as numbered from the anomeric centre) and as such cannot isomerise to adopt a furanose ring structure (but still allows approaching boronic acids unfettered access to the C2,C3-diol).

These results indicate that the negligible observed stability constants (K_{obs}) documented for certain disaccharides cannot be considered solely a function of the availability of the anomeric hydroxyl pair. In the case of the reducing sugars maltose and leucrose it is the inability of the sugars to adopt their furanose forms, and thus a syn-periplanar alignment of the anomeric hydroxyl pair, that inhibits complexation.

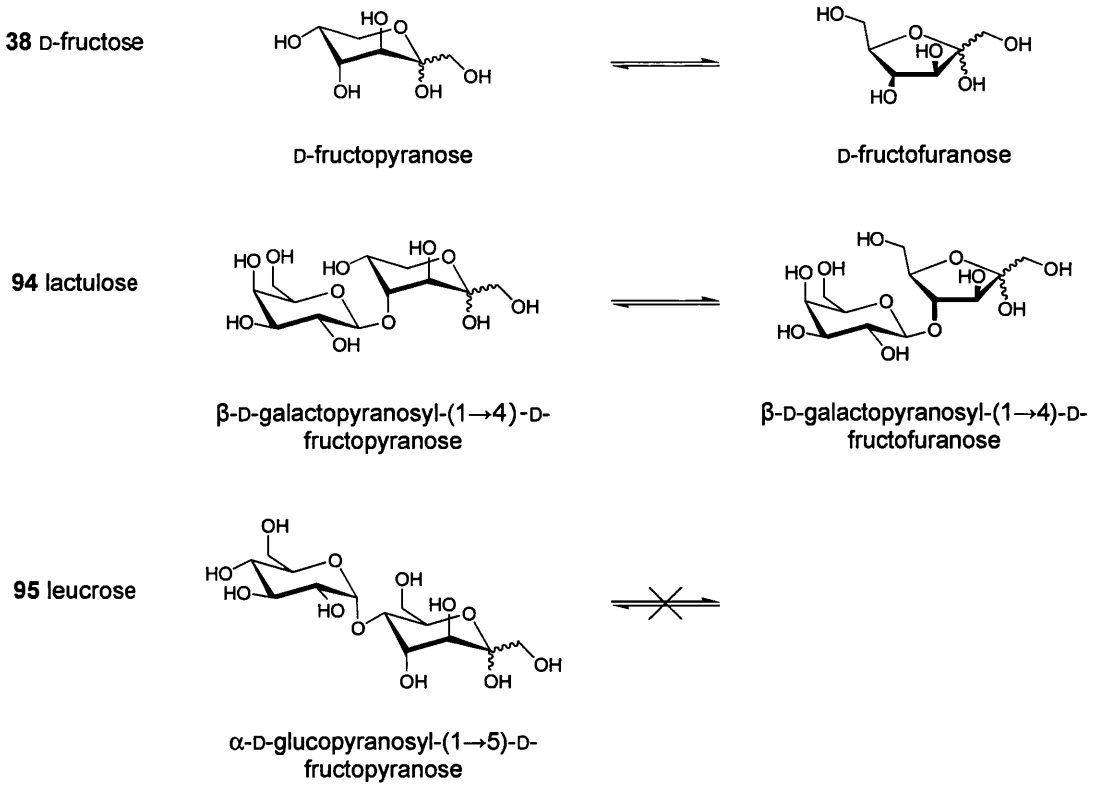

Scheme 35. *D-fructose and its disaccharide derivatives lactulose and leucrose.*[178]

From the pragmatic viewpoint of designing diboronic acid sensors with selectivity for D-glucose, many receptors have relied on an approximate spacing of the two boronic acid units such that the dimensions of the binding pocket mimic that of other established systems.

Whilst the binding sites for the second boronic acid (at the 3,5,6 or 3,4,6 positions of D-glucose) depend on the experimental conditions and the particular boronic acid being investigated,[174,179] there is agreement that the strongest interaction between monoboronic acids and D-glucose occurs with the syn-periplanar hydroxyls on the 1 and 2 positions of α-D-glucofuranose.[131,174,175,178] Given these observations and the known importance of pyranose to furanose interconversion, it has been suggested that in the future design of diboronic acid sensors for saccharides, the pyranose form should not be considered in aqueous systems.[179]

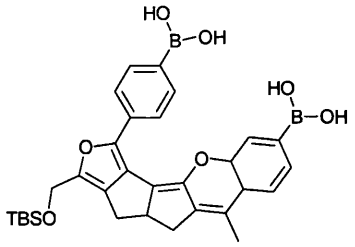

96

Despite these observations Drueckhammer and co-workers successfully used a computer-guided approach to engineer sensor **96**, a receptor specifically designed to complex α-D-glucopyranose at the 1,2 and 4,6 positions.[180] The computational approach produced a rigid molecular scaffold anchoring the two boronic acid groups precisely in space. Defined spatial architecture led the receptor to exhibit a 400-fold greater affinity for D-glucose over any of the other saccharides the receptor was evaluated against. Significantly, ^{1}H NMR confirmed that D-glucose was formed and retained as a stable complex in its pyranose form. Sensor **96** demonstrates that where two point binding is achieved between boronic acids of fixed distances and enforced geometries, different isomeric forms of a saccharide guest may be witnessed within the binding cleft than would have otherwise been predicted from the simple monoboronic acid structural analogues discussed above.

In refining the selectivity of boronic acid appended sensors for saccharides it therefore seems that pre-empting the structure of the guest species or the thermodynamic complex that it will form is non-trivial. It is known that only saccharides with the ability to interconvert between pyranose and furanose forms with an available anomeric hydroxyl pair have so far been reported to interact strongly with boronic acids. It is also generally the case that in aqueous solutions the furanose form of the saccharide will be thermodynamically favoured. However, as illustrated by Drueckhammer and others, in the case of recognition sites with two linked boronic acid fragments this is a function of substrate structure and geometry.

1.4.8 Ditopic Sensors and Competitive Assay Systems

Before concluding this chapter it is worth briefly indicating two closely related areas of sensor design that have emerged to become fruitful areas of research in their own right: ditopic sensors and competitive assay systems. To illustrate these alternative approaches to sensing, one example of each is presented here.

Ditopic Sensors

Ditopic sensors take advantage of two non-equivalent recognition sites. If one is a boronic acid unit, selectivity can be introduced for saccharidic species such as uronic acids, amino sugars and so forth. To achieve this, the second recognition unit must display, and be positioned, such that effective complementarity is observed for both types of functionality present on the guest molecule.

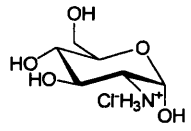

D-glucosamine hydrochloride

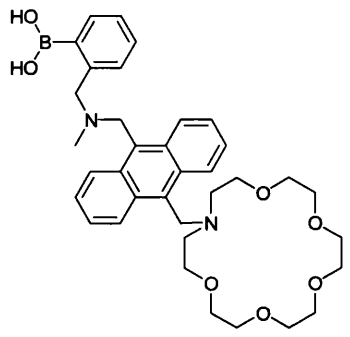

97

Ditopic sensor **97** was reported by Cooper and James in 1997.[181,182] The sensor is similar to the D-glucose selective sensor **68** but has one of the boronic acid units replaced by a monoaza-crown ether receptor, a recognition unit that displayed selectivity for an ammonium terminus. This dual targeted approach induced D-glucosamine hydrochloride selectivity within the system. The observed stability constant (K_{obs}) of sensor **97** with D-glucosamine was 17 M^{-1} in 33.2wt% ethanol in aqueous triethanolamine buffer at pH 7.18.

For a more in depth overview of boronic acid based ditopic fluorescent PET sensors the reader is directed to Appendix 1 on page 267.

Competitive Assay Systems

Unlike the integrated sensors discussed above, competitive assay systems take advantage of an external reporter molecule (generally a commercial dye) complexed within the binding pocket of a receptor. On addition of the required guest to the system the receptor - reporter complex is disrupted as the guest displaces the reporter from the recognition cavity. The release of the reporter molecule into solution affects a change in either colour or fluorescence which is dependant on the reporter molecule used.

Reported by Anslyn and co-workers, the C_3 symmetric tri-podal boronic acid based competitive assay system **98** functioned by displacing 5-carboxyfluorescin on addition of D-glucose-6-phosphate to the system.[183]

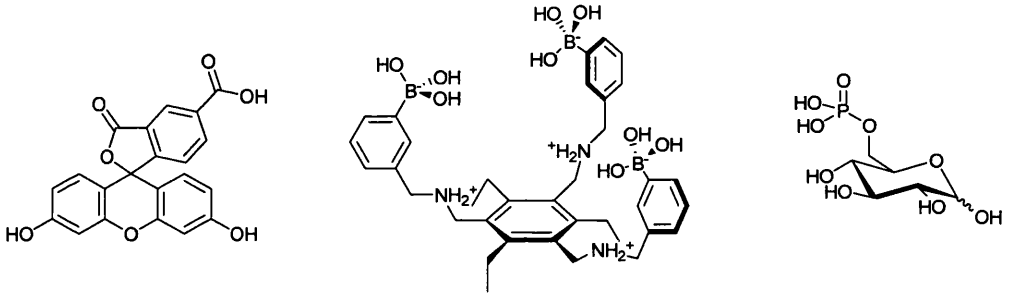

5-carboxyfluorescin (reporter) | **98** (receptor) | D-glucose-6-phosphate (guest)

Visually, addition of the D-glucose-6-phosphate caused a decrease in the absorption of light at 494 nm allowing the concentration of the guest to be monitored directly within the visible spectrum. The observed stability constants (K_{obs}) for receptor **98** were 3×10^2 M^{-1} with 5-carboxyfluorescin and 1.6×10^3 M^{-1} with D-glucose-6-phosphate in an aqueous 70wt% methanol in aqueous HEPES buffer at pH 7.4.

For more information on published competitive assay systems the reader is directed to the extensive reviews on boronic acid sensory systems that have been recently published.[8,9]

1.5 SUMMARY OF INTRODUCTION

- The primary interaction of a boronic acid with a diol is covalent and involves the rapid and reversible formation of a cyclic boronate ester. Boronic acids are therefore ideally suited to the recognition of saccharides in water, overcoming the problem of solvation inherent in synthetic receptors reliant on hydrogen bonding interactions.

- On complexation of a vicinal diol to a boronic acid there is a contraction of the O-B-O bond angle with a concomitant increase in the acidity of the boron species. This phenomenon forms the basis of many of the sensory systems developed around boronic acids.

- Boronic acid – diol complex formation is heavily pH dependent. Rate and stability constants increase by around four and five orders of magnitude, respectively, at pHs above the pK_a of the boronic acid. It has been postulated that these observations can be accounted for by an increase in the rate of the kinetically significant proton transfer mechanism when boron is present as the tetrahedral boronate anion.

- When considering spectrophotometrically derived observed stability constants (K_{obs}) of boronic acids with diols it should be recalled that the observed values have a "medium dependence" on the presence of any Lewis basic components in solution.

- The introduction of a carefully located tertiary amine proximal to the boron centre of a fluorescent sensor permits the sensor to function at lower pH and introduces an "off-on" optical response to the system *via* photoinduced electron transfer (PET).

- The tertiary amine – boronic acid (N-B) interaction in a boronic acid based PET sensor has a strength in the range of 15 to 25 kJ mol^{-1}: to date the exact nature of this interaction has not been established.

- The use of two boronic acid receptors within a binding site introduces saccharide selectivity, permitting saccharides such as D-glucose to be specifically targeted.

- Computational data and observed experimental results indicate that strong binding between boronic acids and saccharides occurs preferentially with saccharides that have an available anomeric hydroxyl pair which has the capacity to conform to a syn-periplanar alignment. In the vast majority of cases this requires formation of the furanose form of the saccharide.

CHAPTER TWO:
Results and Discussion I

The expression "fits like a glove" is an odd one, because there are many different types of gloves and only a few of them are going to fit the situation you are in.

Lemony Snicket

A Series of Unfortunate Events: The Grim Grotto: Book the Eleventh

2 Results and Discussion I

2.1 Overview of Results and Discussion I

During recent years the use of a modular approach in the design and synthesis of new fluorescent PET sensors has been at the fore of the research undertaken towards molecular sensing within the T.D. James research group.

From a design perspective, fluorescent PET sensors are particularly well suited to a modular construct. The compartmentalisation that is derived from the insulated receptor and fluorophore units means that, where the structure allows, these terminal components can be modified largely independently.

In an effort to understand how recognition trends between boronic acid based sensors and saccharides are influenced as a function of the sensor's structure, libraries of compounds were synthesised where single variables were modified sequentially. The development of these libraries has been recently reviewed by us, see Phillips and James,[5,***] and is discussed here as an integral part of the results presented in the next chapter. Work in *Results and Discussion I* includes research undertaken by us as well as by past members of the T. D. James research group.

*** M. D. Phillips and T. D. James, *J. Fluorescence*, 2004, **14**, 549-559.

2.2 MODULAR ASSEMBLY

Rationale

In the design of boronic acid based sensory systems it has been established that two receptor units are required if selectivity is to be achieved for specific saccharides.[158] It has been demonstrated that the *N*-methyl-*o*-(aminomethyl)phenylboronic acid fragment is particularly effective at signalling these binding events *via* PET when correctly positioned alongside a suitable fluorophore.[78]

Retaining the same dual boronic acid recognition units throughout, it was thought advantageous to develop a modular system in which the linker and fluorophore units of these sensors could be modified independently. It was postulated that this approach would afford information on the effect of altering the dimensions of the binding pocket, permit the emission wavelength of the systems to be altered and provide clear data on the role of these individual variables by allowing them to be altered in a controlled manner.

Design of the Molecular Scaffold

In designing a range of modular sensors from which quantitative trends are to be derived, a generic scaffold must be established at the start of the project and adhered to throughout, if a meaningful comparison is to be obtained across the series.

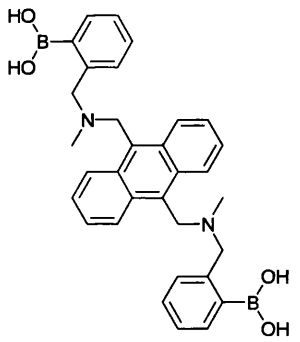

68

Whilst sensors developed around the anthracene core unit (e.g. **68**) have proved to be selective for saccharides such as D-glucose, the rigid core unit (functioning as the scaffold, linker and fluorophore) limits the modifications that can be made to any one

part of the system without influencing the sensor as a whole. Perusing the literature it appears that this limitation holds for a great many sensors.

In adopting a modular approach it was deemed important to design a system in which the receptor, linker and fluorophore units could be connected to the molecular scaffold in such a way as to permit these subunits to be varied independently.

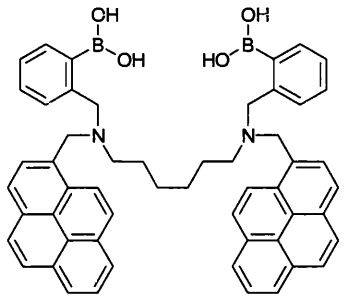

99

Reported in 1995 compound **99** provides an example of a fluorescent PET sensor with clear compartmentalisation of the receptor, linker and fluorophore subunits.[184] Documented by Sandanayake, James and Shinkai, it was found that the stoichiometry of saccharide binding with sensor **99** (i.e. 1:1 or 2:1 saccharide/sensor) could be correlated with a decrease in the fluorescence emission due to the excited state dimer (excimer) complex formed between the two pyrene residues, see Scheme 36 (page 88) broad peak ~ 470 nm. Moreover, the saccharide concentration could be monitored *via* the usual increase in fluorescence emission intensity from the LE state of pyrene as a function of PET, see Scheme 36 (page 88) peaks at 370, 397 and 417 nm. The observed stability constants (K_{obs}) for **99** were 2 000 M^{-1} with D-glucose and 790 M^{-1} with D-galactose in 33wt% methanol in water.[184]

Appleton and Gibson investigated the effect of longer linker units between the two receptor units in this system.[185] 1,6-diaminohexane, 1,7-diaminoheptane, 1,8-diaminooctane, 1,12-diaminododecane and 4,4 -diamino dicyclohexylmethane were introduced, with the observation that six- and seven- carbon linkers conferred the highest selectivity towards D-glucose whereas extended linkers lost the selectivity derived from the cooperative action of the dual recognition units.

Compound **99** was re-synthesised within the James group and the fluorescence properties re-evaluated.[5] The fluorescence titrations of compound **99** (7.5×10^{-7} mol dm^{-3}, λ_{ex} = 342 nm) with different saccharides were carried out in a pH 8.21 aqueous methanolic buffer solution [52.1wt% methanol (KCl, 0.01000 mol dm^{-3}; KH_2PO_4, 0.002752 mol dm^{-3}; Na_2HPO_4, 0.002757 mol dm^{-3})]. The observed stability constants (K_{obs}) with coefficient of determination (r^2) were calculated by the fitting of emission intensity *versus* saccharide concentration using custom written non-linear (Levenberg-Marquardt algorithm) curve fitting.[182] The errors reported are the standard errors obtained from the best fit. Relative fluorescent enhancements (I/I_0) are also reported. The results for **99** with D-glucose were K_{obs} = 260 ± 15 M^{-1} (r^2 = 1.00), I/I_0 = 4.9; with D-galactose K_{obs} = 237 ± 6 M^{-1} (r^2 = 1.00), I/I_0 = 4.2; with D-fructose K_{obs} = 244 ± 26 M^{-1} (r^2 = 0.99), I/I_0 = 3.4 and with D-mannose K_{obs} = 32 ± 3 M^{-1} (r^2 = 0.99), I/I_0 = 3.2.

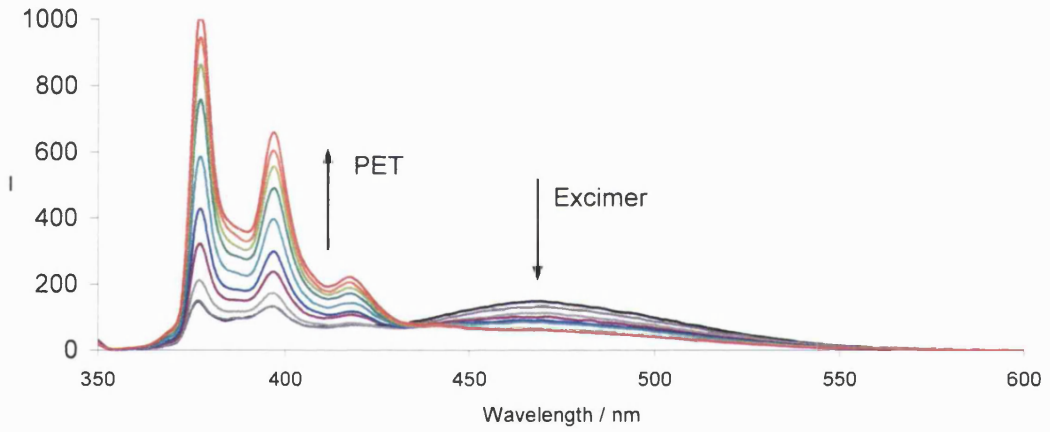

Scheme 36. *The fluorescence emission spectrum of **99** (7.5×10^{-7} mol dm^{-3}, λ_{ex} = 342 nm) with increasing amounts of D-glucose (from 0 to 1.0×10^{-1} mol dm^{-3}) in a pH 8.21 aqueous methanolic buffer solution [52.1 wt% methanol (KCl, 0.01000 mol dm^{-3}; KH_2PO_4, 0.002752 mol dm^{-3}; Na_2HPO_4, 0.002757 mol dm^{-3})].*

In Scheme 36 the long wavelength excimer emission due to π stacking of the pyrene fluorophores can be observed around 470 nm. This fluorescence emission has a somewhat more modest intensity than the emission observed due to the LE state with peaks at 370, 397 and 417 nm. As D-glucose binds to the receptor it forms a rigid 1:1 cyclic structure and in so doing increases the proximity of the boronic acids. It is thought that this interaction levers the two pyrene fluorophores apart so as to increase their separation and reduce the π-π interactions between them. This change in geometry

of the system's components manifests itself in the fluorescence emission spectrum as a clear decrease in excimer emission intensity with added D-glucose.

The increase in the emission intensity from the LE state with increased saccharide concentration, modulated by PET, remains largely unaffected when compared to sensors with single fluorophores.

General Design Assembly

Six carbons separate the two amino nitrogens in the D-glucose selective compound **99**, the same number as separate the two amino nitrogens in the D-glucose selective sensor **68**. The boronic acid groups appended to the two nitrogens of sensor **99** (and **68**) must both take part in a binding event to allow the full fluorescence emission of the system to be restored. The dual recognition sites and their separation are therefore key to the observed saccharide selectivity. With this in mind it was decided that a generic template based on sensor **99** would prove effective. The general design assembly proposed is illustrated in Figure 28.

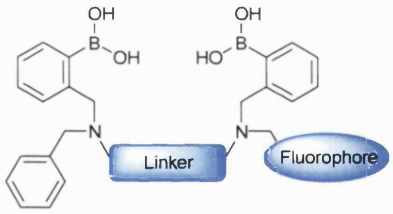

Figure 28: *Receptor and spacer groups remained unchanged throughout. Two N-methyl-o-(aminomethyl)phenylboronic acid groups functioned as the receptor units with a methylene spacer modulating PET.*

This design retains the two boronic acid groups required for selectivity but allows the separation between them to be varied by altering the linker. It also permits the fluorophore to be varied independently and by using only one fluorophore overcomes the problems that may arise from excimer emission, [†††] insolubility, excessive hydrophobicity and steric crowding at the binding pocket.

[†††] Whilst excimer emission can be used to visually determine the stoichiometry of the binding event and advantageously red shifts the fluorescence emission, the comparatively small changes in fluorescence emission intensity do not lend this part of the emission band to accurate signalling of saccharide

2.3 CONTROLLING SUBSTITUTIONS ON POLYAMINES

Background

Synthetically, one of the first challenges faced in forming these products was controlling the regioselectivity of the reaction. The synthesis of modular sensors, with the generic construct illustrated in Figure 28 occurs around the α,ω-alkanediamine linker unit. Although the initial alkanediamine molecule is symmetrical and the terminal amine groups have no regioselective pre-disposition which would allow the researcher to readily differentiate between them, non-equivalent substituents are required at each end of the linker.

The first known fluorescent PET sensors appended with polyamine substituents, e.g. compound **100**, were reported by Czarnik and co-workers in 1989.[186] These systems displayed selectivity for phosphate and functioned in the same way as the boronic acid systems under investigation: a hydrogen bonding interaction at the benzylic amine being used to modulate PET. It is quite conceivable that these phosphate selective receptors could be used in conjunction with boronic acid recognition units in the construct of ditopic sensors. An overview of the documented ditopic fluorescent PET sensors containing boronic acid fragments is contained in Appendix 1 (page 267) and the reader interested in further information on the subject is directed there.

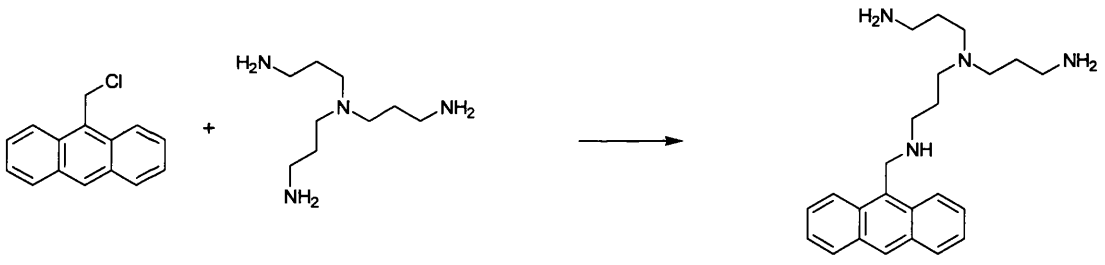

100

Scheme 37. *Synthesis of **100** as prepared by Czarnick and co-workers[186] using an adaptation of a previous literature procedure.[187]*

Our chief interest here is with the transferable synthetic methodology which allows selective substitutions to occur on poly-amino systems. An examination of the synthetic

concentrations. It is also generally the case that sensors with two fluorophore units have observed binding constants (K_{obs}) ~ four times lower than their mono-fluorophore counterparts.

procedure used by Czarnik, Scheme 37, reveals that compound **100** and its 9,10-disubstituted anthracene sister compound were synthesised from the reaction of tris-(3-aminopropyl)amine with 9-(chloromethyl)-anthracene and 9,10-di-(chloromethyl) anthracene respectively.

Previous Findings

We previously investigated the coupling on a model system with similar polyamines and fluorophores halogenated at the benzylic position using conditions analogous to those in Scheme 37.[188] It was our experience, however, that multiple additions occurred with halogenated starting materials, both on the same terminal amines as well as on different amine groups of the same molecule.

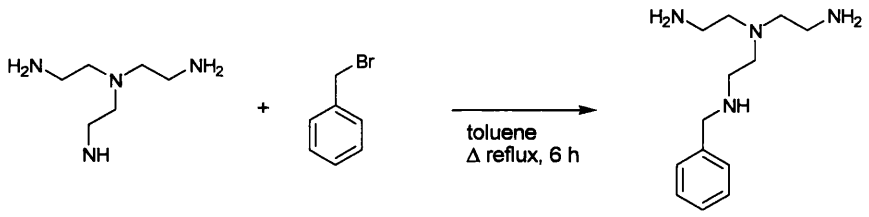

Scheme 38. *The proposed model reaction investigated for the selective substitution of a single aromatic fragment at one amine terminus. A 1:1 mixture of tris-(2-aminoethyl)amine and benzylbromide was utilised.*

Using the model system illustrated in Scheme 38 we rapidly established that exploiting unfavourable interactions, such as those arising from steric bulk, to diminish multiple substitutions from occurring on individual terminal amine nitrogens was not possible. Rather than observing that substitution at newly formed secondary amines was disfavoured. A glut of tertiary amines was observed, these species being far more profuse than would be expected from a statistical prediction. Given the small decrease in basicity (and therefore reactivity) at nitrogen on formation of the benzylic amine and the significant increase in steric crowding, it appears likely that this result is a facet of an increase in stability of the resulting tertiary amine species due to favourable π-π

stacking interactions between the two hydrophobic surfaces of the aromatic substituents.[‡‡‡]

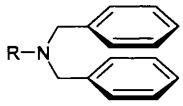

Figure 29. *It appears likely that the preference for multiple substitutions to occur on individual terminal amines is a facet of the increased stability at the resulting tertiary amine due to favourable π-π stacking interactions between the two hydrophobic surfaces of the aromatic substituents.*

To overcome this problem we investigated the use of aldehydes in the coupling of fluorophores with amines. We found that the intermediate imines formed from reacting aldehydes with primary amines, successfully prevented multiple substitutions from occurring on any one nitrogen atom of a given amine terminus.

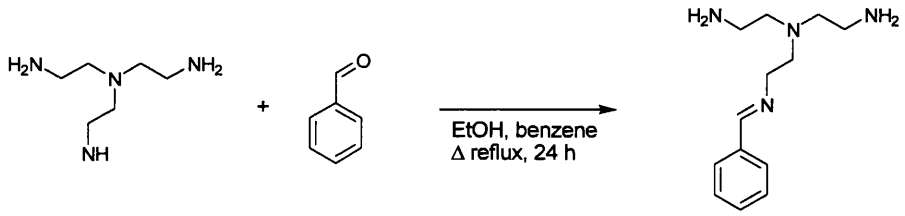

Scheme 39. *The proposed model reaction investigated for the selective substitution of a single aromatic fragment at any given amine terminus. A 1:1 mixture of tris-(2-aminoethyl)amine and benzaldehyde was heated under reflux with the azeotropic removal of water via a Dean Stark head to form the intermediate imine.*

High Dilution Conditions

The problem of substitutions occurring across the same molecule at multiple amino termini presented a more challenging barrier to overcome. During the same investigation the effects of using high dilution conditions indicated that by using an abundance of the polyamine reagent the number of di- and tri-substituted products could be significantly reduced, even if not removed altogether.[188]

The procedure permitted the synthesis of compound **101** and was improved by reacting a six fold equivalent of tris-(2-aminethyl)amine with 9-anthraldehyde, Scheme 40.

[‡‡‡] For comparison, ethylamine has a pK_{aH} = 10.63[189] and *N*-ethyl benzylamine has a pK_{aH} = 10.32.[190] N.B. where amphoteric compounds such as amines are discussed pK_{aH} is used throughout this thesis to refer to the pK_a of the conjugate acid.

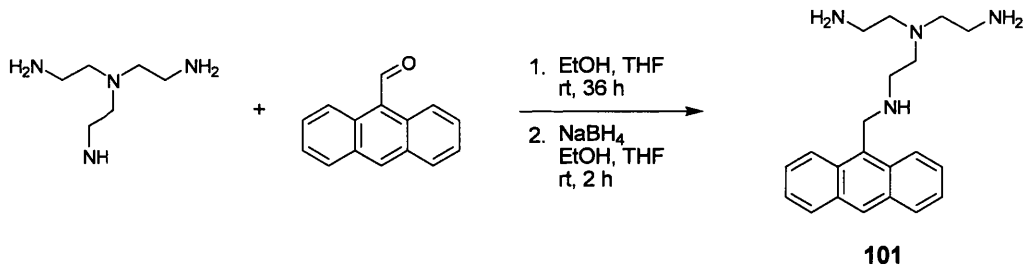

101

Scheme 40. *Increased selectivity was achieved using high dilution conditions coupled with the reductive aminations. 1 eq. of 9-anthraldehyde was added to 6 eq. of tris-(2-aminoethyl)amine.*

Current Work

During the course of our current investigations this procedure allowed the model compounds **102 - 108**, to be synthesised with comparative ease, see Figure 30.

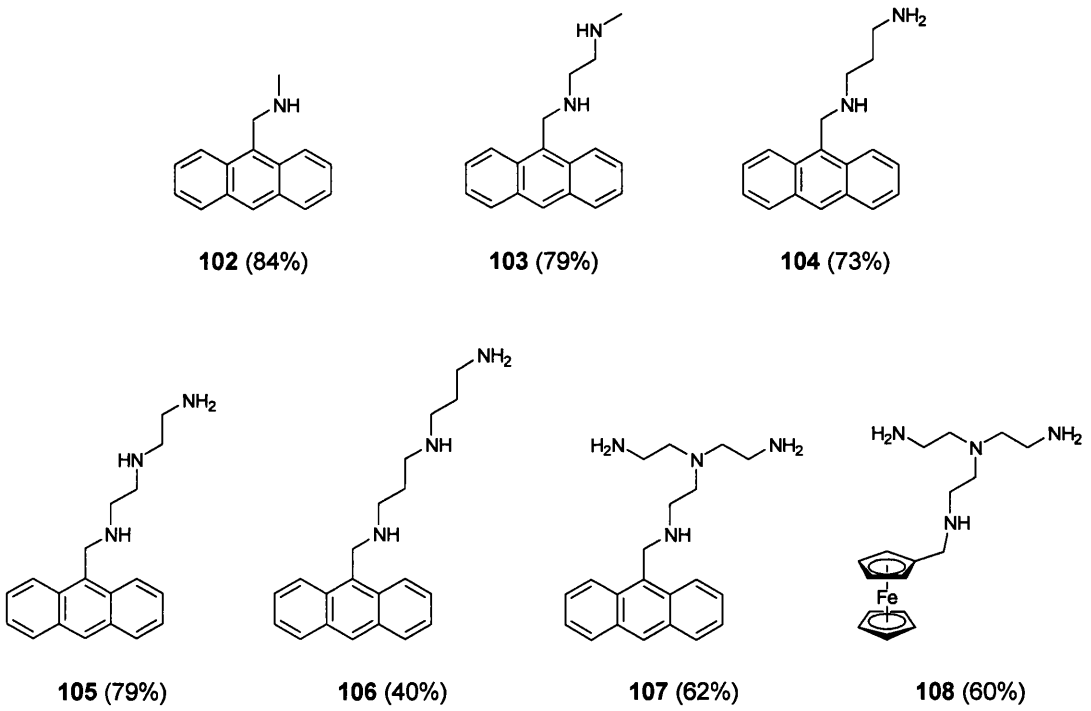

102 (84%) **103** (79%) **104** (73%)

105 (79%) **106** (40%) **107** (62%) **108** (60%)

Figure 30. *Model polyamine fluorescent PET sensors **102-107** and the model electrochemical sensor **108**. The yield obtained following the procedure in Scheme 40 is indicated in brackets.*

From the ^{1}H NMR spectra of these systems it was clear that the desired products accounted for the major species formed, however, the target molecules were rarely isolated entirely pure. It was found that the remaining impurities could be generally ascribed to either un-reacted starting materials or di- and tri-substituted amines. To illustrate this point the ^{1}H NMR spectrum of compound **107**, Figure 31 (page 94), is included. The ^{1}H NMR spectrum of compound **107** is representative of the general trend

observed in these substitution reactions across the series of polyamino alkanes, illustrated in Figure 30.

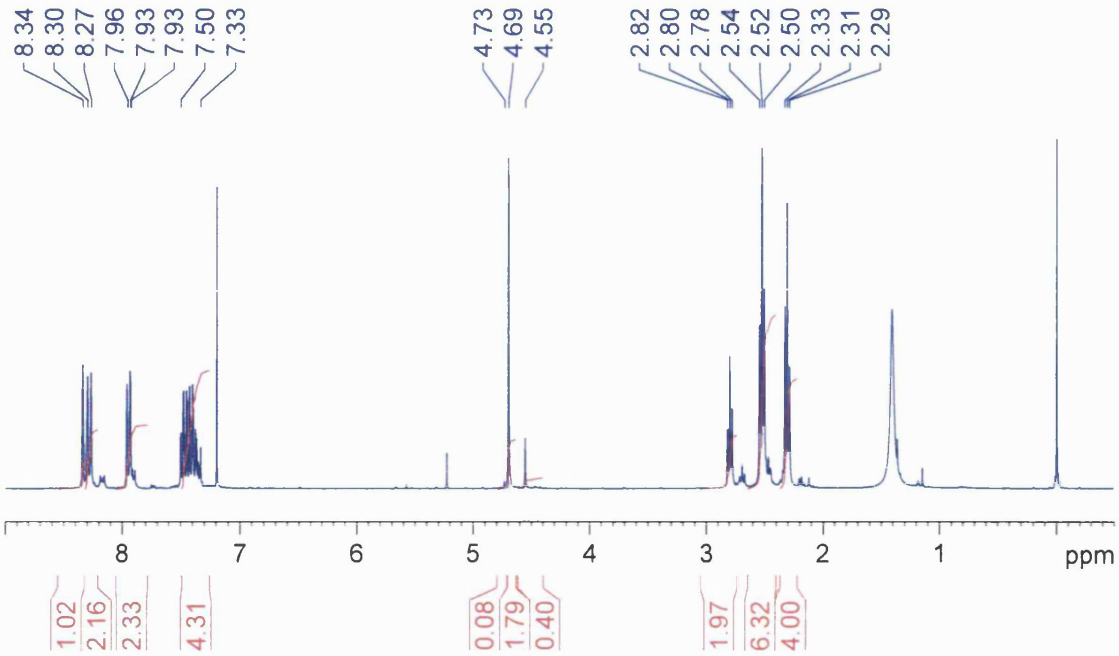

Figure 31. *^{1}H NMR spectrum (300 MHz, $CDCl_3$) of compound **107**, with TMS at 0.00ppm, water at 1.41ppm, DCM at 5.23ppm and the residual solvent peak at 7.19ppm.*

From the ^{1}H NMR spectrum in Figure 31 it can be seen that even under high (6:1 amine/aldehyde) dilution conditions, the reaction mixture has afforded mono-, di- and tri-substituted compounds. These effects can be readily observed by considering the three peaks at 4.55, 4.69 and 4.73ppm respectively which correlate to di-, mono- and tri-substituted tris-(2-aminoethyl)amine respectively, with comparative integral values of ~13, 85 and 2%.

Clearly the reaction yielding the monosubstituted product is favoured, but these experimental conditions led to products with noticeable impurities. The purification of substituted tetra-amines such as compound **107** is non-trivial. The viscous oils do not readily lend themselves to purification techniques such as distillation or silica gel column chromatography and re-crystallisation and filtration cannot be considered for these materials.

2.4 Previous Work within the Group on Modular Systems

2.4.1 Linker Dependence

Synthesis

The work previously undertaken to establish the usefulness of high dilution conditions and reductive aminations on polyamino systems was used in the synthesis of compounds **109**$_{(n=3)}$ - **114**$_{(n=8)}$ with variable linker lengths by Arimori *et al.*, within the T. D. James research group.[188,191,192]

The modular PET sensors **109**$_{(n=3)}$ - **114**$_{(n=8)}$ contained two phenylboronic acid groups, a pyrene fluorophore and a variable linker. The linker was varied from trimethylene **109**$_{(n=3)}$ to octamethylene **114**$_{(n=8)}$. The aim of this research being to elucidate the optimum linker length required for maximum D-glucose selectivity.

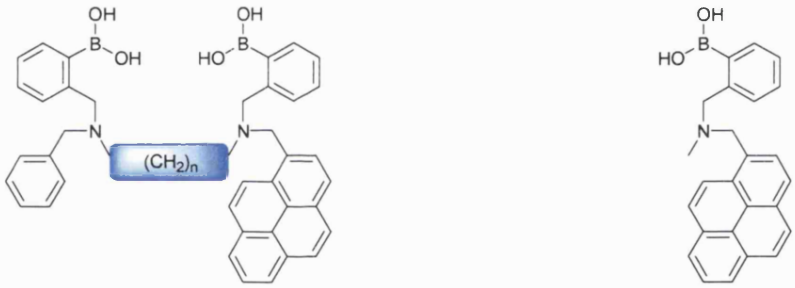

109$_{(n=3)}$
110$_{(n=4)}$
111$_{(n=5)}$
112$_{(n=6)}$
113$_{(n=7)}$
114$_{(n=8)}$

128$_{(pyrene)}$

Figure 32. *The modular PET sensors* ***109***$_{(n=3)}$ - ***114***$_{(n=8)}$ *with monoboronic acid reference compound* ***128***$_{(pyrene)}$.

Linker Synthesis and Saccharide Recognition

As before the required α,ω-alkanediamine was added to benzaldehyde under 5:1 (α,ω-alkanediamine/benzaldehyde) dilution conditions and heated under reflux for 3 hours prior to reduction with sodium borohydride and the subsequent aqueous work up.

The conditions developed for the model polyamine systems, Scheme 40, were improved within the T. D. James research group by Arimori *et al.*[192] by the introduction of a stoichiometric quantity of *p*-toluenesulfonic acid (*p*-TsOH) to the reaction mixture.

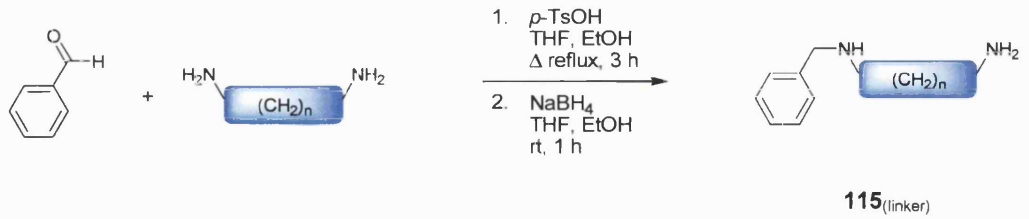

Scheme 41. *Synthesis of core units* ***115***$_{(linker)}$ *where n=3 – 8 under 5:5:1 (amine/p-TsOH/aldehyde) dilution conditions (19-78% yield).*

In carrying out this first step, where high dilution conditions alone were used, an 18% yield of the required *N*-benzyl-1,6-diaminohexane was achieved from benzaldehyde and 1,6-diaminohexane; a significant amount of the disubstituted *N,N*-dibenzylhexane-1,6-diamine was observed in the ^{1}H NMR spectrum (unpublished results). This step was significantly improved with the addition of 1 equivalent of *p*-toluenesulfonic acid to every 1 equivalent of diamine, the enhanced reaction afforded *N*-benzyl-1,6-diaminohexane in 78% yield.

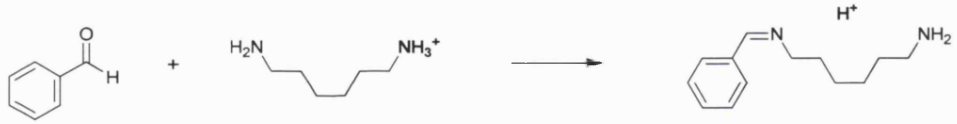

Scheme 42. *Reaction of benzaldehyde with 1,6-hexamethylene diamine in the presence of p-TsOH (1:1:1 amine/p-TsOH/aldehyde).*

The reason for the increased preference towards monosubstituted alkyldiamines in the presence of a stoichiometric amount of *p*-toluenesulfonic acid is generally ascribed to the operation of a crude protection mechanism, Scheme 42. One can envisage half of all the amines present, after addition of the *p*-toluenesulfonic acid, to be protonated, i.e. one ammonium cation present on each molecule of diamine, thus preventing the protonated end of the molecule from reacting, and so driving the equilibrium in favour of the monosubstituted products.

Having isolated the monosubstituted alkyl-diamine, a second reductive amination with 1-pyrenecarboxaldehyde was conducted. The product was then purified by Sephadex®

LH-20 column chromatography (with methanol as eluent) to complete the synthesis of the derivatised linkers **116**$_{(linker)}$, see Scheme 42.

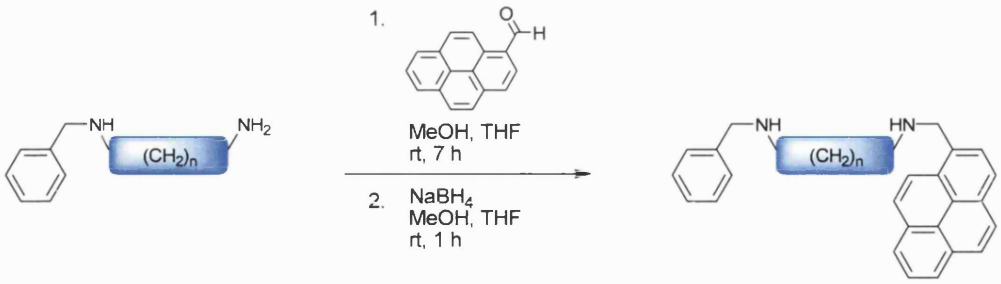

Scheme 43. *Synthesis of compound* ***116***$_{(linker)}$ *where n=3 – 8 (47-86% yield).*

The target molecule was then prepared as in Scheme 44. The final purification step was achieved by reprecipitation of the resulting residue from chloroform in *n*-hexanes to yield a yellow powder, a typical final purification step in the synthesis of a compound containing an *o*-(methylamine)phenylboronic acid fragment.

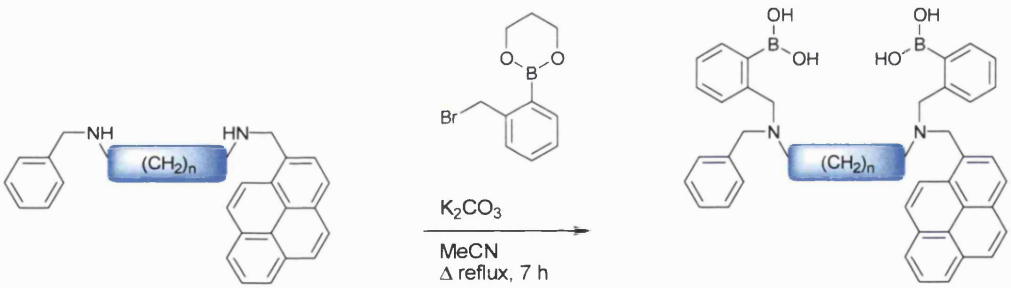

116$_{(linker)}$ **109**$_{(n = 3)}$ **- 114**$_{(n = 8)}$

Scheme 44. *Synthesis of diboronic acid sensors* ***109***$_{(n=3)}$ *-* ***114***$_{(n=8)}$ *(35-83% yield).*

The fluorescence titrations of **109**$_{(n=3)}$ **- 114**$_{(n=8)}$ and **128**$_{(pyrene)}$ (1.0×10^{-7} mol dm^{-3}) with different saccharides were carried out in a pH 8.21 aqueous methanolic buffer solution, as described above (see page 88).[193] The fluorescence intensity of sensors **109**$_{(n=3)}$ **- 114**$_{(n=8)}$ and **128**$_{(pyrene)}$ increased with increasing saccharide concentration. The observed stability constants (K_{obs}) of PET sensors **109**$_{(n=3)}$ **- 114**$_{(n=8)}$ and **128**$_{(pyrene)}$ were calculated by fitting the emission intensity at 397 nm *versus* saccharide concentration and are given in Table 3.

Table 3. Quantum yield (qFM) values for compounds **109**$_{(n=3)}$ - **114**$_{(n=8)}$ and **128**$_{(pyrene)}$ in the absence of saccharides. Observed stability constant (K_{obs}) (determination of coefficient; r^2) and fluorescence enhancements for compounds **109**$_{(n=3)}$ - **114**$_{(n=8)}$ and **128**$_{(pyrene)}$ with monosaccharides. The system with the highest observed stability constant (K_{obs}) is highlighted in red.

sensor		D-glucose		D-galactose	
	qFM	K_{obs} / dm^3 mol^{-1}	fluorescence enhancement	K_{obs} / dm^3 mol^{-1}	fluorescence enhancement
109$_{(n=3)}$	0.16	103 ± 3 (1.00)	3.9	119 ± 5 (1.00)	3.5
110$_{(n=4)}$	0.16	295 ± 11 (1.00)	3.3	222 ± 17 (1.00)	3.7
111$_{(n=5)}$	0.20	333 ± 27 (1.00)	3.4	177 ± 15 (1.00)	3.0
112$_{(n=6)}$	0.24	962 ± 70 (0.99)	2.8	657 ± 39 (1.00)	3.1
113$_{(n=7)}$	0.16	336 ± 30 (0.98)	3.0	542 ± 41 (0.99)	2.9
114$_{(n=8)}$	0.19	368 ± 21 (1.00)	2.3	562 ± 56 (0.99)	2.3
128$_{(pyrene)}$	0.17	44 ± 3 (1.00)	4.5	51 ± 2 (1.00)	4.2

sensor		D-fructose		D-mannose	
	qFM	K_{obs} / dm^3 mol^{-1}	Fluorescence enhancement	K_{obs} / dm^3 mol^{-1}	Fluorescence enhancement
109$_{(n=3)}$	0.16	95 ± 9 (0.99)	3.6	45 ± 4 (1.00)	2.7
110$_{(n=4)}$	0.16	266 ± 28 (0.99)	4.2	39 ± 1 (1.00)	3.4
111$_{(n=5)}$	0.20	433 ± 19 (1.00)	3.4	48 ± 2 (1.00)	3.0
112$_{(n=6)}$	0.24	784 ± 44 (1.00)	3.2	74 ± 3 (1.00)	2.8
113$_{(n=7)}$	0.16	722 ± 37 (1.00)	3.3	70 ± 5 (1.00)	2.7
114$_{(n=8)}$	0.19	594 ± 56 (0.99)	2.3	82 ± 3 (1.00)	2.2
128$_{(pyrene)}$	0.17	395 ± 11 (1.00)	3.6	36 ± 1 (1.00)	3.7

To help visualise the trends in the observed stability constants (K_{obs}) documented in Table 3, the observed stability constants (K_{obs}) of the diboronic acid sensors **109**$_{(n=3)}$ - **114**$_{(n=8)}$ are reported in Figure 33 divided by (i.e. relative to) the observed stability constants (K_{obs}) of their equivalent monoboronic acid analogue **128**$_{(pyrene)}$. In most cases, the observed stability constants (K_{obs}) with diboronic acid sensors **109**$_{(n=3)}$ - **114**$_{(n=8)}$ are higher than for the monoboronic acid sensor **128**$_{(pyrene)}$.

It is known that D-glucose and D-galactose will bind to diboronic acids readily using two sets of diols, thus forming stable, cyclic 1:1 complexes. The allosteric binding of the two boronic acid groups is clearly illustrated by the relative difference between the observed stability constants (K_{obs}) of the equivalent di- and mono-boronic acid

compounds. The observed stability constants (K_{obs}) of the diboronic acid sensors are up to ~ 22 times larger than with their monoboronic acid counterparts, see Figure 33.

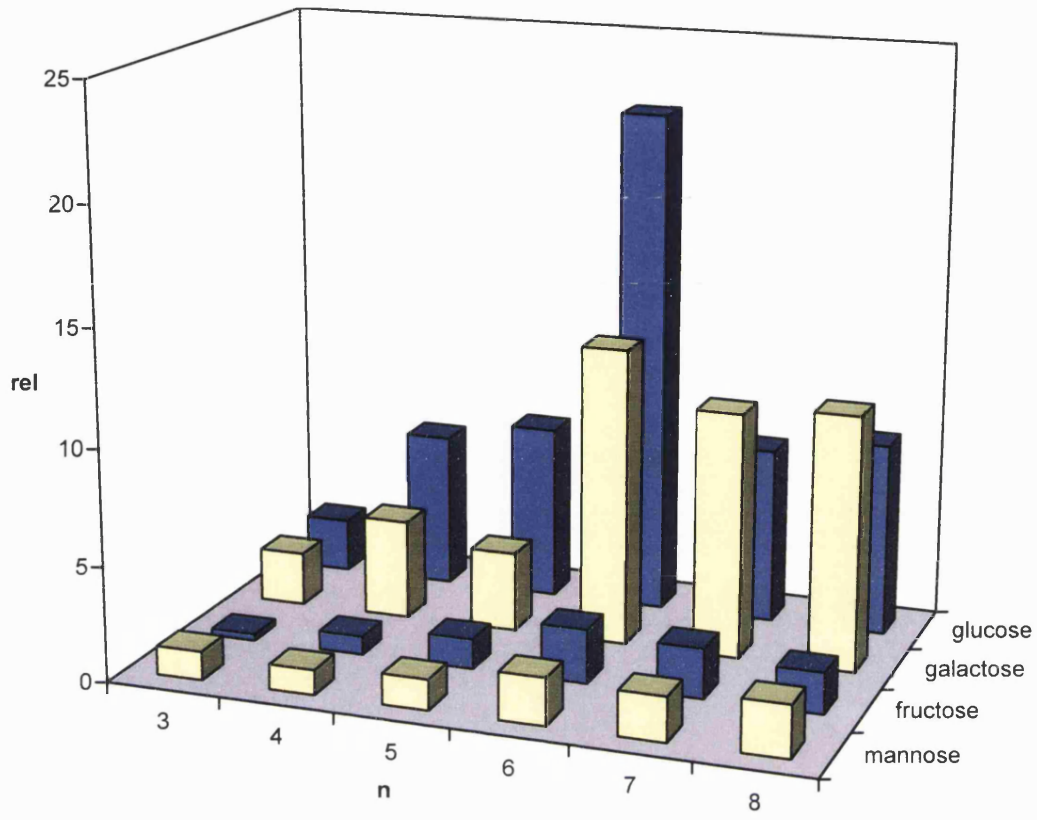

Figure 33. *Observed stability constants (K_{obs}) of* ***109***$_{(n=3)}$ *-* ***114***$_{(n=8)}$ *divided by the observed stability constants (K_{obs}) of* ***128***$_{(pyrene)}$*, to yield relative values with saccharides. The* D*-configuration of the monosaccharides was used throughout this evaluation.*

The observed stability constants (K_{obs}) for the diboronic acid sensors with D-fructose and D-mannose are, at most, twice as strong as with the monoboronic acid sensor **128**$_{(pyrene)}$. Each D-fructose and D-mannose molecule will only bind to one boronic acid unit through one diol. This allows complexes to form with overall 2:1 (saccharide/sensor) stoichiometry. The relative values of *ca.* 2 are indicative of two independent saccharide binding events on each sensor, with no increase in stability derived from cooperative binding.

The highest observed stability constants (K_{obs}) for D-glucose within these systems was obtained by sensor **112**$_{(n=6)}$. The flexible six carbon linker provided the optimal

selectivity for D-glucose over other saccharides, this is in agreement with the observed selectivity of compounds **68** and **99** which also linkers containing six carbon atoms.

Curiously there is an inversion in the selectivity displayed by these systems on going from a six to a seven carbon linker. From Figure 33 it is clear that the trimethylene linked $\mathbf{109}_{(n=3)}$ shows little specificity between D-glucose and D-galactose. Increasing the size of the binding pocket, tetramethylene $\mathbf{110}_{(n=4)}$ through to hexamethylene $\mathbf{112}_{(n=6)}$, induces a clear selectivity for D-glucose, with $\mathbf{112}_{(n=6)}$ providing the strongest binding by far. However, there is an inversion in this selectivity on increasing the linker length to heptamethylene $\mathbf{113}_{(n=7)}$ and octamethylene $\mathbf{114}_{(n=8)}$, with the enlarged binding pocket being D-galactose selective.

This facet was initially ascribed to the difference in configuration of these diastereomers.[192] The 1,2- and 4,6-diols of D-glucose point in the same direction (down), but in D-galactose (the 4-epimer of D-glucose), the 1,2-diol is down and the 4,6-diol is up, this is illustrated in Figure 34. Therefore, not only are the inter-diol distances of D-galactose slightly longer than in D-glucose but the diols are also on opposite faces of the saccharide ring. On this basis it seemed reasonable to expect better complementarity for D-galactose with a larger inter-receptor distance than for D-glucose.

glucose galactose

Figure 34. *The α-D-pyranose forms of glucose and galactose with the 1,2- and 4,6-diols highlighted in red.*

As discussed above (see Section 1.4.7, *The Importance of Pyranose to Furanose Interconversion*, page 72) current thinking requires that we consider saccharidic forms where a syn-periplanar arrangement of the anomeric hydroxyl pair can be attained. Generally this requires formation of the furanose form of the saccharide. However, computational work has shown that in the case of D-galactose the α-D-furanose form of the saccharide is not the only species that can be considered with a syn-periplanar alignment of the anomeric hydroxyl pair.[175]

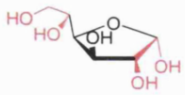

α-D-glucofuranose

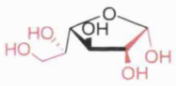

α-D-galactofuranose

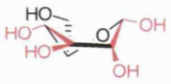

α-D-galactopyranose
(twist boat)

Figure 35. *The α-D-furanose forms of glucose and galactose with the 1,2- and 5,6-diols highlighted in red, as well as the twist boat conformation of the α-D-pyranose form of galactose with the 1,2- and 3,4-diols highlighted in red.*

On complexation of a boronic acid to the diol in the 1,2-position of α-D-galactopyranose a reorientation of the saccharide can afford an acetal ring with a boat or twist boat conformation. This reorientation permits a second boronic acid group to bind with the diol in the 3,4-position producing an energetically stable complex with the pyranose form of the saccharide.

In light of this new data it seems plausible that the preference of D-galactose for a slightly larger binding pocket than D-glucose can be ascribed to the stability of the preferred ring form. D-galactose can generate complexes with boronic acids in its pyranose form, whereas D-glucose will prefer the smaller furanose ring form.

2.4.2 Linker Dependence and Disaccharides

When compared to monosaccharide receptors only a small number of synthetic, boronic acid based receptors for di-[43,194-196] and oligo-saccharides[197-204] currently exist. One reason is the problem associated with positioning the two binding units to create a selective receptor for these larger and more flexible guests. Following the investigation into the effect of linker length on monosaccharides, the selectivity of sensors **109**$_{(n=3)}$ - **114**$_{(n=8)}$ towards disaccharides was probed, see Arimori, Phillips and James.[205,§§§]

For consistency the same disaccharides were evaluated here as were used in the evaluation of sensor **93** (page 77).[178] For the structures of D-glucose, melibiose and maltose, see Scheme 34 (page 78) and for the structures of D-fructose, lactulose and leucrose, see Scheme 35 (page 79). The fluorescence titrations of sensors **109**$_{(n=3)}$ - **114**$_{(n=8)}$ and **128**$_{(pyrene)}$ with different saccharides, were carried out in a pH 8.21 aqueous methanolic buffer solution, as described above (page 88). The fluorescence intensity of

§§§ S. Arimori, M. D. Phillips, and T. D. James, *Tetrahedron Lett.*, 2004, **45**, 1539-1542.

109$_{(n=3)}$ - **114**$_{(n=8)}$ and **128**$_{(pyrene)}$ (1.0×10^{-7} mol dm^{-3}, λ_{ex} = 342 nm) increased with increasing saccharide concentration. The observed stability constants (K_{obs}) of PET sensors **109**$_{(n=3)}$ - **114**$_{(n=8)}$ and **128**$_{(pyrene)}$ were calculated by fitting the emission intensity at 397 nm *versus* saccharide concentration curves. Fluorescence enhancements were calculated by the same method. Where the emission intensity at 397 nm *versus* concentration of saccharide curves failed to describe a distinct plateau the maximum observed fluorescence enhancements were reported. The observed stability constants (K_{obs}) and fluorescence enhancements for **109**$_{(n=3)}$ - **114**$_{(n=8)}$ and **128**$_{(pyrene)}$ are given in Table 4 and are displayed graphically in Figure 36 and Figure 37.

Table 4. Observed stability constant (K_{obs}) (determination of coefficient; r^2) and fluorescence enhancement for the disaccharide complexes of compounds **109**$_{(n=3)}$ - **114**$_{(n=8)}$ and **128**$_{(pyrene)}$.[206]

sensor	melibiose		maltose	
	K_{obs} / dm^3 mol^{-1}	fluorescence enhancement	K_{obs} / dm^3 mol^{-1}	fluorescence enhancement
109$_{(n=3)}$	33 ± 7 (0.98)	2.4	0 ± 2 (0.96)	1.5[a]
110$_{(n=4)}$	77 ± 9 (0.99)	4.9[a]	31 ± 7 (0.98)	3.5 [a]
111$_{(n=5)}$	184 ± 11 (1.00)	3.8	2 ± 1 (0.99)	2.1 [a]
112$_{(n=6)}$	339 ± 17 (1.00)	2.9	52 ± 14 (0.98)	2.3
113$_{(n=7)}$	153 ± 4 (1.00)	3.3	5 ± 1 (1.00)	2.0 [a]
114$_{(n=8)}$	192 ± 30 (0.98)	2.9	22 ± 4 (0.98)	2.4 [a]
128$_{(pyrene)}$	96 ± 5 (1.00)	3.9	5 ± 1 (0.99)	2.1 [a]

sensor	lactulose		leucrose	
	K_{obs} / dm^3 mol^{-1}	fluorescence enhancement	K_{obs} / dm^3 mol^{-1}	fluorescence enhancement
109$_{(n=3)}$	126 ± 14 (0.99)	3.5	29 ± 3 (0.99)	2.5[a]
110$_{(n=4)}$	477 ± 92 (0.95)	4.5	35 ± 2 (1.00)	3.4[a]
111$_{(n=5)}$	616 ± 114 (0.97)	5.0	41 ± 2 (1.00)	3.5[a]
112$_{(n=6)}$	595 ± 30 (1.00)	3.2	69 ± 2 (1.00)	2.9[a]
113$_{(n=7)}$	493 ± 28 (1.00)	3.3	21 ± 5 (0.97)	3.9[a]
114$_{(n=8)}$	528 ± 29 (1.00)	2.6	72 ± 5 (1.00)	2.7[a]
128$_{(pyrene)}$	473 ± 10 (1.00)	3.7	58 ± 3 (1.00)	3.7

[a] Maximum observed fluorescence enhancement.

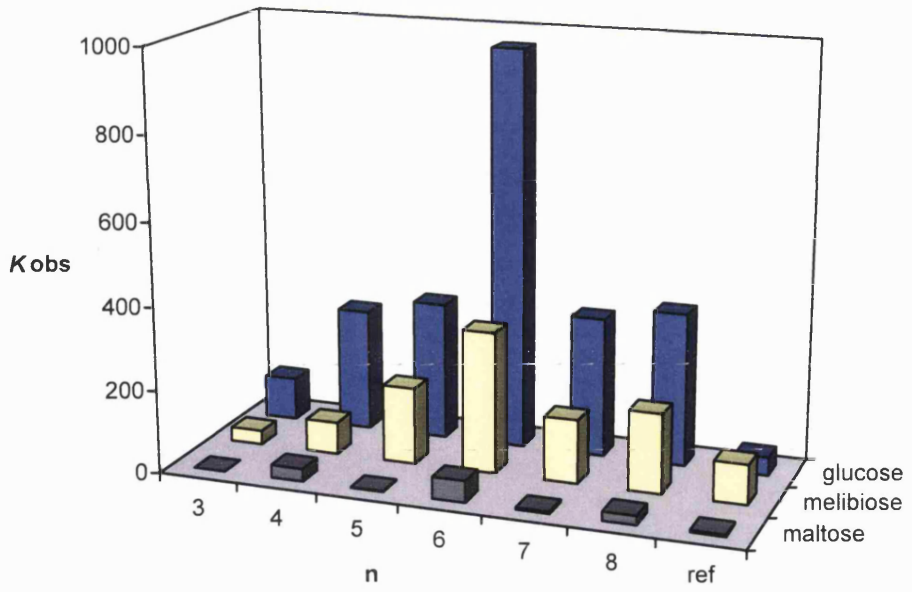

Figure 36. *Observed stability constants (K_{obs}) of the diboronic acid sensors* ***109***$_{(n=3)}$ *-* ***114***$_{(n=8)}$ *and the monoboronic acid reference compound* ***128***$_{(pyrene)}$ *(denoted n = ref) with the* D*-configuration of glucose and its derivatives.*

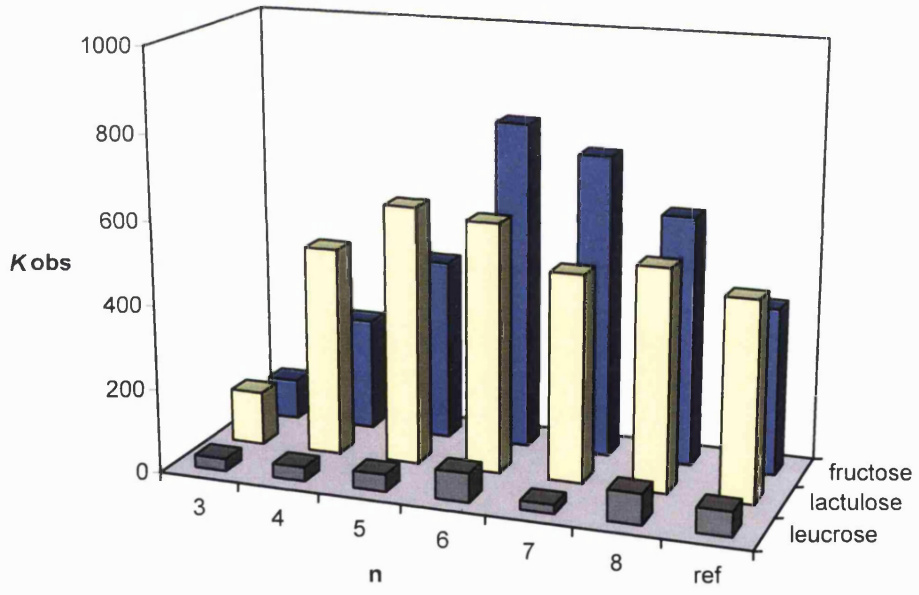

Figure 37. *Observed stability constants (K_{obs}) of the diboronic acid sensors* ***109***$_{(n=3)}$ *-* ***114***$_{(n=8)}$ *and the monoboronic acid reference compound* ***128***$_{(pyrene)}$ *(denoted n = ref) with the* D*-configuration of fructose and its derivatives.*

The observed stability constants (K_{obs}) for compounds **109**$_{(n=3)}$ - **114**$_{(n=8)}$ and **128**$_{(pyrene)}$ with saccharides which have the ability to form a furanose ring with a syn-periplanar anomeric hydroxyl pair (D-glucose, melibiose, D-fructose and lactulose) are large,

consistent with our understanding of the boronic acid diol interaction. Equally, the low or zero values of the observed stability constants (K_{obs}) for saccharides unable to form a furanose ring with a syn-periplanar anomeric hydroxyl pair (maltose and leucrose) are also consistent with current thinking.

The importance of this work compared to previous evaluations is that it was the first to probe the efficacy of diboronic acid units in disaccharide recognition. From previous results it was apparent that the second binding site can bind monosaccharides at their 3, 4, 5 or 6 positions. What had not been examined before was the role of this secondary binding site with disaccharides.

The observed stability constants (K_{obs}) for **109**$_{(n=3)}$ - **114**$_{(n=8)}$ divided by the observed stability constants (K_{obs}) of **128**$_{(pyrene)}$ are displayed in Figure 38. Overall the diboronic acid sensors retain their selectivity for D-glucose over the other saccharides.

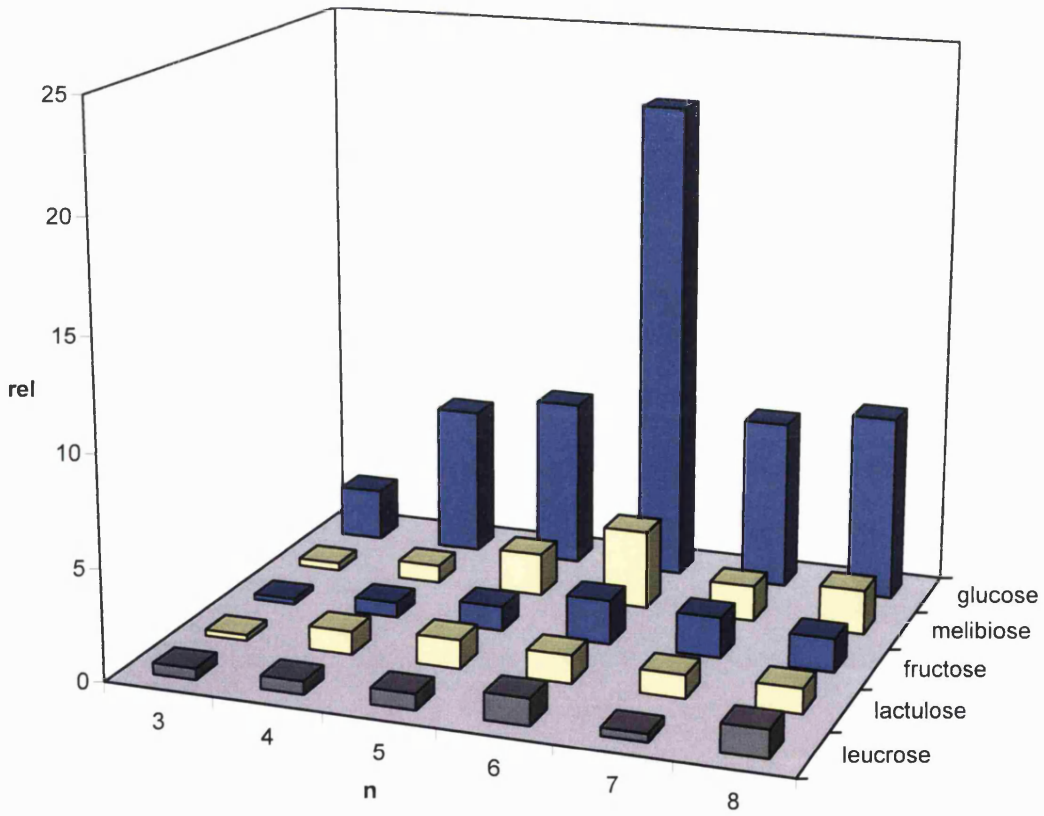

Figure 38. *Observed stability constants (K_{obs}) of* ***109***$_{(n=3)}$ - ***114***$_{(n=8)}$ *divided by the observed stability constants (K_{obs}) of* ***128***$_{(pyrene)}$*, to yield relative values with saccharides. The* D*-configuration of the monosaccharides was used throughout this evaluation.*

It can be seen that the selectivity trend displayed by the sensors towards D-glucose is, to a lesser extent, mirrored by melibiose. An examination of the furanose ring segment of melibiose, Scheme 45, reveals that binding was feasible at the 3,5-positions allowing for the potential formation of a stable cyclic complex.

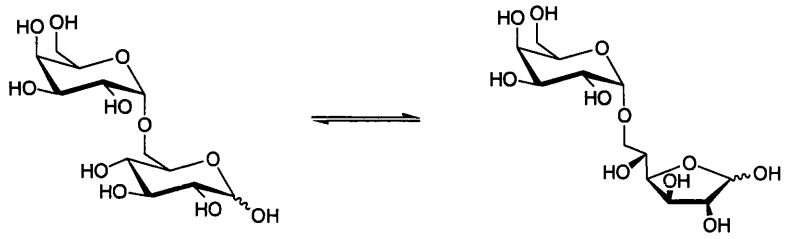

Scheme 45. *The pyranose to furanose interconversion of the glucose ring in melibiose.*

The relative values obtained for maltose were not illustrated in Figure 38 as the relative values were found to fluctuate significantly. The cause of this lies in the value obtained for the observed stability constant (K_{obs}) of reference compound $\mathbf{128}_{(pyrene)}$. As the observed stability constant (K_{obs}) of compound $\mathbf{128}_{(pyrene)}$ with maltose was only 5 ± 1 M^{-1} when the relative values were calculated small changes in the observed stability constants (K_{obs}) were found to manifest large changes in the relative values. Nonetheless, it should be noted that observed stability constants (K_{obs}) for sensors $\mathbf{109}_{(n=3)}$ - $\mathbf{114}_{(n=8)}$ with maltose were small in all cases, with all values contained within the range 0 ± 2 M^{-1} to 52 ± 14 M^{-1}.

It is clear from the data that where the secondary binding sites are blocked on saccharides i.e. on maltose, lactulose and leucrose, no increased stability is derived from the introduction of a second boronic acid unit.

Overall selectivity is retained for the monosaccharides with the ability to form cyclic complexes. An analogous trend is observed for disaccharides which also have the ability to form cyclic complexes, however, the observed stability constants (K_{obs}) are weaker in these instances, a characteristic attributed to the increased steric hindrance at the secondary binding site.

2.4.3 Energy Transfer Systems

The last area of investigation to have been undertaken on modular systems within the T. D. James research group, by Arimori *et al.*[207] was that of energy transfer.

Fluorescence energy transfer is the transfer of excited-state energy from a donor to an acceptor. The transfer occurs as a result of transition dipole-dipole interactions between the donor-acceptor pair.[120] The fluorescent sensor investigated, **117**$_{(phenanthrene\text{-}pyrene)}$, had two phenylboronic acid groups a hexamethylene linker and two different fluorophore groups: phenanthrene and pyrene.

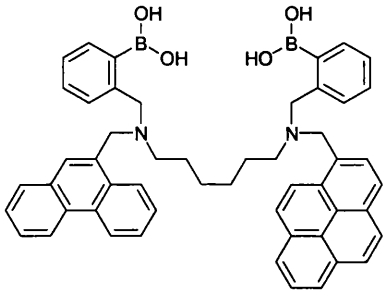

117$_{(phenanthrene\text{-}pyrene)}$

The purpose of constructing sensor **117**$_{(phenanthrene\text{-}pyrene)}$ was to investigate the efficiency of energy transfer from phenanthrene to pyrene as a function of saccharide binding. A similar concept had previously been employed in the construction of a fluorescent calix[4]arene sodium sensor.[208] The excitation and emission wavelengths of the phenanthrene (donor) are 299 nm and 369 nm, respectively, while the excitation and emission wavelengths of the pyrene (acceptor) are 342 nm and 397 (or 417) nm, respectively. The emission wavelength of phenanthrene (369 nm) and excitation wavelength of pyrene (342 nm) overlap. These observations led to the postulation that intramolecular energy transfer from phenanthrene to pyrene could take place in sensor **117**$_{(phenanthrene\text{-}pyrene)}$.

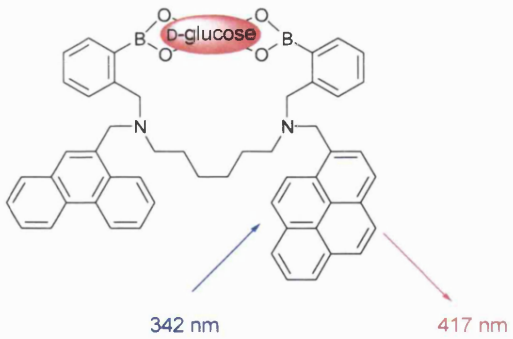

Scheme 46. *Schematic representation of sensor* ***117***$_{(phenanthrene\text{-}pyrene)}$ *with bound D-glucose (depicted as a red ellipse). D-Glucose allows a revival of fluorescence emission from the LE pyrene fluorophore when pyrene is excited directly. Excitation and emission wavelengths are illustrated in blue and red respectively. The colours are used to depict the Stokes shift of the system rather than the actual colour of the light.*

Using light of 342 nm (the λ_{ex} of pyrene) to excite sensor **117**$_{(phenanthrene\text{-}pyrene)}$ leads to long wavelength excimer emission due to π-π interactions between phenanthrene and pyrene, Scheme 47 broad peak ~ 470 nm. PET modulated emission is also observed from the LE state of pyrene, the three distinctive peaks of the emission band visible in Scheme 47 at 370, 397 and 417 nm. The intense peak in Scheme 47 at 342 nm is due to Raleigh scattering of the exciting radiation.

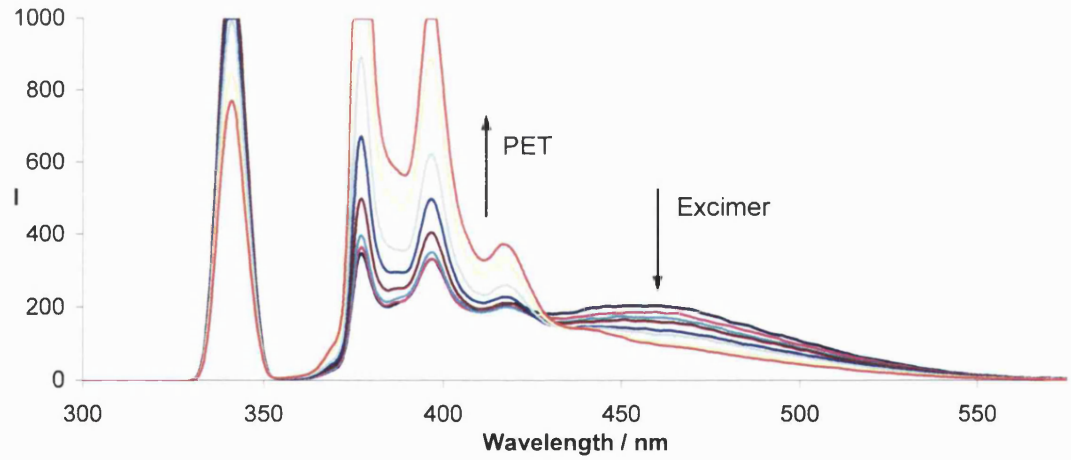

Scheme 47. *Fluorescence intensity versus wavelength for sensor* ***117***$_{(phenanthrene\text{-}pyrene)}$ *(2.5 × 10^{-6} mol dm^{-3}) displaying photoinduced electron transfer and excimer emission with increasing concentrations of D-glucose (from 0 to 1.0 × 10^{-1} mol dm^{-3}) in 52.1 wt% MeOH pH 8.21 phosphate buffer. λ_{ex} = 342 nm.*

If light of 299 nm was used (the λ_{ex} of phenanthrene) to excite sensor **117**$_{(phenanthrene\text{-}pyrene)}$ the fluorescence emission spectrum did not display an emission band around 369 nm as would be expected for phenanthrene. Instead the resulting emission band had an

emission maximum at 417 nm and was identical to the emission observed when pyrene was excited directly, as in Scheme 47. This result can be ascribed to energy transfer from the phenanthrene to the pyrene fluorophore.

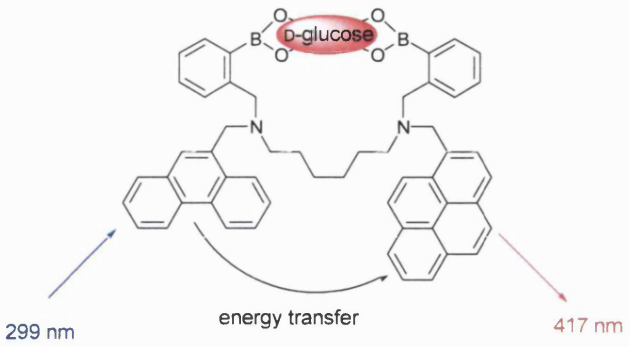

Scheme 48. *Schematic representation of sensor* ***117***$_{(phenanthrene\text{-}pyrene)}$ *with bound* D*-glucose (depicted as a red ellipse). When phenanthrene is excited directly an energy transfer mechanism can occur. Excitation and emission wavelengths are illustrated in blue and red respectively. The colours are used to depict the Stokes shift of the system rather than the actual colour of the light. The non-radiative energy transfer is depicted in black.*

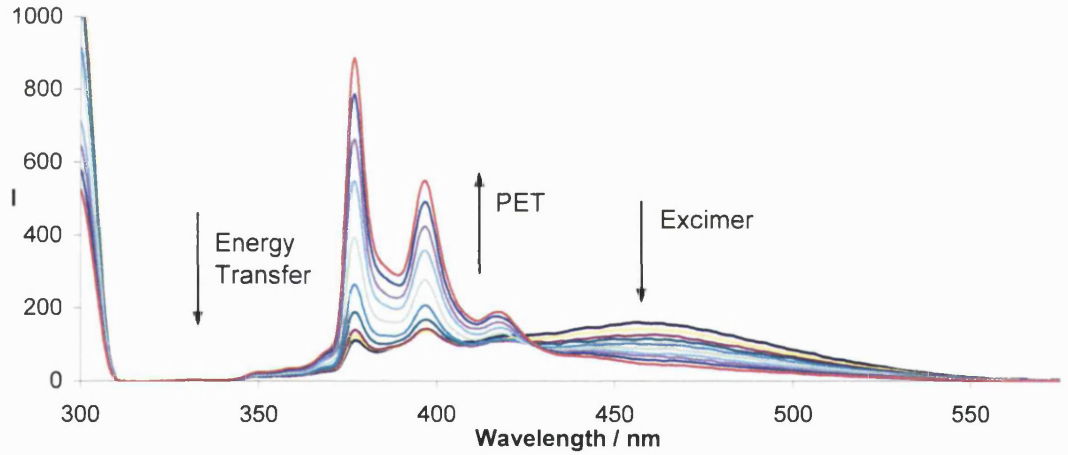

Scheme 49. *Fluorescence intensity versus wavelength for sensor* ***117***$_{(phenanthrene\text{-}pyrene)}$ *(2.5 × 10^{-6} mol dm^{-3}) displaying energy transfer, photoinduced electron transfer and excimer emission with increasing concentrations of* D*-glucose (from 0 to 1.0 × 10^{-1} mol dm^{-3}) in 52.1 wt% MeOH pH 8.21 phosphate buffer.* λ_{ex} *= 299 nm.*

The fluorescence titrations of sensor **117**$_{(phenanthrene\text{-}pyrene)}$ (2.5 × 10^{-6} mol dm^{-3}, λ_{ex} = 299 nm for phenanthrene and λ_{ex} = 342 nm for pyrene) with different saccharides were carried out in a pH 8.21 aqueous methanolic buffer, as described above (page 88). Absorption *versus* concentration plots of sensor **117**$_{(phenanthrene\text{-}pyrene)}$ and the monoboronic acid reference compounds **128**$_{(pyrene)}$ and **129**$_{(phenanthrene)}$ confirmed that the

π-π stacking of sensor **117**$_{(phenanthrene\text{-}pyrene)}$ was solely intramolecular. The fluorescence intensity of sensor **117**$_{(phenanthrene\text{-}pyrene)}$ at 417 nm increased with added saccharide when excited at both 299 and 342 nm, while the excimer emission at 460 nm decreased with added saccharide. The change in excimer emission indicates that the π-π interaction between phenanthrene and pyrene is disrupted on saccharide binding.

The observed stability constants (K_{obs}) of sensor **117**$_{(phenanthrene\text{-}pyrene)}$ (with λ_{ex} = 299 nm and λ_{ex} = 342 nm) were calculated by fitting the emission intensities at 417 nm *versus* concentration of saccharide curves and are given in Table 5. The observed stability constants (K_{obs}) for the diboronic acid sensor **117**$_{(phenanthrene\text{-}pyrene)}$ (λ_{ex} = 299 and 342 nm) with D-glucose were enhanced relative to those of the monoboronic acid reference compounds **128**$_{(pyrene)}$ and **129**$_{(phenanthrene)}$, while the observed stability constants (K_{obs}) for the diboronic acid sensor **117**$_{(phenanthrene\text{-}pyrene)}$ (λ_{ex} = 299 and 342 nm) with D-fructose were reduced relative to those for the monoboronic acid reference compounds **128**$_{(pyrene)}$ and **129**$_{(phenanthrene)}$.

Table 5. Observed stability constants (K_{obs}) (coefficient of determination; r^2) and fluorescence enhancements for compounds **99** and **117**$_{(phenanthrene\text{-}pyrene)}$ with saccharides.[206]

sensor	D-glucose		D-galactose	
	K_{obs} / dm^3 mol^{-1}	fluorescence enhancement	K_{obs} / dm^3 mol^{-1}	fluorescence enhancement
99	260 ± 15 (1.00)	4.9	237 ± 6 (1.00)	4.2
117$_{(phenanthrene\text{-}pyrene)}$[a]	142 ± 12 (0.99)	3.9	74 ± 7 (0.99)	2.2
117$_{(phenanthrene\text{-}pyrene)}$[c]	108 ± 10 (0.99)	2.4	81 ± 8 (0.99)	2.6

sensor	D-fructose		D-mannose	
	K_{obs} / dm^3 mol^{-1}	fluorescence enhancement	K_{obs} / dm^3 mol^{-1}	fluorescence enhancement
99	244 ± 26 (0.99)	3.4	32 ± 3 (0.99)	3.2
117$_{(phenanthrene\text{-}pyrene)}$[a]	76 ± 10 (0.98)	1.7	*b*	*b*
117$_{(phenanthrene\text{-}pyrene)}$[c]	125 ± 11 (0.99)	3.5	8 ± 1 (1.00)	3.5

[a] λ_{ex} = 299 nm, λ_{em} = 417 nm
[b] The K_{obs} and fluorescence enhancement could not be determined because of the small changes in fluorescence.
[c] λ_{ex} = 342 nm, λ_{em} = 417 nm

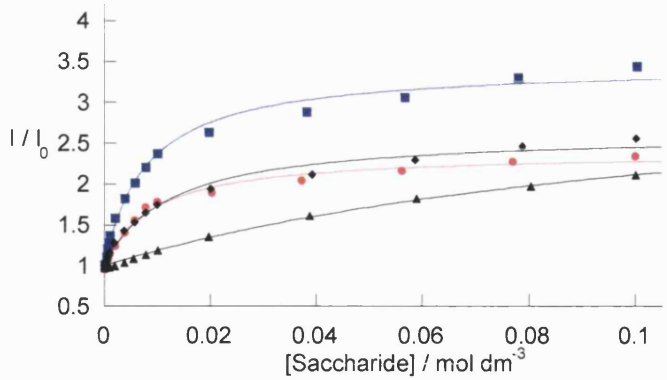

Figure 39. *Relative fluorescence intensity versus saccharide concentration profile of sensor* ***117***$_{(phenanthrene\text{-}pyrene)}$ *(2.5 × 10^{-6} mol dm^{-3}) displaying PET at the pyrene fluorophore with (●) D-glucose, (■) D-fructose, (♦) D-galactose, (▲) D-mannose, in 52.1 wt% MeOH pH 8.21 phosphate buffer.* λ_{ex} *= 342 nm,* λ_{em} *= 417 nm.*

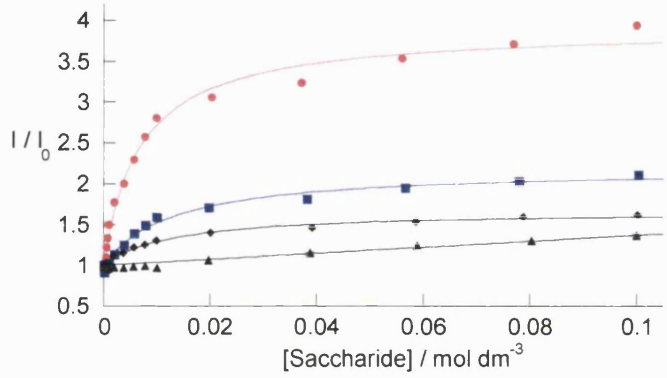

Figure 40. *Relative fluorescence intensity versus saccharide concentration profile of sensor* ***117***$_{(phenanthrene\text{-}pyrene)}$ *(2.5 × 10^{-6} mol dm^{-3}) displaying ET between the phenanthrene and pyrene fluorophores with (●) D-glucose, (■) D-fructose, (♦) D-galactose, (▲) D-mannose, in 52.1 wt% MeOH pH 8.21 phosphate buffer.* λ_{ex} *= 299 nm,* λ_{em} *= 417 nm.*

Sensor **117**$_{(phenanthrene\text{-}pyrene)}$ was particularly noteworthy in that the difference between the observed fluorescence enhancements obtained when excited at phenanthrene (λ_{ex} = 299 nm) and pyrene (λ_{ex} = 342 nm) can be correlated with the molecular structure of the saccharide-sensor complex *via* PET, see Table 5. The fluorescence enhancement of sensor **117**$_{(phenanthrene\text{-}pyrene)}$ with D-glucose was 3.9 times greater when excited at 299 nm and 2.4 times greater when excited at 342 nm. With D-fructose the enhancement was 1.9 times greater when excited at 299 nm and 3.2 times greater when excited at 342 nm. This is to say that the selectivity between D-fructose and D-glucose within the same complex is in fact inverted dependant on the excitation wavelength used. This inversion is clearly displayed in Figure 39 and Figure 40. This result arises from the fact that energy transfer from phenanthrene to pyrene is far more efficient in the 1:1 cyclic

diboronic acid – saccharide complex than in the alternative 2:1 acyclic complex. This approach finally allows for efficient discrimination between saccharides based on their binding motif (*i.e.* the formation of a 1:1 or a 2:1 complex).

2.4.4 Literature Response

Following publication of the modular construct used by the T. D. James research group in the design of boronic acid based fluorescent PET sensors in 2001,[191] two research groups have published further data on libraries of sensors assembled in a modular fashion.

Wang and Co-workers

Wang and co-workers documented the range of diboronic acid sensors Figure 41 (**a**) - (**l**) in 2002.[202,209] It can be seen by examining the generic template used that the sensors are designed around the known core of sensor **68**, the first diboronic acid sensor to display selectivity for D-glucose. In this construct the number of carbon atoms from one *N*-methyl-*o*-(aminomethyl)phenylboronic acid nitrogen atom to the other is increased substantially. Six carbon atoms separate each of the adjacent amine – amide nitrogen atoms with anthracene cores rigidifying this section of the molecule and introducing possible interactions through either π-π stacking or steric encumbrance. The variable linkers examined augment the length of these rigid linkers further still.

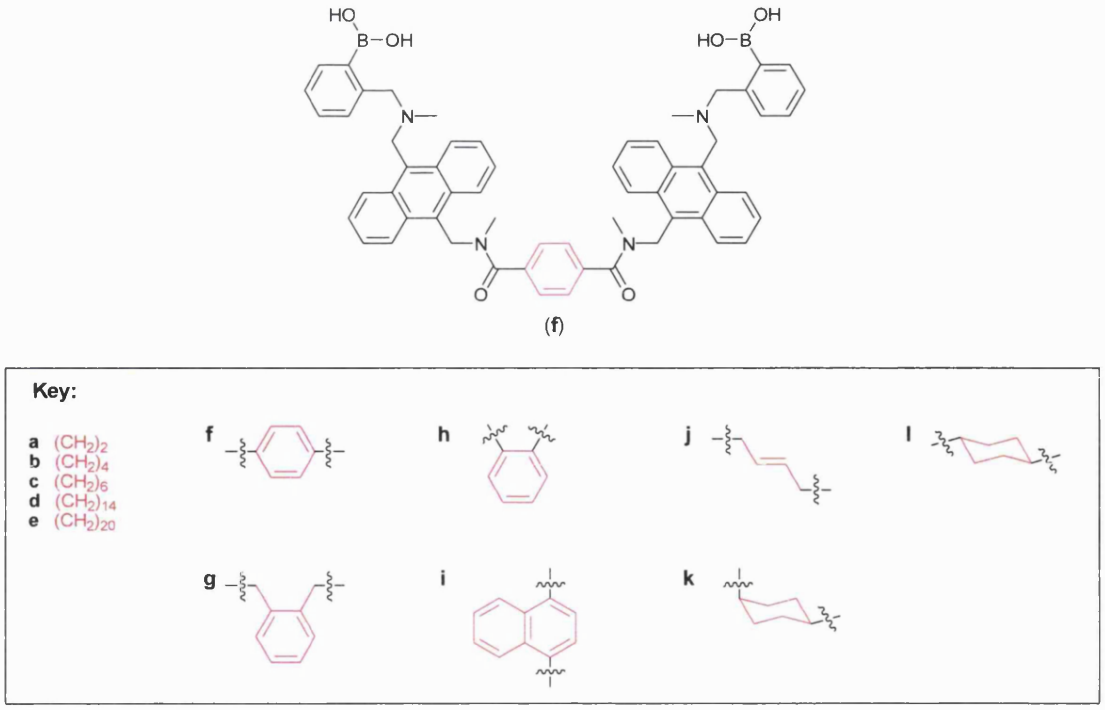

Figure 41. *Range of diboronic acid sensors (**a**) – (**l**) with the interchangeable linker fragments highlighted in red. (**f**) displayed selectivity for sialyl Lewis X and (**g**) displayed selectivity for D-glucose.*

Figure 41 (**f**) with the *para*-benzene linker was found to be selective for sialyl Lewis X.[202] Figure 41 (**g**) with the *ortho*-xylene linker was found to be selective for D-glucose.[209] In replacing the *ortho*-xylene linker of Figure 41 (**g**) with the flexible butyl linker of Figure 41 (**b**) the number of carbon atoms in the linker remained the same but the structural rigidity of the linker was lost, this led to a halving of the observed stability constant (K_{obs}). In reintroducing the rigidity but changing the geometry and spacing of the core unit to the *ortho*-benzene linker Figure 41 (**h**) the observed stability constant (K_{obs}) was seen to decrease further still.

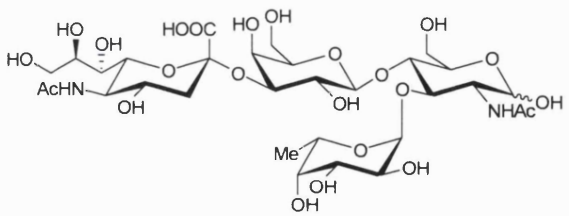

sialyl Lewis X

The observed stability constants (K_{obs}) for the selected sensors in Figure 41 were: (**g**), 34 M^{-1} with D-fructose, 1 470 M^{-1} with D-glucose and 30 M^{-1} with D-galactose; (**b**), 80

M^{-1} with D-fructose, 640 M^{-1} with D-glucose and 110 M^{-1} with D-galactose; (**h**), 280 M^{-1} with D-fructose, 180 M^{-1} with D-glucose and 30 M^{-1} with D-galactose in a solution of 1:1 (v/v) methanol/0.1 M aqueous phosphate buffer solution at pH 7.4. The observed stability constant (K_{obs}) for sensor Figure 41 (**f**) with sialyl Lewis X was not reported.

Hall and co-workers

In an article published in 2004 Hall and co-workers documented the first parallel, solid phase synthesis of modular boronic acid based sensors.[210] The series was developed from a range of common components allowing the rapid assembly of a library of compounds, with the use of semi-preparative high performance liquid chromatography (HPLC) to ensure sensors of satisfactory purity. This approach allowed the structures of the inter amine linkers to be altered (selectivity was once again found for D-glucose with a linker six carbon atoms in length), however, the investigation went on to assess the potential role of a third boronic acid receptor moiety in the recognition of disaccharides (Figure 42) and the effect of introducing unencumbering electron-withdrawing and electron-donating groups *para* to the arylboronic acid (Figure 43).

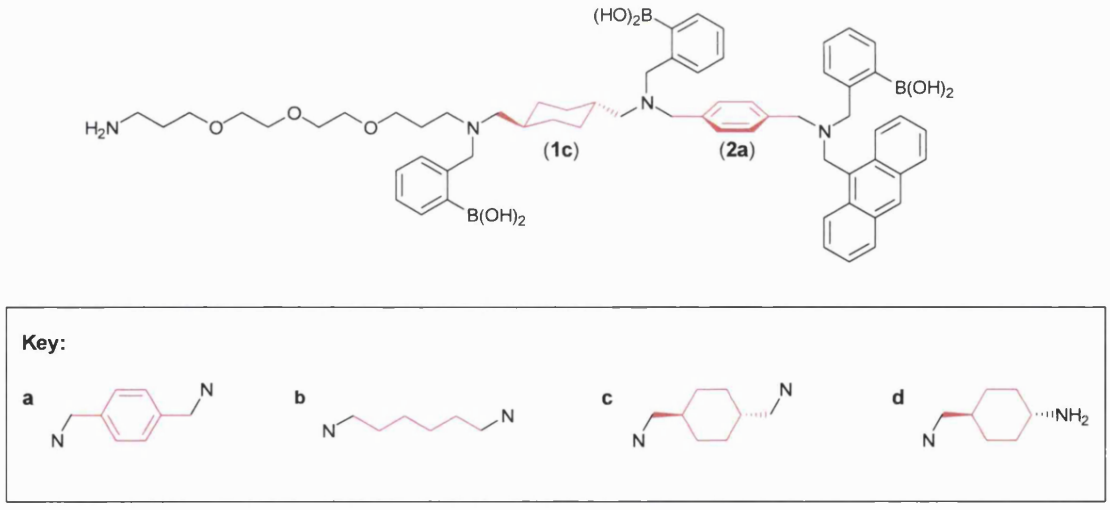

Figure 42. *Triboronic acid sensors assembled via combinatorial synthesis to evaluate the potential of increased allosteric binding effects through three point binding (the interchangeable linker units are highlighted in red).*

The triboronic acid sensors were titrated against four disaccharides: lactulose, melibiose, turanose and trehalose. Across the range of sensors and guests examined no benefit was found from three (*versus* two) boronic acid receptor units. For example the

observed stability constant (K_{obs}) of triboronic acid Figure 42 (**1c, 2a**) with lactulose was 200 M^{-1}, this value can be contrasted with the value obtained for the analogous diboronic acid (**2a** derivative) that displayed an observed stability constant (K_{obs}) of 220 M^{-1} with lactulose in 0.010 mol dm^{-3} phosphate buffer at pH 7.8 in a 1:1 water/methanol mixture.

Building on these observations Hall and co-workers examined the dependence of complexation on the electronic characteristics of the arylboronic acid receptors. By altering the Lewis acidity at boron it was believed that two main features in the molecular recognition event could be altered: the strength of the binding interaction with the saccharides and the strength of the N-B interaction controlling the fluorescence intensity. This hypothesis was tested by introducing electron-withdrawing and electron-donating groups at the *para* position of the arylboronic acid ring.

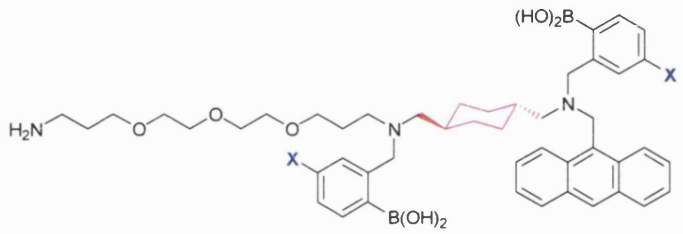

Figure 43. *Diboronic acid modular systems with an interchangeable linker section (highlighted in red) and interchangeable electron-withdrawing and electron donating groups para to the arylboronic acid (highlighted in blue).*

Five substituent groups were considered in all: methoxy, fluoro, methoxycarbonyl, cyano and nitro, with *para*-substituent parameters, σ_p: -0.12, 0.15, 0.44, 0.70 and 0.81, respectively.[211] If Figure 43 is considered and lactulose is used as the model disaccharide, the binding measurements display a qualitative trend that electron poor phenylboronic acids are preferable for binding. This observation was rationalised on the basis that on increasing the Lewis acidity at boron the N-B interaction becomes stronger developing more of a tetrahedral character at boron. This in turn reduces the ring strain in the developing boronic ester. In addition to this, acidifying boron and reducing its pK_a also provides the substantial benefit of allowing the sensor to function at lower pH.

Table 6. Observed stability constants (K_{obs}) for the general structure illustrated in Figure 43 with lactulose, determined in 0.010 mol dm^{-3} phosphate buffer at pH 7.8 in a 1:1 water/methanol mixture.

X	Linker	σ_p	(K_{obs}) / dm^3 mol^{-1}
OMe	(**c**)	-0.12	150
F	(**c**)	0.15	585
CN	(**c**)	0.70	1020
CN	(**b**)	0.70	1870

In enhancing the observed stability constants (K_{obs}) the use of methoxycarbonyl, cyano and nitro groups appeared to be particularly effective. Overall the largest observed stability constant (K_{obs}) reported with lactulose was with the diboronic acid illustrated in Figure 43 with a hexamethylene linker (**b**) and a *para*-cyano electron withdrawing group.[210]

2.5 SUMMARY OF RESULTS AND DISCUSSION I

- A degree of control can be imparted in the substitution of polyamines by conducting reductive aminations under high dilution conditions and in the presence of a Brønsted acid.

- Optimum D-glucose selectivity is obtained across the range of modular diboronic acid sensors **109**$_{(n=3)}$ - **114**$_{(n=8)}$ when the two amine nitrogens are separated by a linker six carbon atoms in length.

- The change in selectivity from D-glucose to D-galactose as a function of the increasing dimensions of the binding pocket can be ascribed to the relative availability of syn-periplanar hydroxyl pairs and the stability of D-glucose in its furanose form and D-galactose in a twist boat conformation of its pyranose form.

- Where significant binding was observed between diboronic acids and disaccharide, the disaccharide possessed a terminal residue that could interconvert between its pyranose and furanose forms.

- Where the above condition was met steric crowding at the secondary binding site was thought to reduce the strength of the complex formed between the diboronic acid and disaccharide, compared to the complex formed between the same diboronic acid and the analogous monosaccharide.

- Intramolecular energy transfer between suitable fluorophores provides a highly efficient way of discriminating between saccharides based on the binding motif of the complex formed.

CHAPTER THREE:
Results and Discussion II

The most exciting phrase to hear in science, the one that heralds new discoveries, is not 'Eureka!' but rather, 'Hmm... That's funny...'

Isaac Asimov

3 Results and Discussion II

3.1 Overview of Results and Discussion II

In continuing the evaluation of modular fluorescent sensors the next structural feature to be examined was the fluorophore. This chapter discusses the work undertaken by us in this regard and in particular addresses the methods by which compounds containing the *N*-methyl-*o*-(aminomethyl)phenylboronic acid fragment are synthesised.

In examining the scientific literature surrounding boronic acid based PET sensors it is often the case that the focus of published articles is on the evaluation and performance of the sensors. This has led to an apparent paucity in the number of articles which discuss the synthetic methodologies used to construct these sensors in any depth.

Our aim was to develop efficient, robust and generally applicable synthetic strategies in the design, construction and purification of sensors containing the N-methyl-o-(aminomethyl)phenylboronic acid fragment.

In order to achieve this generally applicable synthetic strategy, reactions were designed to proceed in a hierarchical manner *via* common intermediates. The careful choice of common precursors permitted a number of complex molecules to be constructed through the convergent assembly of generic subunits, thus introducing chemical simplicity and efficiency of assembly into the synthetic routes.

Having established robust synthetic methodologies for the diboronic acid sensors **133**$_{(pyrene)}$ - **137**$_{(2\text{-naphthalene})}$ and synthesised their respective monoboronic acid reference compounds **128**$_{(pyrene)}$ - **132**$_{(2\text{-naphthalene})}$ these techniques were applied to the construction of an entirely novel type of diboronic acid based fluorescent PET sensor. A route was therefore designed and the pair of diboronic acid tipped tweezers **162** synthesised.

3.2 Fluorophore Dependence in Modular Systems

Given the understanding developed in the previous chapter regarding the influence of the linker length in modular PET sensors for saccharides, as well as the advantages of using energy transfer to determine selectivity, the next structural feature to be evaluated was the fluorophore appended to the modular sensor, see Arimori, Consiglio, Phillips and James.[212,****]

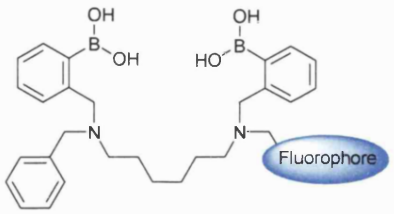

133$_{(pyrene)}$ - **137**$_{(2\text{-naphthalene})}$

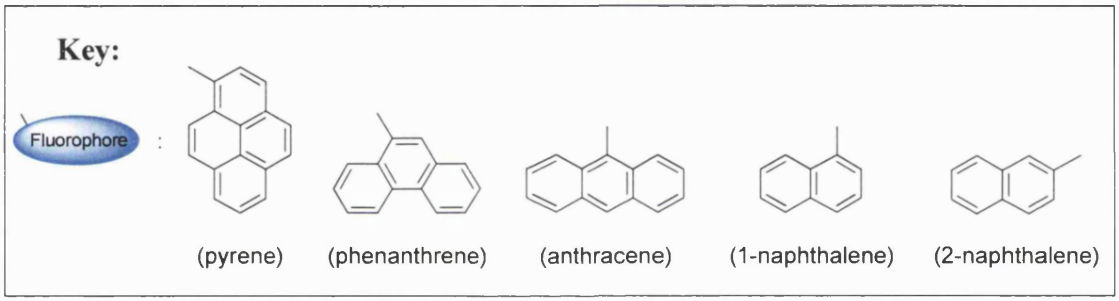

Figure 44. *Generic template for the five diboronic acid sensors with variable fluorophore units* ***133***$_{(pyrene)}$ - ***137***$_{(2\text{-naphthalene})}$.

The fluorophores chosen are all commercially available as their aldehyde derivatives, comparatively inexpensive and have similar photophysical properties.

Sensors **133**$_{(pyrene)}$ - **137**$_{(2\text{-naphthalene})}$ all utilise the same general structural motif, this is illustrated in Figure 44. The two phenylboronic acid receptors introduce saccharide selectivity while the hexamethylene linker governs the dimensions of the binding cleft, with a proven bias towards D-glucose selectivity.

**** S. Arimori, G. A. Consiglio, M. D. Phillips, and T. D. James, *Tetrahedron Lett.*, 2003, **44**, 4789-4792.

3.3 MONOBORONIC ACID REFERENCE COMPOUNDS

In order to determine the binding stoichiometry of the complexes formed within the binding sites of the diboronic acid based sensors **133**$_{(pyrene)}$ - **137**$_{(2\text{-naphthalene})}$ and elucidate the benefits gained from allosteric interactions, these systems must be contrasted against analogous monoboronic acid reference compounds. These reference compounds **128**$_{(pyrene)}$ - **132**$_{(2\text{-naphthalene})}$ shall be discussed first.

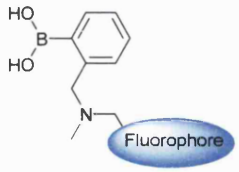

128$_{(pyrene)}$ - **132**$_{(2\text{-naphthalene})}$

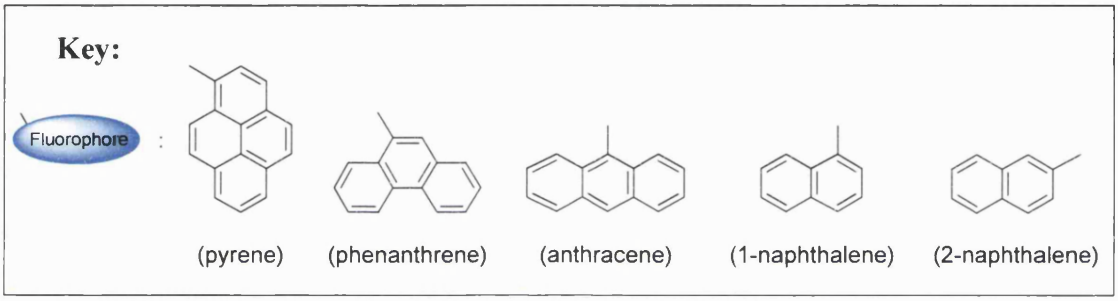

Figure 45. *Generic template for the five monoboronic acid reference compounds with variable fluorophore units* ***128***$_{(pyrene)}$ - ***132***$_{(2\text{-naphthalene})}$.

3.3.1 Methodology

Arimori et al.

Reference compounds **128**$_{(pyrene)}$ - **132**$_{(2\text{-naphthalene})}$ were initially investigated within our research group.[212] The ^{1}H NMR spectra of the compounds synthesised indicated that the correct compounds had been produced and permitted the fluorescence titration experiments of compounds **128**$_{(pyrene)}$ - **132**$_{(2\text{-naphthalene})}$ to be run with saccharides.

Not only was their insufficient material left for a full characterisation following the fluorescence evaluation, it was also felt that the synthetic route that had been employed could be significantly improved upon.

Previous Synthetic Route

The initial synthesis had been achieved by means of coupling methylamine to the required aldehyde *via* a reductive amination. Following reduction the reaction mixture was extracted from water in chloroform and dried to afford the intermediate amine. The amine was dissolved in acetonitrile and coupled with 2-(2-(bromomethyl)phenyl)-1,3,2-dioxaborinane (**124**) in the presence of potassium carbonate. After heating under reflux the reaction mixture was condensed dissolved in chloroform, acidified and washed with brine. The organic phase was then re-condensed and the product re-precipitated from chloroform in *n*-hexanes.

Objective

The above procedure provides a fair representation of the synthetic strategies typically employed in the construction of boronic acid based fluorescent PET sensors. It was our intention to develop a synthetic protocol that would allow compounds such as the monoboronic acid reference compounds $\mathbf{128}_{(\text{pyrene})}$ - $\mathbf{132}_{(\text{2-naphthalene})}$ to be generated *via* robust laboratory procedures and to afford these compounds with excellent levels of purity.

It was therefore decided that the entire range of monoboronic acid reference compounds $\mathbf{128}_{(\text{pyrene})}$ - $\mathbf{132}_{(\text{2-naphthalene})}$ would be completely resynthesised and new synthetic paths derived. Within the remit of this research our objective was not only to synthesise the compounds but to thoroughly interrogate the synthetic procedures involved in obtaining compounds containing the *N*-methyl-*o*-(aminomethyl)phenylboronic acid fragment.

Generic Synthetic Routes

The construction of boronic acid based PET sensors is frequently challenging. Therefore the idea of establishing generic routes for the synthesis of these compounds is a most desirable one.

In considering a global synthetic route various steps were earmarked as being crucial in the synthesis of boronic acid based PET sensors. It became rapidly clear that the largest obstacle encountered in forming the desired compounds in good yield and with high levels of purity was the final step. The obtuse handling characteristics typical of compounds containing the *N*-methyl-*o*-(aminomethyl)phenylboronic acid fragment

makes purification of these compounds particularly challenging. Purification of the final product is non-trivial and although techniques such as reprecipitation and solvent washes are common in this area they cannot be exclusively relied upon to deliver the final product cleanly.

To overcome this pitfall it was postulated that synthetic routes should be engineered so as to allow the products of the penultimate step to be obtained with particularly high levels of purity. It was envisaged that with this caveat in place the final coupling of the boronic acid and amine fragments stood the best chance of yielding the desired target molecules cleanly.

3.3.2 Retrosynthetic Analysis

In designing the synthetic route to the monoboronic acid reference compounds **128**$_{(pyrene)}$ - **132**$_{(2\text{-naphthalene})}$ the above proposal (Section 3.3.1) necessitates that the coupling of the *o*-methyl phenylboronic acid and the amine occurs last. In a retrosynthetic analysis of compounds **128**$_{(pyrene)}$ - **132**$_{(2\text{-naphthalene})}$ it therefore became apparent that a boronic acid such as the commercially available *o*-formyl phenylboronic acid could be used with an *N*-methyl(aminomethyl) derivative of the required fluorophore, see Scheme 50.

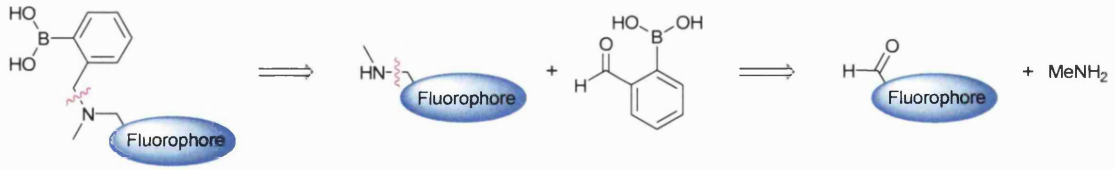

Scheme 50. *Retrosynthetic analysis of monoboronic acid reference compounds* **128**$_{(pyrene)}$ - **132**$_{(2\text{-naphthalene})}$. *The symbol* ~~ *is used to indicate the location of the proposed decouplings.*

As there is only a single amine in the intermediate *N*-methyl(aminomethyl) derivative of the fluorophore there is no scope for complications arising from substitution occurring on multiple functional groups as was the case earlier, see Section 2.3 (page 90). This should permit a reductive amination between the required aldehyde and methylamine to occur directly.

3.3.3 Synthesis of the N-Methyl(aminomethyl) Fluorophore Derivatives

Initial Reaction Conditions

The synthesis of the *N*-methyl(aminomethyl) derivative of anthracene **102**$_{(anthracene)}$ had already been undertaken during our course of investigations in Section 2.3 (see *Controlling Substitutions on Polyamines*, page 90) and is illustrated in Scheme 51, below.

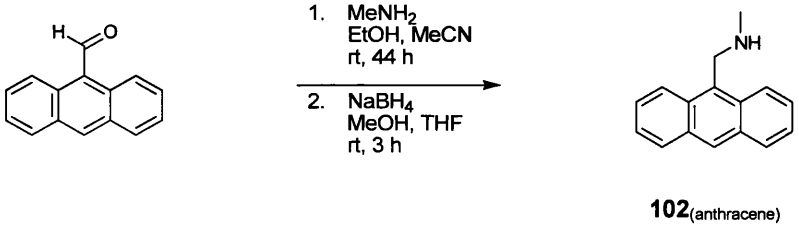

102$_{(anthracene)}$

Scheme 51. *Synthesis of compound* **102**$_{(anthracene)}$ *(84% yield).*

As the precursor to the final target molecule it was important that this product be isolated with high levels of purity. During the initial synthesis of the model compounds **102** - **108** (page 93), the purpose of which had been to establish the efficacy of high dilution conditions, a routine purification consisting of removal of the solvents under reduced pressure, followed by a solvent extraction had been sufficient. Whilst the ^{1}H NMR spectrum indicated that product **102**$_{(anthracene)}$ was isolated with reasonable purity, small quantities of side products were present. Having used 1 equivalent of 9-anthraldehyde, 2 equivalents of methylamine and 3 equivalents of sodium borohydride it was possible that contaminants in the final reaction mixture could take the form of the reduced derivative of 9-anthraldehyde (anthracen-9-yl-methanol), methylamine or the sodium and boron salts pertaining to the consumed sodium borohydride. A purification method that would categorically ensure the removal of all these components from the reaction mixture was required.

Improved Aqueous Wash

The procedure in Scheme 51 was repeated using methylamine (2.5 equivalents) and pyrene-1-carboxaldehyde (recrystalised from ethanol), see Scheme 52. Whilst the reaction conditions used were similar a more meticulous solvent extraction was

conducted in the work up. Following extraction into dichloromethane the organic phase was repeatedly washed with water to ensure the removal of any sodium and boron salts and the removal of all of the remaining methylamine. The presence of the amine base was verified by monitoring the pH of the aqueous phase after mixing. The initially basic organic layer was washed until the aqueous phases being removed repeatedly afforded a neutral pH.

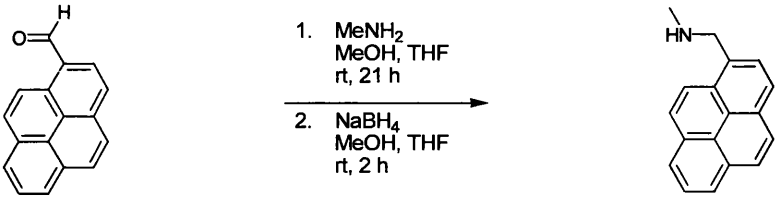

118(pyrene)

Scheme 52. *Synthesis of amine* ***118***$_{(pyrene)}$ *(70% yield).*

This procedure proved effective at removing any remaining methylamine, however, this purification technique assumed that all of the pyrene-1-carboxaldehyde had been consumed in the reaction and did not provide a pathway for the removal of any unwanted organic products such as the resulting pyren-1-yl-methanol.

Formation of the Hydrochloride Salts

To circumvent this flaw a further purification step was introduced, see Scheme 53. Having subjected the organic layer to an extensive aqueous wash to remove any remaining methylamine the organic phase was then dried over magnesium sulfate, filtered and gaseous hydrogen chloride (> 99%) bubbled directly through the dry solution of dichloromethane and amine **118**$_{(pyrene)}$.

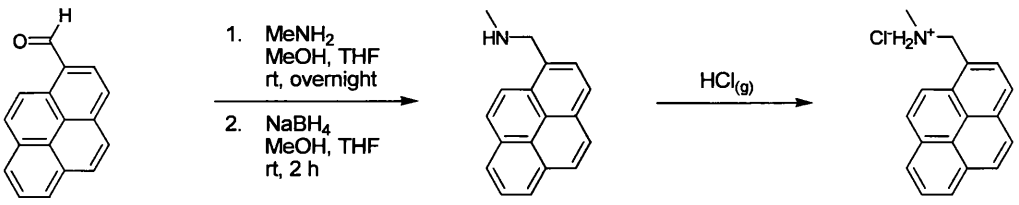

118(pyrene) **119**(pyrene)

Scheme 53. *Synthesis of amine* ***118***$_{(pyrene)}$ *(99% yield) with subsequent formation of the ammonium hydrochloride salt* ***119***$_{(pyrene)}$ *(the reaction proceeded with 87% overall yield).*

This interconversion of amine **118**$_{(pyrene)}$ to its ammonium hydrochloride salt **119**$_{(pyrene)}$ occurred with formation of the ammonium salt in dry dichloromethane as a highly insoluble cream precipitate. As this procedure caused no discernable changes to occur to the properties of the pyren-1-yl-methanol, the ammonium salt and aromatic alcohol could be readily separated. The resulting precipitate was slurried across a glass sinter and flushed with dry dichloromethane to yield the product **119**$_{(pyrene)}$ with high levels of purity. For clarity this procedure is depicted in

Scheme **54**.

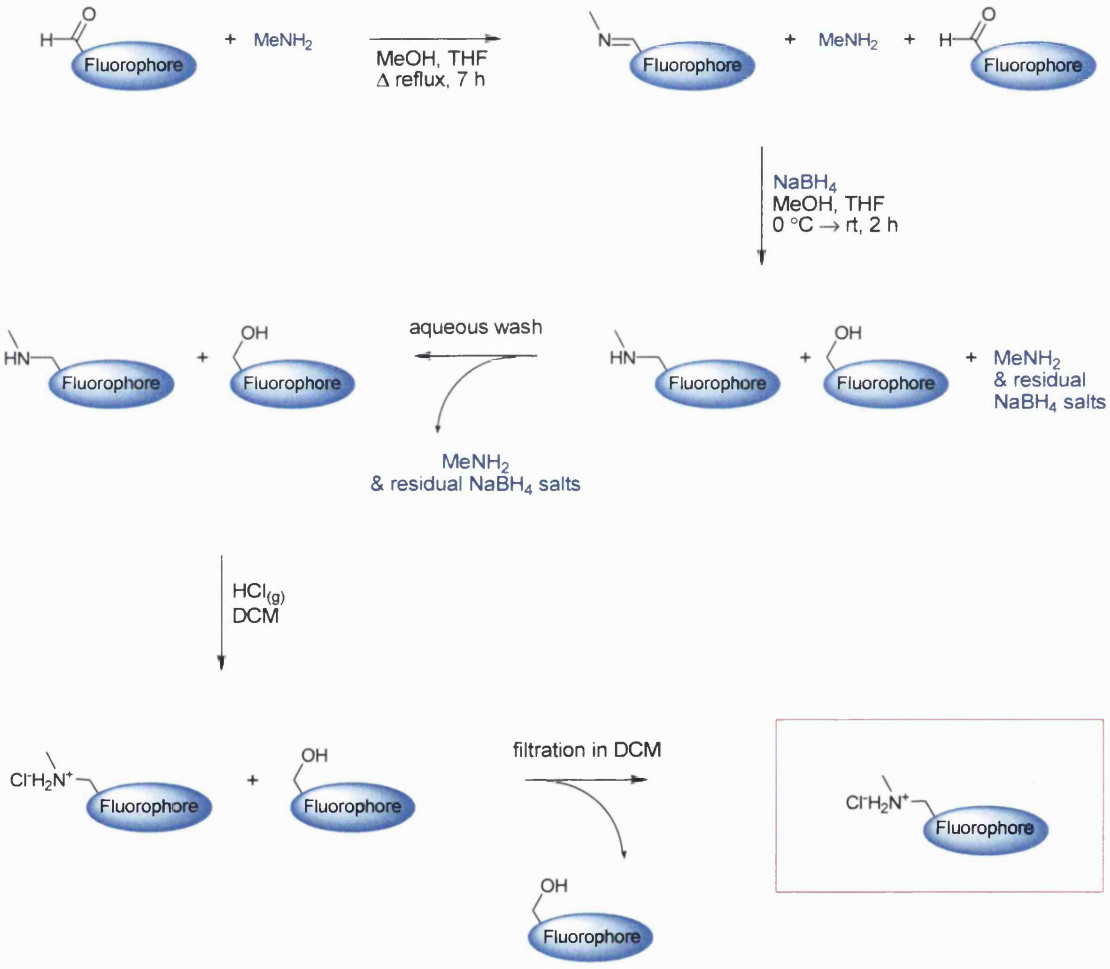

Scheme 54. *Schematic representation of the synthetic route and purification rationale developed for the isolation of the ammonium hydrochloride salts* ***119***$_{(pyrene)}$ *-* ***123***$_{(2\text{-}naphthalene)}$ *with high levels of purity. For clarity* $MeNH_2$, $NaBH_4$ *and the derivatives of* $NaBH_4$ *are indicated in blue.*

This approach proved highly successful and was found to be applicable for all of the compounds used regardless of the fluorophore. All five compounds were therefore

isolated as their ammonium hydrochloride salts *via* the generic route detailed in Scheme 55.

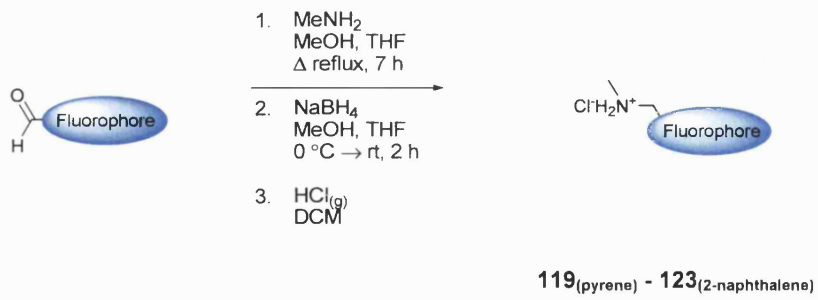

119$_{(pyrene)}$ - **123**$_{(2\text{-naphthalene})}$

Scheme 55. *Synthesis of compounds* ***119***$_{(pyrene)}$ - ***123***$_{(2\text{-naphthalene})}$ *(68-91% yield).*

The purity of these precursors was readily apparent from the ^{1}H NMR spectra obtained. To qualify this assertion the spectrum of the ammonium salt **121**$_{(anthracene)}$ is illustrated in Figure 46.

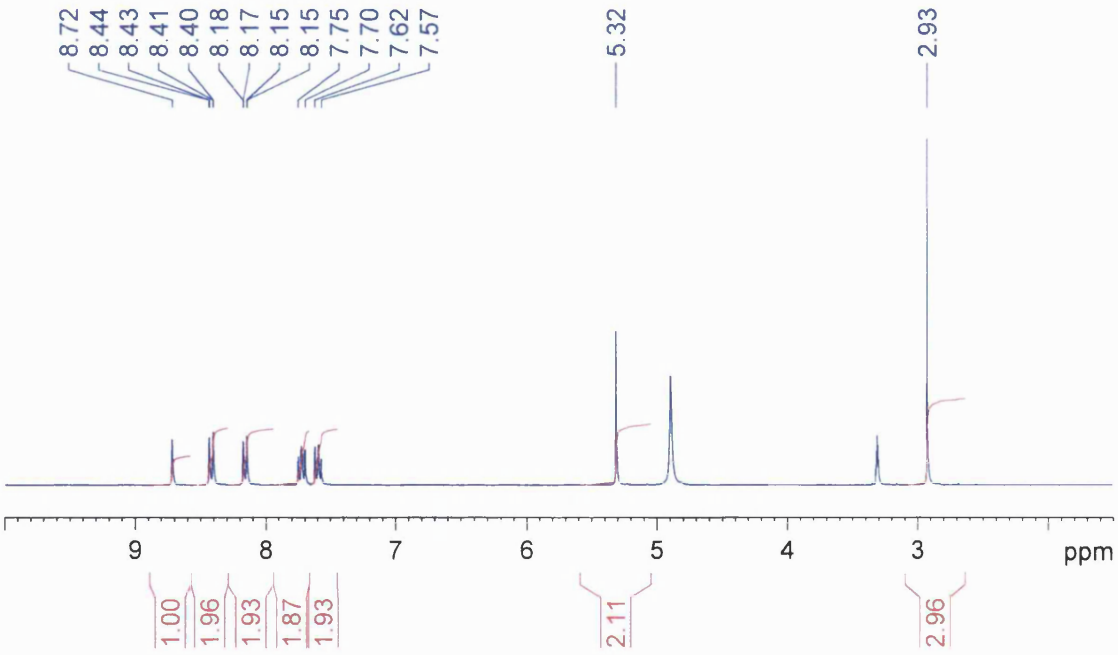

Figure 46. *^{1}H NMR spectrum (300 MHz, MeOD) of compound* ***121***$_{(anthracene)}$*, with the residual solvent peak at 3.31ppm and water at 4.90ppm. For clarity only the outer peaks of the two aromatic ddd are given.*

Although the initial reason for the formation of the hydrochloride salt was to gain an extra handle in the purification of the boronic acid precursor it is the case that ammonium salts are substantially more stable than their amine counterparts, this allowed compounds **119**$_{(pyrene)}$ - **123**$_{(2\text{-naphthalene})}$ to be stored (dark at room temperature)

with no discernable degradation being observed over the course of these investigations. It is also the case that ammonium salts are far more amenable to the majority of characterisation methods routinely used than their amine counter parts, this trait permitted a comprehensive physical analysis to be carried out across the series of compounds **119**$_{(pyrene)}$ - **123**$_{(2\text{-naphthalene})}$, see Figure 47.

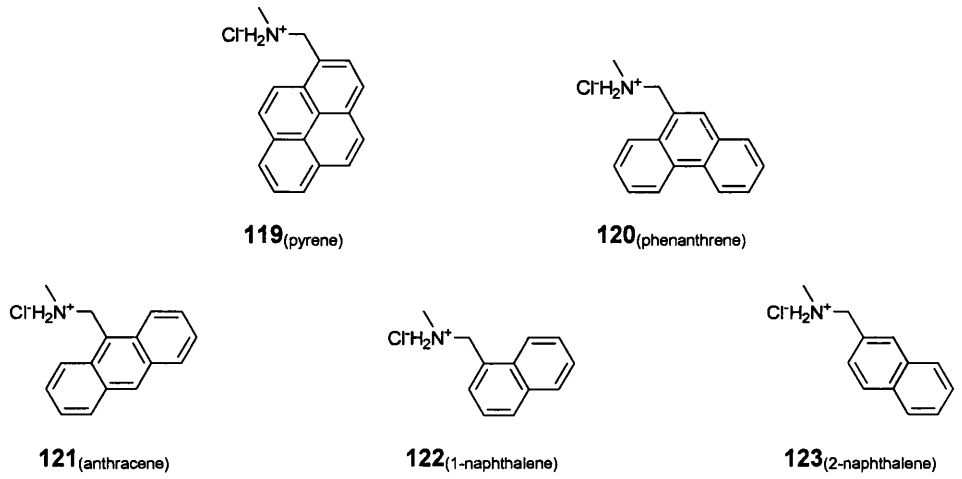

Figure 47. *Hydrochloride salt precursors* ***119***$_{(pyrene)}$ - ***123***$_{(2\text{-naphthalene})}$ *of the monoboronic acid reference compounds* ***128***$_{(pyrene)}$ - ***132***$_{(2\text{-naphthalene})}$.

3.3.4 Attachment of the Phenylboronic Acid Fragment

o-Formyl Phenylboronic Acid

The second precursor required in the final overall step was the *o*-methyl phenylboronic acid fragment. The commercially available *o*-formyl phenylboronic acid has been successfully used in the direct coupling of this fragment with amines, as illustrated in Scheme 56.[159]

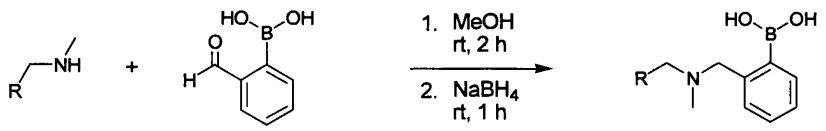

Scheme 56. *Reductive amination of o-formyl phenylboronic acid with a secondary amine. Typical conditions are indicated.*[159]

It should be noted, however, that compounds **119**$_{(pyrene)}$ - **123**$_{(2\text{-naphthalene})}$ were isolated not as amine bases but as ammonium hydrochloride salts. This introduced an additional

step in attempting to couple the two precursors *via* a reductive amination as the amine base must be freed before the amination can occur. If the reductive amination is attempted in one pot and sodium hydroxide added directly to the starting materials a Cannizzaro reaction[83] is (not unexpectedly) observed to occur, the aldehyde group of the *o*-formyl phenylboronic acid undergoing disproportionation.

The amine base can be freed with aqueous sodium hydroxide and then extracted in dichloromethane prior to the reaction. This was done and the coupling of the ammonium salt **122**$_{(1\text{-naphthalene})}$ with *o*-formyl phenylboronic acid attempted.

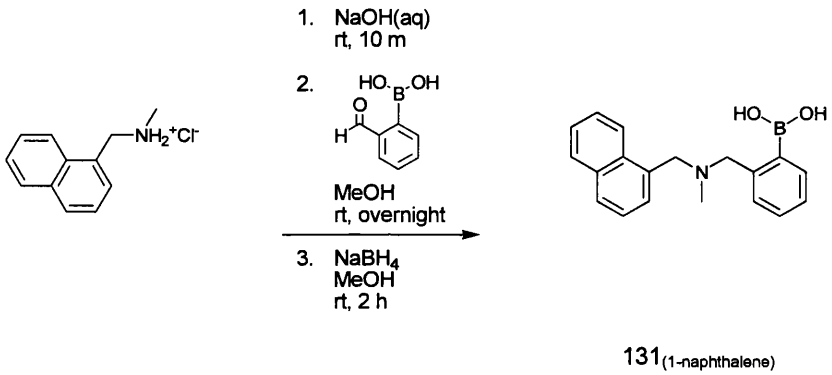

Scheme 57. *Attempted synthesis* ***131***$_{(1\text{-naphthalene})}$ *from the ammonium salt* ***122***$_{(1\text{-naphthalene})}$ *and o-formyl phenylboronic acid.*

From the ^{1}H NMR spectrum of the filtered reaction mixture it was apparent that the reaction had not proceeded cleanly, moreover this method afforded a poor yield. Dissolution in chloroform and reprecipitation in *n*-hexanes failed to generate a precipitate. Other methods of purification were therefore investigated and the product was re-generated tripling the quantities of starting material used (from ~ 40 mg to ~ 120 mg of the ammonium salt **122**$_{(1\text{-naphthalene})}$). It was the case that a minimum of 100 mg of the limiting reagent was required in these reactions to ensure the product was generated with sufficient mass for the purification step to be viable.

One avenue to be investigated was column chromatography on neutral alumina. Neutral alumina thin layer chromatography (TLC) of the reaction mixture indicated good separation with two spots visible and retardance factors (R_fs) of 0.69 and 0.22 (5:95 methanol/dichloromethane,). The reaction mixture was subject to column chromatography on neutral alumina and these two fractions isolated. The fraction corresponding to an R_f of 0.22 appeared to comprise mainly of the unreacted compound

122$_{(1\text{-naphthalene})}$ in its free amine base form. The fraction corresponding to an R_f of 0.69 appeared to contain the desired product, boronic acid **131**$_{(1\text{-naphthalene})}$, as well as number of other impurities. The ^{1}H NMR spectrum of this fraction in deuterated chloroform is illustrated in Figure 48.

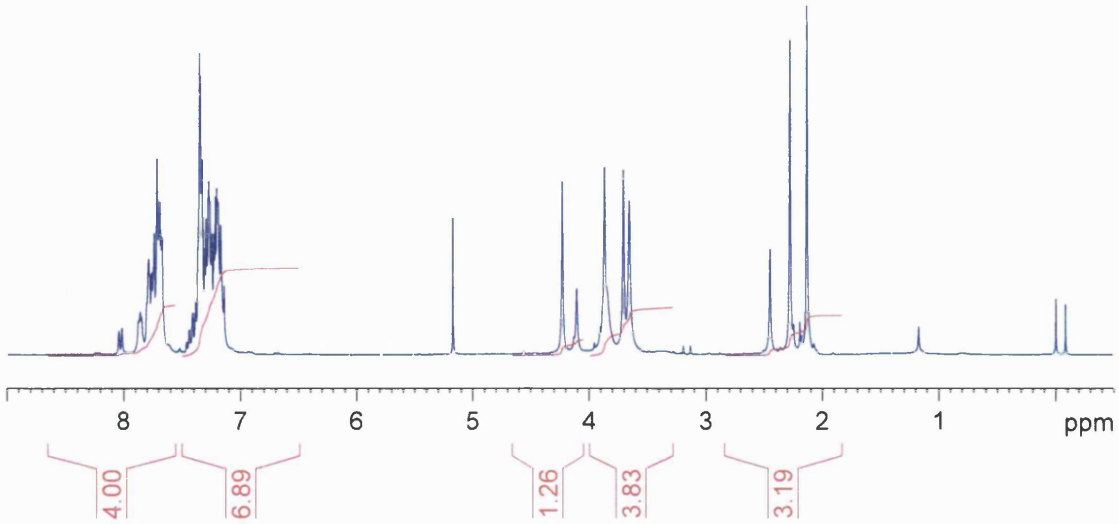

Figure 48. *^{1}H NMR spectrum (300 MHz, $CDCl_3$) of the reaction mixture isolated from the reaction in Scheme 57.*

The ^{1}H NMR spectrum in Figure 48 represents a good example of the difficulties associated in characterising boronic acids. From the structure of boronic acid **131**$_{(1\text{-naphthalene})}$ one would expect three singlets in the alkyl region: two from the two isolated CH_2 groups and one from the isolated CH_3 group, as well as signals accounting for eleven protons in the aromatic region from the benzene and naphthalene moieties. Considering the alkyl region in Figure 48, the numerous signals between 1.5 and 4.5ppm might be instinctively ascribed to the presence of gross impurities, however, it should be remembered that boronic acids condense to form trimers. So in the deuterated chloroform used to run the ^{1}H NMR of boronic acid **131**$_{(1\text{-naphthalene})}$ the boronic acid may be present in both its monomeric and trimeric forms, see Figure 49. The presence of the trimer can be verified by the additional doublets formed just downfield of the left hand aromatic multiplet, the signal being a telltale characteristic often observed in the ^{1}H NMR spectra of phenylboronic acid anhydrides.

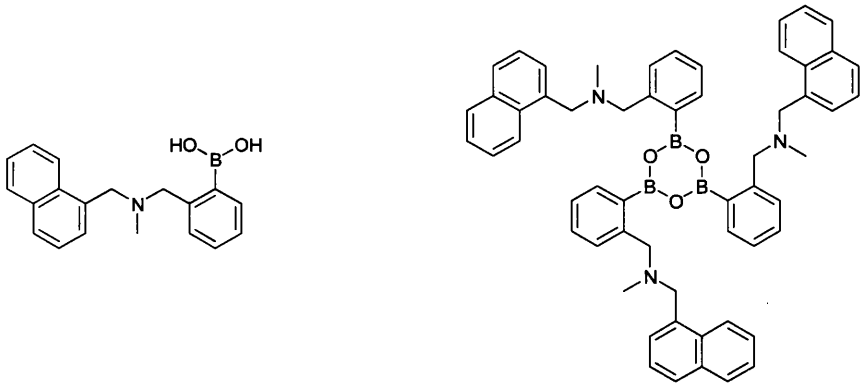

Figure 49. *Monomeric and trimeric forms of compound* ***131***$_{(1\text{-naphthalene})}$.

This trimerisation of boronic acids presents an additional complication in interpreting NMR spectra when attempting to ascertain the purity of the sample. Nevertheless, the number of signals generated in Figure 48 and their relative integrals indicated that boronic acid **131**$_{(1\text{-naphthalene})}$ had not been isolated cleanly, unreacted phenylboronic acid derivatives were also present.

In an effort to improve the separation of these compounds on neutral alumina columns the reaction was repeated on a number of occasions with ammonium salts of different fluorophores and with a range of eluent systems and alumina mesh sizes.

Unfortunately conditions were not found for the chromatographic separation that allowed the target molecule to be obtained independently from other compounds. However, during the course of these investigations it was shown that introducing ≥ 1 equivalent of triethylamine or potassium carbonate at the start of the reaction, the reaction could be conducted in one pot without the need to free the amine base before commencing the reaction (it was postulated that the bases could be subsequently removed in the chromatographic step).

Protected *o*-Bromo Benzylboronic Acids

Whilst the direct use of commercially available compounds would be advantageous other routes were now considered. The most common sources of *o*-methyl phenylboronic acid fragments to be reported for these couplings are protected *o*-bromo benzylboronic acids. The two precursors typically used are the boronic acids **124** and **127**, see Figure 50.

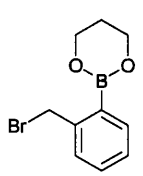

124

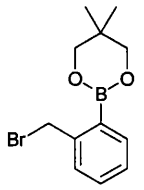

127

Figure 50. *Compound **124**, 2-(2-(bromomethyl)phenyl)-1,3,2-dioxaborinane and compound **127**, 2-(2-(bromomethyl)phenyl)-5,5-dimethyl-1,3,2-dioxaborinane.*

Both compounds **124** and **127** are derived from *o*-tolylboronic acid, see Scheme 58. The two commonly used protecting groups: 1,3-propanediol and neopentyl glycol, are added prior to bromination and allow the intermediate and final compounds in Scheme 58 to be purified by silica gel flash column chromatography.

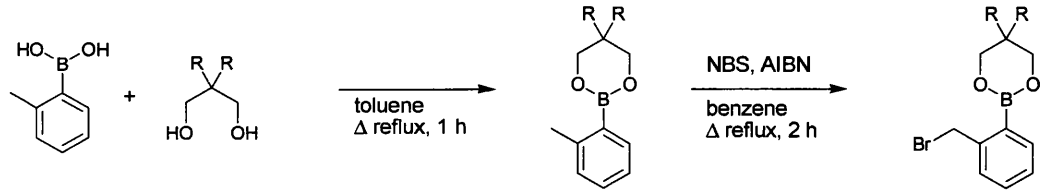

Scheme 58. *1,3-propanediol (R = H) and neopentyl glycol (R = Me) are both routinely used in the protection of o-tolylboronic acid. Typically water is removed from the system in the first step to drive the reaction towards the desired intermediate product.*

When considering the role of compounds **124** and **127** it should be noted that one of them will represent a precursor in the final step of the overall synthetic route for the monoboronic acid reference compounds $\mathbf{128}_{(\text{pyrene})}$ - $\mathbf{132}_{(\text{2-naphthalene})}$. It was therefore the aim to isolate one of these compounds with an exacting level of purity, the ability of **124** and **127** to be purified by silica gel flash column chromatography being crucial to this step.

In evaluating the 1,3-propanediol and neopentyl glycol protecting groups, both intermediates **125** and **126** were synthesised. Of the two diols, neopentyl glycol was considered to be the most suitable candidate for the protection.

125 **126**

Figure 51. *Compound **125**, 2-o-tolyl-1,3,2-dioxaborinane and compound **126**, 5,5-dimethyl-2-o-tolyl-1,3,2-dioxaborinane.*

Unlike 1,3-propanediol, neopentyl glycol is a solid at room temperature making it more amenable to handling. When interrogated by ^{1}H NMR neopentyl glycol produces two sharp singlets instead of two sets of compact multiplets, a welcome feature considering the potential complexity of the ^{1}H NMR spectra generated by boronic acids. Neopentyl glycol also forms a stronger complex with phenylboronic acid than 1,3-propanediol does, making compounds **126** and **127** more stable than compounds **125** and **124**, but even with this increased stability the cleavage of the ligand is remarkably facile after boronic acid **127** has been complexed to an amine. It is also the case that the overall yield of the protected *o*-bromo benzylboronic acid appears to be higher when neopentyl glycol is used,[158,210,213,214] minimising the amount of *o*-tolylboronic acid that is required in the formation of this compound.[††††]

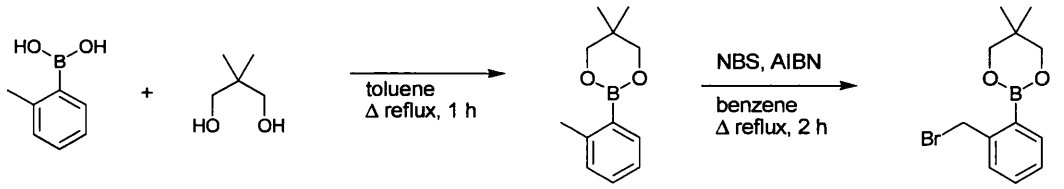

126 **127**

Scheme 59. *Synthesis of compounds **126** and **127**. In the first step, the benzene commonly used as solvent was replaced by toluene. A Dean Stark head was fitted to allow the azeotropic removal of water to generate intermediate **126** (92% yield). N-Bromosuccinimide (NBS) and 2,2'-azobisisobutyronitrile (AIBN) were used in the second step to afford boronic acid **127** (99% yield).*

[††††] *o*-Tolylboronic acid is a comparatively expensive starting material. The compound's retail price in the Sigma-Aldrich Co. Handbook 2005-2006 was £ 21.30 g^{-1} and was typically used in 5 g batches.

Attachment of the Protected *o*-Bromo Benzylboronic Acid

With compound **127** and the ammonium hydrochloride salts **119**$_{(pyrene)}$ - **123**$_{(2\text{-naphthalene})}$ isolated purely it was postulated that the coupling of these compounds should proceed readily and cleanly, see Scheme 60.

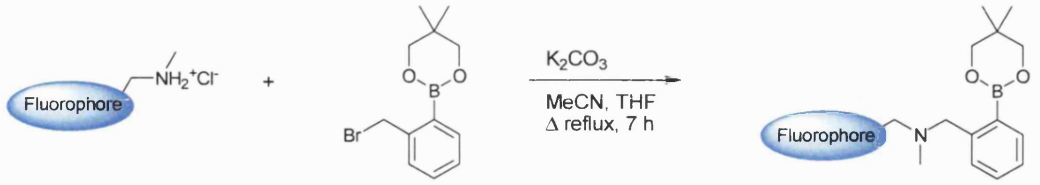

119$_{(pyrene)}$ - **123**$_{(2\text{-naphthalene})}$ **127** **128**$_{(pyrene)}$ - **132**$_{(2\text{-naphthalene})}$

Scheme 60. *Synthesis of the monoboronic acid reference compounds* ***128***$_{(pyrene)}$ - ***132***$_{(2\text{-naphthalene})}$ *from* ***119***$_{(pyrene)}$ - ***123***$_{(2\text{-naphthalene})}$ *and* ***127***.

From the viewpoint of sensor design the presence or absence of the neopentyl glycol protecting group on the final product was not a concern. The sensors would be evaluated at micromolar concentrations in aqueous methanolic solutions with millimolar concentrations of saccharides, the facile displacement of the protecting group under these conditions would not produce any noticeable interference in the fluorescence titrations. However, there was one prerequisite, both for characterisation and fluorescence titrations the compound must be isolated entirely as its protected or deprotected form, not as a mixture.

Reprecipitation from Chloroform in Ultrasounding *n*-Hexanes

The reaction was first conducted with the ammonium salt **123**$_{(2\text{-naphthalene})}$ and boronic acid **127**. Potassium carbonate was used to carry out the reaction and free the ammonium hydrochloride salt in one pot. The work up consisted of a solvent wash followed by a reprecipitation from chloroform (~ 2 $cm^3\ g^{-1}$) in *n*-hexanes (~ 60 $cm^3\ g^{-1}$) whilst the *n*-hexanes were subject to ultrasound. This procedure produced a pale yellow powder but the ^1H NMR spectrum indicated that this method of purification had not afforded the 2-naphthalene appended product cleanly. More success was to be had with this method when compounds were used that had been appended with larger fluorophores.

^{1}H NMR Spectra

At the same time as establishing a purification method for the boronic acids, challenges were faced in establishing protocols for the characterisation of these compounds by NMR. A good example of this is given by the product of the reaction of the ammonium salt **121**$_{(anthracene)}$ and boronic acid **127**. The reaction mixture was initially purified by a solvent wash and reprecipitation in an ultrasound bath, which afford a crude mass of 45%. The routine ^{1}H NMR experiment of the resultant precipitate, before drying, afforded the rather promising spectrum illustrated in Figure 52.

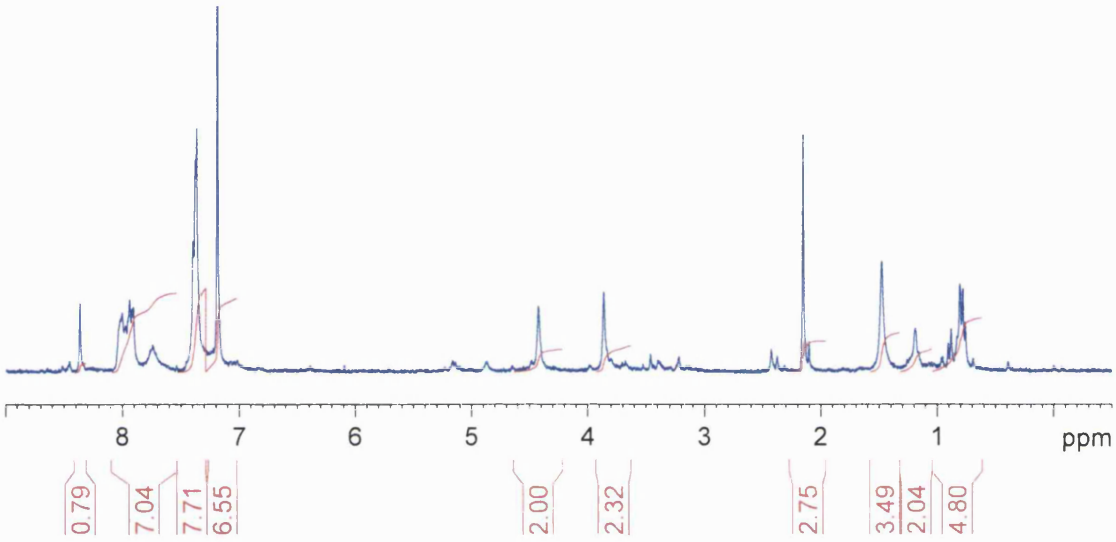

Figure 52. *^{1}H NMR spectrum (300 MHz, $CDCl_3$) of the wet compound afforded from the reaction of the ammonium salt **121**$_{(anthracene)}$ and boronic acid **127** followed by a solvent wash (DCM washed with water) and reprecipitation from chloroform in n-hexanes subject to ultrasound.*

In the ^{1}H NMR spectrum of the deprotected form of the ammonium salt **121**$_{(anthracene)}$ we would expect three peaks in the alkyl region and would later find these peaks to be at 2.09ppm (3H, s, NCH_3), 3.75ppm (2H, s, phenyl ArCH_2) and 4.30ppm (2H, s, anthryl ArCH_2), see Figure 53. There were also two alkyl peaks to be considered due to neopentyl glycol which might still have been complexed, we had found boronic acid **127** to display neopentyl glycol's alkyl peaks at 0.96ppm (6H, s, $OCH_2C(CH_3)_2CH_2O$) and 3.71ppm (4H, s, $OCH_2C(CH_3)_2CH_2O$).

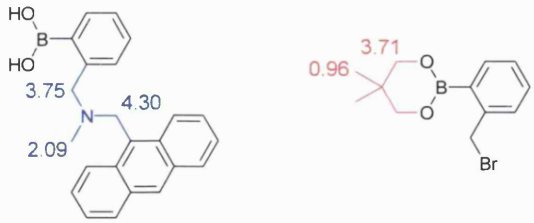

Figure 53. *The values in ppm of the signals observed for the selected alkyl regions of the ammonium salt* ***121***$_{(anthracene)}$ *(blue) and boronic acid* ***127*** *(red) in* ^{1}H *NMR spectra (300 MHz,* $CDCl_3$*).*

Given the promising result in Figure 52 the compound was re-condensed and dried *in vacuo* for five hours to ensure the removal of any remaining solvent. The ^{1}H NMR experiment was then rerun on the dry sample, the resultant ^{1}H NMR spectrum is illustrated in Figure 54.

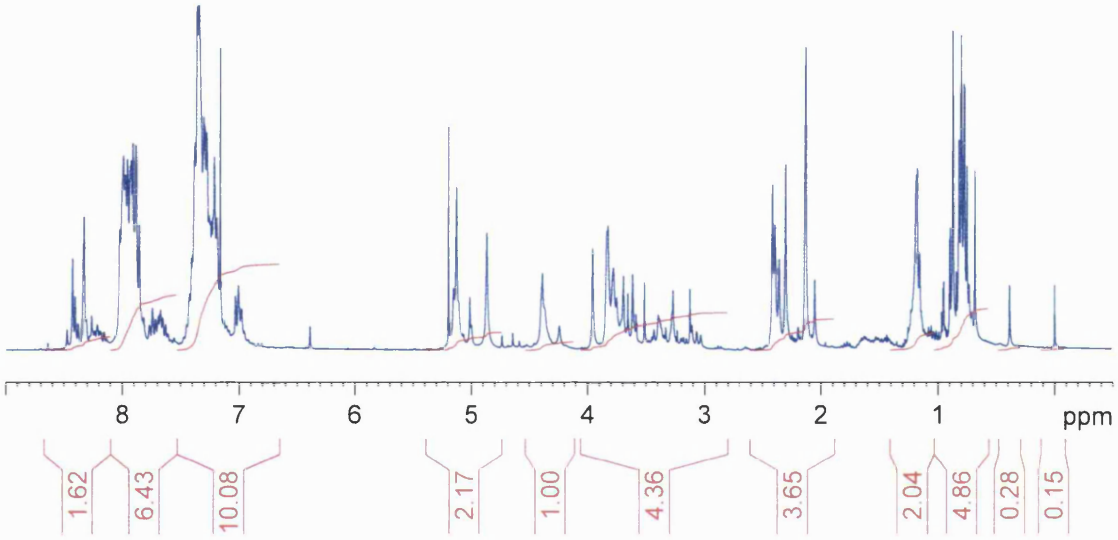

Figure 54. ^{1}H *NMR spectrum (300 MHz,* $CDCl_3$*) of the dry compound afforded from the reaction of the ammonium salt* ***121***$_{(anthracene)}$ *and boronic acid* ***127*** *followed by a solvent wash (DCM washed with water), reprecipitation from chloroform in n-hexanes subject to ultrasound and five hours on a high vacuum line.*

From Figure 54 the increase in complexity of this spectrum and apparently large increase in sample impurity is clear. In our experience obtaining dissimilar results from identical ^{1}H NMR experiments of the same boronic acid samples was commonplace.

If the deuterated chloroform used in Figure 54 was replaced by deuterated methanol (d_4 was used throughout) then the resulting spectrum of the dry product yielded a clear spectrum with fewer peaks. The benefit of using deuteric solvents in inhibiting the formation of trimers in these systems therefore became readily apparent, however, due

to the large appended fluorophores present these compounds displayed poor solubility in such solvents.

The use of mixed deuterated solvents in these experiments to avoid trimerisation had been previously reported by our group and the use of different blends of deuterated solvents was assessed here.[192] The optimum solvent blend in running the NMR experiments of the boronic acid based sensors was found to be a mixture of deuterated chloroform (0.8 cm^3) and deuterated methanol (2 drops). This mixture was found to effectively dissolve the compounds, inhibit trimerisation and minimise the discrepancy between the expected chemical shifts of compounds in deuterated chloroform and that observed in our blend.

Having overcome the issue of excessive signals in the ^1H NMR spectra from the trimeric forms of the boronic acids, the compounds examined in Figure 52 and Figure 54 still appeared impure by ^1H NMR. ^{11}B NMR revealed three peaks, a broad peak at 30.3ppm indicative of an sp^2 hybridised boronic acid, a broad peak at 9.6ppm indicative of an sp^3 hybridised boronate anion and a sharp peak at 19.1ppm indicative of the sp^2 hybridised protected boronic ester. From these results the weakness of relying solely on a solvent wash and a reprecipitation became apparent, as did the consequent need for a more effective purification method.

3.3.5 Column Chromatography

Work on purifying the desired monoboronic acid reference compounds by neutral alumina column chromatography began to prove successful with the product of the reaction between the ammonium salt **119**$_{(pyrene)}$ and boronic acid **127** being isolated with moderate purity, unfortunately it was isolated in both its free boronic acid and complexed forms.

Apart from providing poor separation, the potential of neutral alumina chromatography was limited to separating the protected and deprotected boronic acids. Ideally a method was required not only of purifying these two compounds but of ensuring the compounds were fully converted to either one form or the other, thus optimising the yield.

The use of silica gel column chromatography to deprotect boronic acids complexed to neopentyl glycol had been documented previously.[158] It should be noted that in the literature precedent the compound was chromatographed after the purification step had occurred, the sole purpose of the chromatographic step therefore being to remove the protecting group. In a similar step we repeated this procedure and found that the mixture of protected and deprotected compound **128**$_{(pyrene)}$ could be fully deprotected by passing the mixture down a silica gel plug, thus affording the boronic acid entirely in its deprotected form and with 57% overall yield.

It should be recalled that deprotection of the phenylboronic acid fragments **126** and **127** did not occur on silica gel, see Scheme 59. As discussed in Section 1.4.4 (page 54) the introduction of a suitably positioned amine group proximal to the boron centre generates a N-B interaction. This change in acidity at the boron centre is sufficient to allow the mildly acidic environment within the silica gel column to now fully deprotect compound **128**$_{(pyrene)}$.

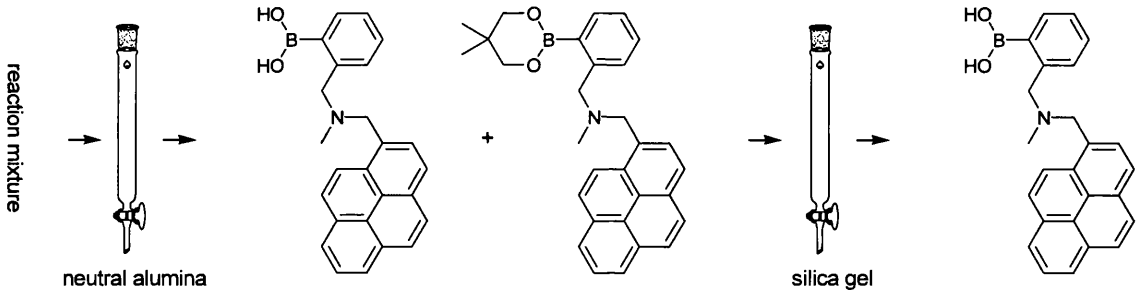

Scheme 61. *Schematic representation of the procedure involving purification of the reaction mixture by neutral alumina column chromatography to yield the required boronic acid and ester, and removal of the neopentyl glycol protecting group by silica gel column chromatography.*

In refining this purification, which now required two consecutive chromatographic steps, it was postulated that deprotection and separation could be conducted simultaneously.

To this end the use of silica gel column chromatography was examined. It is rare that silica gel column chromatography is reported in the purification of compounds containing the free *N*-methyl-*o*-(aminomethyl)phenylboronic acid fragment and we did not find a literature precedent which used silica gel as a genuine purification technique (as opposed to a deprotection technique).

Remarkably the R_fs of compounds **128**$_{(pyrene)}$ - **132**$_{(2\text{-naphthalene})}$ on silica gel TLCs ranged between 0.35 and 0.46 (10:90 methanol/dichloromethane elution). However, it was found that the R_fs observed by TLC were somewhat deceptive. Compounds **128**$_{(pyrene)}$ - **132**$_{(2\text{-naphthalene})}$ exhibit markedly different properties when in the bulk mobile phase of a silica gel column as compared to when they are on the flat surface of a silica gel TLC plate. The reluctance of these compounds to travel in the mobile phase of a column required a polar gradient elution to be used allowing the impurities to be driven off the column before reclaiming the desired target molecules.

A typical TLC obtained from spotting the fractions collected on running a flash column is illustrated in Figure 55, the procedure used for successful purification is detailed in the figure caption. It should be noted that the R_f of the monoboronic acid is not indicative of how the compound behaves on the column. The compound in fraction 2 does have a far lower R_f than the compound in fractions 6-19.

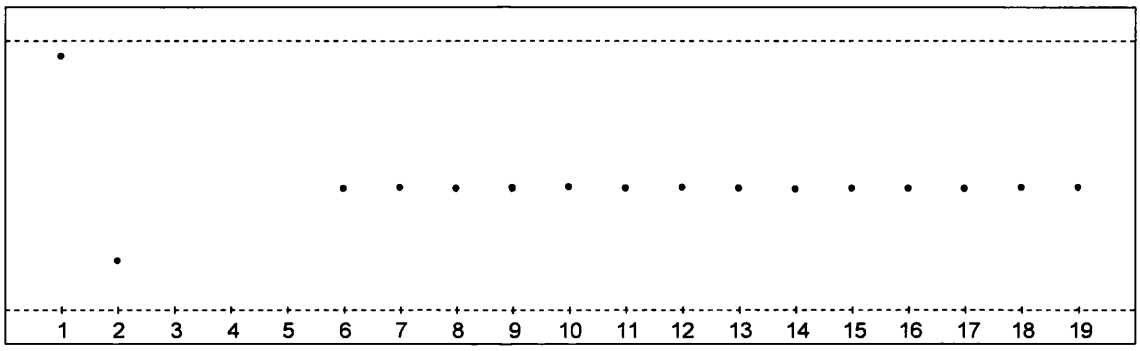

Figure 55. *TLC of fractions 1-19 collected during the purification of compound* **129**$_{(phenanthrene)}$*. The plate was aluminium backed, coated with a 0.20 mm layer of silica gel 60 with fluorescent indicator* UV_{254} *and eluted with 10:90 MeOH/DCM. All spots were visible under UV* (λ_{ex} *254 nm or 365 nm), fraction 1 could also be visualised with vanillin and fraction 2 with ninhydrin. 407 mg of crude material was loaded onto a silica gel 60 column 3 cm in diameter and 19 cm in height with 5:95 MeOH/DCM as eluent. The procedure took ~ 7 hours to run and required the availability of ~ 4 L of MeOH and ~ 4 L of DCM. Once loaded the column was kept under pressure and the mobile phase kept moving whenever possible. The gradient elution proceeded as follows (eluent ratios are given as MeOH/DCM): F1 (600* cm^3*, 5:95)* $\rightarrow$ *(300* cm^3*, 10:90); F2 (200* cm^3*, 10:90)* $\rightarrow$ *(500* cm^3*, 15:85)* $\rightarrow$ *(200* cm^3*, 20:80); F3 (800* cm^3*, 20:80); F4 (250* cm^3*, 25:75); F5 (250* cm^3*, 25:75)* $\rightarrow$ *(250* cm^3*, 30:70); F6 (250* cm^3*, 30:70)* $\rightarrow$ *(250* cm^3*, 35:65); F7 (250* cm^3*, 35:65); F8 (250* cm^3*, 40:60); F9 (250* cm^3*, 40:60); F10 (250* cm^3*, 75:25); F11 (225* cm^3*, 75:25); F12 (225* cm^3*, 90:10); F13 (250* cm^3*, 90:10); F14 (225* cm^3*, 90:10); F15 (225* cm^3*, 90:10); F16 (900* cm^3*, 90:10); F17 (350* cm^3*, 90:10); F18 (225* cm^3*, 90:10); F19 (100* cm^3*, 90:10).*

It was imperative in running these flash silica gel columns that the elution was continuous. Due to the separation between compounds, comparatively large fractions could be collected to accommodate the ~ 6-7 litres of eluent typically required. It should also be noted that due to the volumes involved the minimum mass of crude material this

purification worked for was 100 mg, in instances where any less was used it was not possible to visualise the products by TLC.

Whilst this chromatographic step represented a somewhat unorthodox use of a silica gel column, the almost Sisyphean effort involved was worth investing as, if done correctly, the product could be reclaimed from the column and the compound obtained pure. Due to the acidic environment of the column, and the use of neopentyl glycol as a protecting group, purification and deprotection did indeed occur simultaneously. Flash column chromatography on silica gel therefore afforded compounds **128**$_{(pyrene)}$ - **132**$_{(2\text{-naphthalene})}$ directly and purely *via* the parallel synthesis illustrated in Scheme 62 - Scheme 66.

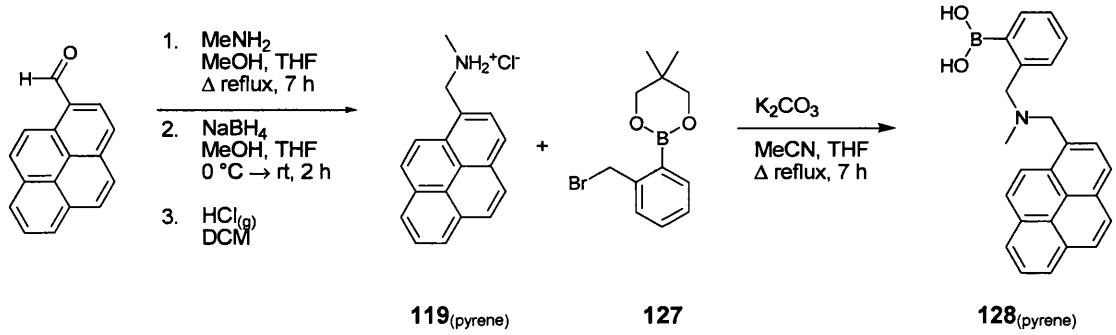

Scheme 62. *Synthesis of compound* ***128***$_{(pyrene)}$ *(final step 82% yield).*

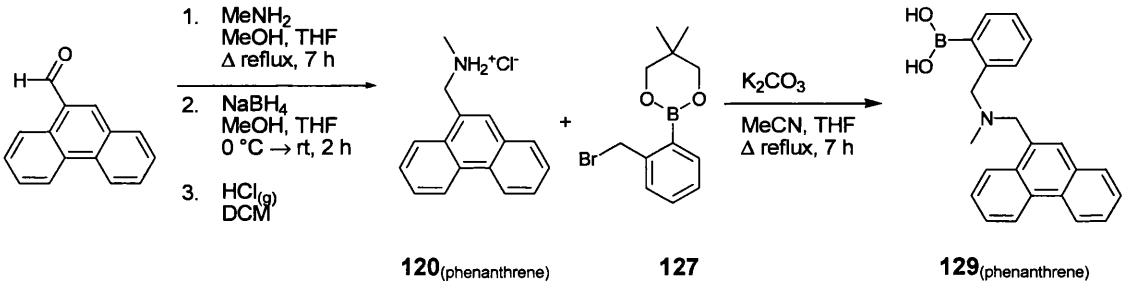

Scheme 63. *Synthesis of compound* ***129***$_{(phenanthrene)}$ *(final step 69% yield).*

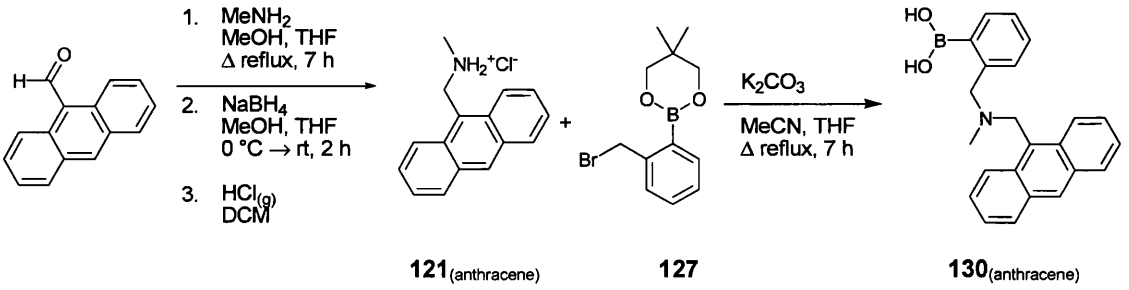

Scheme 64. *Synthesis of compound* ***130***$_{(anthracene)}$ *(final step 80% yield).*

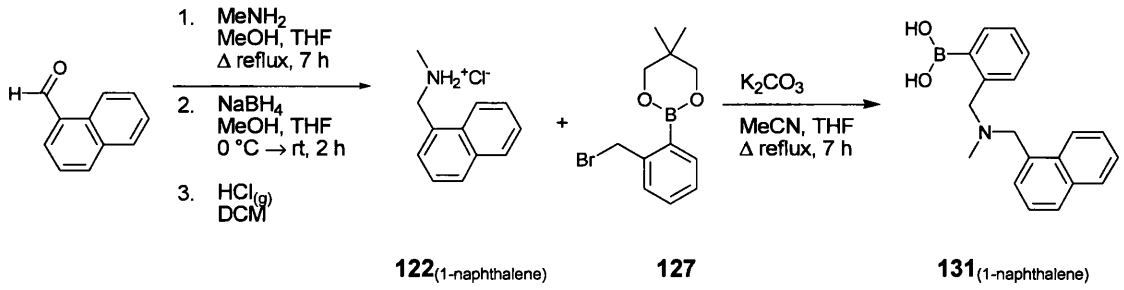

Scheme 65. *Synthesis of compound* ***131****(1-naphthalene) (final step 74% yield).*

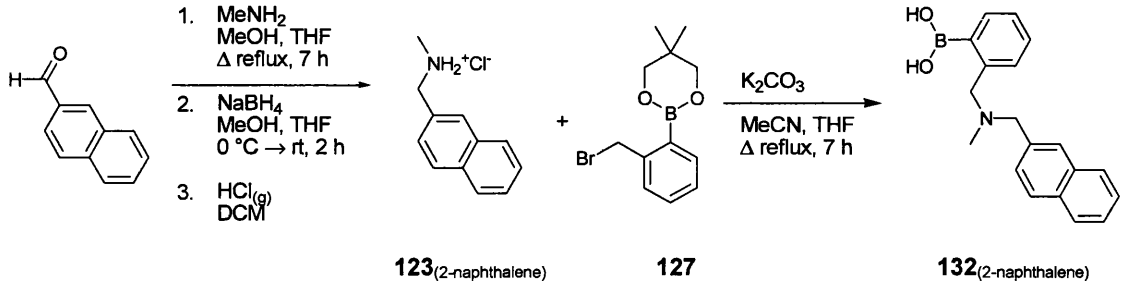

Scheme 66. *Synthesis of compound* ***132****(2-naphthalene) (final step 42% yield).*

To give an example of the effectiveness of this synthetic route and the power of the purification technique, the ^{1}H NMR spectrum of compound **130**$_{(anthracene)}$ is illustrated in Figure 56. The spectrum is typical of the ^{1}H NMR spectra obtained for compounds **128**$_{(pyrene)}$ - **132**$_{(2\text{-naphthalene})}$ and when contrasted against the previous ^{1}H NMR spectra presented in this section illustrates the exceptional purity of this compound following chromatography. The blend of deuterated solvents inhibits trimerisation.

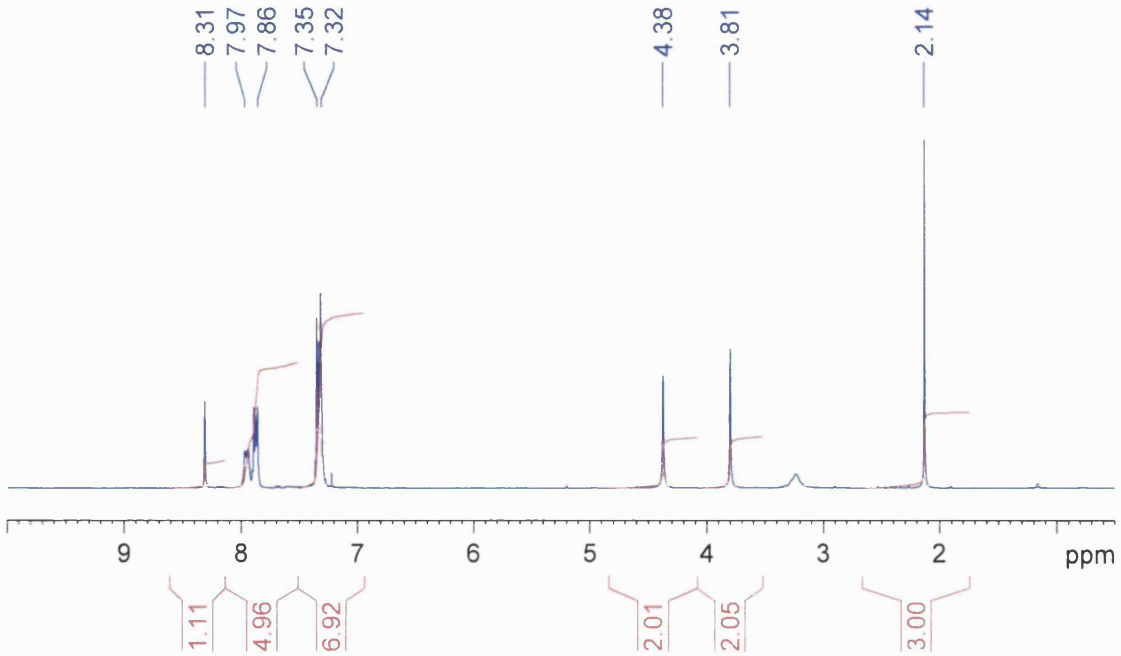

Figure 56. *^{1}H NMR spectrum (300 MHz, $CDCl_3$ with a few drops of MeOD) of compound* ***130***$_{(anthracene)}$*, with residual solvent peaks at 3.24ppm (MeOH) and 7.22ppm ($CHCl_3$).*

The purity of these reference compounds allowed them to be characterised completely and permitted a broader spread of analytical procedures to be undertaken than is often undertaken for this class of compounds.

2D heteronuclear multiple bond connectivity (HMBC) experiments were devised using **130**$_{(anthracene)}$ to elucidate the absolute structural assignment of the alkyl peaks in the ^{1}H NMR spectra. Unusually, for this class of compound, low resolution and high resolution mass spectrometry (LRMS and HRMS) yielded the molecular ion peaks of the target molecules, obviating the need to rely on the pseudo-molecular ion peaks of derived complexes. A procedure was devised and implemented for the acquisition of reproducible melting points, see *Experimental* for details. Indeed the only characterisation method to remain elusive was elemental analysis. This was an unsurprising result given the known resilience of the *N*-methyl-*o*-(aminomethyl)-phenylboronic acid fragment toward combustion. This property was well documented in the early work conducted on boronic acids[215] and has led to the wide spread application of boron acids and boronates in modern fire retardants.[216]

To put the strength of the synthetic methodology developed here into context it should be noted that the monoboronic acid reference compound **128**$_{(pyrene)}$ has been reported in

six different scientific publications since 1995. In those six publications no structural data has been reported whatsoever regarding the characterisation of compound $\mathbf{128}_{(\text{pyrene})}$.[184,191,192,205,207,212]

The synthetic methodology documented above has permitted us to isolate compound $\mathbf{128}_{(\text{pyrene})}$ in excellent purity and as such has allowed us to report, within this thesis: the retardance factor (R_f), melting point, elemental analysis, infra red spectrum, ^{1}H NMR spectrum, ^{11}B NMR spectrum, ^{13}C NMR spectrum, low resolution mass spectrum and high resolution mass spectrum.

Denouement

In designing synthetic routes for the construction of sensors containing the *N*-methyl-o-(aminomethyl)phenylboronic acid fragment particular attention must be paid to the final step: the coupling of the amine moiety to the phenylboronic acid moiety. In the synthesis of the boronic acid reference compounds $\mathbf{128}_{(\text{pyrene})}$ - $\mathbf{132}_{(\text{2-naphthalene})}$ described above we have documented synthetic procedures which allow for the required intermediate compounds to be isolated with exacting levels of purity and which thus permit the final reaction to proceed cleanly. Furthermore, purification of the target molecules by affinity chromatography has been achieved and is detailed herein, as are the procedural nuances developed to permit a meaningful structural analysis.

The chromatographic purification has afforded the desired compounds with unprecedented levels of purity and by a means which would appear to be generally applicable to other fluorescent sensors containing the *N*-methyl-o-(aminomethyl)-phenylboronic acid fragment.

3.4 DIBORONIC ACID MODULAR SENSORS

The second stage in undertaking the examination of fluorophore dependence in modular systems was the evaluation and synthesis of the diboronic acid sensors themselves.

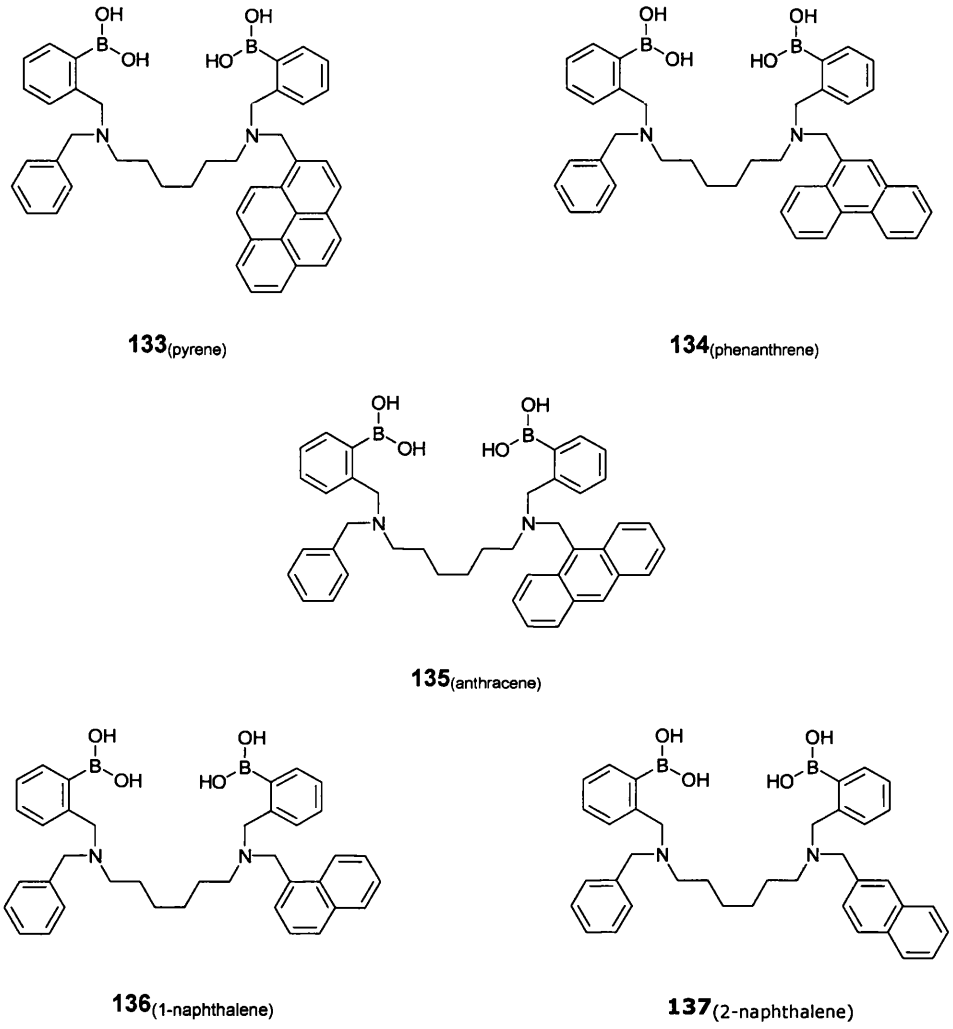

Figure 57. *Modular sensors* ***133****(pyrene)* *-* ***137****(2-naphthalene)* *with modified fluorophore subunits.*

As with the monoboronic acid reference compounds **128**(pyrene) - **132**(2-naphthalene) the diboronic acid sensors **133**(pyrene) - **137**(2-naphthalene) were initially investigated by Arimori *et al.* within our research group.[212] In this instance there was sufficient material remaining and of high enough purity to allow us to characterise the diboronic acid sensors **133**(pyrene) - **137**(2-naphthalene) isolated by our predecessors.

Generally Applicable Synthetic Routes

Although target molecules **133**$_{(pyrene)}$ - **137**$_{(2\text{-naphthalene})}$ had been isolated, the main premise of our work remained the same: the development of robust and generally applicable synthetic routes for the formation of fluorescent sensors containing the *N*-methyl-*o*-(aminomethyl)phenylboronic acid fragment.

Having established effective methods for the handling, synthesis and purification of the monoboronic acid reference compounds **128**$_{(pyrene)}$ - **132**$_{(2\text{-naphthalene})}$, these techniques were applied and furthered in the synthesis of the diboronic acid sensors **133**$_{(pyrene)}$ - **137**$_{(2\text{-naphthalene})}$.

Previous Synthetic Route

As with the work on linker dependence, Section 2.4.1 (page 95), Arimori *et al.* synthesised the diboronic acid systems **133**$_{(pyrene)}$ - **137**$_{(2\text{-naphthalene})}$ from the 1,6-hexamethylene diamine core up. Using the same synthetic procedures as in the construction of sensors **109**$_{(n=3)}$ - **114**$_{(n=8)}$ with varying linker units,[192] 5:1 (amine/aldehyde) dilution conditions were used with 5 equivalents of *p*-toluenesulfonic acid to control the number of substitutions occurring on the amine.[212]

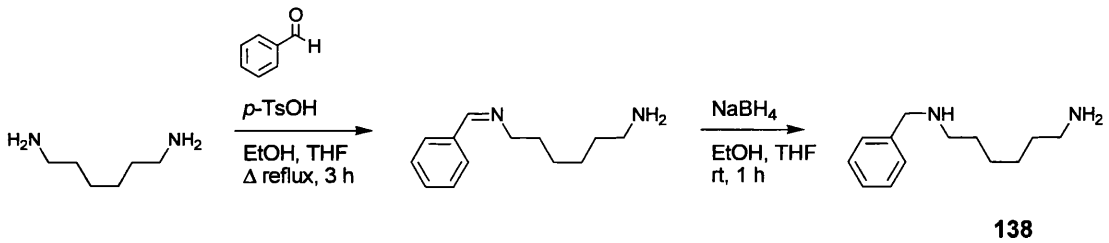

138

Scheme 67. *Synthesis of compound **138** under 5:5:1 (amine/p-TsOH/aldehyde) dilution conditions (78% yield).*[212]

The second reductive amination with the required aldehyde of the fluorophore gave the corresponding disubstituted diamines which were purified by Sephadex® LH-20 column chromatography (with methanol as eluent) to complete the synthesis of the derivatised linkers **144**$_{(fluorophore)}$, see Scheme 68.

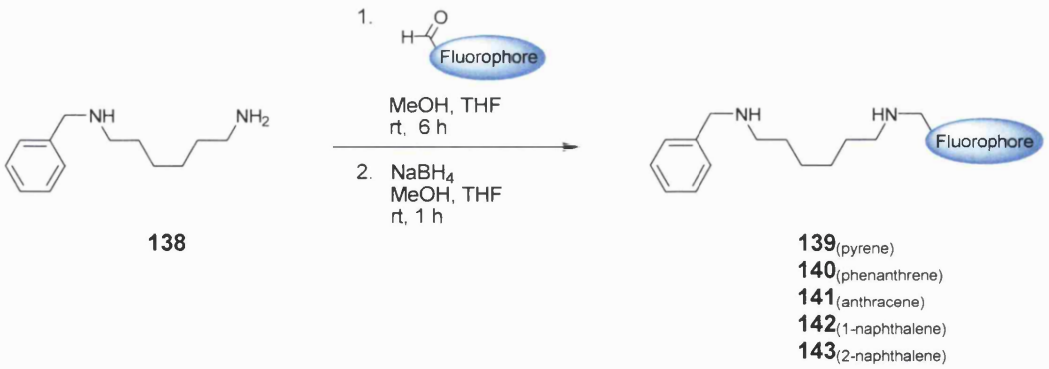

138

139$_{(pyrene)}$
140$_{(phenanthrene)}$
141$_{(anthracene)}$
142$_{(1\text{-}naphthalene)}$
143$_{(2\text{-}naphthalene)}$

Scheme 68. *Synthesis of compounds* ***139***$_{(pyrene)}$ *-* ***143***$_{(2\text{-}naphthalene)}$ *(37-86% yield).*[212]

Insertion of the phenylboronic acid receptor units was achieved by the addition of 2-(2-bromobenzyl)-1,3,2-dioxaborinane to a solution of potassium carbonate and the required intermediate core unit **139**$_{(pyrene)}$ - **143**$_{(2\text{-}naphthalene)}$ in acetonitrile, see Scheme 69. Purification was achieved by reprecipitation from chloroform in *n*-hexanes.

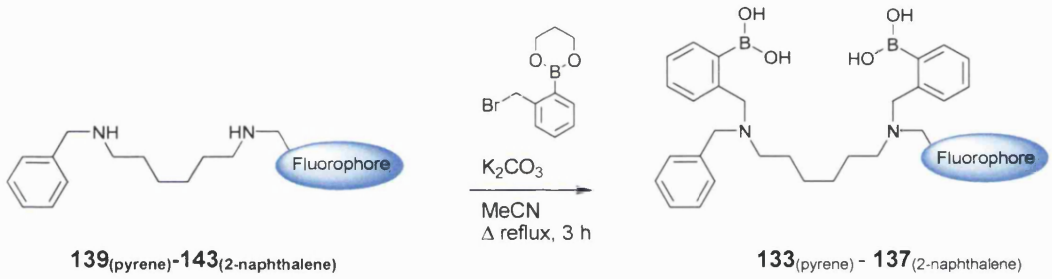

139$_{(pyrene)}$-**143**$_{(2\text{-}naphthalene)}$

133$_{(pyrene)}$ - **137**$_{(2\text{-}naphthalene)}$

Scheme 69. *Synthesis of diboronic acids* ***133***$_{(pyrene)}$ *-* ***137***$_{(2\text{-}naphthalene)}$ *(35-56% yield).*[212]

3.4.1 Proposed Synthetic Methodology

As established for the monoboronic acid reference compounds **128**$_{(pyrene)}$ - **132**$_{(2\text{-}naphthalene)}$, the key to the synthesis of compounds containing the *N*-methyl-*o*-(aminomethyl)-phenylboronic acid fragment is the clean coupling of the boronic acid and amine moieties in the final step from stringently purified precursors.

The choice of the boronic acid precursor **127** and its ability to couple with both amines and ammonium salts had already been determined, our efforts now focused on the use and applicability of the 5:1 dilution conditions in functionalising the diamine linkers.

Retrosynthetic Analysis

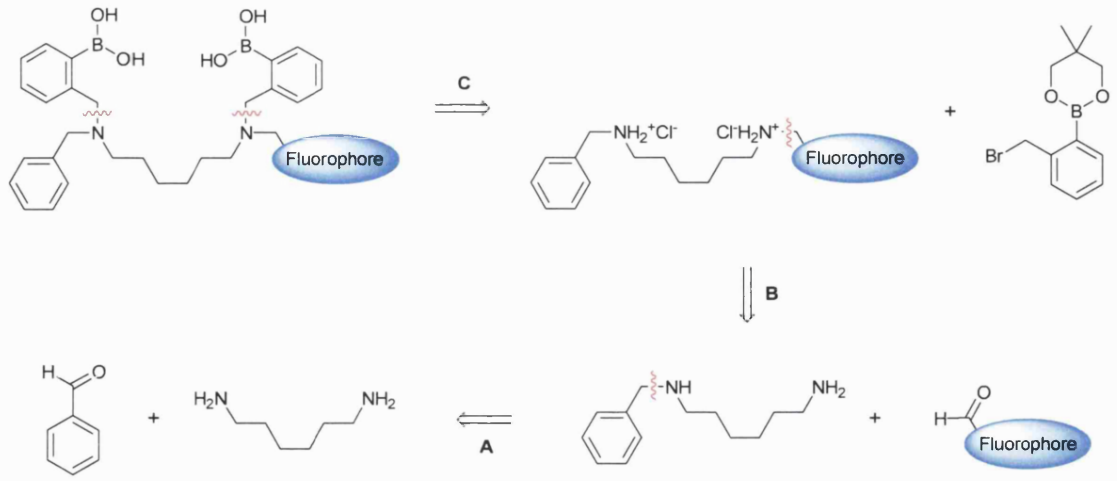

Scheme 70. *Retrosynthetic analysis of the diboronic acid sensors* ***133***$_{(pyrene)}$ *-* ***137***$_{(2\text{-naphthalene})}$*. The symbol ~~~ is used to indicate the location of the proposed decouplings.*

As demonstrated in the previous section, if the precursors to the final step could be isolated purely, step **C** in Scheme 70 should afford the target molecules in good yields and with high levels of purity. Therefore with a route for the coupling of the diboronic acid and amine moieties already successfully established and the diboronic acid sensors **133**$_{(pyrene)}$ - **137**$_{(2\text{-naphthalene})}$ already obtained, steps **A** and **B** in Scheme 70 were tackled. The aim here was to devise a route to the disubstituted diamine core units which would afforded them in reasonable yield and with high levels of purity.

3.4.2 *Implementation*

5:1 Dilution Conditions

In forming the core unit, the first step, regioselective substitution of a single electrophile on to the α,ω-alkanediamine linker was crucial in controlling the purity of the final compound. Whilst largely effective with 1,6-hexamethylene diamine it was felt that the 5:1 (amine/aldehyde) dilution conditions used to couple benzaldehyde with the diamine linker in the presence of 5 equivalents of *p*-toluenesulfonic acid could be improved upon.

Under ideal circumstances high dilution conditions are designed to offer a statistical bias in the way the reaction proceeds. The basic concept is that as each molecule of aldehyde is introduced to the system it will find itself mainly surrounded by molecules

of unreacted hexamethylene diamine. If these unreacted molecules of hexamethylene diamine do genuinely outweigh their already monosubstituted derivatives (and it is known that both species have similar reactivities) then it is reasonable to expect a tendency towards the formation of the monosubstituted derivative over that of the disubstituted derivative.

10:1 Dilution Conditions with a Four Hour Dropwise Addition

The reaction conditions were investigated further and dilution increased to 10:1 (amine/aldehyde, with 10 equivalents *p*-toluenesulfonic acid), which provided a modest increase in selectivity. When 10:10:1 (amine/*p*-toluenesulfonic acid/aldehyde) dilution conditions were used in conjunction with a ≥ 4 hour dropwise addition of the aldehyde to the system, it was found that the monosubstituted hexamethylene diamine derivative could be obtained almost exclusively.

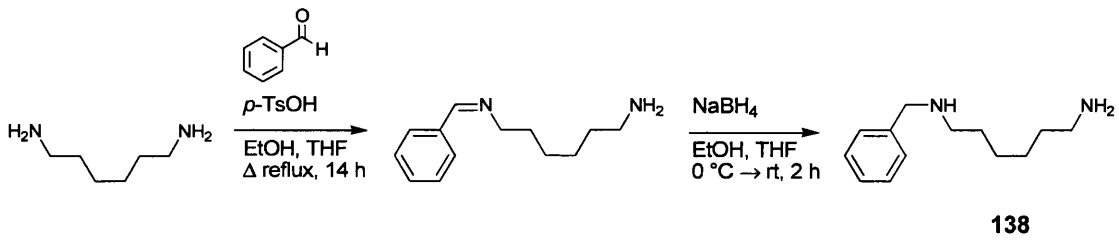

138

Scheme 71. *Synthesis of compound **138** under 10:10:1 (amine/p-TsOH/aldehyde) dilution conditions with a ≥ 4 h dropwise addition of the aldehyde (77% yield).*

There was confidence with this procedure that, after the reductive amination, the monosubstituted molecule **138** and the un-reacted hexamethylene diamine accounted for the vast majority of amine containing compounds in the reaction vessel. To ensure no hexamethylene diamine could go on to react in the next step, the reaction mixture was extracted in dichloromethane and subjected to a rigorous solvent wash, as was described in the synthesis of the monoboronic acid reference compounds $\mathbf{128}_{(\text{pyrene})}$ - $\mathbf{132}_{(\text{2-naphthalene})}$, see Section 3.3.3, *Improved Aqueous Wash* (Page 123).

This method substantially improved the purity of compound **138** and was found to be applicable in the addition of other aldehydes to the 1,6 hexamethylene diamine linker, such as 1-pyrenecarboxaldhyde, see Scheme 72.

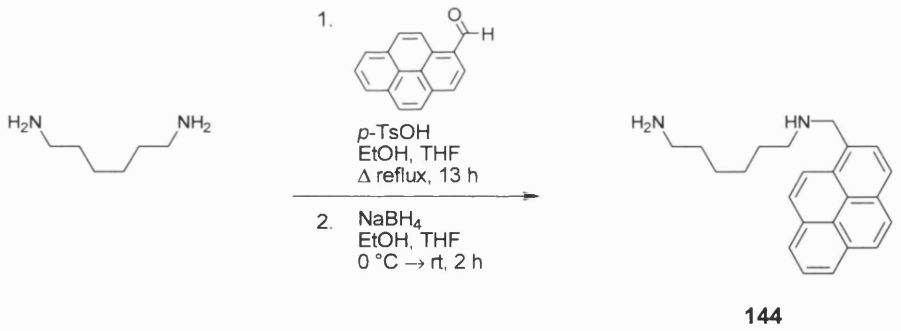

144

Scheme 72. *Synthesis of **144** under 10:10:1 (amine/p-TsOH/aldehyde) dilution conditions with a ≥ 4 h dropwise addition of the aldehyde (96% yield).*

The ^{1}H NMR spectrum of compound **144** obtained using the procedure in Scheme 72, is displayed in Figure 58. The NMR spectrum clearly shows that substitution on 1,6-hexamethylene diamine can be efficiently controlled using 10:1 dilution conditions and a 4 hour addition.

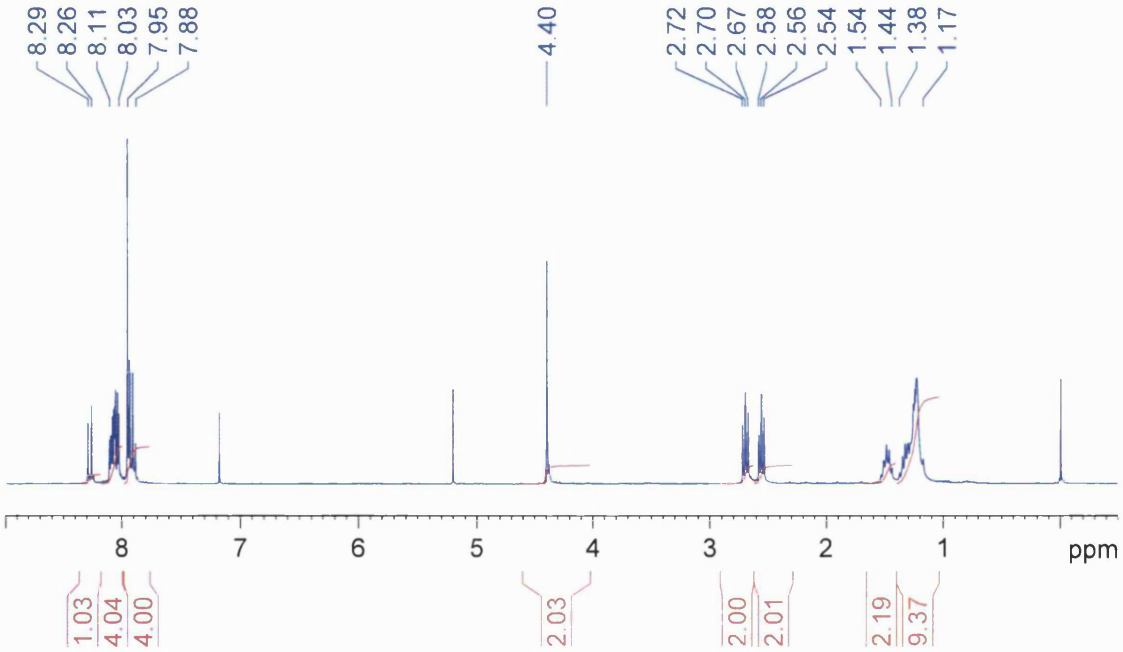

Figure 58. *^{1}H NMR spectrum (300 MHz, $CDCl_3$) of compound **144**, with TMS at 0.00ppm, water masked ~ 1.23ppm giving rise to the inflated integral value for the multiplet in the range 1.17-1.38ppm, DCM at 5.20ppm and the residual solvent peak at 7.17ppm.*

3.4.3 Applicability of High Dilution Conditions

Whilst these conditions proved particularly effective for controlling aminations on 1,6-hexamethylene diamine the route could not be considered generally applicable. At the

start of this project the evaluation of high dilution conditions in controlling substitutions on polyamines (page 90) had uncovered certain unexpected results, complications arising in the substitution of fluorophores on to α,ω-alkanediamines of particular chain lengths. A good example of this comes from the reaction of 9-anthraldehyde with ethylene diamine under 6:1 (amine/aldehyde) dilution conditions.

π-π Interactions

Under 6:1 dilution conditions the reaction afforded the disubstituted form of ethylene diamine in unprecedented levels, the highest being a ratio of 78% disubstituted product to 22% monosubstituted product. The likelihood is that the separation between the two aromatic surfaces in the intermediate disubstituted di-imine **145** was such that the hydrophobic π-π interactions furnished the compound with significant stabilisation.

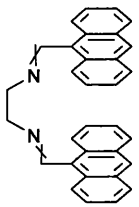

145

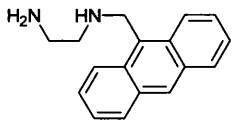

146

With the propensity of 9-anthraldehyde and ethylene diamine to form substances such as the di-imine **145** it was considered unrealistic that high dilution conditions would be obtained that could provide an efficient or reliable route to the monosubstituted diamine **146**.

Intramolecular Ring Closure

Reactions were also undertaken between diamines and compounds with more than one reactive functional group. This introduced the issue of intramolecular ring closure. For example the reaction between 1,6-hexamethylene diamine and isophthaloyl dichloride, Scheme 73, would be expected to occur when these two reagents were introduced to each other regardless of the dilution conditions used, the role of these reagents will be discussed in Section 3.6 (page 166).

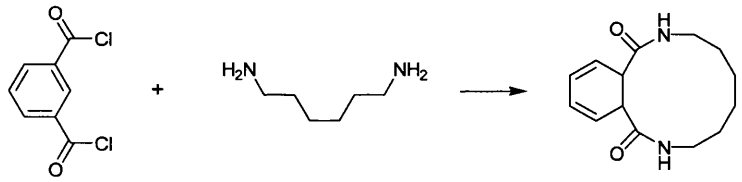

Scheme 73. *Expected intramolecular ring closure between 1,6-hexamethylene diamine and isophthaloyl dichloride.*

Conclusion

With the 10:1 dilution conditions and slow dropwise addition of the aldehyde it had became possible to isolate monosubstituted derivatives of 1,6-hexamethylene diamine purely. Whilst the high dilution conditions functioned well for the reaction of this particular diamine with compounds containing a single electrophilic centre, it was felt that the route was neither efficient nor generally applicable.

The high dilution method required 90% of the starting amine to be discarded in the first step and as discussed above the exact conditions and outcome of the reactions were dependent on the length and branching of the alkyl chain in the polyamine substrate, as well as the solubility and functionality of the fluorophore. These variables forced the reaction conditions to be fine tuned by the researcher in each instance, introducing procedural variations into these synthetic routes on a case-by-case basis.

To circumvent this synthetic prestidigitation and to overcome the challenges introduced by multiple electrophilic centres, protecting group chemistry was considered.

3.4.4 Protecting Group Chemistry

A plethora of protecting groups exist for amines and have been extensively reviewed elsewhere.[217-219] In selecting a suitable protecting group for our purposes the main criteria was that it should allow a mono-protected α,ω-alkanediamine to be isolated cleanly.

The protecting group chosen was *tert*-butoxycarbonyl (Boc). Not only are Boc protecting agents inexpensive and commercially available but the ubiquitous use of Boc in protecting group chemistry ensures a wealth of documented experimental information. Of particular relevance to our synthetic needs, Boc is acid labile and can be cleaved

using hydrochloric acid, allowing deprotection and formation of the ammonium hydrochloride salt of the compound to occur in one pot.

The most common direct method for the preparation of Boc mono-protected α,ω-alkanediamines was developed by Krapcho *et al.*[220,221] and is analogous to the high dilution method developed for the monosubstituted compounds **138** and **144** above. To 6-7 equivalents of the α,ω-alkanediamine, at 0 °C, Krapcho *et al.* added di-*tert*-butyl dicarbonate (Boc_2O) dropwise. We had previously investigated the use of Boc_2O when considering methods to achieve selective substitutions on the polyamines discussed in Section 2.3 (page 90), however, there is little to distinguish this method of introducing a single substituent to a diamine from the reductive amination under 10:1 dilution conditions discussed above.

Selective Synthesis of Carbamate Protected Polyamines

An alternative and rather more versatile procedure was reported by Christensen and co-workers in 2002 which proved to be more efficient in its use of starting materials and particularly well suited to our needs.[222] Reporting on the synthesis of Boc, benzyloxycarbonyl (Cbz), and allyloxycarbonyl (Alloc) protected polyamines Christensen and co-workers used alkyl phenyl carbonates as protecting agents. This method has been reported to permit primary and secondary amines to be distinguished by the selective protection of primary amines under kinetic control. Moreover, the route allows mono-protected α,ω-alkanediamines to be obtained exclusively with exacting levels of purity. The mono-protected α,ω-alkanediamines were afforded from reactions performed with 1:1.1 (amine/protecting group) stoichiometry by directly mixing the reactants in one pot.

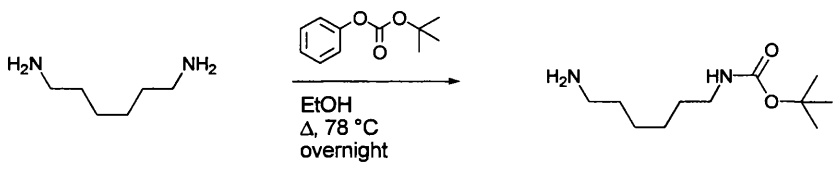

147

Scheme 74. *Synthesis of compound **147** (45% yield).*

As should be expected from the direct addition of *tert*-butyl phenyl carbonate to hexamethylene diamine, no regioselectivity was displayed in the reaction itself. The reaction mixture therefore afforded a combination of un-, mono- and di-substituted products. The pivotal step in isolating the mono-protected component in this procedure occurs during the ingenuously simple and effective purification. Following completion of the reaction the solvent is removed under reduced pressure. Water is added to the residue, the acidity adjusted to pH = 3 and the aqueous phase washed with dichloromethane. The acidity of the aqueous phase is then adjusted to pH = 14 allowing the final product to be extracted cleanly in dichloromethane. This procedure is represented schematically in Scheme 75.

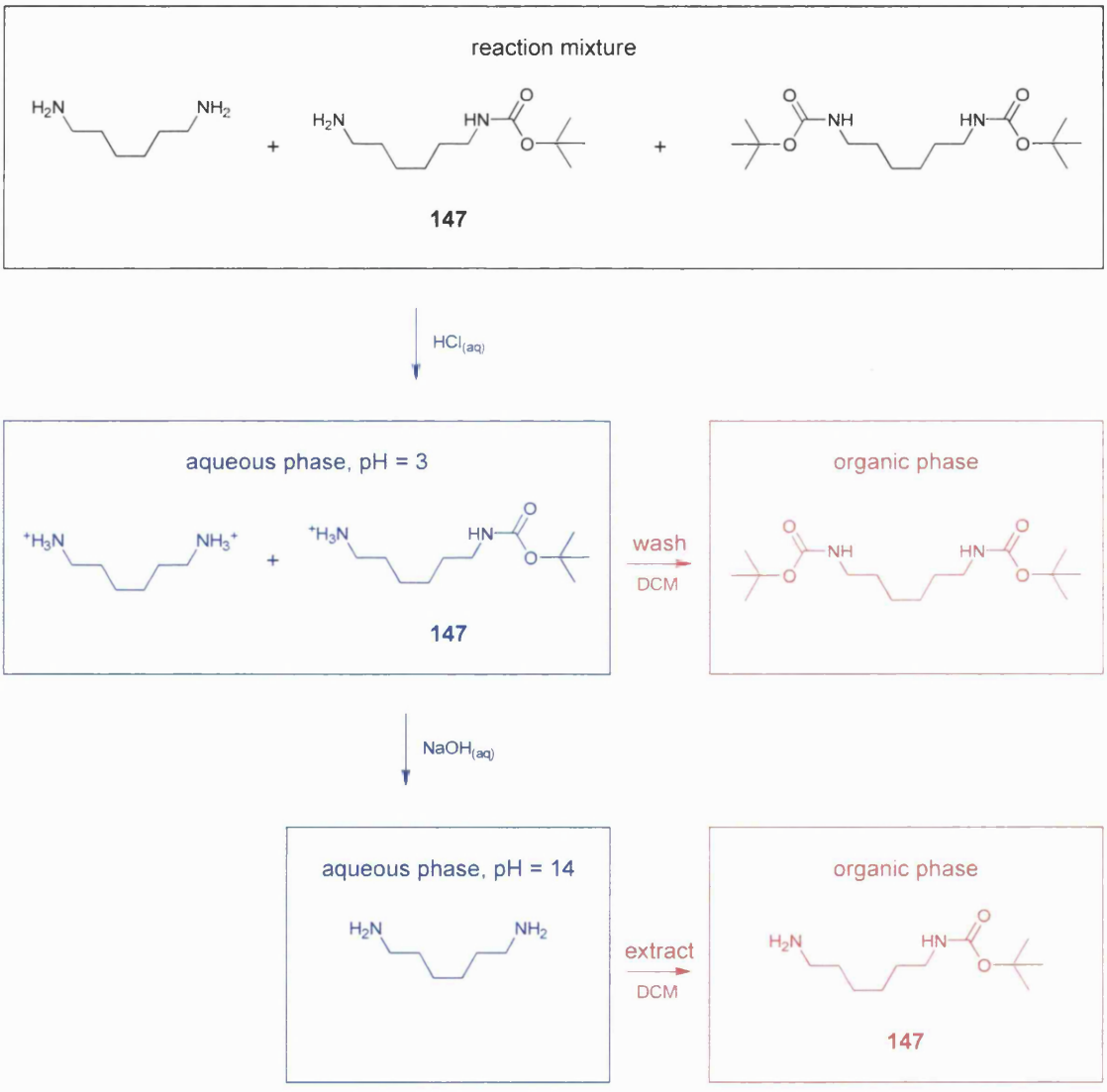

Scheme 75. *Schematic representation of the procedure used to obtain compound **147** cleanly from the reaction mixture via a solvent extraction.*

In adopting the procedure developed by Christensen and co-workers we chose to carry out the purification twice so as to ensure the isolation of compound **147** with excellent levels of purity, this afforded compound **147** in 45% yield.

In choosing this procedure as the first step in our synthetic route it should be recalled that compound **138** had been afforded in 77% yield under high dilution conditions and the method used by Krapcho *et al.* generated compound **147** in 75% yield.[220] It should be recalled, however, that these high dilution methods involve the loss of a significant amount (5-9 equivalents) of the α,ω-alkanediamine.

tert-Butyl phenyl carbonate is inexpensive (£14.20 for 25 g), even cheaper than the ubiquitous Boc_2O (£15.50 for 25 g) and yet it does not suffer from the undesired handling properties (Boc_2O: mp 23 °C,[223] R:10-26-36/37/38).‡‡‡‡ Moreover, the cost of reagents and the ruggedness of the synthetic procedure allowed us to scale the reaction up. *tert*-Butyl phenyl carbonate (26.5 g, 137 mmol) and 1,6-hexamethylene diamine (16.1 g, 138 mmol) reacted to yield 13.0 g of compound **147** in 44% yield and with excellent purity.

The ability to mono-protect our starting linker, cleanly and in such large batches, made this protection route the method of choice for functionalising 1,6-hexamethylene diamine in the opening step.

Thermal Degradation

It is well known that the Boc protecting group is susceptible to thermal cleavage. Therefore in conducting the synthesis of compound **147** the temperature should be maintained below ~ 80 °C.[222] In practice we found controlling the temperature of the reaction with a digital contact thermometer set at 78 °C functioned adequately in the synthesis of **147**.

This was not the case in the synthesis of compound **148**. When compound **148** was reacted with benzaldehyde at 78 °C overnight, thermal degradation became an issue. Whilst compound **148** can be afforded pure from the reaction mixture by silica gel

‡‡‡‡ The price comparison is based on the compounds' retail prices in the Sigma-Aldrich Co. Handbook 2005-2006. Risk phrases are as based on the information displayed on the product labels, R10, Flammable; R26, Very toxic by inhalation; R36/37/38, Irritating to eyes, respiratory system and skin.[224]

column chromatography (no decomposition was witnessed on silica),[225,226] the yield of the desired product was found to be about half (35%) of the yield when the reaction was conducted at room temperature overnight (67%). If the reaction was conducted under reflux conditions then these side products, disubstituted or unreacted 1,6-hexamethylene diamines, were generated in overwhelming quantities.

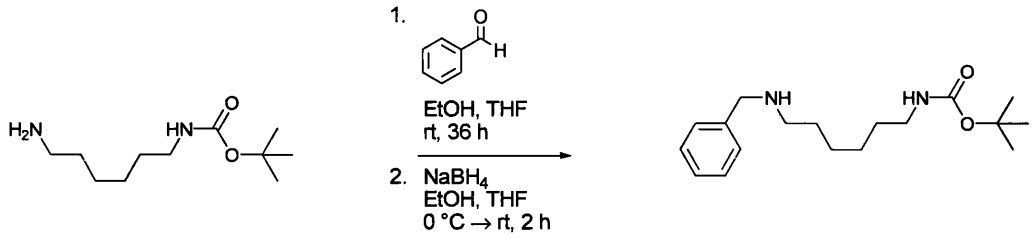

147 148

Scheme 76. *Synthesis of compound **148** (67% yield).*

As is usual with amides the splitting pattern observed for the CH_2 group adjacent to the carbamate NH in ^{1}H NMR spectra appeared as a triplet in deuterated methanol but as a doublet of triplets in deuterated chloroform, see page 188.[227] This characteristic, coupled with the downfield shift of the multiplet, permitted the ratio between protected and unprotected amine groups to be readily and unambiguous determined in these studies.

Deprotection

With compound **148** isolated cleanly, the protecting group was to be removed. In removing the Boc group the roles of heat, trifluoroacetic acid (TFA) and hydrochloric acid were assessed. Whilst TFA represents one of the most common reagents for removal of Boc groups, formation of the diammonium hydrochloride salt, compound **149**, was particularly appealing. To ensure both amine groups were converted to their hydrochloride salts, concentrated hydrochloric acid in ethyl acetate was used.

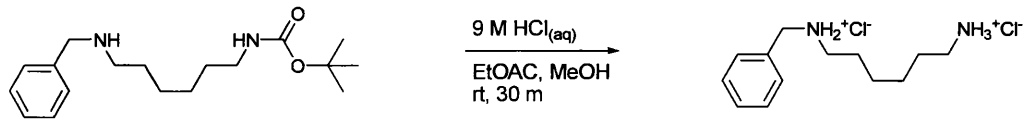

148 149

Scheme 77. *Deprotection of compound **148** to yield the ammonium hydrochloride salt **149** (62% yield).*

As discussed in the previous section (Section 3.3, page 120) the advantage of forming the ammonium hydrochloride salt is two fold. First it allows the compounds to be isolated with exacting levels of purity, see the ^{1}H NMR spectrum in Figure 59, second it ensures their longevity. The ammonium salt **149** represented the common precursor to all of the diboronic acid sensors **133**$_{(pyrene)}$ - **137**$_{(2\text{-naphthalene})}$ therefore the ability to store compound **149** in a stable form was vital.

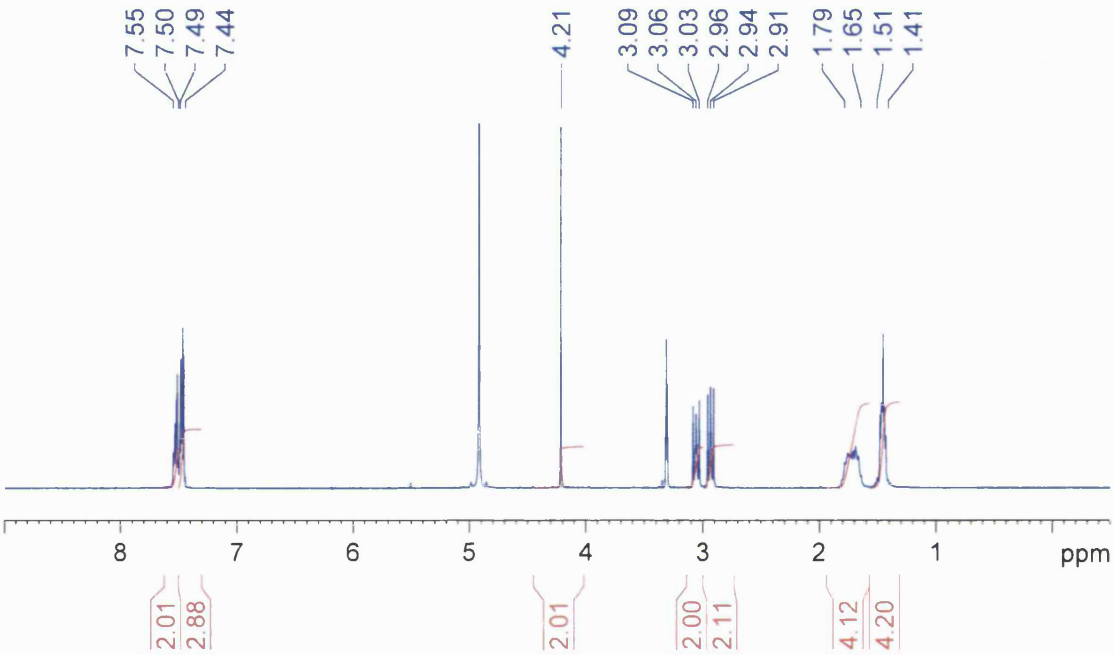

Figure 59. *^{1}H NMR spectrum (300 MHz, MeOD) of the ammonium salt **149** with the residual solvent peak at 3.31ppm and water at 4.92ppm.*

Formation of the Core Unit

When required for use the ammonium salt **149** was basified to free the amine base and generate amine **150**, allowing a reductive amination to be conducted cleanly on the one remaining primary amine. The reaction was modelled with 9-anthraldhyde, see Scheme 78, the overall reaction scheme to the generic core unit **151**$_{(fluorophore)}$ being illustrated in Scheme 79.

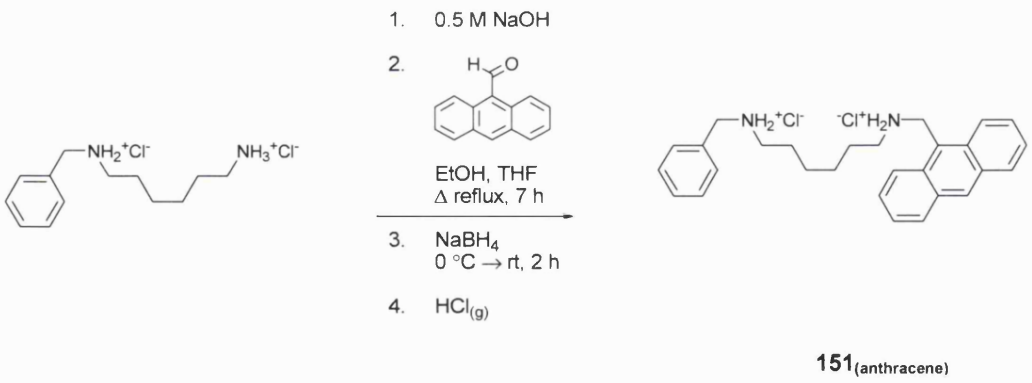

Scheme 78. *Synthesis of the ammonium salt* ***151*** *(anthracene) (34%yield).*

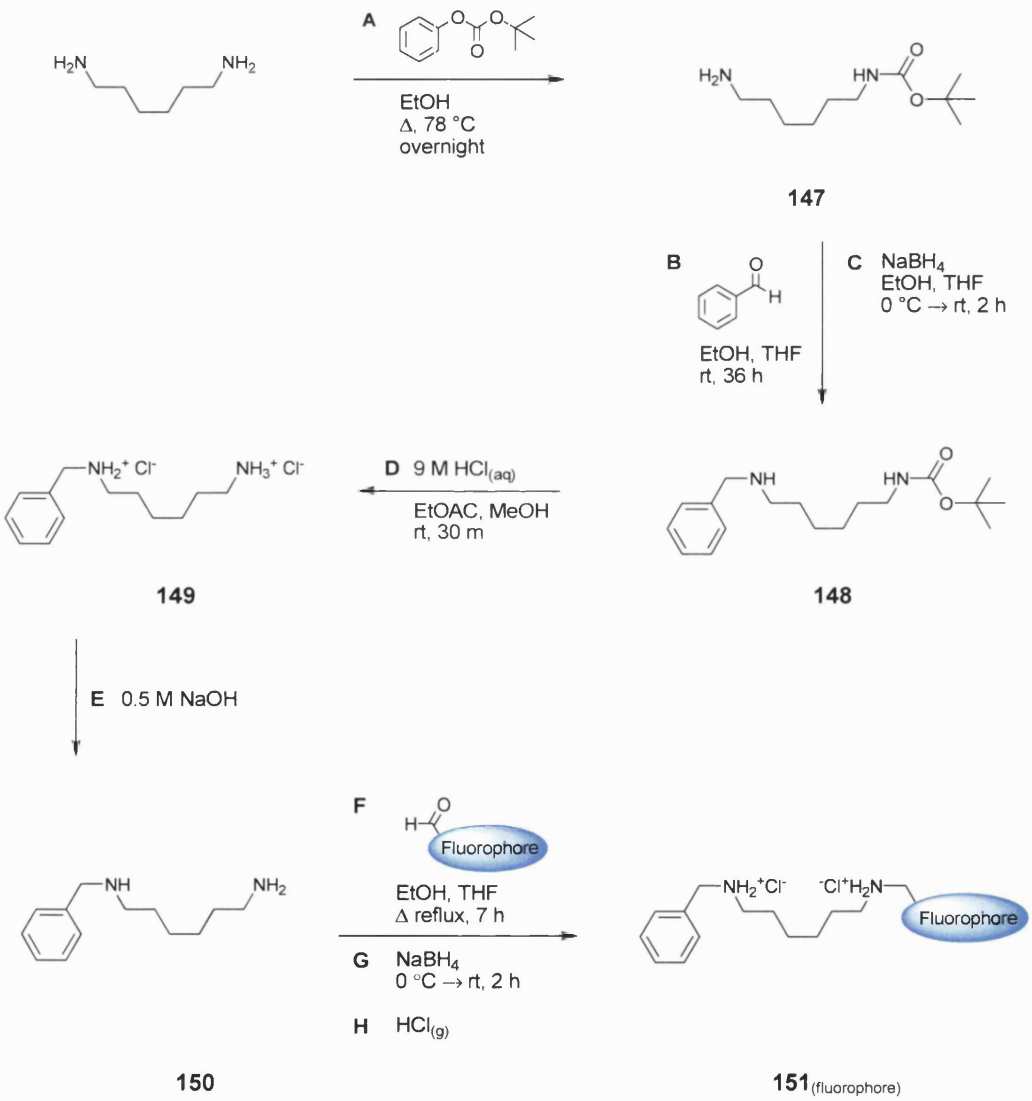

Scheme 79. *The overall synthetic route required to yield compound* ***151*** *(fluorophore). (**A**) introduction of tert-butyl phenyl carbonate; (**B** and **C**) introduction of benzaldehyde; (**D**) deprotection with HCl(aq); (**E**) formation of the amine base; (**F, G** and **H**) introduction of the required aldehyde.*

Denouement

Given the successful method developed in Section 3.3 (page 120) for the coupling and purification of *o*-methyl phenylboronic acid fragments with amines and given that we had already fully characterised the diboronic acid sensors **133**$_{(pyrene)}$ - **137**$_{(2\text{-naphthalene})}$, our role in the development of an enhanced synthetic methodology for these compounds was complete.

The synthetic route in Scheme 79 not only provides an efficient route to the ammonium salt **151**$_{(anthracene)}$ (and analogous core units with other appended fluorophores) but also provides access to the 1,6-hexamethylene diamine linker as a selectively mono-protected carbamate. The method fulfils our initial aim; by utilising a series of reproducible steps the outcome of the synthesis is no longer dependent on the subtle differences between reagents and the individual procedural variations introduced by the researcher but is robust and reproducible.

Selective regiochemical control of the intermediates, by protection of the initially indistinguishable amine functional groups, permits the incorporation of this methodology into other synthetic steps. Formation of mono-protected α,ω-alkanediamines is key to the novel tweezers system we shall discuss below (Section 3.6, page 166).

Mono-protected α,ω-alkanediamines also have the potential to allow the construction of entire series of poly-substituted core units. For example, the synthesis of a library containing modular fluorescent PET sensors with two non-equivalent fluorophores has been proposed. This library would probe the energy transfer properties between all 2^4 non-equivalent combinations of appended fluorophores that could be generated from the pyrene, phenanthrene, anthracene, 1-naphthalene and 2-naphthalene.

3.5 FLUORESCENCE TITRATIONS

The fluorescence titrations of the diboronic acid sensors **133**$_{(pyrene)}$ - **137**$_{(2\text{-naphthalene})}$ and their respective monoboronic acid reference compounds **128**$_{(pyrene)}$ - **132**$_{(2\text{-naphthalene})}$ were conducted.[212]

3.5.1 Measurement Conditions and Results

The fluorescence titrations of the monoboronic acid reference compounds **128**$_{(pyrene)}$ - **132**$_{(2\text{-naphthalene})}$ and the diboronic acid sensors **133**$_{(pyrene)}$ - **137**$_{(2\text{-naphthalene})}$ with D-glucose, D-galactose, D-fructose and D-mannose were carried out in an aqueous methanolic buffer solution [52.1wt% methanol at pH 8.21 (KCl, 0.01000 mol dm^{-3}; KH_2PO_4, 0.002752 mol dm^{-3}; Na_2HPO_4, 0.002757 mol dm^{-3})].[228] The fluorescence intensity of the diboronic acid sensors **133**$_{(pyrene)}$ - **137**$_{(2\text{-naphthalene})}$ increased with increasing saccharide concentration. The observed stability constants (K_{obs}) of PET sensors **133**$_{(pyrene)}$ - **137**$_{(2\text{-naphthalene})}$ and **128**$_{(pyrene)}$ - **132**$_{(2\text{-naphthalene})}$ were calculated by the fitting of emission intensity *versus* saccharide concentration curves.[229] The emission wavelengths used for each fluorophore in determining the emission intensity are detailed in Table 7. The observed stability constants (K_{obs}) calculated are reported in Table 8 and Table 9.

Table 7. Fluorescence measurement conditions

fluorophore	concentration / mol dm^{-3}	λ_{ex} / nm	λ_{em} / nm
pyrene	$1.0\ 10^{-6}$	342	397
phenanthrene	5.0×10^{-6}	299	369
anthracene	1.0×10^{-6}	370	420
1-naphthalene	2.5×10^{-6}	275	335
2-naphthalene	2.5×10^{-6}	274	335

Table 8. Observed stability constants (K_{obs}) (coefficient of determination; r^2) and fluorescence enhancements for the saccharide complexes of sensors **128**$_{(pyrene)}$ - **132**$_{(2\text{-naphthalene})}$ and **133**$_{(pyrene)}$ - **137**$_{(2\text{-naphthalene})}$.

sensor	D-glucose		D-galactose	
	K_{obs} / dm^3 mol^{-1}	fluorescence enhancement	K_{obs} / dm^3 mol^{-1}	fluorescence enhancement
133$_{(pyrene)}$	962 ± 70 (0.99)	2.8	657 ± 39 (1.00)	3.1
128$_{(pyrene)}$	44 ± 3 (1.00)	4.5	51 ± 2 (1.00)	4.2
134$_{(phenanthrene)}$	325 ± 58 (0.97)	1.5	611 ± 101 (0.97)	1.4
129$_{(phenanthrene)}$	30 ± 7 (0.98)	1.5	77 ± 12 (0.98)	1.4
135$_{(anthracene)}$	441 ± 76 (0.98)	3.2	536 ± 31 (1.00)	3.1
130$_{(anthracene)}$	61 ± 3 (1.00)	3.4	93 ± 6 (1.00)	3.0
136$_{(1\text{-naphthalene})}$	417 ± 60 (0.98)	6.1	1072 ± 68 (0.99)	5.4
131$_{(1\text{-naphthalene})}$	52 ± 1 (1.00)	5.7	78 ± 5 (1.00)	5.0
137$_{(2\text{-naphthalene})}$	532 ± 57 (0.99)	4.2	894 ± 66 (0.99)	4.1
132$_{(2\text{-naphthalene})}$	35 ± 2 (1.00)	4.5	49 ± 4 (1.00)	4.3

Table 9. Observed stability constants (K_{obs}) (coefficient of determination; r^2) and fluorescence enhancements for the saccharide complexes of sensors **128**$_{(pyrene)}$ - **132**$_{(2\text{-naphthalene})}$ and **133**$_{(pyrene)}$ - **137**$_{(2\text{-naphthalene})}$.

sensor	D-fructose		D-mannose	
	K_{obs} / dm^3 mol^{-1}	fluorescence enhancement	K_{obs} / dm^3 mol^{-1}	fluorescence enhancement
133$_{(pyrene)}$	784 ± 44 (1.00)	3.2	74 ± 3 (1.00)	2.8
128$_{(pyrene)}$	395 ± 11 (1.00)	3.6	36 ± 1 (1.00)	3.7
134$_{(phenanthrene)}$	1013 ±126(0.98)	1.4	134 ± 18 (0.98)	1.4
129$_{(phenanthrene)}$	548 ± 55 (0.99)	1.4	58 ± 8 (0.98)	1.4
135$_{(anthracene)}$	1000 ± 69 (0.99)	3.0	111 ± 6 (1.00)	2.8
130$_{(anthracene)}$	713 ± 35 (1.00)	3.0	61 ± 3 (1.00)	3.0
136$_{(1\text{-naphthalene})}$	964 ± 41 (1.00)	5.5	101 ± 3 (1.00)	5.0
131$_{(1\text{-naphthalene})}$	529 ± 45 (0.99)	5.4	46 ± 1 (1.00)	5.2
137$_{(2\text{-naphthalene})}$	1068 ± 63 (1.00)	3.8	98 ± 4 (1.00)	3.5
132$_{(2\text{-naphthalene})}$	399 ± 34 (0.99)	4.6	40 ± 2 (1.00)	3.8

To help visualize the trends of the observed stability constants (K_{obs}) in Table 8 and Table 9, the stability constants of the diboronic acid sensors **133**$_{(pyrene)}$ - **137**$_{(2\text{-naphthalene})}$ are reported in Figure 60 divided by the stability constants of the analogous monoboronic acid reference compounds **128**$_{(pyrene)}$ - **132**$_{(2\text{-naphthalene})}$.

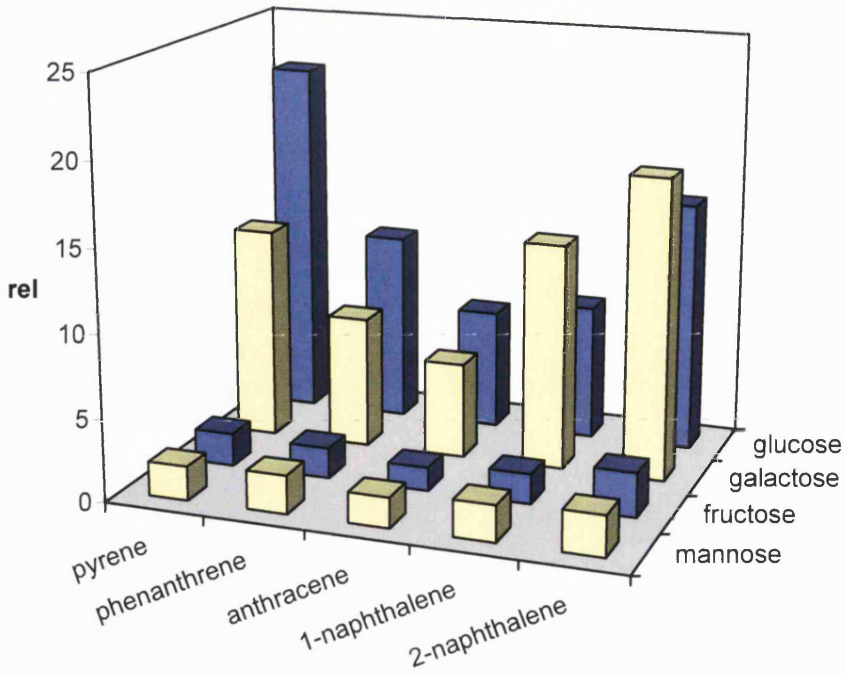

Figure 60. *Observed stability constants (K_{obs}) of the diboronic acid sensors **133**$_{(pyrene)}$ - **137**$_{(2\text{-naphthalene})}$ divided by the observed stability constants (K_{obs}) of the corresponding monoboronic acid reference compounds **128**$_{(pyrene)}$ - **132**$_{(2\text{-naphthalene})}$ to yield relative values with saccharides. The D-configuration of the monosaccharides was used throughout this evaluation.*

3.5.2 Inference

It could be thought that altering the appended fluorophore on the modular diboronic acid systems would simply lead to fluorescent sensors with different emission and excitation wavelengths. As can be readily observed from the bar graph in Figure 60 this was not the case.

The relative stabilities clearly illustrate that an increase in selectivity is obtained by cooperative binding through the formation of 1:1 cyclic systems. The large enhancement of the relative stability observed for the 1:1 cyclic systems (formed with D-glucose and D-galactose) are clearly contrasted with the small two fold enhancement observed for the 2:1 acyclic systems (formed with D-fructose and D-mannose).

The results in Figure 60 indicate that the best match between receptor and guest is for sensors **133**$_{(pyrene)}$, **134**$_{(phenanthrene)}$ and **135**$_{(anthracene)}$ with D-glucose and for sensors **136**$_{(1\text{-naphthalene})}$ and **137**$_{(2\text{-naphthalene})}$ with D-galactose.

The bar graph in Figure 60 describes a saddle like trend from pyrene through to 2-naphthalene with a change in selectivity from D-glucose to D-galactose occurring in the middle of the series. To account for such a trend these results must be a function of more than one variable.

Solvation

The first factor to be considered was the size of the fluorophore's π-surface. From Figure 60 it can be observed that the largest relative value was for sensor **133**$_{(pyrene)}$ with D-glucose. Pyrene, with four fused benzene rings, represents the largest fluorophore in the series and as such endows sensor **133**$_{(pyrene)}$ with the largest planar aromatic π-surface of any of the sensors **133**$_{(pyrene)}$ - **137**$_{(2\text{-naphthalene})}$. As the size of the fluorophore is reduced to three fused benzene rings in phenanthrene and anthracene the relative values are seen to diminish. As the fluorophore size decreases further still to the two fused benzene rings in 1- and 2-naphthalene there is a distinct change in the direction of the trend, the relative values increase, with a concomitant change in selectivity from D-glucose to D-galactose. Given the proximity of the fluorophore's planar aromatic π-surface to the binding pocket it seemed reasonable to infer that the hydrophobicity within the binding pocket would be a function of the size of the fluorophore. If so sensor **133**$_{(pyrene)}$ would therefore have the most hydrophobic environment within the binding pocket of any of the sensors **133**$_{(pyrene)}$ - **137**$_{(2\text{-naphthalene})}$, this environment being observed to have the best D-glucose selectivity across the series.

To rationalise these observed changes in terms of the complementarity between the hydrophobicities of the monosaccharides and sensors **136**$_{(1\text{-naphthalene})}$ - **137**$_{(2\text{-naphthalene})}$ the reported hydration values for the monosaccharides were examined. From the literature it appears that establishing the hydration characteristics of monosaccharides such as D-glucose and D-galactose is non-trivial, however, there is general agreement that D-galactose is slightly more hydrophobic than D-glucose.[230-232] The opposite of what we would expect based on the above observations.

The interactions between aromatic hydrocarbons and monosaccharides in aqueous solutions have been determined. Janado *et al.* documented that aqueous solutions of D-galactose were found to dissolve more benzene, naphthalene and biphenyl than the

equivalent aqueous solutions of D-glucose.[233,234] A result consistent with D-galactose being the more hydrophobic of the two saccharides.

In attempting to establish a rationale for the values displayed in Figure 60 a number of factors have to be considered: the size, orientation and proximity of the fluorophores in sensors **133**$_{(pyrene)}$ - **137**$_{(2\text{-naphthalene})}$ to the binding pocket; the hydrophobicities of the monosaccharides in their relative compositions and the manner in which complexation with boronic acids will change this (as discussed above D-glucose will predominantly favour the α-D-glucofuranose form and D-galactose will favour an α-D-galactofuranose or α-D-galactopyranose (twist-boat) form)[32,176] as well as the covalent interactions of the saccharide hydroxyl groups with the diboronic acid receptors on binding. Rationalising these trends in a quantitative manner would therefore require a considerable computational effort given the complex and dynamic nature of these systems, however, in considering these experimental observations a number of important features come to light.

Since Emil Fischer's seminal article of 1894 in which the hydrated polar groups within yeast's binding site were described as a locked gate that could only be opened by the key polar groups of α-glucosides (and not β-glucosides) much work has been done on understanding the cause of such well defined stereospecific recognition.[235,236] Whilst the physical fit of the "key" within the "lock" could be intuitively understood, further research demonstrated that selectivity was not just a facet of enthalpic stabilisation but relied intimately on the increase in entropy that occurred when water was displaced from the binding site. In turn this entropic stabilisation had to be played off against the decrease in entropy that occurred when the perturbed solvent shell surrounding the saccharide was displaced.

For most of the hexoses and pentoses there is little overall difference in hydrophobicity, nevertheless, it is the case that very slight differences in the stereochemical configuration of monosaccharides' hydroxyl groups can lead to significant changes in solvation properties. One of the most significant deviations from the general trend within the hexoses is the presence of an axial C4 hydroxyl group.[231,237] This facet has been documented to cause D-galactose to have a substantially diminished fit in water compared to D-glucose and as such the two monosaccharides have been categorised as having markedly different hydration properties (i.e. whilst their observed

hydrophobicities may appear to be similar, the degree of disorder they introduce to the water molecules surrounding them is quite different.).[230,232,238]

Water molecules are therefore crucial in controlling the selective recognition of saccharides within aqueous systems and it is the case that the restructuring of perturbed surface water provides an important force in controlling these molecular associations.[239] Therefore if correctly approached the solvation effects observed within our simple diboronic acid sensors may provide the impetus for a more refined discrimination to be made between the molecular recognition of D-glucose and D-galactose in aqueous systems through careful control of the hydrophobicity of the binding pocket.

This observation may prove of particular interest not only in sensor design but also in regard to the significant work being undertaken on saccharide transport through organic membranes (such as lipid bilayers) *via* boronic acid carriers. In these systems D-galactose is noticeable by its absence as, to date, no data has been reported regarding the transport of D-galactose through hydrophobic membranes using boronic acid carriers.[240-245]

Steric Crowding

If the size of the fluorophore's π surface was the only factor to be considered, little difference would be expected between the results observed for sensors **136**$_{(1\text{-naphthalene})}$ and **137**$_{(2\text{-naphthalene})}$. This was not the case. In comparing sensors **136**$_{(1\text{-naphthalene})}$ and **137**$_{(2\text{-naphthalene})}$ there was no difference in size between the fluorophore's hydrophobic π-surfaces, only a difference in connectivity and therefore the relative alignment of the fluorophores with regard to the binding cleft. In explaining the difference between the relative values, the number of *peri*-hydrogens on the fluorophores was considered. The fluorophore with the highest number of *peri*-hydrogens is anthracene with two, then pyrene, phenanthrene and 1-naphthalene with one each and then 2-naphthalene with none, this is illustrated in Figure 61.

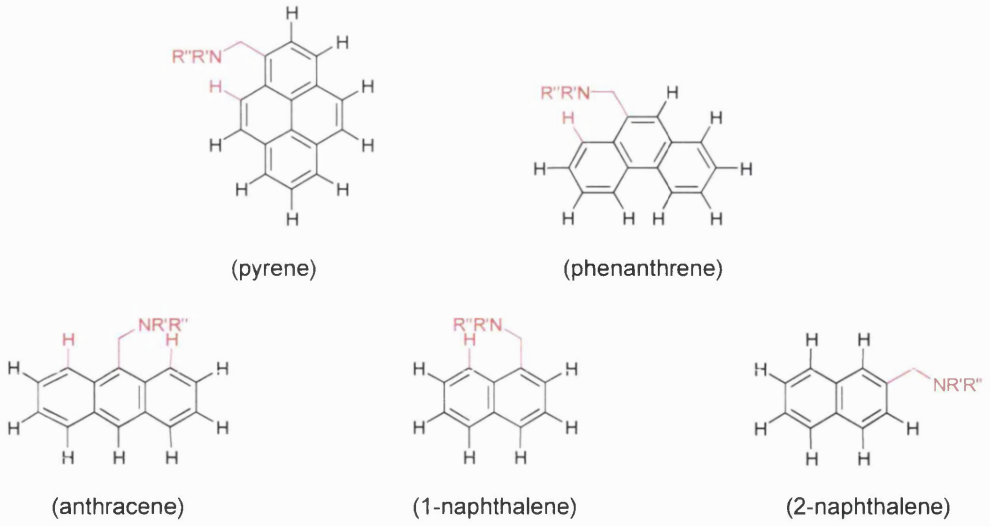

Figure 61. *The five fluorophores used for the mono- and di-boronic acid systems. For clarity the methylamine fragment, peri-hydrogen and their bonds are highlighted in red. The two groups are illustrated here in their eclipsed conformation.*

This ties in well with the observed results in the bar graph of Figure 60. Anthracene with the greatest number of *peri*-hydrogens displays the lowest relative stability. These *peri*-hydrogens can be considered to increase the steric crowding within the binding pocket and as such this hypothesis seems quite reasonable. It also fits the increase in sensitivity observed for 2-naphthalene over 1-naphthalene.

Denouement

These results demonstrate that in a fluorescent PET saccharide sensor with two phenylboronic acid groups, a hexamethylene linker and a fluorophore, the choice of the fluorophore is crucial. The fluorophore not only defines the emission wavelength but also influences the environment within the binding site with the overall selectivity being fluorophore dependent.

An informed decision will therefore have to be taken in the future design of fluorescent sensors, such that the polarity of the chosen guest species complements the solvation within the binding pocket. Whilst not a direct premise of complementarity between hydrophobicity of the appended fluorophore of the sensor and the pyranose form of the guest monosaccharide, it appears to be the case that boronic acids display enhanced selectivity for D-glucose over D-galactose when the hydrophobicity of the binding pocket is increased.

In addition to considering solubility, a minimisation of the *peri*-hydrogens should reduce steric crowding within the binding pocket and, as demonstrated with D-glucose and D-galactose, increase the relative stability of complexes formed with diboronic acid sensors.

3.6 MOLECULAR TWEEZERS

3.6.1 Design Rationale

Background

Coined by Chen and Whitlock in 1978 the term "molecular tweezers" was first used to describe simple molecular receptors (i.e. receptor **152**) containing two aromatic tips tethered by a rigid linker unit. In the case of receptor **152** the rigid diyne linker positioned the tweezers' aromatic caffeine tips ~ 7 Å apart, this pre-organisation of the acyclic receptor prevented self-association whilst permitting aromatic guest molecules to intercalate between the two tips and thus form stable complexes.[246,247]

152

Molecular tweezers soon progressed to utilise not only the π-stacking interactions generated between the aromatic pincers and guest molecules but also to use functional group complementarity. Hydrogen bonding groups were embedded within the binding cavity to interact with the corresponding groups present on the guest molecules, see Figure 62.[248-250]

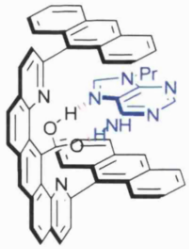

Figure 62. *Interaction between the molecular tweezers **153** (black) and 9-propyladenine (blue), hydrogen bonds are denoted in red.*

In studying these molecular tweezers their attributes became clear. The ability of these host systems to display conformational flexibility whilst retaining a defined three dimensional shape proved particularly effective in advancing the degree of specificity

observed in synthetic receptors.[251,252] The efficacy of using conformational pre-organisation in the design of flexible supramolecular receptors has been demonstrated by a number of research groups and is reflected in the number of outstanding publications this work has generated.[253-268]

Proposed Structure

Following the fluorescence evaluation of the diboronic acid sensors **133**$_{(pyrene)}$ - **137**$_{(2\text{-}naphthalene)}$ and monoboronic acid reference compounds **128**$_{(pyrene)}$ - **132**$_{(2\text{-}naphthalene)}$ in Section 3.5, it became clear that constructing a pair of molecular tweezers tipped with two large aromatic fluorophore units could be of potential benefit in enhancing the selectivity between specific saccharides by further augmenting the hydrophobicity within the binding pocket. With the results of the dipyrenyl, diboronic acid modular sensor **99** in mind (see pages 87 and 88 where compound **99** was discussed and found to discriminate between D-glucose and D-galactose with observed stability constants (K_{obs}) as different as 2 000 M^{-1} with D-glucose and 790 M^{-1} with D-galactose in 33wt% methanol in water)[5,184,185] and considering the potential advantages of allowing a degree of conformational flexibility to be designed into the active recognition site, the structure of the diboronic acid fluorescent PET sensor **162** was postulated.

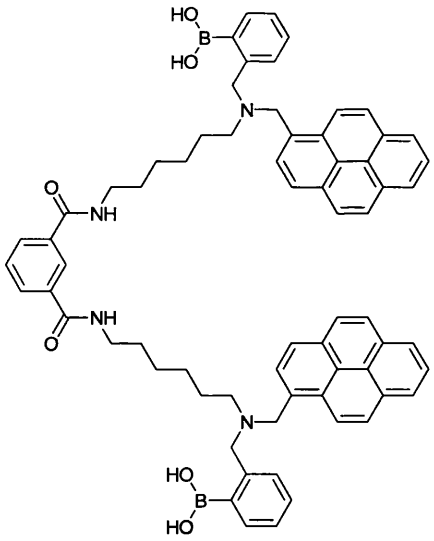

162

As can be seen from the structure of compound **162** the *o*-phenylboronic acid units, tertiary amines and pyrenyl fluorophores are positioned so as to permit fluorescence to be controlled *via* PET.

The dual boronic acid units permit saccharide selectivity *via* two point binding with the two pyrene units augmenting the hydrophobicity within the binding pocket. Noticeably the two hexamethylene linkers will introduce a degree of conformational flexibility into the system whilst the general dimensions of the binding cavity are already known to be effective for saccharide recognition.

Isophthalamide Cores

Supramolecular recognition units based around isophthalamide cores have been synthesised previously and it is often the case in these systems that the amide groups are directly involved in the recognition event.[269-273] One example that illustrates this hydrogen bonding interaction well is the complexation between the macrocyclic tetra-amide **154** and barbital, Figure 63.[274]

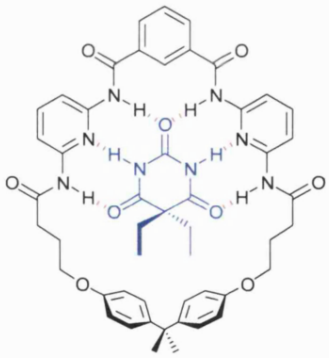

Figure 63. *Macrocyclic tetra-amide **154** (black) with complexed barbital (blue). Hydrogen bonding is denoted in red.*

Although it was not perceived that these hydrogen bonding interactions would be directly involved in the recognition of monosaccharides the possibility exists that these hydrogen bond donors could play a significant role in the recognition of larger guests. Strictly the proposed molecular tweezers **162** could be denoted as a ditopic sensor and as such the roles of intermolecular interactions, including hydrogen bonding,[275,276] solvophobic effects,[277] steric encumbrance and covalent complexation *via* the boronic acid groups could all come into play and influence the host – guest selectivity.

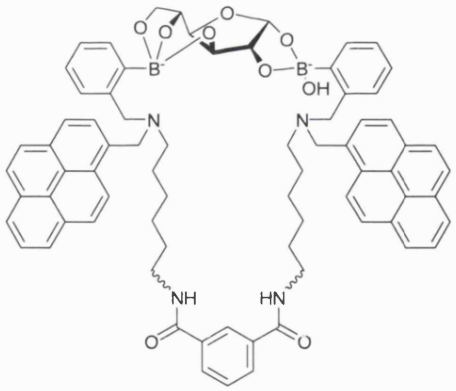

Figure 64. *A potential binding motif in the complexation of α-D-glucofuranose by the molecular tweezers* ***162***.

Interlocked Molecules

The isophthalamide unit has been used extensively by Leigh and co-workers in the synthesis of mechanically interlinked supramolecular molecules. This work was sparked off by the serendipitous observation that isophthaloyl dichloride was found to self assemble with *para*-xylene diamine to produce the [2]catenane **155**, see Scheme 80.[278,279] The observed self-assembly has allowed for a wide spread of interlocked ring systems to be investigated[280-285] and has also permitted the synthesis of rotaxane based molecular switches, systems where macrocycles self assemble around functionalised molecular threads and shuttle back and forth in response to external stimuli.[286-291]

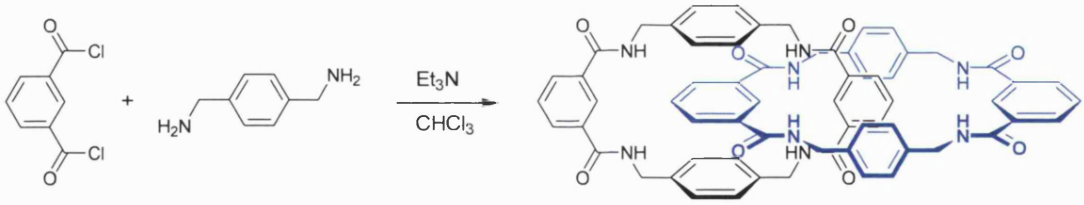

Scheme 80. *Synthesis of the [2]catenane* ***155****, for clarity one ring is depicted in black and one in blue.*

Although the [2]catenane **156** is formed primarily on the basis of the strength of the π-π stacking interactions developed between the aromatic rings, hydrogen bonding interactions have also been observed in catenanes with larger ring apertures. This arises from the rotation of one of the isophthalamide carbonyls to position the hydrogen bond accepting oxygen between two proximal hydrogen bonding amide NHs on the adjacent macrocycle. In more concentrated environments such observations should be recalled when considering the molecular tweezers **162**.

3.6.2 Retrosynthetic Analysis

When the initial retrosynthetic analysis of the proposed molecular tweezers **162** was undertaken, high dilution conditions were being used to synthesise the diboronic acid compounds **133**$_{(pyrene)}$ - **137**$_{(2\text{-naphthalene})}$. With this in mind the retrosynthetic analysis illustrated in Scheme 81 was proposed.

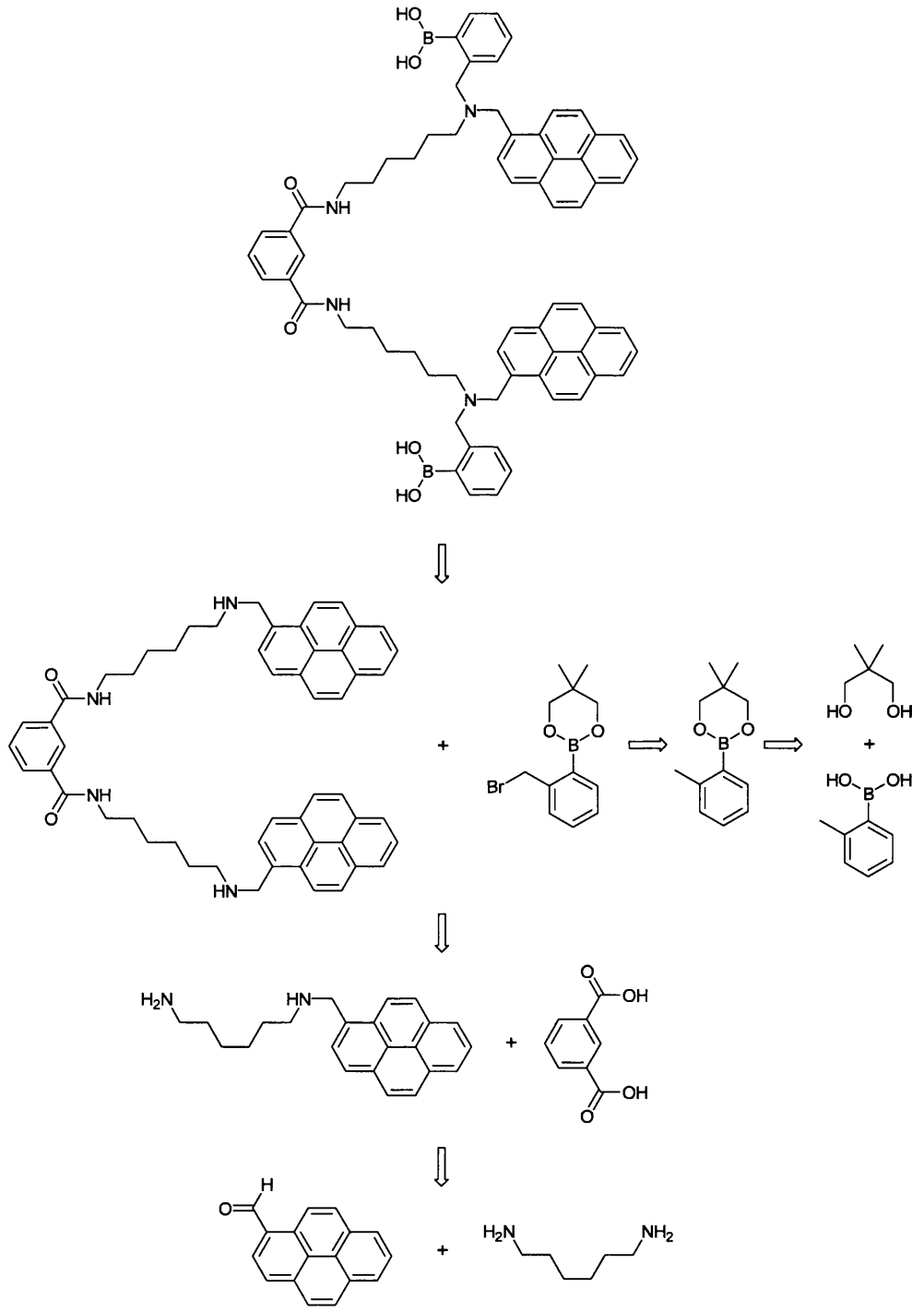

Scheme 81. *Initial retrosynthetic analysis for the construction of the proposed molecular tweezers.*

Protecting Group Chemistry

As the pitfalls of using high dilution conditions became apparent the proposed coupling of isophthalic acid to a diamine became one of the major driving forces in using protecting group chemistry to achieve monosubstituted diamines. If a protecting group such as Boc were to be appended to one end of the diamine then isophthaloyl dichloride could be used in lieu of isophthalic acid without any concerns arising from reactions occurring at the secondary amine.[292] This would increase the probability that reactions would proceed cleanly, that they would be driven to completion and that the di-carbamate product generated could be readily purified.

Hierarchical Approach

The procedure for isolating mono-protected diamines has been discussed above (Section 3.4.4, page 150) and by using the same mono Boc-protected hexamethylene diamine **147** here the synthesis of these boronic acid based sensors proceeded with common intermediates being used extensively.

This hierarchical approach is demonstrated in the second retrosynthetic analysis, illustrated in Scheme 82. To aid visualisation the retrosynthetic coupling required to form the previously generated intermediate compounds **127** and **147** are denoted in blue in Scheme 82. With this colour code in place the strength of a hierarchical approach should hopefully be clear. In synthesising compound **162** seven couplings were proposed in Scheme 82 of which three had already been undertaken and could now be prepared in large batches.

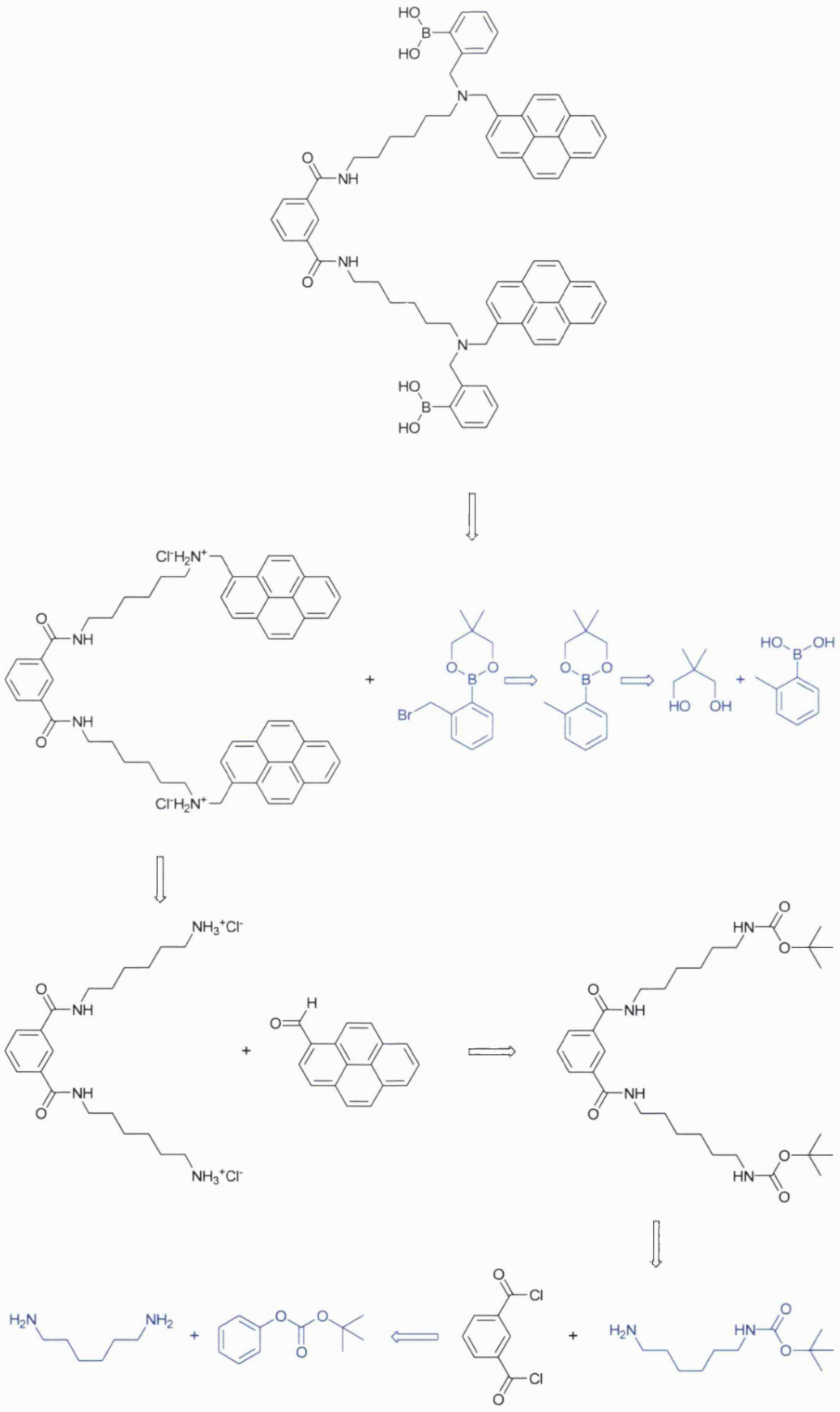

Scheme 82. *Retrosynthetic analysis for the construction of the proposed molecular tweezers. The hierarchical approach employed is illustrated here by denoting common intermediates in blue.*

3.6.3 Precursor Synthesis

With one nitrogen atom of compound **147** now under the aegis of the carbamate protecting group the single unprotected amine group present on compound **147** could be reacted directly with isophthaloyl dichloride.[270] The comparatively facile reaction proposed is illustrated in Scheme 83. The reaction was found to proceed to completion within 3 hours and required only a solvent wash to isolate compound **157** in high yields (96%) and with excellent levels of purity. The reaction was also found to be quite amenable to scale up with > 5 g batches being prepared.

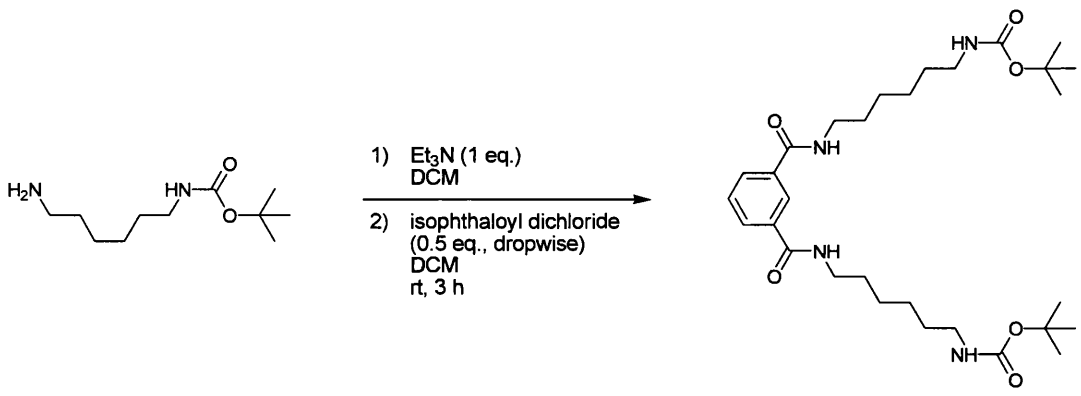

Scheme 83. *Synthesis of compound **157**.*

Cleavage of the Boc groups was achieved with hydrochloric acid (32%) in ethyl acetate. This permitted the Boc groups to be cleaved and the stable ammonium hydrochloride salt **158** to be obtained in one-pot and in quantitative yield.

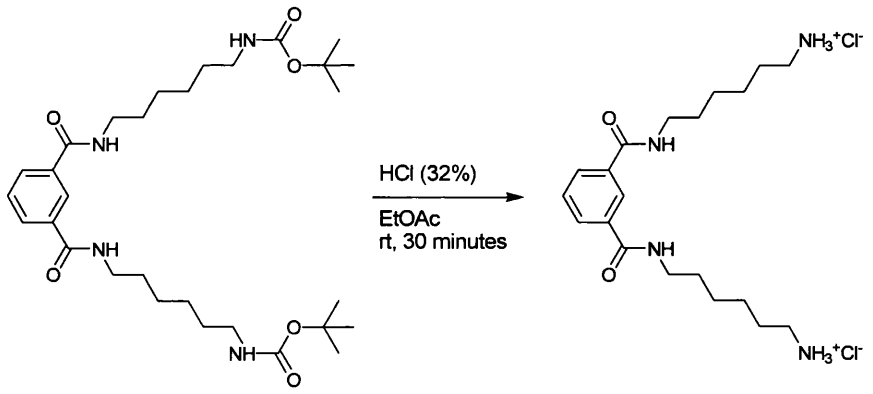

Scheme 84. *Synthesis of the ammonium salt **158**.*

Addition of the Dual Pyrene Fluorophore Units

It had been thought that addition of the two pyrene fluorophores to the ammonium hydrochloride salt **158** would be a facile step proceeding *via* a dual reductive amination, see Scheme 85, and in a manner analogous to the reactions previously examined (see the discussion on the pyrenyl hydrochloride salt $\mathbf{119}_{(pyrene)}$, page 127). As will be discussed below the physical attributes of the ammonium salt **161** (and its intermediates) introduced a number of unforeseen challenges. Although this coupling worked first time, it proceeded in low yield and it was thought advantageous that the step be refined to allow the product (and it must be recalled that the ammonium salt **161** represented the final intermediate in this overall reaction scheme) to be isolated in higher yield and with consistently high levels of purity.

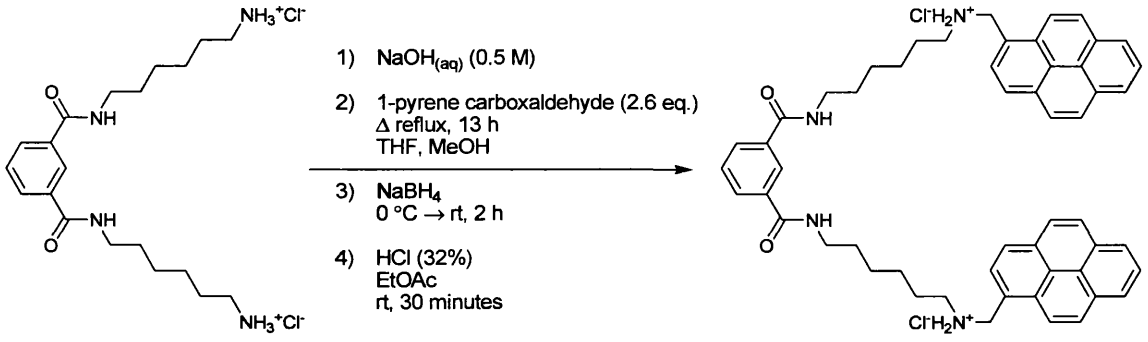

Scheme 85. *Proposed synthesis of the ammonium salt **161**.*

Reaction (3.6.3) 1

Initially the reductive amination was attempted using the same procedure as for the diboronic acid sensors $\mathbf{133}_{(pyrene)}$ - $\mathbf{137}_{(2\text{-naphthalene})}$. The amine base of the ammonium salt **158** was freed with sodium hydroxide (0.5 M) and then extracted from the aqueous phase in dichloromethane (3 ×). The recombined organic phases were condensed and the residue dissolved in a methanol/tetrahydrofuran solution to which 1-pyrene carboxaldehyde (2.6 equivalents) was added. The system was heated overnight under reflux conditions and it was found that the reaction had produced the di-, mono- and un-substituted imine derivatives of compound **158**. Following reduction with sodium borohydride the desired product was extracted in dichloromethane (3 ×) from aqueous sodium hydroxide (0.5 M). The recombined organic phases were washed with water (5

×), dried over magnesium sulfate and filtered. To the resulting product was added ethyl acetate and concentrated hydrochloric acid (32%) to form the hydrochloride salt.

Following vacuum filtration (in dry ethyl acetate, subject to ultrasound) the resulting powder appeared to be speckled with both yellow and brown products. The solid was therefore heated under reflux in absolute ethanol, slowly cooled to 0 °C, vacuum filtered, and dried *in vacuo* to isolate the ammonium salt **161** as a brown powder in 24% (39.8 mg) yield.

Reaction (3.6.3) 2

Whilst the reaction had proceeded with high levels of purity, the 24% yield was considered to be rather low for a reductive amination (this can be contrasted with the 91% yield obtained for the analogous pyrenyl ammonium hydrochloride salt **119**$_{(pyrene)}$, page 127). To proceed to the next step and formation of diboronic acid **162** it was necessary to increase the yield and scale the reaction up. With concerns regarding the solubility of compound **158** in the initial biphasic solvent wash we sought to bypass this procedure (extraction of the free amine from aqueous sodium hydroxide). The ammonium salt **158** (1 equivalent) was therefore directly mixed into a solution of 1-pyrene carboxaldehyde (2.2 equivalents) in the presence of triethylamine (2 equivalents). The reaction mixture was heated under reflux conditions for 8 hours. Following reduction and purification as above the yield of compound **161** was found to have decreased to 14% (57 mg).

Reaction (3.6.3) 3

With concerns regarding the basicity of the reaction mixture, the ammonium salt **158** was again extracted from sodium hydroxide in dichloromethane (3 ×) but this time the recombined organic phases were washed with water (3 ×) to neutralise the pH. It is the case that aminations are acid catalysed, with optimal conditions in the pH region 1-7.[293,§§§§] The reaction was then repeated and worked up as before only to find the yield had decreased further still to 12% (40 mg).

§§§§ Given the solvents present in solution the apparent pH of the reaction mixture was often crudely determined by adding a drop of the reaction mixture to pH indicator paper (0-14), allowing the strip to dry and then adding a few drops of water to the indicator paper.

Reactions (3.6.3) 4-7

The synthetic approach utilised in Reaction (3.6.3) 3 was used in a number of subsequent trials where the use of silica gel flash column chromatography was evaluated in the purification of the intermediate free amine **159**.

The initial attempts to use silica gel flash column chromatography were stifled by the nature of the reaction mixture being purified. Whilst the reaction mixture was apparently soluble in dichloromethane it was the case that as the volume of dichloromethane above the top face of the silica in the column decreased the reaction mixture was prone to precipitate, agglomerate and form a gelatinous plug across the top face of the silica. This disk of material was impermeable to the flow of eluent above it and when formed would block the column entirely.

Where smaller scales were used to circumvent this issue it was found that the product was entirely amenable to purification *via* silica gel flash column chromatography. Following trial purifications on silica it was found that the mass of material used in the initial loading of the columns was crucially important. The maximum amount of reaction mixture that could be used per unit area of the horizontal cross section of the column was ~ 25 mg cm^{-2}. This loading constraint coupled with the use of large bore diameter columns therefore allowed the desired product to be obtained on reasonable scales.

In optimising the reaction mixture for the chromatographic purification a solvent wash was carried out before each column to ensure the removal of any derivatives from the spent sodium borohydride. In these solvent washes the same adhesive gel was found to aggregate as a colloid suspension between the water and dichloromethane phases. Whilst the handling characteristics of this gel were unenviable and the compound had been assumed to be an impurity in Reaction (3.6.3) 1, Reaction (3.6.3) 2 and Reaction (3.6.3) 3 the presence of this material impinged significantly on the manner in which the columns in Reactions (3.6.3) 4-7 were run.

With chromatographic conditions established the reaction was scaled up and in conducting the solvent wash on this larger scale an unaccountably large mass of material was formed at the water/dichloromethane interface. When analysed by ^{1}H

NMR it was found that this supposed impurity was in fact the required intermediate amine **159**.

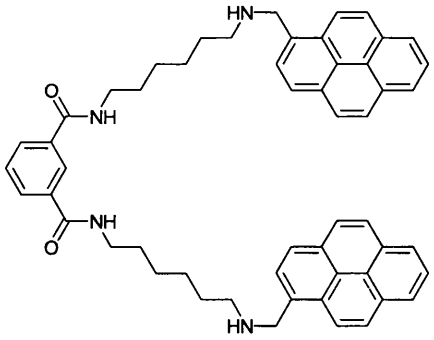

159

As the importance of manipulating such an unwieldy intermediate became apparent, it was found that the solvent extraction of amine **159** must be conducted with ~ 400 cm^3 of dichloromethane g^{-1} of amine. Furthermore it had to be ensured that any precipitate at the water/dichloromethane interface was taken up into the organic layer in each extraction. With this in mind the effectiveness of using a re-precipitation was re-considered (having proved effective in Reaction (3.6.3) 1, Reaction (3.6.3) 2 and Reaction (3.6.3) 3). It was also the case that although the chromatographic technique had proved amenable to scale up the yields had remained low (8%, 39.9 mg; 20%, 93.5 mg; 19%, 1.58 g), one possible source of this yield decrease was thought to be, as mentioned before, the initial extraction form sodium hydroxide in the first step. The use of a mild base to provide an alternative one-pot deprotection was therefore reconsidered.

Reaction (3.6.3) 8

The ammonium hydrochloride salt **158**, 1-pyrene carboxaldehyde and potassium carbonate were mixed directly in one-pot. Initially no reaction was observed to occur in solution. Although acidic conditions are favoured it had been our experience that reductive aminations would proceed readily in the presence of 10 equivalents of amine base (see Section 2.3, page 90). It was therefore unlikely that pH was the only factor involved. The solubility of various bases in methanol was examined and it was found that potassium carbonate was only very sparingly soluble at room temperature. Whilst it was known that sufficient base was dissolved under reflux conditions to drive the formation of the final step in the formation of the monoboronic acid reference

compounds **128**$_{(pyrene)}$ - **132**$_{(2\text{-naphthalene})}$, we postulated that harsher conditions would help drive the formation of intermediate imine **160**. On addition of the more soluble caesium carbonate to compound **158** and 1-pyrene carboxaldehyde in methanol/tetrahydrofuran the rate of reaction was found to increase substantially under the same reaction conditions.

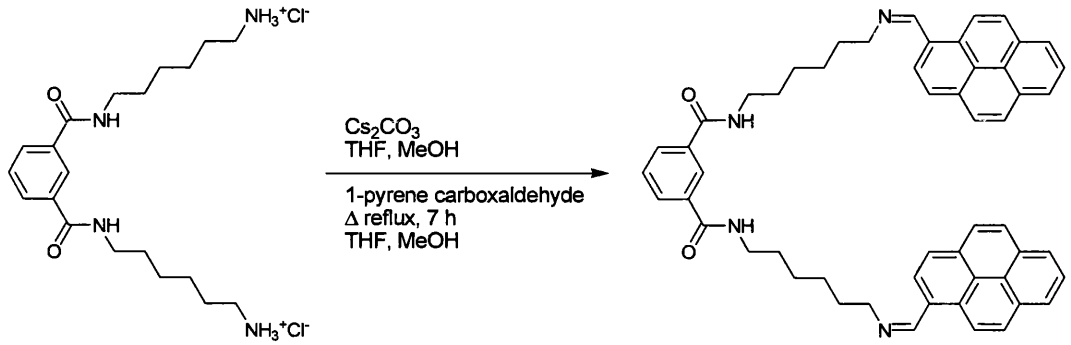

Scheme 86. *Enhanced formation of intermediate imine **160** through the use of Cs_2CO_3.*

The handling procedures developed for the solvent extraction of amine **159** from water in dichloromethane were employed in this step as detailed above. After formation of the hydrochloride salt the product was dried *in vacuo* prior to its dissolution in the minimal amount of boiling dichloromethane. With all of the hydrochloride salt dissolved the reaction was heated under reflux conditions for a further hour before being allowed to cool slowly to room temperature. The resulting suspension was slurried over a glass sinter, vacuum filtered and dried *in vacuo* to afford the ammonium hydrochloride salt **161** in 68% (365 mg) yield.

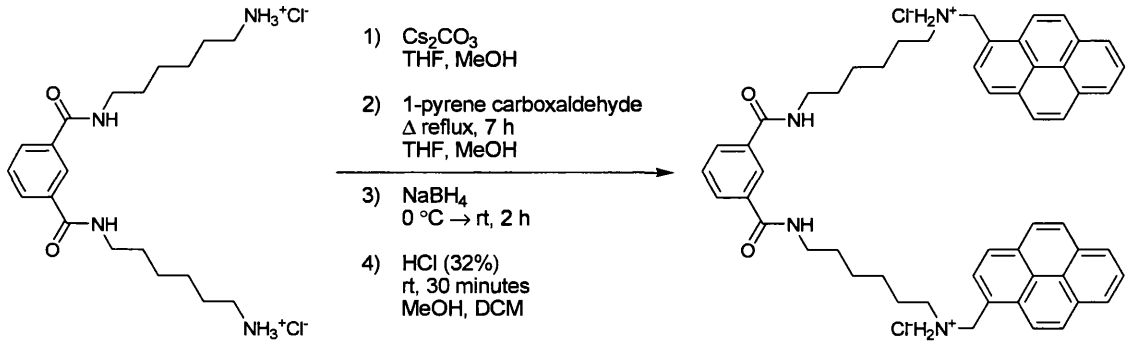

Scheme 87. *Synthesis of* the ammonium salt ***161***.

Reaction (3.6.3) 8 therefore demonstrated the effectiveness of using caesium carbonate in a methanol/tetrahydrofuran solvent mixture, nullifying the need to carry out a preliminary solvent wash. Given the handling and solubility properties of the compounds involved in this step the one-pot approach developed here was most desirable and increased the isolable yield of this reaction by ~ 3 fold.

Characterisation by NMR

The lack of solubility of the ammonium hydrochloride salt **161** presented a challenge not only in the reaction vessel itself but also when attempting to characterise the sample by NMR. Dissolution was only directly possible in deuterated dimethyl sulfoxide (DMSO), which caused significant spectral line broadening in ^{1}H NMR spectra, or very sparingly in deuterated methanol (whilst subject to ultrasound), although this solvent caused certain peaks to be masked under the residual water peak (at 25 °C).

The most effective way of ascertaining the structure was found to be by re-forming the free amine base **159**. This could be done directly in the NMR tube by adding deuterated chloroform to compound **161** in the presence of triethylamine (1 equivalent) or by adding deuterated methanol to compound **161** in the presence of caesium carbonate (1 equivalent). Therefore, to ensure completeness, both compounds **159** and **161** are characterised in the *Experimental* section of this thesis.

From the dual characterisation employed a feature became readily apparent in the ^{13}C NMR spectra of amine **159** that was absent in the ^{13}C NMR spectra of the ammonium salt **161** (and its precursors **157** and **158**). The difference was that the peaks pertaining to the carbon nuclei along (and adjacent to) the amide backbone (the isophthalamido Ar*C*-1/3 and *C*ONHCH$_2$*C*H$_2$ positions) were split. This splitting can be ascribed to the presence of *cis*- and *trans*-amide rotamers in solution.

3.6.4 Synthesis of the Molecular Tweezers

Once again in approaching the final step the general synthetic methodology developed for the construction of the monoboronic acid reference compounds **128**$_{(pyrene)}$ - **132**$_{(2\text{-}naphthalene)}$ with varied fluorophores was put into practice here.

Having isolated compounds **127** and **161** with high levels of purity it was thought that these two moieties should couple under reflux conditions in the presence of a mild base such as potassium carbonate. Neopentyl glycol should then be readily removed on a silica gel column with the chromatographic step allowing the desired product to be isolated cleanly.

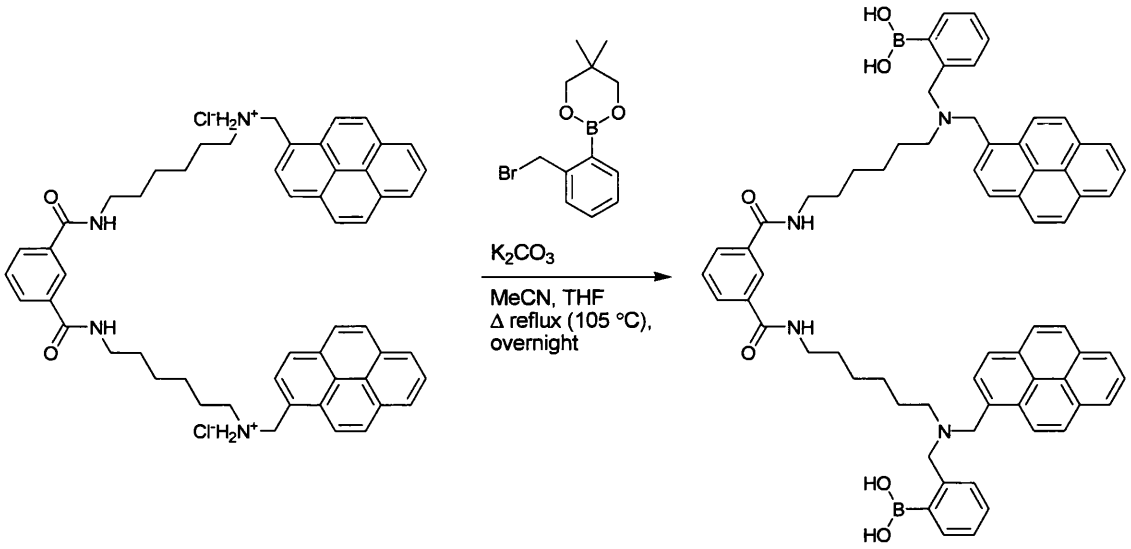

Scheme 88. *The initial conditions employed for the formation of compound **162** using boronic acid **127** (4 eq.) and K_2CO_3 (10 eq.).*

Following the reaction conditions established for the monoboronic acid reference compounds **128**$_{(pyrene)}$ - **132**$_{(2\text{-naphthalene})}$, compound **161** (1 equivalent) was added to a stirred flask of tetrahydrofuran and acetonitrile. To this was added potassium carbonate (10 equivalents) and boronic acid **127** (4 equivalents). The mixture was heated under reflux conditions (at 105 °C) for 13 hours. After cooling the solvents were removed under reduced pressure and the residue extracted in dichloromethane (3 ×) from water adjusted to pH 7 using small volumes of aqueous hydrochloric acid (1 M). The organic phases were recombined, dried and subject to flash silica gel column chromatography. Analysing the fractions it appeared that the diboronic acid tweezers had been made and deprotected but not isolated cleanly. From ^{1}H NMR spectra a number of signals were observed shadowing the desired peaks. It seemed probable that as well as the desired diboronic acid **162**, signals were being generated from derivatives of compound **161** that had not been fully substituted.

By TLC differentiating between these compounds proved challenging, the un-, mono- and di-substituted forms of compound **161** would raise as one elongated spot, behaviour which was mirrored on the silica gel column. As chromatographic separation on silica gel between the mono- and di-substituted forms of compound **161** appeared non-trivial using the highly polar gradient elution developed for the monoboronic acid reference compounds **128**$_{(pyrene)}$ - **132**$_{(2\text{-naphthalene})}$ (where only monosubstituted boronic acids could be formed) it was decided that if the reaction could be driven to ensure the formation of the thermodynamic product this hurdle could be overcome.

The Importance of Potassium Carbonate

One quirk of the reaction which had become apparent in the previous reaction was the choice of base used. When added to a solution of tetrahydrofuran and acetonitrile at room temperature potassium carbonate appeared insoluble. When the system was heated the potassium carbonate dissolved sparingly, nevertheless it was felt that a more soluble base might favour our needs. Repeating the reaction but this time using the readily soluble caesium carbonate the conditions were tweaked to ensure formation of the diboronic acid. To the ammonium hydrochloride salt **161** (1 equivalent) in a stirred flask of tetrahydrofuran and acetonitrile was added caesium carbonate (10 equivalents) and boronic acid **127** (3 equivalents). The mixture was heated under reflux conditions (at 105 °C) for 5 hours after which time a further batch of caesium carbonate (9 equivalents) and boronic acid **127** (2 equivalents) was added and the system heated under reflux conditions (at 95 °C) for a further 19 hours. Following the same solvent extraction and flash column chromatography as before, the various components of the reaction mixture were isolated cleanly and analysed to reveal that absolutely none of the desired product had been generated with the unreacted starting materials being recovered.

Bizarrely this use of caesium carbonate, differing only from potassium carbonate by its counter cation and enhanced solubility, completely inhibited the reaction of boronic acid **127** with compound **161**. Discussions with Tony James indicated that the result was not unique to this reaction but had been observed by him and others within the Shinkai research group during the work conducted in the mid-nineties and appeared to be a general observation (unpublished results).[118,119,158] Therefore whilst potassium carbonate is only sparingly soluble in the tetrahydrofuran/acetonitrile solvent system

employed (a feature which would normally be considered detrimental) this characteristic is in fact critical to the outcome of these reactions.

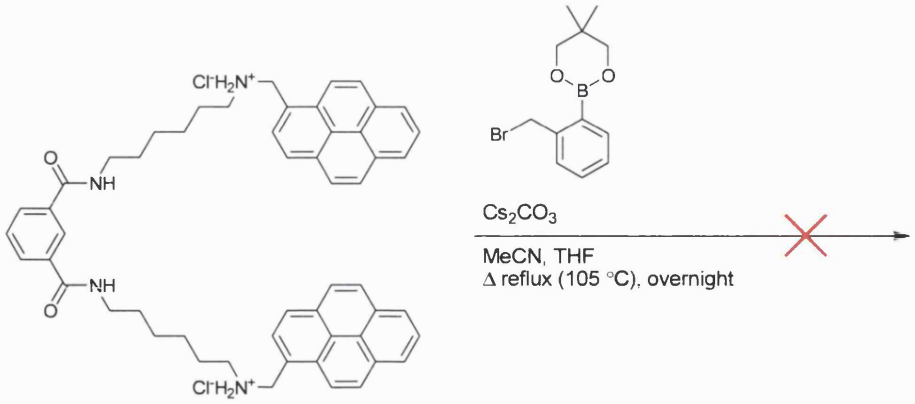

Scheme 89. *The reaction of boronic acid **127** with compound **161** is inhibited by Cs_2CO_3.*

With potassium carbonate as base the above reaction was repeated. To compound **161** (1 equivalent) in dry tetrahydrofuran and dry acetonitrile was added potassium carbonate (20 equivalents) and boronic acid **127** (3 equivalents). Although the monoboronic acid reference compounds $\mathbf{128}_{(pyrene)}$ - $\mathbf{132}_{(2\text{-naphthalene})}$ had been heated under reflux at (105 °C) this temperature was well above the boiling points of either of the two solvents (tetrahydrofuran bp = 66 °C and acetonitrile bp = 82 °C)[294] and given the vigorousness of the boil the temperature was reduced to 95 °C. After 11 hours the reaction mixture was analysed by silica gel TLC and three discrete spots were found at R_fs in the vicinity of the R_f expected from the product.

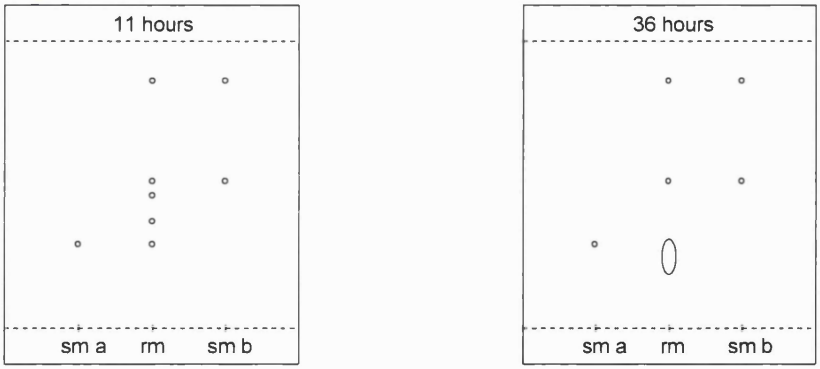

Figure 65. *Silica gel TLC of the reaction mixture (10:90 MeOH/DCM elution) after 11 hours and then 36 hours, where rm denotes reaction mixture, sm denotes starting material and a is compound **161** in the presence of Cs_2CO_3 and b is boronic acid **127**.*

From the TLC taken after 11 hours, illustrated in Figure 65, it was apparent that the reaction was underway but had not reached completion, with compound **161** probably present in its unreacted, mono- and di-substituted forms. A second batch of potassium carbonate (40 equivalents) and boronic acid **127** (3 equivalents) was added and the temperature raised to 105 °C as it was postulated that this slight change in temperature may again impinge on the solubility of potassium carbonate in solution.

After a further 24 hours of heating under reflux the progress of the reaction was checked and it was found that, as before, the reaction had progressed but the discrete spots afforded before had now amalgamated to produce a single elongated spot.

Flash Column Chromatography

As it had been demonstrated that these compounds moved down silica gel columns more readily than the monoboronic acid references compounds **128**$_{(pyrene)}$ - **132**$_{(2\text{-}naphthalene)}$ and it was the case that a more refined discrimination was required given the possibility of mono- and di-substituted products being present with similar R_f values, the column was loaded in a less polar eluent (3:97 methanol/dichloromethane) and the polarity was raised far more slowly than with the monoboronic acid systems.

Nonetheless, as the column fractions were isolated and analysed it was again found that the behaviour of the compounds on a flat silica gel TLC plate did not necessarily reflect their behaviour in the bulk silica gel environment found within the column. The TLC of the isolated fractions is illustrated (and experimental conditions detailed) in Figure 66.

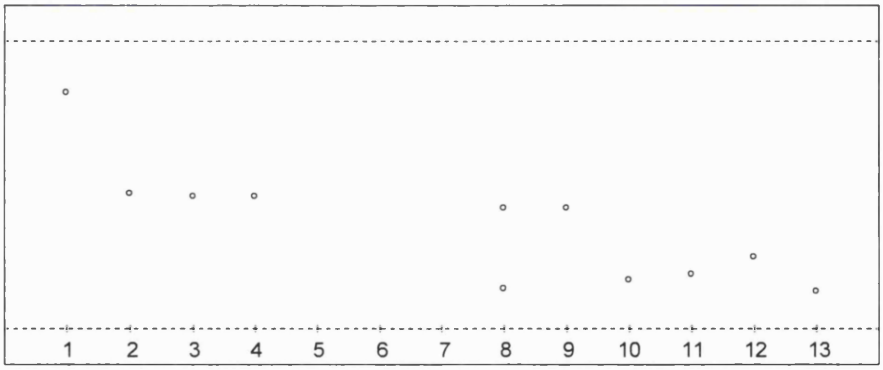

Figure 66. *TLC of fractions 1-13 collected during the purification of compound **162**. The plate was aluminium backed, coated with a 0.20 mm layer of silica gel 60 with fluorescent indicator UV_{254} and eluted with 10:90 MeOH/DCM. All spots were visible under UV (λ_{ex} 254 nm or 365 nm). 157 mg of compound **161** was used at the outset of the reaction and the crude material was loaded onto a silica gel 60 column 2 cm in diameter and 12 cm in height with 3:97 MeOH/DCM as eluent. Once loaded the column was kept under pressure and the mobile phase kept moving whenever possible. The gradient elution proceeded as follows (eluent ratios are given as MeOH/DCM): F1 (500 cm^3, 3:97); F2 (200 cm^3, 3:97); F3 (200 cm^3, 3:97); F4 (200 cm^3, 3:97); F5 (200 cm^3, 3:97); F6 (250 cm^3, 3:97); F7 (250 cm^3, 3:97); F8 (300 cm^3, 3:97) → (500 cm^3; 10:90); F9 (500 cm^3, 15:85) → (300 cm^3; 25:75); F10 (200 cm^3, 25:75) → (500 cm^3; 50:50) → (100 cm^3; 90:10); F11 (500 cm^3, 90:10); F12 (500 cm^3, 90:10); F13 (400 cm^3, 90:10).*

Monoboronic Acid Tipped Molecular Tweezers

Following analysis by ^{1}H NMR, fraction 10 was found to contain the monoboronic acid **163**.

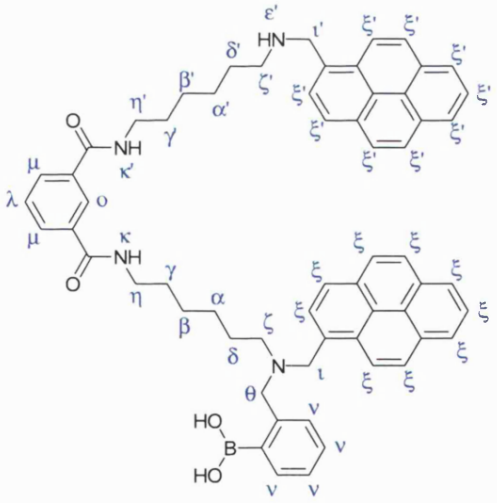

163

The ^{1}H NMR spectrum of fraction 10 is illustrated in Figure 67. For clarity the signals are labelled and related to the corresponding environments on compound **163**. Primed letters denote protons on the unsubstituted side of the molecule.

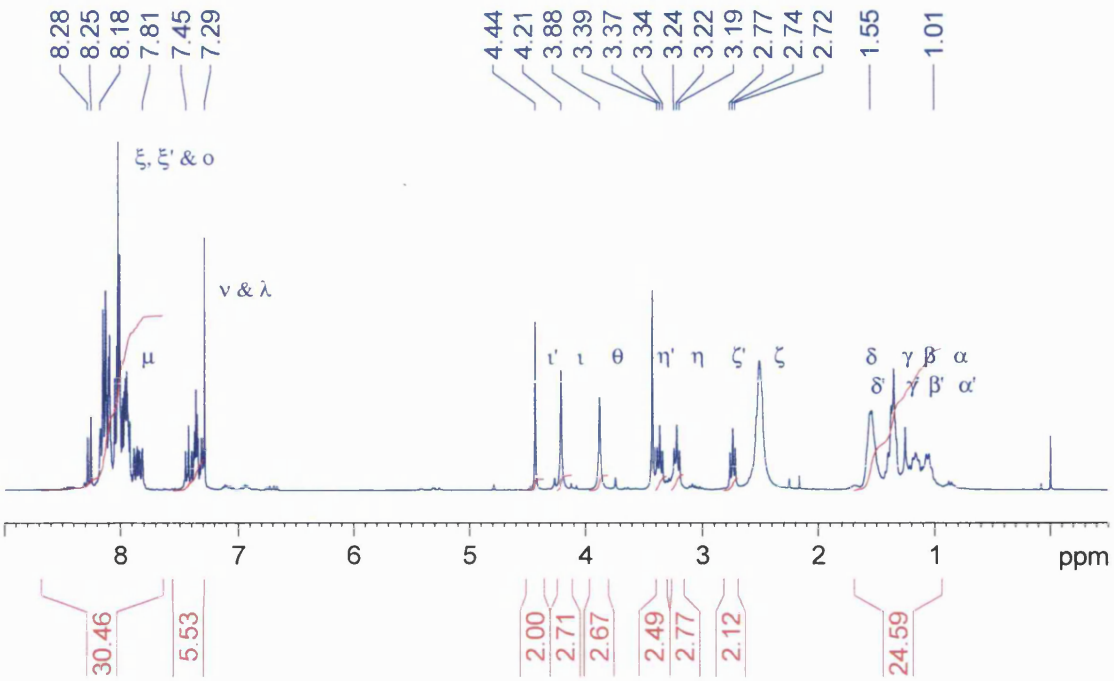

Figure 67. *^{1}H NMR spectrum (300 MHz, $CDCl_3$ with a few drops of MeOD) of compound **163** with TMS at 0.00ppm, water at 2.51ppm and the residual solvent peaks at 3.43ppm (MeOH) and 7.29ppm ($CHCl_3$).*

Expanding the ^{1}H NMR spectrum of Figure 67 in Figure 68, it is possible to see that the signals corresponding to the substituted half of the molecule outweigh the un-substituted half in a ratio of ~ 2.0:2.7. This ratio is indicative of the presence of a small amount (i.e. a 1:0.18 ration of mono-/di- substituted compound) of the fully disubstituted tweezers and is consistent with the values of the integrals obtained across the full ^{1}H NMR spectrum in Figure 67.

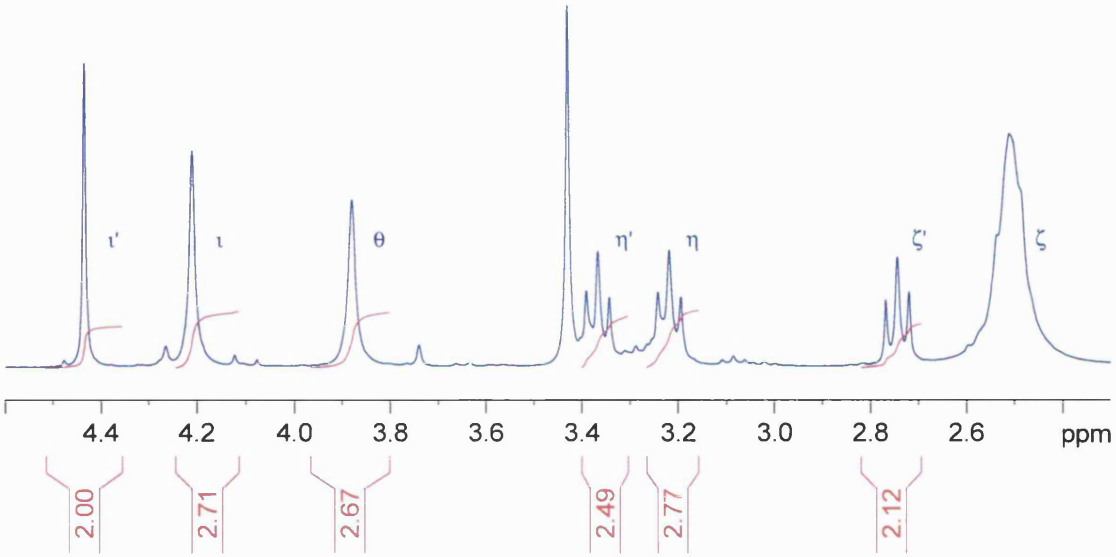

Figure 68. *Expansion of the ^1H NMR spectrum in Figure 67, the triplet expected for ζ is masked by the water peak at 2.51ppm and the singlet at 3.43ppm is due to residual solvent (MeOH).*

3.6.5 Isolation and Characterisation

Diboronic Acid Tipped Molecular Tweezers

Curiously the R_f of fraction 12 was higher than that of fraction 11 on the TLC plate. When fraction 12 was examined it was found to contain the desired diboronic acid tipped molecular tweezers **162** exclusively (as did fraction 13). The disparity in the behaviour of mobile phases on TLC and in the column has been discussed before. Thankfully the separation was sufficient so as to allow the diboronic acid molecular tweezers to be isolated independently from their monoboronic acid analogues.

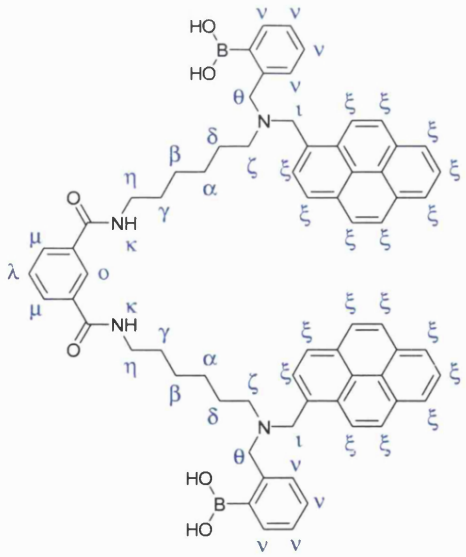

162

The ^{1}H NMR spectrum of the molecular tweezers **162** is displayed in Figure 69. For clarity the signals are labelled and related to the corresponding environments of compound **162**.

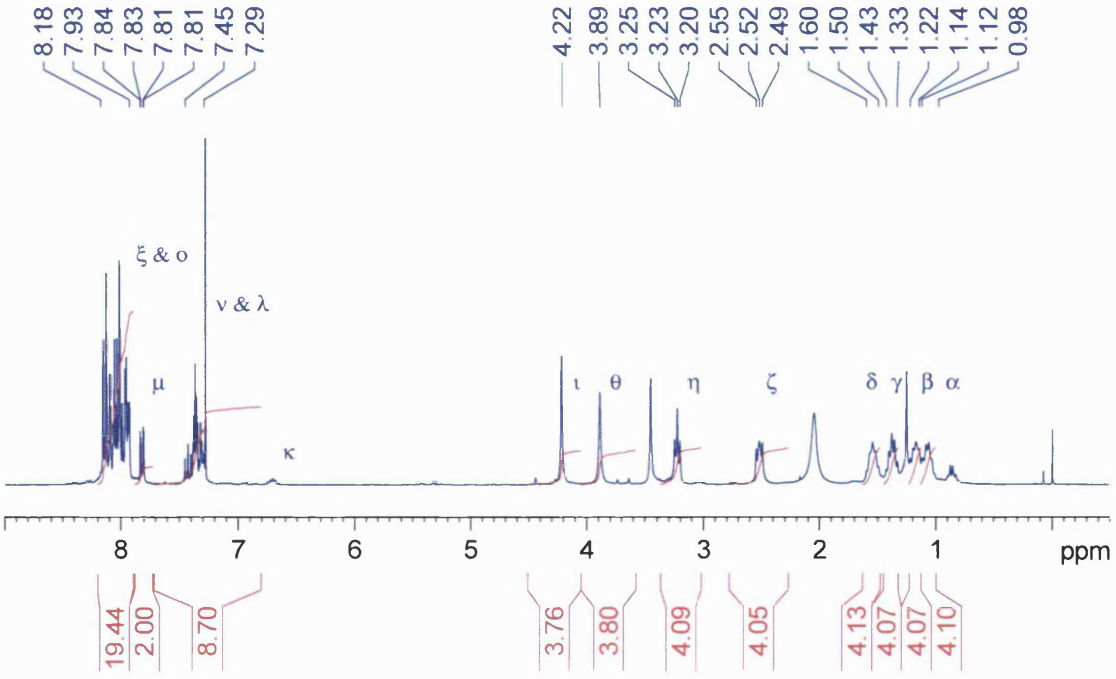

Figure 69. *^{1}H NMR spectrum (300 MHz, $CDCl_3$ with a few drops of MeOD) of compound **162** with TMS at –0.06ppm, silicone grease at 0.01ppm, grease[295] at 0.77-0.83ppm and 1.19ppm, water at 1.74ppm, MeOH at 3.39ppm, amide NH at 6.50-6.54 and $CHCl_3$ at 7.21ppm. For clarity only the outer peaks of the α, β, γ and δ triplets of triplets are peak picked.*

Given that the signals from the CH_2(ζ) and CH_2(η) protons (proximal to the amine and amide groups respectively) could be unambiguously determined, the use of 2D correlated spectroscopy (COSY) NMR experiments permitted the signals from the CH_2 α, β, γ and δ protons down the length of the alkyl chains to be ascribed in a stepwise manner. This technique also revealed the presence of the signal from the isophthalamido Ar*H*-5(λ) proton under the signals arising from the phenyl Ar*H*(ν) protons and the isophthalamido Ar*H*-2(ο) proton under the signals arising from the pyrenyl Ar*H*(ξ).

One curiosity in the ^{1}H NMR spectrum of the molecular tweezers **162** pertaining to the use of the deuterated methanol/chloroform blend was the presence of a small triplet at 6.71ppm in Figure 69. 2D COSY NMR confirmed that the signal was due to the amide NH protons, however, the integral was around a fifth smaller than anticipated. It was also the case that the amide protons did not split the signal corresponding to the CH_2(η) protons in this spectrum. As this spectrum was re-run the presence of a signal from the amide NH and the splitting of the CH_2(η) proximal to the amide was found to vary depending on the particular ratio of deuterated methanol dropped into the deuterated chloroform.

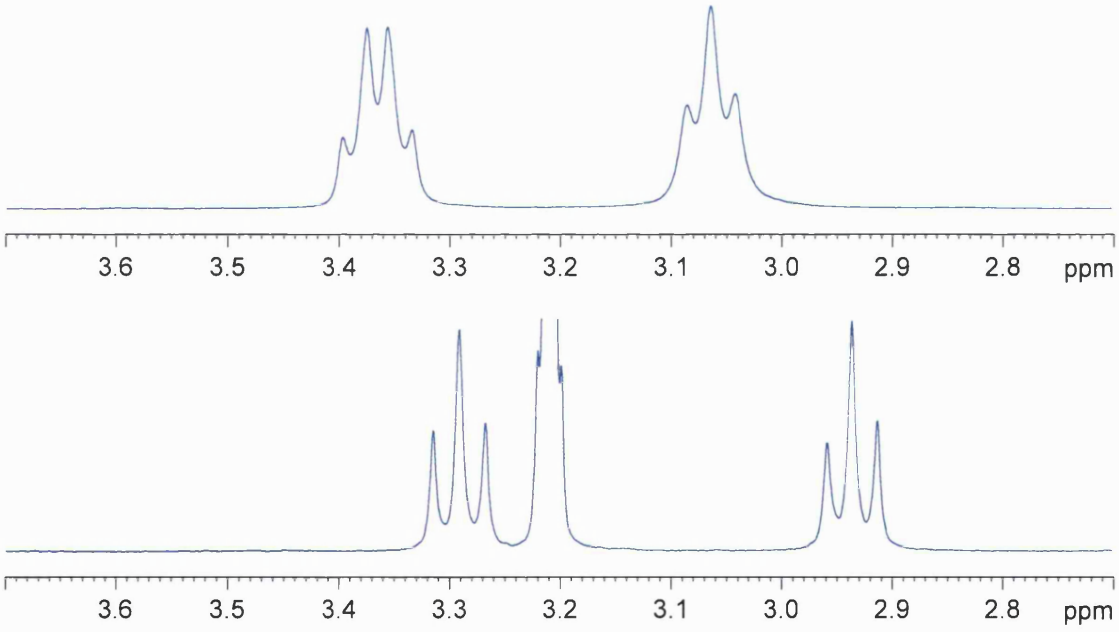

Figure 70. *Expansion of the ^{1}H NMR spectra of the Boc protected compound **157** in $CDCl_3$ (top, displaying the distinctive $NHCH_2$ doublet of triplets) and MeOD (bottom).*

Considering the limiting cases for the analogous Boc protected compound **157** a doublet of triplets is observed in deuterated chloroform (Figure 70, top) and a triplet is observed

in deuterated methanol (Figure 70, bottom). Therefore with regards to the behaviour of the amide protons, the deuterated methanol/chloroform blend represented something of a halfway house.

Cis and *Trans* Amide Rotamers

Having fully characterised the ^{1}H NMR spectrum *via* 2D COSY NMR spectroscopy the use of a 400 MHz spectrometer was obtained and a ~ 9 hour ^{13}C PENDANT NMR experiment run (the full range of experiments run to characterise this 1059 Da compound containing 2 quadrupolar boron nuclei was conducted on the 12 mg of product isolated from fraction 12). As with amine **159**, *cis* and *trans* amide rotamers caused the splitting of certain carbon signals in the ^{13}C NMR spectra. In the case of the molecular tweezers **162** two of the carbon signals were seen to split.

With the use of 2D HMQC NMR it became possible to ascribe all of the signals from carbon nuclei on the alkyl CH_2 (α, β, γ and δ) environments as well as the carbonyl C=O carbons. With these environments ascribed to particular signals the splitting could be accounted for and was indeed found to occur on the carbonyl C=O and CONHCH_2(η) carbons.

Denouement

The isolation of compound **162** confirmed the applicability of the general design approach developed previously within this thesis. Having decided upon the particular structure of the molecular tweezers **162**, our protocols first permitted the synthetic route to be rationally designed and, second, permitted the synthetic assembly to proceed through robust and readily accessible synthetic procedures. This approach afforded the target molecules with high levels of purity and as such provides an effective and generally applicable route for the construction of fluorescent PET sensors containing the *N*-methyl-*o*-(aminomethyl)phenylboronic acid fragment.

3.7 SUMMARY OF RESULTS AND DISCUSSION II

- A generally applicable design strategy is reported for the synthesis of compounds containing the *N*-methyl-*o*-(aminomethyl)phenylboronic acid fragment.

– The design strategy takes advantage of protecting group chemistry to afford cleanly substituted (poly)amines functionalised to suit the needs of the researcher.

– Subsequent formation of the corresponding hydrochloride salts affords scrupulously purified intermediates, a condition which allows formation of the desired boronic acids to occur with excellent levels of purity.

– By forming fully protected and stable intermediate compounds a hierarchical approach may be incorporated into the design strategy to provide ready access to multiple synthetic targets from common intermediates.

- Generally applicable synthetic techniques are reported for the synthesis of compounds containing the *N*-methyl-*o*-(aminomethyl)phenylboronic acid fragment.

– Conditions for the formation of required Boc protected amines, intermediate ammonium hydrochloride salts and the final couplings of boronic acids with amines are detailed.

– It has been demonstrated that the final purification and concurrent deprotection of the mono- and di-boronic acids can be reliably and reproducibly achieved by means of silica gel flash column chromatography.

- During the synthesis of the three distinct sets of compounds discussed in this thesis, we report forty compounds from:

– The complete parallel synthesis of five monoboronic acid reference compounds.

– A refined route for five diboronic acid sensors.

– The complete synthesis of a novel pair of diboronic acid tipped molecular tweezers.

CHAPTER FOUR: Experimental

Fillet of a fenny snake,
In the caldron boil and bake;
Eye of newt, and toe of frog,
Wool of bat, and tongue of dog,
Adder's fork, and blind-worm's sting,
Lizard's leg, and owlet's wing,-
For a charm of powerful trouble,
Like a hell-broth boil and bubble.

Double, double toil and trouble;
Fire burn, and caldron bubble.

William Shakespeare

Macbeth

4 Experimental

4.1 General Procedures

Solvents and Reagents

Solvents and reagents were reagent grade unless stated otherwise and were purchased from Acros Organics, Avocado Research Chemicals Ltd, Fisher Scientific UK, Frontier Scientific Europe Ltd, Lancaster Synthesis Ltd and Sigma-Aldrich Company Ltd and were used without further purification, unless stated otherwise. Where dry solvents were required, dichloromethane and acetonitrile were distilled from calcium hydride, whilst toluene, tetrahydrofuran, hexane and diethyl ether were distilled from sodium benzophenone ketyl, under a nitrogen atmosphere.

Chromatography

Thin layer chromatography was performed using commercially available Merck or Macherey-Nagel aluminium backed plates coated with a 0.20 mm layer of silica gel 60 with fluorescent indicator UV_{254}. These plates were visualised using either ultraviolet light of 254 nm or 365 nm wavelength, or by staining the plates with vanillin or ninhydrin solution. Silica gel column chromatography was carried out using Davisil LC 60A silica gel (35-70 μm).

Nuclear Magnetic Resonance Spectra

Nuclear magnetic resonance spectra were run in chloroform-D, methyl-D_3 alcohol-D, dimethyl-D_6 sulfoxide or a blend of chloroform-D (~ 0.8 cm^3) and methyl-D_3 alcohol-D (2 drops). Where a Bruker AVANCE 300 was used ^1H spectra were recorded at 300.22 MHz, ^{11}B spectra at 96.32 MHz and $\{^1H\}$-^{13}C at 75.50 MHz. Where a Bruker AVANCE 400 was used ^1H spectra were recorded at 400.13 MHz and $\{^1H\}$-^{13}C at 100.62 MHz. Chemical shifts (δ) are expressed in parts per million and are reported relative to the residual solvent peak or to tetramethylsilane as an internal standard in ^1H and $\{^1H\}$-^{13}C spectra. Chemical shifts (δ) are expressed in parts per million and are reported relative to boron trifluoride diethyl etherate as an external standard in ^{11}B spectra. The multiplicities and general assignments of the spectroscopic data are denoted as: singlet (s), doublet (d), triplet, (t), quartet (q), quintet (quin), doublet of

doublets (dd), doublet of doublets of doublets (ddd), doublet of doublets of doublets of doublets (dddd), doublet of triplets (dt), triplet of triplets (tt), unresolved multiplet (m), apparent (app), broad (br) and aryl (Ar). Where stated the $\{^1H\}$-^{13}C NMR spectra were subject to the polarisation that is nurtured during attached nucleus testing (PENDANT) technique, resulting in primary and tertiary carbon atoms having a different phase to secondary and quaternary carbon atoms.[296] The phases are reported as (+) positive phase and (-) negative phase. In certain instances the structural assignments reported for the ^1H NMR spectra were elucidated with the aid of correlated spectroscopy (COSY), heteronuclear multiple quantum coherence (HMQC) and heteronuclear multiple bond connectivity (HMBC) NMR experiments.

Infrared Spectra

Infrared spectra were obtained (following internal background calibration) in the range 600-4000 cm^{-1} from KBr discs, thin films or $CDCl_3$ solutions using a Perkin-Elmer 1600 FT spectrometer. Characteristic absorption peaks are reported in wavenumbers (cm^{-1}).

Mass Spectra

Mass spectra were recorded by the EPSRC National Mass Spectrometry Service Centre, Swansea. Electron impact (EI) and chemical ionisation (CI) analyses were performed in positive ionisation mode. Low resolution EI and CI measurements were performed on a Micromass Quattro II triple quadrupole instrument, with ammonia as the CI reagent gas. Electrospray ionisation measurements were performed in both positive and negative ionisation modes (ES+ and ES- respectively). For low resolution measurements the sample was loop injected into a stream of 1:1 methanol/dichloromethane, on a Waters ZQ4000 single quadrupole mass spectrometer or Mariner API-TOF with reflectron detector mass spectrometer. High resolution EI, CI, ES+ and ES- measurements were conducted on either a Finnigan MAT95 high resolution double focussing mass spectrometer or a MAT900 high resolution double focussing mass spectrometer with tandem ion trap. For EI and CI measurements heptacosa (perfluorotributylamine) was used as the reference compound. Both low and high resolution fast atom bombardment (FAB or liquid secondary ion mass spectrometry, LSIMS) analyses were performed, in positive or negative ionisation mode, on either a Finnigan MAT95 high resolution double focussing mass spectrometer or a MAT900 high resolution double focussing

mass spectrometer with tandem ion trap, using *meta*-nitrobenzyl alcohol (NBA) as the matrix liquid.

Elemental Analyses

Elemental analyses were performed by the Department of Chemistry, University of Bath, using an Exeter Analytical Inc CE-440 Elemental Analyzer.

Melting Points

Capillary melting points were determined using a Büchi 535 melting point apparatus. The readings were taken from a mercury-in-glass thermometer and are reported uncorrected as the meniscus point (unless stated otherwise), rounded to the nearest 1 °C with a heating ramp rate of 0.5 °C minute^{-1}. In instances where a reproducible liquid meniscus could not be obtained the onset point (onset) was recorded instead and is noted.[297] Where the sample changed colour or evolved gas during or after the melt, thermal decomposition (dec) is noted.[298] In the case of the aromatic boronic acids the manner in which they were heated greatly influenced the melting point.[215,299] For these samples heating commenced at a temperature which did not induce sintering at the capillary-sample interface. The temperature was then increased gradually. With a preliminary melting point established the temperature was ramped at 1 °C minute^{-1} from 10 °C below the expected melting point and then maintained at a ramp rate of 0.5 °C minute^{-1} from 5 °C below the expected melting point until completion of the melting point determination.

Fluorescence Measurements

Fluorescence measurements were performed on a Perkin-Elmer Luminescence Spectrophotometer LS 50b, utilising Starna Silica (quartz) cuvets with 10 mm path lengths, four faces polished. Data was collected *via* the Perkin-Elmer FL Winlab software package. All pH measurements taken during fluorescence experiments were recorded on a Hanna Instruments HI 9321 Microprocessor pH meter which was routinely calibrated using Fisher Chemicals standard buffer solutions (pH 4.0 - phthalate, 7.0 – phosphate, and 10.0 - borate). All solvents used in fluorescence measurements were HPLC or Fluorescence grade and the water was deionised. All saccharides used in fluorescence measurements were certified as ≥ 99% pure.

4.2 MODEL COMPOUNDS

4.2.1 6:1 Dilution Conditions and Compounds **102-108**

Anthracen-9-ylmethyl-methyl-amine

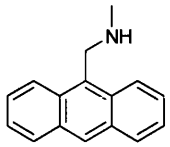

102

To a stirred solution of methylamine (2 M solution in methanol, 5.00 cm^3, 10.0 mmol) in ethanol (30 cm^3) and acetonitrile (30 cm^3) was added 9-anthraldehyde (1.00 g, 4.85 mmol). The system was stirred for 44 hours at room temperature after which time the reaction mixture was condensed under reduced pressure. Methanol (35 cm^3) and tetrahydrofuran (35 cm^3) were added and the system stirred for 10 minutes at room temperature prior to the addition of sodium borohydride (0.90 g, 23.8 mmol). 3 hours stirring at room temperature followed after which the methanol was removed from the suspension under reduced pressure. Sodium hydroxide (0.1 M solution in water, 10 cm^3) and water (50 cm^3) were added. The product was extracted from the aqueous phase in dichloromethane (3 × 30 cm^3), the organic phases recombined, dried over magnesium sulfate and filtered. The solvent was removed *in vacuo* to afford the title compound **102** as yellow needles (0.90 g, 84%); mp 51-52 °C, lit 45-48 °C (re-crystallised from *n*-hexanes);[300] δ_H (300 MHz, $CDCl_3$) 2.59 (3H, s, NHC*H*$_3$), 4.62 (2H, s, anthryl ArC*H*$_2$), 7.36-7.49 (4H, m, anthryl Ar*H*), 7.93 (2H, d, $^3J_{HH}$ 9.0, anthryl Ar*H*), 8.27 (2H, d, $^3J_{HH}$ 8.9, anthryl Ar*H*), 8.33 (1H, s, anthryl Ar*H*); δ_C (75 MHz, $CDCl_3$) 31.3, 48.1, 124.5, 125.3, 126.5, 127.6, 129.5, 130.7, 131.9; *m/z* (EI) 222.1201 ($[M]^+$. $C_{16}H_{15}N$ requires 222.1205), (EI) 221 (73%, $[M]^+$), 191 (100, $[M - NHCH_3]^+$).

N-Anthracen-9-ylmethyl-N-methyl-ethane-1,2-diamine

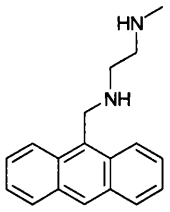

103

To a stirred solution of N^1-methyl-ethane-1,2-diamine (2.60 cm^3, 29.8 mmol), ethanol (30 cm^3) and acetonitrile (30 cm^3) was added 9-anthraldehyde (1.01 g, 4.90 mmol). The system was stirred for 69 hours at room temperature after which time the reaction mixture was condensed under reduced pressure. Methanol (30 cm^3) and tetrahydrofuran (30 cm^3) were added and the system stirred for 10 minutes at room temperature prior to the addition of sodium borohydride (1.34 g, 35.4 mmol). 5 hours stirring at room temperature followed after which the solvent was removed under reduced pressure. Sodium hydroxide (0.1 M solution in water, 2 cm^3) and water (50 cm^3) were added. The product was extracted from the aqueous phase in dichloromethane (3 × 30 cm^3). The organic phase was washed using water (2 × 50 cm^3), dried over magnesium sulfate and filtered. The remaining solvents were removed by evaporation under reduced pressure to afford the title compound **103** as a viscous brown oil (1.01 g, 79%); δ_H (300 MHz, $CDCl_3$) 2.32 (3H, s, NC*H*$_3$), 2.65-2.69 (2H, m, C*H*$_2$$CH_2NCH_3$), 2.91-2.95 (2H, m, C*H*$_2$$NCH_3$), 4.66 (2H, s, anthryl ArC*H*$_2$), 7.36-7.48 (4H, m, anthryl Ar*H*), 7.91-7.94 (2H, m, anthryl Ar*H*), 8.25-8.28 (2H, m, anthryl Ar*H*), 8.32 (1H, s, anthryl Ar*H*); δ_C (75 MHz, $CDCl_3$) 36.7, 46.2, 50.0, 52.0, 124.5, 125.3, 126.5, 127.6, 129.4, 129.6, 129.7, 130.7, 131.9, 132.1; *m/z* (CI) 365 (100%, $[M + H]^+$).

N-Anthracen-9-ylmethyl-propane-1,3-diamine

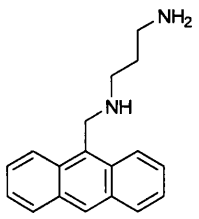

104

To a stirred solution of propane-1, 3-diamine (4.90 cm^3, 58.7 mmol), ethanol (30 cm^3) and acetonitrile (30 cm^3) was added 9-anthraldehyde (2.00 g, 9.70 mmol). The system was stirred for 45 hours at room temperature after which time the reaction mixture was condensed under reduced pressure. Methanol (60 cm^3) was added and the system stirred for 10 minutes at room temperature prior to the addition of sodium borohydride (1.35 g, 35.7 mmol). 6 hours stirring at room temperature followed, sodium hydroxide (1 M solution in water, 5 cm^3) and water (50 cm^3) were added before the solvents were removed under reduced pressure. Water (50 cm^3) was added to the reaction mixture and the products extracted from the aqueous phase in dichloromethane (3 × 30 cm^3), dried over magnesium sulfate and filtered. The remaining solvents were removed by evaporation under reduced pressure to afford the title compound **104** as a viscous brown oil (1.86 g, 73%); δ_H (300 MHz, $CDCl_3$) 1.71 (2H, tt, $^3J_{HH}$ 6.9, $^3J_{HH}$ 6.9, $CH_2CH_2CH_2NH_2$), 2.78 (2H, t, $^3J_{HH}$ 6.8, anthryl $ArCH_2NHCH_2$), 2.93 (2H, t, $^3J_{HH}$ 7.0, CH_2NH_2), 4.71 (2H, s, anthryl $ArCH_2$), 7.43-7.58 (4H, m, anthryl Ar*H*), 8.00 (2H, app d, $^3J_{HH}$ 8.3, anthryl Ar*H*), 8.34 (2H, app d, $^3J_{HH}$ 8.9, anthryl Ar*H*), 8.38 (1H, s, anthryl Ar*H*); δ_C (75 MHz; $CDCl_3$) 32.2, 41.1, 46.0, 49.0, 124.3, 125.4, 126.7, 127.8, 129.6, 130.7, 131.4, 131.9; *m/z* (FAB) 264.1634 ($[M]^+$. $C_{18}H_{20}N_2$ requires 264.1626), (FAB) 265 (38%; $[M + H]^+$), 191 (100, $[M - NH(CH_2)_3NH_2]^+$).

***N*-(2-Amino-ethyl)-*N*-anthracen-9-ylmethyl-ethane-1,2-diamine**

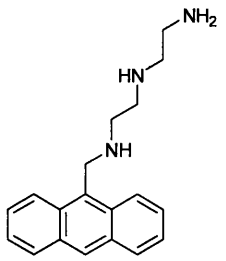

105

To a stirred solution of N^1-(2-amino-ethyl)-ethane-1,2-diamine (3.20 cm^3, 29.5 mmol), ethanol (30 cm^3) and acetonitrile (30 cm^3) was added 9-anthraldehyde (1.01 g, 4.90 mmol). The system was stirred for 42 hours at room temperature after which time the reaction mixture was condensed under reduced pressure. Methanol (35 cm^3) and tetrahydrofuran (30 cm^3) were added and the system stirred for 10 minutes at room temperature prior to the addition of sodium borohydride (0.90 g, 23.8 mmol). 22 hours stirring at room temperature followed. Sodium hydroxide (0.1 M solution in water, 4 cm^3) and water (50 cm^3) were added prior to the removal of the solvents under reduced pressure. Water (50 cm^3) was added to the reaction mixture and the product extracted from the aqueous phase in dichloromethane (3×30 cm^{-3}), dried over magnesium sulfate and filtered. The remaining solvents were removed by evaporation under reduced pressure to afford **105** as a viscous brown oil (1.13 g, 79%); δ_H (300 MHz, $CDCl_3$) 2.60 (2H, t, $^3J_{HH}$ 5.7, CH_2CH_2), 2.72 (2H, t, $^3J_{HH}$ 5.9, CH_2CH_2), 2.78 (2H, t, $^3J_{HH}$ 5.7, CH_2CH_2), 2.99 (2H, t, $^3J_{HH}$ 5.8, CH_2CH_2), 4.75 (2H, s, anthryl $ArCH_2$), 7.40-7.57 (4H, m, anthryl Ar*H*), 8.01 (2H, app d, $^3J_{HH}$ 8.3, anthryl Ar*H*), 8.36 (2H, app d, $^3J_{HH}$ 9.1, anthryl Ar*H*), 8.40 (1H, s, anthryl Ar*H*); δ_C (75 MHz, $CDCl_3$) 42.2, 46.0, 49.7, 50.1, 52.8, 124.6, 125.3, 126.5, 127.6, 129.6, 130.7, 131.9, 132.2; *m/z* (FAB) 294.1974 ([M + H]$^+$. $C_{19}H_{24}N_3$ requires 294.1970), (FAB) 294 (24%, [M + H]$^+$), 191 (100, [M – $NH(CH_2)_2NH(CH_2)_2NH_2$]$^+$).

N-(3-Amino-propyl)-N-anthracen-9-ylmethyl-propane-1,3-diamine

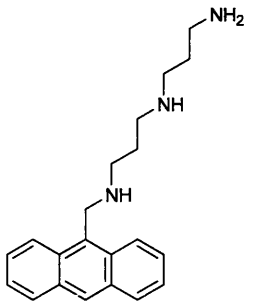

106

To a stirred solution of N^2-(3-amino-propyl)-propane-1,3-diamine (4.60 cm^3, 32.9 mmol), ethanol (30 cm^3) and acetonitrile (40 cm^3) was added 9-anthraldehyde (1.13 g, 5.45 mmol). The system was stirred for 38 hours at room temperature after which time the reaction mixture was condensed under reduced pressure. Methanol (30 cm^3) was added and the system stirred for 10 minutes at room temperature prior to the addition of sodium borohydride (0.90 g, 23.8 mmol). 7 hours stirring at room temperature followed before the solvent was removed under reduced pressure. Sodium hydroxide (5 M solution in water, 1 cm^3) and water (50 cm^3) were added. The aqueous phase was washed with diethyl ether (2 × 30 cm^3) before extraction of the product in dichloromethane (3 × 30 cm^3). The resulting organic phase was then washed using water (2 × 50 cm^3) before drying over magnesium sulfate and filtering. The remaining solvents were removed by evaporation under reduced pressure to afford the title compound **106** as a viscous brown oil (0.63 g, 40%); δ_H (300 MHz, $CDCl_3$) 1.55 (2H, tt, $^3J_{HH}$ 6.9, $^3J_{HH}$ 6.9, anthryl $ArCH_2NHCH_2CH_2CH_2$), 1.76 (2H, tt, $^3J_{HH}$ 6.8, $^3J_{HH}$ 6.8, $CH_2CH_2CH_2NH_2$), 2.58-2.71 (6H, m, anthryl $ArCH_2NHCH_2CH_2CH_2NHCH_2$), 2.95 (2H, t, $^3J_{HH}$ 6.8, CH_2NH_2), 4.71 (2H, s, anthryl $ArCH_2$), 7.43-7.56 (4H, m, anthryl Ar*H*), 8.00 (2H, app d, $^3J_{HH}$ 8.3, anthryl Ar*H*), 8.34 (2H, app d, $^3J_{HH}$ 8.7, anthryl Ar*H*), 8.39 (1H, s, Ar*H*); δ_C (75 MHz, $CDCl_3$) 30.7, 34.2, 40.9, 46.3, 48.4, 49.1, 49.6, 124.6, 125.3, 126.4, 127.5, 129.5, 130.7, 131.9, 132.2; *m/z* (FAB) 322.2281 ($[M + H]^+$. $C_{21}H_{28}N_3$ requires 322.2283), (FAB) 322 (39%; $[M + H]^+$), 191 (100, $[M - NH(CH_2)_3NH(CH_2)_3NH_2]^+$).

N'-(2-Amino-ethyl)-N'-{2-[(anthracen-9-ylmethyl)-amino]-ethyl}-ethane-1,2-diamine

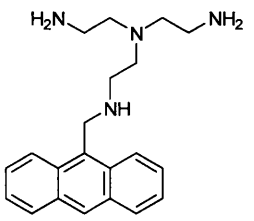

107

To a stirred solution of tris-(2-aminoethyl)amine (5.00 cm^3, 33.4 mmol), ethanol (30 cm^3) and acetonitrile (30 cm^3) was added 9-anthraldehyde (1.15 g, 5.57 mmol). The system was stirred for 114 hours at room temperature after which time the reaction mixture was condensed under reduced pressure. Methanol (40 cm^3) was added and the system stirred for 10 minutes at room temperature prior to the addition of sodium borohydride (0.90 g, 23.8 mmol). 2 hours stirring at room temperature followed after which sodium hydroxide (0.1 M solution in water, 2 cm^3) and water (50 cm^3) were added prior to the removal of the solvents under reduced pressure. The product was dissolved in water (50 cm^3) and impurities extracted using diethyl ether (2 × 75 cm^3). The product was then extracted from the aqueous phase in dichloromethane (3 × 30 cm^3). The organic phase washed with water (50 cm^3), dried over magnesium sulfate and filtered. The organic solvent was removed by evaporation under reduced pressure to afford the title compound **107** as a viscous dark orange oil (1.16g, 62%); δ_H (300 MHz, $CDCl_3$) 2.31 (4H, t, $^3J_{HH}$ 6.0, CH_2CH_2), 2.52 (6H, t, $^3J_{HH}$ 6.1, CH_2), 2.80 (2H, d, $^3J_{HH}$ 6.0, CH_2), 4.69 (1H, s, anthryl $ArCH_2$), 7.33-7.50 (4H, m, anthryl Ar*H*), 7.95 (2H, app d, $^3J_{HH}$ 7.7, anthryl Ar*H*), 8.28 (2H, app d, $^3J_{HH}$ 9.2, anthryl Ar*H*), 8.34 (1H, s, anthryl Ar*H*); δ_C (75 MHz, $CDCl_3$) 39.9, 45.6, 54.8, 56.9, 124.5, 125.4, 126.6, 129.6, 130.7, 131.9; *m/z* (FAB) 337.2397 ($[M + H]^+$. $C_{21}H_{29}N_4$ requires 337.2392), (CI) 337 (5%; $[M + H]^+$), 191 (100, $[M - NH(CH_2)_2N((CH_2)_2NH_2)_2]^+$).

N-(2-Amino-ethyl)-N-{2-[(ferrocenylmethyl)-amino]-ethyl}-ethane-1,2-diamine

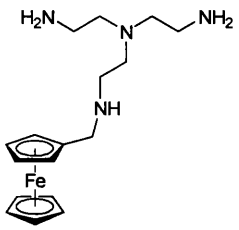

108

To a stirred solution of tris-(2-aminoethyl)amine (5.00 cm^3, 33.4 mmol), ethanol (30 cm^3) and acetonitrile (30 cm^3) was added ferrocene carboxaldehyde (1.19 g, 5.57 mmol). The system was stirred for 95 hours at room temperature after which time the reaction mixture was condensed under reduced pressure. Methanol (40 cm^3) was added and the system stirred for 10 minutes at room temperature prior to the addition of sodium borohydride (0.90 g, 23.8 mmol). 2 hours stirring at room temperature followed after which sodium hydroxide (0.1 M solution in water, 2 cm^3) and water (50 cm^3) were added prior to the removal of the solvents under reduced pressure. The product was dissolved in water (50 cm^3) and washed with diethyl ether (2 × 75 cm^3). The product was then extracted from the aqueous phase in dichloromethane (3 × 30 cm^3). The organic phase was washed with water (50 cm^3), dried over magnesium sulfate and filtered. The organic solvent was dried *in vacuo* to afford the title compound **108** as a viscous red oil (1.15 g, 60%); δ_H (300 MHz, $CDCl_3$) 2.46 (12H, m, CH_2CH_2), 3.55 (2H, s, ferrocenyl ArCH_2), 4.14 (7H, s, ferrocenyl Ar*H*), 4.24 (2H, s, ferrocenyl Ar*H*); δ_C (75 MHz, $CDCl_3$) 40.6, 47.6, 55.2, 58.4, 69.5, 69.9, 70.5.

4.2.2 10:1 Dilution Conditions with 4 Hour Addition and Compounds **138-144**

***N*-benzylhexane-1,6-diamine**

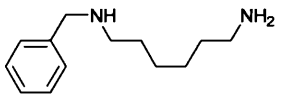

138

Hexamethylene diamine (3.85 g, 33.1 mmol) and *p*-toluenesulfonic acid monohydrate (6.76 g, 35.5 mmol) were dissolved in absolute ethanol (100 cm^3) and the system heated under reflux. Benzaldehyde (349 mg, 3.29 mmol) was dissolved in dry tetrahydrofuran (180 cm^3) and added dropwise to the heated solution *via* a pressure equalised dropping funnel over a 10 hour period. The system was then heated under reflux for a further 4 hours. Sodium borohydride (1.82 g, 48.0 mmol) was carefully added to the system with stirring at 0 °C. The system was allowed to return to room temperature and stirred for a further 2 hours. Dilute hydrochloric acid (1 M, 10 cm^3) was added and the solvent removed under reduced pressure. The residue was extracted from dilute sodium hydroxide (0.5 M, 50 cm^3) in dichloromethane (3 × 30 cm^3), the organic phases were recombined, washed with water (10 × 30 cm^3), dried over magnesium sulfate and filtered. The product was dried *in vacuo* to afford the title compound **138** as a yellow oil (250 mg, 77%); ν (Film)/cm^{-1} 3290, 2925, 2853, 1602, 735, 698; δ_H (300 MHz, $CDCl_3$) 1.17-1.47 (8H, m, $NHCH_2(CH_2)_4CH_2NH_2$), 2.51-2.62 (4H, m, $NHCH_2(CH_2)_4CH_2NH_2$), 3.71 (2H, s, benzyl $ArCH_2$), 7.16-7.26 (5H, m, benzyl Ar*H*); δ_C (75 MHz, $CDCl_3$) 27.2 (-), 27.6 (-), 30.5 (-), 34.2 (-), 42.6 (-), 49.8 (-), 54.5 (-), 127.2 (+), 128.5 (+), 128.8 (+), 140.9 (-); *m/z* (CI) 207 (100%, $[M + H]^+$).

N-Pyren-1-ylmethyl-hexane-1,6-diamine

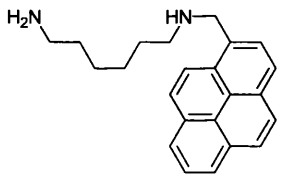

144

Hexamethylene diamine (3.64 g, 31.3 mmol) and *p*-toluenesulfonic acid monohydrate (6.18 g, 32.5 mmol) were dissolved in absolute ethanol (180 cm^3) and the system heated under reflux. Pyrene-1-carboxaldehyde (656 mg, 2.85 mmol) was dissolved in dry tetrahydrofuran (250 cm^3) and added dropwise to the heated solution *via* a pressure equalised dropping funnel over a 7 hour period. The system was then heated under reflux for a further 5 hours. Sodium borohydride (605 mg, 16.0 mmol) was carefully added to the system with stirring at 0 °C. The system was allowed to return to room temperature and stirred for a further 2 hours. Dilute hydrochloric acid (1 M, 10 cm^3) was added and the solvent removed under reduced pressure. The residue was extracted from dilute sodium hydroxide (0.5 M, 50 cm^3) in dichloromethane (3 × 30 cm^3), the organic phases recombined, washed with water (10 × 30 cm^3), dried over magnesium sulfate and filtered. The product was dried *in vacuo* to afford the title compound **144** as a mustard yellow powder (903 mg, 96%); ν (KBr)/cm^{-1} 2927, 2856, 841; δ_H (300 MHz, $CDCl_3$) 1.17-1.38 (6H, m, $(CH_2)_3$), 1.44-1.54 (2H, m, CH_2), 2.56 (2H, t, $^3J_{HH}$ 6.9, NH_2CH_2), 2.70 (2H, t, $^3J_{HH}$ 7.2, CH_2CH_2NH), 4.40 (2H, s, pyrenyl $ArCH_2$), 7.88-7.95 (4H, m, pyrenyl Ar*H*), 8.03-8.11 (4H, m, pyrenyl Ar*H*), 8.28 (1H, app d, $^3J_{HH}$ 9.2, pyrenyl Ar*H*); δ_c PENDANT (75 MHz, $CDCl_3$) 27.2 (-), 27.7 (-), 30.6 (-), 34.2 (-), 42.6 (-), 50.4 (-), 52.3 (-), 123.6 (+), 125.1 (+), 125.3 (-), 125.35 (+), 125.42 (-), 125.45 (+), 126.2 (+), 127.37 (+), 127.40 (+), 127.9 (+), 128.0 (+), 129.4 (-), 131.0 (-), 131.2 (-), 131.7 (-), 134.5 (-); *m/z* (ES^+) 331.2169 ($[M + H]^+$. $C_{23}H_{27}N_2$ requires 331.2169), (CI) 331 (100%, $[M + H]^+$).

4.3 MODULAR SYSTEMS

4.3.1 Phenylboronic Acid Precursors **125-127**

2-*o*-Tolyl-1,3,2-dioxaborinane

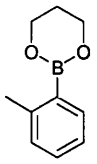

125

o-Tolylboronic acid (1.07 g, 7.87 mmol) and 1,3-propanediol (0.70 cm^3, 9.69 mmol) were mixed in toluene (30 cm^3). A Dean Stark head was fitted and the reaction mixture heated under reflux for 15 hours. The reaction mixture was allowed to cool before being washed with water (3 × 30 cm^3). The mixture was then condensed under reduced pressure and dichloromethane (30 cm^3) added. This organic phase was then washed with water (3 × 30 cm^3), dried over magnesium sulfate, filtered and dried *in vacuo* to afford the title compound **125** as a yellow oil (1.06 g, 76%); $\nu_{max}(CHCl_3)/cm^{-1}$ 3056, 3015, 2953, 2896, 1599, 1569, 1482, 1308, 1154; δ_H (300 MHz, $CDCl_3$) 1.97 (2H, dddd, $^3J_{HH}$ 5.5, $^3J_{HH}$ 5.5, $^3J_{HH}$ 5.5, $^3J_{HH}$ 5.5, $OCH_2CH_2CH_2O$), 2.43 (3H, s, CH_3), 4.09 (4H, t, $^3J_{HH}$ 5.5, $OCH_2CH_2CH_2O$), 7.06 (2H, app dd, $^3J_{HH}$ 7.4, $^3J_{HH}$ 7.4, Ar*H*), 7.19 (1H, app ddd, $^3J_{HH}$ 7.2, $^3J_{HH}$ 7.2, $^4J_{HH}$ 1.8, Ar*H*), 7.63 (1H, app d, $^3J_{HH}$ 7.4, Ar*H*); δ_B (96 MHz, $CDCl_3$) 28.5; δ_C (75 MHz, $CDCl_3$) 22.8 (+), 27.8 (-), 62.3 (-), 125.0 (+), 130.38 (+), 130.39 (+), 135.2 (+), 144.4 (-); *m/z* (ES+) 194.1345 ($[M + NH_4]^+$. $C_{10}H_{17}O_2BN$ requires 194.1347), (EI) 176 (100%, $[M]^+$).

5,5-dimethyl-2-*o*-tolyl-1,3,2-dioxaborinane

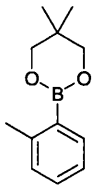

126

2-Tolylboronic acid (5.02 g, 36.9 mmol) and 2,2-dimethyl-1,3-propanediol (4.54 g, 43.5 mmol) were mixed in toluene (100 cm^3). A Dean Stark head was fitted and the reaction mixture heated under reflux for 1 hour. The amber reaction mixture was condensed under reduced pressure, purified by flash column chromatography on silica gel (with dichloromethane as eluent) and dried *in vacuo* to yield the title compound **126** as a colourless oil (6.90 g, 92%); R_f (DCM) 0.76; Found: C, 70.4; H, 8.3; N, 0.2. $C_{12}H_{17}BO_2$ requires C, 70.6; H, 8.4; N, 0.0%; ν (Film)/cm^{-1} 3063, 3016, 2963, 2887, 1599, 1570, 1476, 1306, 1138; δ_H (300 MHz, $CDCl_3$) 0.94 (6H, s, $OCH_2C(CH_3)_2CH_2O$), 2.43 (3H, s, $ArCH_3$), 3.68 (4H, s, $OCH_2C(CH_3)_2CH_2O$), 7.04-7.21 (3H, m, Ar*H*), 7.64-7.67 (1H, m, Ar*H*); δ_B (96 MHz, $CDCl_3$) 28.3; δ_C PENDANT (75 MHz, $CDCl_3$) 22.3 (+), 22.8 (+), 32.1 (-), 72.7 (-), 125.1 (+), 130.4 (+), 130.5 (+), 135.3 (+), 144.4 (-); *m/z* (EI) 204.1313 ($[M]^+$. $C_{12}H_{17}O_2B$ requires 204.1316), (EI) 204 (100%, $[M]^+$).

2-[2-(bromomethyl)phenyl]-5,5-dimethyl-1,3,2-dioxaborinane

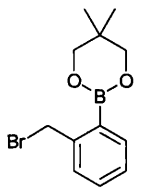

127

N-Bromosuccinimide (6.47 g, 36.3 mmol) and 2,2'-azobisisobutyronitrile (476 mg, 2.90 mmol) were added to a stirred solution of compound **126** (6.66 g, 32.6 mmol) in benzene (50 cm^3). A condenser was fitted and the system allowed to equilibrate at 60 °C. After 5 minutes at 60 °C the temperature was further raised and the system heated under reflux for 2 hours. The reaction mixture was then allowed to cool to room temperature, filtered and the filtrate condensed under reduced pressure. The resulting product was purified by flash column chromatography on silica gel (with dichloromethane as eluent) and dried *in vacuo* to yield the title compound **127** as a colourless oil (9.13 g, 99%); R_f (DCM) 0.77; ν (Film)/cm^{-1} 3064, 2981, 2891, 1599, 1569, 1477, 1305, 1129, 648; δ_H (300 MHz, $CDCl_3$) 0.96 (6H, s, $OCH_2C(CH_3)_2CH_2O$), 3.71 (4H, s, $OCH_2C(CH_3)_2CH_2O$), 4.84 (2H, s, $ArCH_2$), 7.14-7.96 (4H, m, Ar*H*); δ_B (96 MHz, $CDCl_3$) 27.9; δ_C PENDANT (75 MHz, $CDCl_3$) 22.4 (+), 32.2 (-), 35.0 (-), 72.8 (-), 128.0 (+), 130.7 (+), 131.0 (+), 136.1 (+), 144.0 (-); *m/z* (ES+) 300.0768 ($[M + NH_4]^+$. $C_{12}H_{20}O_2NBBr$ requires 300.0765), (EI) 283 (100%, $[M]^+$).

4.3.2 Ammonium Hydrochloride Salts **119**$_{(pyrene)}$-**123**$_{(2\text{-naphthalene})}$

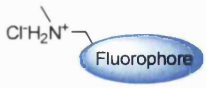

119$_{(pyrene)}$ - **123**$_{(2\text{-naphthalene})}$

General procedure for the preparation of compounds 119$_{(pyrene)}$- 123$_{(2\text{-naphthalene})}$

A solution of the required aldehyde (1 eq.) and methylamine (2.5 eq.) in tetrahydrofuran (0.2 mol dm^{-3}) and methanol (0.2 mol dm^{-3}) was heated under reflux for 7 hours. The system was allowed to cool to room temperature, placed in an ice bath and sodium borohydride (3 eq.) was added in portions. Stirring continued at room temperature for 2 hours before the careful addition of hydrochloric acid (1 M, 10 cm^3). The system was stirred for a further 10 minutes before removal of the solvents under reduced pressure. The resulting residue was then extracted in dichloromethane (3 × 30 cm^3) from sodium hydroxide (0.5 M, 30 cm^3). The organic phases were recombined, washed with water (≥ 5 × 30 cm^3) until neutral pH was obtained, dried over magnesium sulfate and filtered. An excess of gaseous hydrogen chloride was bubbled through the filtrate, which was subsequently purged with nitrogen gas and condensed under reduced pressure. Dichloromethane (25 cm^3) was added to the ammonium hydrochloride salt. The suspension was then slurried over a glass sinter and washed with dichloromethane (3 × 30 cm^3) prior to the removal of all solvent from it *in vacuo* to afford the required title compound **119**$_{(pyrene)}$ - **123**$_{(2\text{-naphthalene})}$.

Methyl-pyren-1-ylmethyl-ammonium chloride

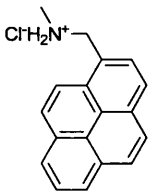

119$_{(pyrene)}$

Following the protocol laid out in the general procedure (page 207) and utilising: pyrene-1-carboxaldehyde (1.17 g, 5.09 mmol), 2 M methylamine in methanol (7.00 cm^3, 14.0 mmol), tetrahydrofuran (50 cm^3), methanol (50 cm^3) and sodium borohydride (1.23 g, 35.0 mmol) the reaction afforded the title compound **119**$_{(pyrene)}$ as a cream powder (1.30 g, 91%); mp 243-244 °C (dec); Found: C, 76.4; H, 5.8; N, 5.0. $C_{18}H_{16}NCl$ requires C, 76.7; H, 5.7; N, 5.0%; ν (KBr)/cm^{-1} 3040, 2967, 2843, 2783, 2503, 1604, 1590, 845; δ_H (300 MHz, MeOD) 2.89 (3H, s, NC*H*$_3$), 4.98 (2H, s, pyrenyl ArC*H*$_2$), 8.08-8.22 (4H, m, pyrenyl Ar*H*), 8.29-8.34 (4H, m, pyrenyl Ar*H*), 8.44 (1H, app d, $^3J_{HH}$ 9.4, pyrenyl Ar*H*); δ_c PENDANT (75 MHz, MeOD) 34.0 (-), 51.1 (+), 123.4 (-), 125.90 (+), 125.94 (+), 126.4 (+), 126.5 (-), 127.4 (-), 127.6 (-), 128.1 (-), 128.7 (-), 130.16 (-), 130.23 (-), 130.6 (-), 131.5 (+), 132.4 (+), 133.0 (+), 134.3 (+); *m/z* (FAB) 246.1283 ([M - Cl]$^+$. $C_{18}H_{16}N$ requires 246.1283), (FAB) 246 (46%, [M - Cl]$^+$), 215 (100, [M - NH_2CH_3Cl]$^+$).

Methyl-phenanthren-9-ylmethyl-ammonium chloride

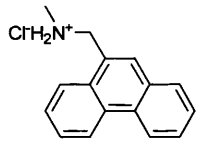

120$_{(phenanthrene)}$

Following the protocol laid out in the general procedure (page 207) and utilising: phenanthrene-9-carboxaldehyde (341 mg, 1.65 mmol), 2 M methylamine in methanol (2.10 cm^3, 4.20 mmol), tetrahydrofuran (30 cm^3), methanol (30 cm^3) and sodium borohydride (405 mg, 10.7 mmol) the reaction afforded the title compound **120**$_{(phenanthrene)}$ as a white powder (288 mg, 68%); mp 223 °C (dec); ν (KBr)/cm^{-1} 2936, 2825, 2749, 2688, 2462, 1576, 743, 726; δ_H (300 MHz, MeOD) 2.77 (3H, s, NC*H*$_3$), 4.65 (2H, s, phenanthryl ArC*H*$_2$), 7.53-7.70 (4H, m, phenanthryl Ar*H*), 7.87-7.89 (2H, m, phenanthryl Ar*H*), 8.07-8.12 (1H, m, phenanthryl Ar*H*), 8.66-8.69 (1H, m, phenanthryl Ar*H*), 8.73-8.8.78 (1H, m, phenanthryl Ar*H*); δ_c PENDANT (75 MHz, MeOD) 34.2 (+), 51.5 (-), 124.2 (+), 125.0 (+), 125.2 (+), 127.5 (-), 128.8 (+), 128.9 (+), 129.1 (+), 130.0 (+), 130.5 (+), 131.1 (-), 132.0 (+), 132.5 (-), 132.6 (-), 132.7 (-); *m/z* (FAB) 222.1291 ([M - Cl]$^+$. $C_{16}H_{16}N$ requires 222.1283), (FAB) 222 (100%, [M - Cl]$^+$).

Anthracen-9-ylmethyl-methyl-ammonium chloride

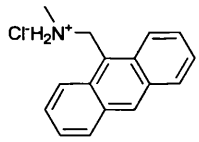

121$_{(anthracene)}$

Following the protocol laid out in the general procedure (page 207) and utilising: 9-anthraldehyde (1.85 g, 8.98 mmol), 2 M methylamine in methanol (11.5 cm^3, 23.0 mmol), tetrahydrofuran (90 cm^3), methanol (30 cm^3) and sodium borohydride (1.96 g, 51.9 mmol) the reaction afforded the title compound **121**$_{(anthracene)}$ as a yellow powder (1.64 g, 71%); mp 248 °C (dec); Found: C, 74.3; H, 6.2; N, 5.4. $C_{16}H_{16}NCl$ requires C, 74.6; H, 6.3; N, 5.4%; ν (KBr)/cm^{-1} 2914, 2731, 2441, 730; δ_H (300 MHz, MeOD) 2.93 (3H, s, NCH_3), 5.32 (2H, s, anthryl ArCH_2), 7.60 (2H, app ddd, $^3J_{HH}$ 8.5, $^3J_{HH}$ 6.6, $^4J_{HH}$ 1.0, anthryl Ar*H*), 7.73 (2H, app ddd, $^3J_{HH}$ 8.9, $^3J_{HH}$ 6.6, $^4J_{HH}$ 1.3, anthryl Ar*H*), 8.16 (2H, app dd, $^3J_{HH}$ 8.5, $^4J_{HH}$ 0.6, anthryl Ar*H*), 8.42 (2H, app dd, $^3J_{HH}$ 9.0, $^4J_{HH}$ 0.8, anthryl Ar*H*), 8.72 (1H, s, anthryl Ar*H*); δ_c PENDANT (75 MHz, MeOD) 34.4 (+), 45.8 (-), 123.3 (-), 124.5 (+), 127.0 (+), 129.3 (+), 131.1 (+), 132.1 (+), 132.6 (-), 133.3 (-); *m/z* (FAB) 222.1290 ([M - Cl]$^+$. $C_{16}H_{16}N$ requires 222.1283), (FAB) 222 (69%, [M - Cl]$^+$), 191 (100, [M - NH_2CH_3Cl]$^+$).

Methyl-naphthalen-1-ylmethyl-ammonium chloride

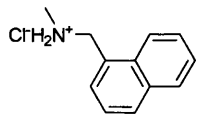

122$_{(1\text{-naphthalene})}$

Following the protocol laid out in the general procedure (page 207) and utilising: 1-naphthaldehyde (2.32 g, 14.9 mmol), 2 M methylamine in methanol (18.6 cm^3, 37.2 mmol), tetrahydrofuran (30 cm^3), methanol (30 cm^3) and sodium borohydride (1.76 g, 46.5 mmol) the reaction afforded the title compound **122**$_{(1\text{-naphthalene})}$ as a white powder (2.50 g, 81%); mp 188 °C (dec), lit 187-188 °C (re-crystallised from isopropanol);[301] Found: C, 68.9; H, 6.6; N, 6.6. $C_{12}H_{14}NCl$ requires C, 69.4; H, 6.8; N, 6.7%; ν (KBr)/cm^{-1} 2983, 2752, 2421, 1597, 1576, 1513; δ_H (300 MHz, MeOD) 2.72 (3H, s, NC*H*$_3$), 4.61 (2H, s, naphthyl ArC*H*$_2$), 7.43-7.61 (4H, m, naphthyl Ar*H*), 7.86-7.92 (2H, m, naphthyl Ar*H*), 8.08 (1H, app d, $^3J_{HH}$ 8.5, naphthyl Ar*H*); δ_c PENDANT (75 MHz, MeOD) 34.0 (+), 50.9 (-), 124.2 (+), 126.9 (+), 128.0 (+), 128.91 (-), 128.92 (+), 130.5 (+), 130.7 (+), 132.0 (+), 133.0 (-), 135.8 (-); *m/z* (FAB) 172.1122 ([M - Cl]$^+$. $C_{12}H_{14}N$ requires 172.1126), (FAB) 172 (100%, [M - Cl]$^+$).

Methyl-naphthalen-2-ylmethyl-ammonium chloride

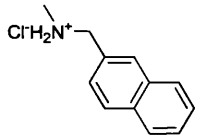

123$_{(2\text{-naphthalene})}$

Following the protocol laid out in the general procedure (page 207) and utilising: 2-naphthaldehyde (1.21 g, 7.73 mmol), 2 M methylamine in methanol (10.0 cm^3, 20.0 mmol), tetrahydrofuran (30 cm^3), methanol (30 cm^3) and sodium borohydride (0.94 g, 24.8 mmol) the reaction afforded the title compound **123**$_{(2\text{-naphthalene})}$ as a white powder (1.26 g, 79%); mp 230 °C (dec), lit 232-233 °C (re-crystallised from EtOH);[302] Found: C, 69.2; H, 6.5; N, 6.7. $C_{12}H_{14}NCl$ requires C, 69.4; H, 6.8; N, 6.7%; ν (KBr)/cm^{-1} 2934, 2757, 2700, 2411, 1601, 1589, 1510; δ_H (300 MHz, MeOD) 2.77 (3H, s, NCH_3), 4.37 (2H, s, naphthyl ArCH_2), 7.54-7.60 (3H, m, naphthyl Ar*H*), 7.90-8.02 (4H, m, naphthyl Ar*H*); δ_c PENDANT (75 MHz, MeOD) 33.6 (+), 54.1 (-), 127.9 (+), 128.3 (+), 128.6 (+), 129.2 (+), 129.6 (+), 130.3 (-), 130.6 (+), 131.2 (+), 135.1 (-), 135.4 (-); *m/z* (FAB) 172.1132 ($[M - Cl]^+$. $C_{12}H_{14}N$ requires 172.1126), (FAB) 172 (100%, $[M - Cl]^+$).

4.3.3 Monoboronic Acid Reference Compound **128**$_{(pyrene)}$-**132**$_{(2\text{-}naphthalene)}$

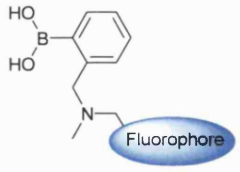

119$_{(pyrene)}$ - **123**$_{(2\text{-naphthalene})}$

General procedure for the preparation of compounds 128$_{(pyrene)}$- 132$_{(2\text{-naphthalene})}$

To a solution of the required ammonium hydrochloride salt **119**$_{(pyrene)}$ - **123**$_{(2\text{-naphthalene})}$ (1 eq.) in tetrahydrofuran (0.05 mol dm^{-3}) and acetonitrile (0.05 mol dm^{-3}) was added an excess of potassium carbonate (~ 10 eq.). The solution was stirred for 10 minutes before 2-(2-bromobenzyl)-1, 3-dioxaborinane **127** (1.1 eq.) was added and the system heated under reflux for 7 hours. The solvent was removed under reduced pressure. The residue was slurried in water (50 cm^3) and adjusted to pH ~ 7 with hydrochloric acid (2 M). The suspension was extracted in dichloromethane (3 × 50 cm^3). The organic phases were recombined and the solvent removed under reduced pressure. The resulting oil was purified by flash column chromatography on silica gel (methanol/dichloromethane, gradient elution: loading with a 5:95 ratio and incrementing the relative amount of methanol in 5% steps to 40:60 before moving to 75:25 and finally 90:10). The desired fractions were re-condensed, filtered in dichloromethane and dried *in vacuo* to afford the required title compound **128**$_{(pyrene)}$ - **132**$_{(2\text{-naphthalene})}$.

(2-Borono-benzyl)-methyl-pyren-1-ylmethyl-amine

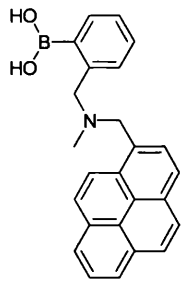

128$_{(pyrene)}$

Following the protocol laid out in the general procedure (page 213) and utilising: the ammonium hydrochloride salt **119**$_{(pyrene)}$ (48 mg, 0.170 mmol), potassium carbonate (125 mg, 0.904 mmol) and the boronic ester **127** (63 mg, 0.223 mmol) in tetrahydrofuran (100 cm^3) and acetonitrile (100 cm^3) the reaction afforded the title compound **128**$_{(pyrene)}$ as a yellow powder (53 mg, 82%); R_f (10:90 MeOH/DCM) 0.40; mp 170-172 °C (dec); Found: C, 79.3; H, 5.6; N, 3.7. $C_{25}H_{22}BNO_2$ requires C, 79.2; H, 5.9; N, 3.7%; ν (KBr)/cm^{-1} 3040, 2943, 2834, 1597, 1344, 1003, 842; δ_H (300 MHz, $CDCl_3$ with a few drops of MeOD) 2.15 (3H, s, NC*H*$_3$), 3.76 (2H, s, phenyl ArC*H*$_2$), 4.12 (2H, s, pyrenyl ArC*H*$_2$), 7.20-7.24 (1H, m, phenyl Ar*H*), 7.28-7.33 (2H, m, phenyl Ar*H*), 7.83-7.97 (7H, m, Ar*H*), 8.02-8.05 (3H, m, Ar*H*); δ_B (96 MHz, $CDCl_3$ with a few drops of MeOD) 28.0; δ_C (75 MHz, $CDCl_3$ with a few drops of MeOD): 40.1, 55.6, 63.8, 122.0, 123.5, 123.6, 123.8, 124.0, 124.2, 124.9, 126.2, 126.39, 126.44, 126.6, 127.6, 128.8, 129.6, 129.9, 130.2, 140.4; *m/z* (ES+) 380.1815 ($[M + H]^+$. $C_{25}H_{23}O_2NB$ requires 380.1816), (ES+) 380 (100%, $[M + H]^+$).

[2-Borono-benzyl]-methyl-phenanthren-1-ylmethyl-amine

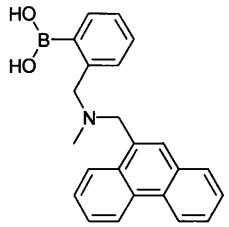

129$_{(phenanthrene)}$

Following the protocol laid out in the general procedure (page 213) and utilising: the ammonium hydrochloride salt **120**$_{(phenanthrene)}$ (187 mg, 0.725 mmol), potassium carbonate (2.30 g, 16.6 mmol) and the boronic ester **127** (240 mg, 0.848 mmol) in tetrahydrofuran (100 cm^3) and acetonitrile (100 cm^3) the reaction afforded the title compound **129**$_{(phenanthrene)}$ as a white powder (178 mg, 69%); R_f (10:90 MeOH/DCM) 0.45; mp 139 °C (dec); ν (KBr)/cm^{-1} 3055, 2940, 1597, 1567, 1496, 1340, 1003, 746; δ_H (300 MHz, $CDCl_3$ with a few drops of MeOD) 2.26 (3H, s, NCH_3), 3.76 (2H, s, phenyl ArCH_2), 4.01 (2H, br s, phenanthryl ArCH_2), 7.18-7.32 (3H, m, phenyl Ar*H*), 7.42-7.47 (1H, m, Ar*H*), 7.50-7.61 (3H, m, Ar*H*), 7.66 (1H, s, Ar*H*), 7.70-7.84 (3H, m, Ar*H*), 8.59 (1H, app d, $^3J_{HH}$ 8.1, phenanthryl Ar*H*), 8.63 (1H, app d, $^3J_{HH}$ 8.3, phenanthryl Ar*H*); δ_B (96 MHz, $CDCl_3$ with a few drops of MeOD) 28.4; δ_C (75 MHz, $CDCl_3$ with a few drops of MeOD) 40.0, 55.8, 63.3, 120.8, 121.4, 123.1, 124.8, 124.9, 125.1, 125.2, 126.0, 126.7, 126.9, 127.7, 128.1, 128.8, 128.9, 129.0, 129.2, 129.5, 133.8, 139.6; *m/z* (ES+) 356.1817 ($[M + H]^+$. $C_{23}H_{23}O_2NB$ requires 356.1816), (ES+) 356 (100%, $[M + H]^+$).

Anthracen-9-ylmethyl-(2-borono-benzyl)-methyl-amine

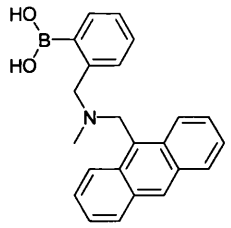

130$_{(anthracene)}$

Following the protocol laid out in the general procedure (page 213) and utilising: the ammonium hydrochloride salt **121**$_{(anthracene)}$ (253 mg, 0.982 mmol), potassium carbonate (673 mg, 4.87 mmol) and the boronic ester **127** (350 mg, 1.24 mmol) in tetrahydrofuran (100 cm^3) and acetonitrile (100 cm^3) the reaction afforded the title compound **130**$_{(anthracene)}$ as a yellow powder (280 mg, 80%); R_f (10:90 MeOH/DCM) 0.46; mp 128 °C (dec); ν (KBr)/cm^{-1} 3048, 2946, 2849, 1595, 1340, 1001, 731; δ_H (300 MHz, $CDCl_3$ with a few drops of MeOD) 2.09 (3H, s, NC*H*$_3$), 3.75 (2H, s, phenyl ArC*H*$_2$), 4.30 (2H, s, anthryl ArC*H*$_2$), 7.24-7.33 (7H, m, Ar*H*), 7.80-7.92 (5H, m, anthryl Ar*H*), 8.25 (1H, s, anthryl Ar*H*); δ_B (96 MHz, $CDCl_3$ with a few drops of MeOD) 28.8; δ_C (75 MHz, $CDCl_3$ with a few drops of MeOD) 42.2, 50.6, 65.7, 124.8, 125.2, 126.2, 128.0, 128.1, 128.6, 129.4, 130.3, 131.2, 131.6, 131.7, 135.9, 141.7; *m/z* (ES+) 356.1814 ($[M + H]^+$. $C_{23}H_{23}O_2NB$ requires 356.1816), (ES+) 356 (100%, $[M + H]^+$).

(2-Borono-benzyl)-methyl-naphthalen-1-ylmethyl-amine

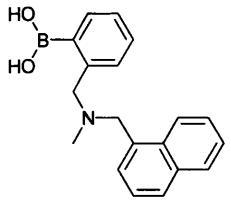

131$_{(1\text{-naphthalene})}$

Following the protocol laid out in the general procedure (page 213) and utilising: the ammonium hydrochloride salt **122**$_{(1\text{-naphthalene})}$ (200 mg, 0.963 mmol), potassium carbonate (2.71 g, 19.6 mmol) and the boronic ester **127** (326 mg, 1.15 mmol) in tetrahydrofuran (100 cm^3) and acetonitrile (100 cm^3) the reaction afforded the title compound **131**$_{(1\text{-naphthalene})}$ as a cream powder (218 mg, 74%); R_f (10:90 MeOH/DCM) 0.35; mp 117 °C (dec); ν (KBr)/cm^{-1} 3048, 3002, 2943, 2837, 1597, 1560, 1507, 1340, 1003, 779; δ_H (300 MHz, $CDCl_3$ with a few drops of MeOD) 2.19 (3H, s, NC*H*$_3$), 3.73 (2H, s, phenyl ArC*H*$_2$), 3.95 (2H, br s, naphthyl ArC*H*$_2$), 7.15-7.21 (1H, m, Ar*H*), 7.23-7.31 (2H, m, Ar*H*), 7.32-7.42 (4H, m, Ar*H*), 7.69-7.82 (4H, m, Ar*H*); δ_B (96 MHz, $CDCl_3$ with a few drops of MeOD) 28.2; δ_C (75 MHz, $CDCl_3$ with a few drops of MeOD) 41.7, 56.7, 65.0, 124.1, 125.4, 126.1, 126.4, 127.9, 129.0, 129.9, 132.6, 134.2, 141.5; *m/z* (ES+) 306.1656 ($[M + H]^+$. $C_{19}H_{21}O_2NB$ requires 306.1660), (ES+) 306 (100%, $[M + H]^+$).

(2-Borono-benzyl)-methyl-naphthalen-2-ylmethyl-amine

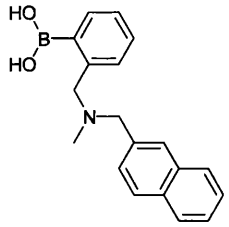

132$_{(2\text{-naphthalene})}$

Following the protocol laid out in the general procedure (page 213) and utilising: the ammonium hydrochloride salt **123**$_{(2\text{-naphthalene})}$ (269 mg, 1.30 mmol), potassium carbonate (1.85 g, 13.4 mmol) and the boronic ester **127** (414 mg, 1.46 mmol) in tetrahydrofuran (100 cm^3) and acetonitrile (100 cm^3) the reaction afforded the title compound **132**$_{(2\text{-naphthalene})}$ as a white powder (165 mg, 42%); R_f (10:90 MeOH/DCM) 0.44; mp 136-137 °C (dec); ν (KBr)/cm^{-1} 3052, 3003, 2939, 2784, 1598, 1568, 1507, 1340, 1007, 751; δ_H (300 MHz, $CDCl_3$ with a few drops of MeOD) 2.08 (3H, s, NCH_3), 3.65 (4H, s, $ArCH_2NCH_3CH_2Ar$), 7.06-7.13 (1H, m, Ar*H*), 7.18-7.27 (2H, m, Ar*H*), 7.29-7.42 (3H, m, Ar*H*), 7.61 (1H, s, naphthyl Ar*H*), 7.68-7.82 (4H, m, Ar*H*); δ_B (96 MHz, $CDCl_3$ with a few drops of MeOD) 28.1; δ_C (75 MHz, $CDCl_3$ with a few drops of MeOD) 40.9, 60.8, 64.5, 126.4, 126.6, 127.7, 127.8, 128.0, 128.1, 128.7, 129.0, 130.1, 133.3, 133.58, 133.59, 134.1, 136.0, 141.7; *m/z* (ES+) 306.1664 ($[M + H]^+$. $C_{19}H_{21}O_2NB$ requires 306.1660), (ES+) 306 (78%, $[M + H]^+$), 320 (100, $[M + H + Me]^+$).

4.3.4 Functionalised 1,6-Hexamethylene Diamine Intermediates **147-151** *(anthracene)*

tert-Butyl 6-aminohexylcarbamate

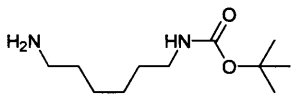

147

tert-Butyl phenyl carbonate (8.50 cm^3, 45.8 mmol) was added to a stirred solution of hexamethylene-1,6-diamine (5.12 g, 44.0 mmol) in absolute ethanol (50 cm^3). The system was fitted with a condenser and heated at 78 °C overnight, allowed to cool and condensed under reduced pressure. Dichloromethane (100 cm^3) was added and extracted with water (4 × 75 cm^3). For each extraction the pH of the aqueous phase was monitored and adjusted with hydrochloric acid (2 M) such that $3 \leq pH \leq 7$. The aqueous phases were collected in a flask pre-filled with sodium hydroxide (50 cm^3, 1 M). Ensuring that $pH \geq 14$ the resulting aqueous phase was extracted with dichloromethane (5 × 100 cm^3). These organic phases were recombined, condensed (to 100 cm^3) and subject to the above purification a second time by first extracting with water (4 × 75 cm^3, $3 \leq pH \leq 7$) and then by extracting from the combined aqueous phases ($pH \geq 14$) with dichloromethane (5 × 100 cm^3). These organic phases were recombined, dried over magnesium sulfate, filtered and dried *in vacuo* to afford the title compound **147** as a peach suspension (4.25 g, 45%); ν $(CDCl_3)/cm^{-1}$ 3456, 3018, 2980, 2932, 2858, 1708, 1508; δ_H (300 MHz, $CDCl_3$) 1.07 (2H, s, NH_2), 1.23-1.30 (4H, m, $NH_2(CH_2)_2(CH_2)_2(CH_2)_2NH$), 1.33-1.43 (13H, m, $CH_2(CH_2)_2CH_2CH_2NHCOOC(CH_3)_3$), 2.61 (2H, t, $^3J_{HH}$ 4.5, NH_2CH_2), 3.03 (2H, dt, $^3J_{HH}$ 4.9, $^3J_{HH}$ 4.9, CH_2NH), 4.77 (1H, br s, $NHCO$); δ_H (300 MHz, MeOD) 1.18-1.52 (17H, m, $(CH_2)_4CH_2NHCOOC(CH_3)_3$), 2.66 (2H, t, $^3J_{HH}$ 7.4, NH_2CH_2), 2.93 (2H, t, $^3J_{HH}$ 6.9, CH_2NH); δ_C PENDANT (75 MHz, $CDCl_3$) 26.8(+), 26.9(+), 28.6(-), 30.3(+), 33.9(+), 40.6(+), 42.3(+), 78.8(+), 156.3(+); *m/z* (ES+) 217.1908 ($[M + H]^+$. $C_{11}H_{25}N_2O_2$ requires 217.1911), (EI) 217 (26%, $[M + H]^+$), 57 (100, $[M - NH_2C_6H_{12}NHCOO]^+$).

***tert*-Butyl 6-(benzylamino)hexylcarbamate**

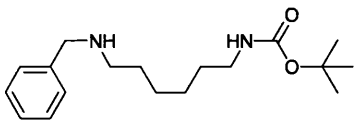

148

A solution of *tert*-butyl 6-aminohexylcarbamate **147** (1.91 g, 8.82 mmol) and benzaldehyde (1.79 g, 16.9 mmol) in tetrahydrofuran (100 cm^3) and ethanol (100 cm^3) was stirred under a nitrogen atmosphere for 36 hours. The system was placed in an ice bath and sodium borohydride (1.95 g, 51.7 mmol) was added. Stirring continued at room temperature for 2 hours before the careful addition of hydrochloric acid (1 M, 10 cm^3). The solvents were removed under reduced pressure, prior to the addition of water (65 cm^3) and sodium hydroxide (10 cm^3, 1 M). The aqueous phase was extracted with dichloromethane (5 × 30 cm^3), the organic phases were recombined dried over magnesium sulfate, filtered and condensed under reduced pressure to afford a pale yellow oil. This was purified by flash column chromatography on silica gel (methanol/dichloromethane, gradient elution) and dried *in vacuo* to afford the title compound **148** as a studded, colourless oil (1.82 g, 67%); R_f (10:90 MeOH/DCM) 0.43; ν (film)/cm^{-1} 3343, 3085, 3061, 3027, 2975, 2930, 2856, 1699, 1520; δ_H (300 MHz, $CDCl_3$) 1.18-1.30 (4H, m, $NH(CH_2)_2(CH_2)_2(CH_2)_2NH$), 1.31-1.45 (13H, m, $NHCH_2CH_2(CH_2)_2CH_2CH_2NHCOOC(CH_3)_3$), 2.54 (2H, t, $^3J_{HH}$ 7.2, $ArCH_2NHCH_2$), 3.01 (2H, dt, $^3J_{HH}$ 6.6, $^3J_{HH}$ 6.6, CH_2NHCO), 3.70 (2H, s, $ArCH_2$), 4.57 (1H, br s, NHCO), 7.13-7.28 (5H, m, ArH); δ_H (300 MHz, MeOD) 1.18-1.27 (4H, m, $NH(CH_2)_2(CH_2)_2(CH_2)_2NH$), 1.30-1.48 (13H, m, $CH_2(CH_2)_2CH_2CH_2NHCOOC(CH_3)_3$), 2.47 (2H, t, $^3J_{HH}$ 7.5, $ArCH_2NHCH_2$), 2.91 (2H, t, $^3J_{HH}$ 6.9, CH_2NHCO), 3.64 (2H, s, benzyl $ArCH_2$), 7.11-7.25 (5H, m, benzyl ArH); δ_C PENDANT (75 MHz, $CDCl_3$) 27.1 (-), 27.4 (-), 28.8 (+), 30.39 (-), 30.42 (-), 40.9 (-), 49.7 (-), 54.5 (-), 79.3 (-), 127.3 (+), 128.5 (+), 128.8 (+), 140.9 (-), 156.4 (-); *m/z* (ES+) 307.2376 ($[M + H]^+$. $C_{18}H_{31}N_2O_2$ requires 307.2380), (CI) 307 (63%, $[M + H]^+$), 233 (100, $[M - OC(CH_3)_3]^+$).

N^1-benzylhexane-1,6-diammonium dichloride

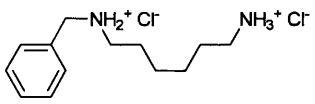

149

tert-Butyl 6-(benzylamino)hexylcarbamate **148** (37 mg, 0.121 mmol) was dissolved in a solution of hydrochloric acid (5 cm^3, S.G. 1.16, 32%), ethyl acetate (50 cm^3) and methanol (10 cm^3) and then stirred at room temperature for 30 minutes. The solution was condensed under reduced pressure using methanol to aid the removal of solvents azeotropically. Dichloromethane (25 cm^3) was added to the residue and gaseous hydrogen chloride bubbled through the suspension. The suspension was subsequently purged with nitrogen, slurried over a glass sinter and washed with dichloromethane (3 × 30 cm^3) prior to the removal of all solvent from it *in vacuo* to afford the title compound **149** as a white powder (21 mg, 62%); ν (KBr)/cm^{-1} 2957, 2802, 2708, 2614, 2558, 2405, 2211, 2026, 1589, 1571, 1499; δ_H (300 MHz, MeOD) 1.41-1.51 (4H, m, $NH_2Cl(CH_2)_2(CH_2)_2(CH_2)_2NH_3Cl$), 1.65-1.79 (4H, m, $NH_2ClCH_2CH_2(CH_2)_2CH_2CH_2NH_3Cl$), 2.94 (2H, t, $^3J_{HH}$ 7.6, benzyl $ArCH_2NH_2ClCH_2$), 3.06 (2H, t, $^3J_{HH}$ 8.0, CH_2NH_3Cl), 4.21 (2H, s, benzyl $ArCH_2$), 7.44-7.49 (3H, m, benzyl *ArH*), 7.50-7.55 (2H, m, benzyl *ArH*); δ_C PENDANT (75 MHz, MeOD) 27.3 (+), 27.5 (+), 28.7 (+), 40.9 (+), 48.9 (+), 52.7 (+), 130.7 (-), 131.1 (-), 131.4 (-), 133.0 (+); *m/z* (ES-) 277.1241 ([M - H]. $C_{13}H_{23}Cl_2N_2$ requires 277.1244), (ES-) 277 (100%, [M - H]).

***N*-[(anthracen-9-yl)methyl]-*N*-benzylhexane-1,6-diammonium dichloride**

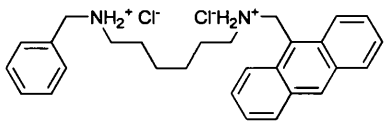

151$_{(anthracene)}$

N^1-benzylhexane-1,6-diammonium chloride **149** was added to sodium hydroxide (50 cm^3, 0.5 M) and stirred for 10 minutes. The amine base was then extracted with dichloromethane (3 × 30 cm^3). The organic phases were recombined, washed with brine (3 × 30 cm^3) and condensed under reduced pressure. To the free amine base (76 mg, 0.368 mmol) in absolute ethanol (20 cm^3) and dry tetrahydrofuran (20 cm^3) was added 9-anthraldehyde (121 mg, 0.587 mmol) and the solution heated under reflux conditions for 7 hours. The system was placed in an ice bath and sodium borohydride (129 mg, 3.41 mmol) was added. Stirring continued at room temperature for 2 hours before the careful addition of hydrochloric acid (1 M, 10 cm^3). The solvents were removed under reduced pressure, prior to the extraction of the intermediate in dichloromethane (3 × 30 cm^3) from sodium hydroxide (0.5 M, 30 cm^3). The organic phases were recombined, washed with water (≥ 5 × 30 cm^3) until neutral pH was obtained, dried over magnesium sulfate and filtered. An excess of gaseous hydrogen chloride was bubbled through the filtrate, it was subsequently purged with nitrogen gas and condensed under reduced pressure. Dichloromethane (25 cm^3) was added to the ammonium hydrochloride salt. The suspension was then slurried over a glass sinter and washed with dichloromethane (3 × 30 cm^3) prior to the removal of all solvent from it *in vacuo* to afford the title compound **151**$_{(anthracene)}$ as a yellow powder (59 mg, 34%); mp 142-144 °C (dec.); ν (KBr)/cm^{-1} 2938, 2785, 736; δ_H (300 MHz, MeOD) 1.46-1.51 (4H, m, $NH_2Cl(CH_2)_2(CH_2)_2(CH_2)_2NH_2Cl$), 1.75-1.88 (4H, m, $NH_2ClCH_2CH_2(CH_2)_2CH_2CH_2NH_2Cl$), 3.06 (2H, t, $^3J_{HH}$ 8.0, $PhCH_2NH_2ClCH_2$), 3.30-3.36 (2H, m, anthryl $CH_2NH_2ClCH_2Ar$), 4.22 (2H, s, benzyl $ArCH_2$), 5.33 (2H, s, anthryl CH_2Ar), 7.44-7.49 (3H, m, benzyl Ar*H*), 7.50-7.55 (2H, m, benzyl Ar*H*), 7.60 (2H, ddd, $^3J_{HH}$ 8.5, $^3J_{HH}$ 6.7, $^4J_{HH}$ 0.8, anthryl Ar*H*), 7.73 (2H, ddd, $^3J_{HH}$ 8.9, $^3J_{HH}$ 6.7, $^4J_{HH}$ 1.4, anthryl Ar*H*), 8.16 (2H, dd, $^3J_{HH}$ 8.5, $^4J_{HH}$ 1.1, anthryl Ar*H*), 8.43 (2H, dd, $^3J_{HH}$ 8.9, $^4J_{HH}$ 0.8, anthryl Ar*H*), 8.72 (1H, s, anthryl Ar*H*); δ_C PENDANT (75 MHz, MeOD) 27.2 (+), 27.3 (+), 27.4 (+), 27.5 (+), 44.6 (+), 49.9 (+), 52.8 (+), 124.6 (-), 127.0 (-), 129.3 (-), 130.7 (-), 131.07 (-),

131.10 (-), 131.42 (-), 131.44 (-), 132.1 (-), 132.7 (+), 133.3 (+); *m/z* (ES+) 397.2641 ($[M - 2Cl - H]^+$. $C_{28}H_{33}N_2$ requires 397.2638), (ES+) 397 (37%, [M - 2Cl - H]), 191 (100, $[M - PhCH_2NH_2Cl(CH_2)_6NH_2Cl]^+$).

4.3.5 Characterisation of Modular Diamine Intermediates **139**$_{(pyrene)}$-**143**$_{(2\text{-naphthalene})}$

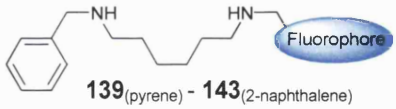

139$_{(pyrene)}$ - **143**$_{(2\text{-naphthalene})}$

139$_{(pyrene)}$ - **143**$_{(2\text{-naphthalene})}$

Nota Bene

For completeness Section 4.3.5 details the synthetic procedure employed by Arimori *et al.* in generating the modular diamine intermediates **139**$_{(pyrene)}$ - **143**$_{(2\text{-naphthalene})}$. The characterisation of intermediates **139**$_{(pyrene)}$ - **143**$_{(2\text{-naphthalene})}$ was undertaken by us from raw data previously collected. No material remained to carry out further analysis first hand.

General procedure for the preparation of compounds **139**$_{(pyrene)}$ - **143**$_{(2\text{-naphthalene})}$

N^1-benzylhexane-1,6-diamine **138** (1 eq.) and the required aldehyde (1.2 eq.) were stirred at room temperature for 7 hours under a nitrogen atmosphere in 1:1 methanol/tetrahydrofuran. Sodium borohydride (3.6 eq.) was then added to the solution prior to stirring at room temperature for 1 hour. The solvent was removed under reduced pressure and the residue dissolved in chloroform. The chloroform phase was washed with water, dried over magnesium sulfate and the solvent removed under reduced pressure. The residue was purified by gel filtration (Sephadex LH-20, methanol as eluent) to afford the required title compound **139**$_{(pyrene)}$ - **143**$_{(2\text{-naphthalene})}$.

_N_-benzyl-_N_-pyren-1-ylmethyl-hexane-1,6-diamine

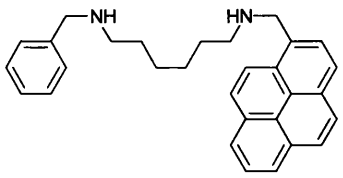

139$_{(pyrene)}$

Using a two step modification of the protocol laid out in the general procedure (page 224) and utilising: N^1-benzylhexane-1,6-diamine **138** (500 mg, 2.42 mmol), pyrene-1-carboxaldehyde (669 mg, 2.91 mmol), methanol (12 cm^3) and tetrahydrofuran (12 cm^3) the resulting intermediate imine, N^1-benzyl-N^6-((pyren-1-yl)methylene)hexane-1,6-diamine, was isolated in 940 mg (93%) yield. N^1-benzyl-N^6-((pyren-1-yl)-methylene)hexane-1,6-diamine (500 mg, 1.19 mmol) was reduced with sodium borohydride (230 mg, 6.08 mmol) and worked up as detailed above. The two step procedure afforded the title compound **139**$_{(pyrene)}$ as a yellow oil (468 mg, 86% overall); δ_H (300 MHz, $CDCl_3$) 1.21-1.34 (4H, m, $NH(CH_2)_2(CH_2)_2(CH_2)_2NH$), 1.41-1.47 (2H, m, phenyl $ArCH_2NHCH_2CH_2$), 1.49-1.57 (2H, m, pyrenyl $ArCH_2NHCH_2CH_2$), 2.55 (2H, t, $^3J_{HH}$ 7.2, phenyl $ArCH_2NHCH_2$), 2.75 (2H, t, $^3J_{HH}$ 7.4, pyrenyl $ArCH_2NHCH_2$), 3.75 (2H, s, phenyl $ArCH_2$), 4.50 (2H, s, pyrenyl $ArCH_2$), 7.15-7.25 (5H, m, phenyl Ar*H*), 7.95-8.10 (4H, m, pyrenyl Ar*H*), 8.15-8.22 (4H, m, pyrenyl Ar*H*), 8.37 (1H, app d, $^3J_{HH}$ 9.2, pyrenyl Ar*H*); δ_C (75 MHz, $CDCl_3$) 27.4, 30.2, 49.5, 50.0, 51.9, 54.1, 54.2, 123.2, 124.7, 125.0, 125.1, 125.9, 126.9, 127.0, 127.5, 127.6, 128.1, 128.4, 129.1, 131.3, 134.2; m/z (EI) 420 (89%, $[M]^+$), 329 (100, $[M - C_6H_5CH_2]^+$).

_N_-benzyl-_N_-phenanthren-9-ylmethyl-hexane-1,6-diamine

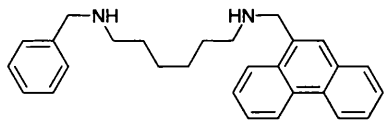

140$_{(phenanthrene)}$

Following the protocol laid out in the general procedure (page 224) and utilising: N^1-benzylhexane-1,6-diamine **138** (150 mg, 0.727 mmol), phenanthrene-9-carboxaldehyde (182 mg, 0.882 mmol), methanol (5 cm^3), tetrahydrofuran (5 cm^3) and sodium borohydride (100 mg, 2.64 mmol) the reaction afforded the title compound **140**$_{(phenanthrene)}$ as a yellow oil (209 mg, 73%); δ_H (300 MHz, $CDCl_3$) 1.25-1.51 (8H, m, $NHCH_2(CH_2)_4CH_2NH$), 2.59 (2H, t, $^3J_{HH}$ 7.2, phenyl $ArCH_2NHCH_2$), 2.75 (2H, t, $^3J_{HH}$ 7.2, phenanthryl $ArCH_2NHCH_2$), 3.75 (2H, s, phenyl $ArCH_2$), 4.24 (2H, s, phenanthryl $ArCH_2$), 7.20-7.34 (5H, m, phenyl Ar*H*), 7.53-7.63 (4H, m, phenanthryl Ar*H*), 7.71 (1H, s, phenanthryl Ar*H*), 7.84 (1H, app d, $^3J_{HH}$ 7.4, phenanthryl Ar*H*), 8.13-8.15 (1H, m, phenanthryl Ar*H*), 8.63 (1H, app d, $^3J_{HH}$ 8.2, phenanthryl Ar*H*), 8.68-8.71 (1H, m, phenanthryl Ar*H*); δ_C (75 MHz, $CDCl_3$) 27.7, 27.8, 30.4, 30.5, 49.7, 50.4, 52.4, 54.4, 122.7, 123.4, 124.5, 126.45, 126.51, 126.6, 126.86, 126.92, 127.1, 128.4, 128.58, 128.64, 130.3, 130.96, 131.13, 131.8, 134.4, 140.5.

_N_-anthracen-9-ylmethyl-_N_-benzyl-hexane-1,6-diamine

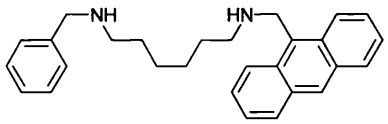

141$_{(anthracene)}$

Following the protocol laid out in the general procedure (page 224) and utilising: N^1-benzylhexane-1,6-diamine **138** (516 mg, 2.50 mmol), 9-anthraldehyde (620 mg, 3.01 mmol), methanol (12 cm^3), tetrahydrofuran (12 cm^3) and sodium borohydride (847 mg, 22.4 mmol) the reaction afforded the title compound **141**$_{(anthracene)}$ as a yellow oil (369 mg, 37%); δ_H (300 MHz, $CDCl_3$) 1.25-1.60 (8H, m, $NHCH_2(CH_2)_4CH_2NH$), 2.61 (2H, t, $^3J_{HH}$ 7.2, phenyl $ArCH_2NHCH_2$), 2.87 (2H, t, $^3J_{HH}$ 7.2, anthryl $ArCH_2NHCH_2$), 3.77 (2H, s, phenyl $ArCH_2$), 4.71 (2H, s, anthryl $ArCH_2$), 7.22-7.35 (5H, m, phenyl Ar*H*), 7.43-7.56 (4H, m, anthryl Ar*H*), 8.01 (2H, app d, $^3J_{HH}$ 7.7, anthryl Ar*H*), 8.34 (2H, app d, $^3J_{HH}$ 8.3, anthryl Ar*H*), 8.40 (1H, s, anthryl Ar*H*); δ_C (75 MHz, $CDCl_3$) 27.4, 30.1, 45.9, 49.5, 50.6, 54.1, 124.2, 124.9, 126.1, 126.9, 127.1, 128.1, 128.4, 129.2, 130.3, 131.6; *m/z* (EI) 396 (23%, $[M]^+$), 191 (100, $[M - C_6H_5CH_2NH(CH_2)_6NH]^+$).

***N*-benzyl-*N*-naphthalen-1-ylmethyl-hexane-1,6-diamine**

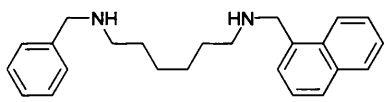

142$_{(1\text{-naphthalene})}$

Following the protocol laid out in the general procedure (page 224) and utilising: N^1-benzylhexane-1,6-diamine **138** (300 mg, 1.45 mmol), 1-naphthaldehyde (272 mg, 1.74 mmol), methanol (7 cm^3), tetrahydrofuran (7 cm^3) and sodium borohydride (197 mg, 5.21 mmol) the reaction afforded the title compound **142**$_{(1\text{-naphthalene})}$ as a yellow oil (388 mg, 77%); δ_H (300 MHz, $CDCl_3$) 1.27-1.39 (4H, m, $NH(CH_2)_2(CH_2)_2(CH_2)_2NH$), 1.47-1.58 (4H, m, $NHCH_2CH_2(CH_2)_2CH_2CH_2NH$), 2.61 (2H, t, $^3J_{HH}$ 7.2, phenyl $ArCH_2NHCH_2$), 2.73 (2H, t, $^3J_{HH}$ 7.2, naphthyl $ArCH_2NHCH_2$), 3.78 (2H, s, phenyl $ArCH_2$), 4.22 (2H, s, naphthyl $ArCH_2$), 7.12-7.33 (5H, m, phenyl Ar*H*), 7.40-7.54 (4H, m, naphthyl Ar*H*), 7.76 (1H, app d, $^3J_{HH}$ 7.8, naphthyl Ar*H*), 7.85 (1H, app d, $^3J_{HH}$ 8.2, naphthyl Ar*H*), 8.11 (1H, app d, $^3J_{HH}$ 8.6, naphthyl Ar*H*); δ_C (75 MHz, $CDCl_3$) 27.39, 27.42, 30.2, 49.5, 50.0, 51.7, 54.1, 123.5, 125.3, 125.4, 125.8, 125.9, 126.7, 127.5, 128.0, 128.2, 128.6, 133.7, 136.0.

N-Benzyl-N-naphthalen-2-ylmethyl-hexane-1,6-diamine

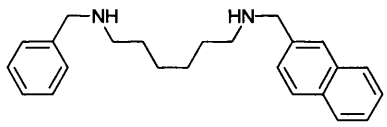

143$_{(2\text{-naphthalene})}$

Following the protocol laid out in the general procedure (page 224) and utilising: N^1-benzylhexane-1,6-diamine **138** (200 mg, 0.969 mmol), 2-naphthaldehyde (187 mg, 1.20 mmol), methanol (5 cm^3), tetrahydrofuran (5 cm^3) and sodium borohydride (136 mg, 3.60 mmol) the reaction afforded the title compound **143**$_{(2\text{-naphthalene})}$ as a yellow oil (468 mg, 54%); δ_H (300 MHz, $CDCl_3$) 1.25-1.54 (8H, m, $NHCH_2(CH_2)_4CH_2NH$), 2.58-2.67 (4H, m, $NCH_2(CH_2)_4CH_2NH$), 3.77 (2H, s, phenyl $ArCH_2$), 3.94 (2H, s, naphthyl $ArCH_2$), 7.21-7.32 (5H, m, phenyl Ar*H*), 7.43-7.47 (3H, m, naphthyl Ar*H*), 7.75 (1H, s, naphthyl Ar*H*), 7.79-7.82 (3H, m, naphthyl Ar*H*); δ_C (75 MHz, $CDCl_3$) 27.3, 29.5, 30.3, 49.5, 54.1, 125.5, 126.0, 126.4, 126.6, 126.8, 127.6, 127.7, 128.0, 128.1, 128.4, 129.1, 129.3, 132.6, 133.4, 138.1, 140.5; *m/z* (ES+) 347 (100%, $[M + H]^+$).

4.3.6 Characterisation of Modular Diboronic Acid Sensors **133**$_{(pyrene)}$-**137**$_{(2\text{-naphthalene})}$

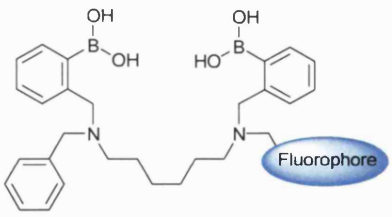

133$_{(pyrene)}$ - **137**$_{(2\text{-naphthalene})}$

Nota Bene

For completeness Section 4.3.6 details the synthetic procedure employed by Arimori *et al.* in generating the modular diboronic acid sensors **133**$_{(pyrene)}$ - **137**$_{(2\text{-naphthalene})}$. The characterisation of the modular diboronic acid sensors **133**$_{(pyrene)}$ - **137**$_{(2\text{-naphthalene})}$ was undertaken by us either from raw data previously collected or, where possible, directly from the original compounds themselves.

High Resolution Mass Spectra

The diboronic acid sensors **133**$_{(pyrene)}$ - **137**$_{(2\text{-naphthalene})}$ failed to show distinct molecular ion peaks when analysed by electron impact, chemical ionisation or fast atom bombardment mass spectrometry. The spectra generated displayed signals above the expected *m/z* value of the molecular ion peaks and when compound **133**$_{(pyrene)}$ was analysed up to a *m/z* of 2100 a clear molecular ion peak at 1375 was observed. This signal reflected the presence of a dimerised species and the molecular ion peak was found to match well with the theoretical isotope pattern for $[2M - H]^+$. On this basis a number of pseudo-molecular ion peaks of dimerised species have been ascribed. As the molecular weights of the observed peaks approached or exceeded 1200 Da in all cases, high resolution mass spectrometry was not undertaken.

General procedure for the preparation of compounds **133**$_{(pyrene)}$ - **137**$_{(2\text{-naphthalene})}$

A solution of compound **139**$_{(pyrene)}$ - **143**$_{(2\text{-naphthalene})}$ (1 eq.), potassium carbonate (4 eq.) and 2-(2-bromobenzyl)-1, 3-dioxaborinane (2.4 eq.) in dry acetonitrile (0.1 mol dm^{-3}) was heated under reflux, in a nitrogen atmosphere for 7 hours. The solvent was condensed under reduced pressure and the residue dissolved in chloroform. The chloroform phase was washed with water, dried over magnesium sulfate and the solvent

removed under reduced pressure. The residue was re-precipitated from chloroform in *n*-hexanes and dried *in vacuo* to afford the title compounds **133**$_{(pyrene)}$ - **137**$_{(2\text{-naphthalene})}$.

***N*-benzyl-*N*, *N*-bis-{2-borono-benzyl}-*N*-pyren-1-ylmethyl-1,6-diaminoalkane**

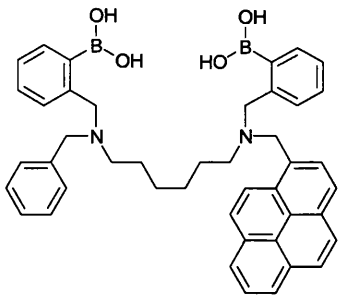

133$_{(pyrene)}$

Following the protocol laid out in the general procedure (page 230) and utilising: diamine **139**$_{(pyrene)}$ (291 mg, 0.423 mmol), 2-(2-bromobenzyl)-1,3,2-dioxaborinane (422 mg, 1.66 mmol), potassium carbonate (380 mg, 2.75 mmol) and dry acetonitrile (10 cm^3) the reaction afforded the title compound **133**$_{(pyrene)}$ as a yellow powder (162 mg, 34%); mp 165-168 °C, lit 165-168 °C;[192] Found: C, 76.6; H, 6.7; N, 3.8. $C_{44}H_{46}B_2N_2O_4$ requires C, 76.8; H, 6.7; N, 4.0%; δ_H (300 MHz, $CDCl_3$ with a few drop of MeOD) 1.25-1.55 (8H, m, $NHCH_2(CH_2)_4CH_2NH$), 2.21-2.30 (2H, m, phenyl $ArNHCH_2$), 2.44-2.53 (2H, m, pyrenyl $ArCH_2NHCH_2$), 3.47 (2H, s, $ArCH_2$), 3.61 (2H, s, $ArCH_2$), 3.89 (2H, s, $ArCH_2$), 4.23 (2H, s, $ArCH_2$), 7.06-7.42 (11H, m, Ar*H*), 7.79-8.23 (11H, m, Ar*H*); δ_C (75 MHz, $CDCl_3$ with a few drop of MeOD) 24.4, 24.8, 26.9, 27.1, 51.8, 53.2, 54.2, 57.1, 61.2, 62.0, 123.2, 124.7, 125.1, 125.3, 126.0, 127.3, 127.4, 127.5, 127.6, 128.4, 128.6, 129.6, 129.9, 130.1, 131.3, 131.3, 136.1, 141.6, 141.8; *m/z* (FAB) 1375 (21%, $[2M - H]^+$), 1243 (100, $[2M - CH_2C_6H_4B(OH)_2]^+$).

_N_-Benzyl-_N'_,_N'_-bis-[2-borono-benzyl]-_N'_-phenaththren-2-ylmethyl-hexamethylene-1,6-diamine

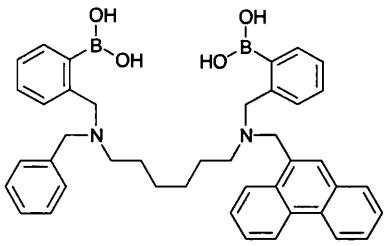

134$_{(phenanthrene)}$

Following the protocol laid out in the general procedure (page 230) and utilising: diamine **140**$_{(phenanthrene)}$ (150 mg, 0.378 mmol), 2-(2-bromobenzyl)-1,3,2-dioxaborinane (232 mg, 0.910 mmol), potassium carbonate (210 mg, 1.52 mmol) and dry acetonitrile (7 cm^3) the reaction afforded the title compound **134**$_{(phenanthrene)}$ as a yellow powder (136 mg, 54%); Found: C, 75.7; H, 6.9; N, 4.2. $C_{42}H_{46}B_2N_2O_4$ requires C, 75.9; H, 7.0; N, 4.2%; mp 162-165 °C; δ_H (300 MHz, $CDCl_3$ with a few drop of MeOD) 1.21-1.54 (8H, m, $NHCH_2(CH_2)_4CH_2NH$), 2.28-2.36 (2H, m, phenyl $ArCH_2NHCH_2$), 2.50-2.54 (2H, m, phenanthryl $ArCH_2NHCH_2$), 3.52-3.56 (2H, m, $ArCH_2$), 3.61-3.73 (2H, m, $ArCH_2$), 3.84 (2H, s, $ArCH_2$), 3.99 (2H, s, $ArCH_2$), 7.02-7.92 (20H, m, Ar*H*), 8.63-8.70 (2H, m, Ar*H*); δ_C (75 MHz, $CDCl_3$ with a few drop of MeOD) 24.5, 24.6, 27.0, 27.1, 53.6. 55.2, 57.1, 61.1, 62.0, 64.3, 122.3, 122.8, 124.6, 126.2, 126.3, 126.5, 127.1, 127.3, 128.2, 128.9, 129.3, 129.7, 129.8, 130.1, 130.4, 130.6, 130.7, 130.9, 131.0, 131.1, 135.7, 141.4; *m/z* (FAB) 1205 (100%, $[2(M - H) - C_6H_5B(OH)_2 - H]^+$)

_N_-anthracen-9-ylmethyl-_N_-benzyl-_N'_,_N'_-bis- [2-borono-benzyl]-hexamethylene-1,6-diamine

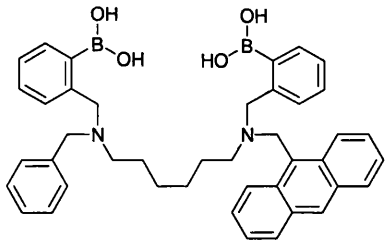

135(anthracene)

Following the protocol laid out in the general procedure (page 230) and utilising: diamine **141**(anthracene) (300 mg, 0.756 mmol), 2-(2-bromobenzyl)-1,3,2-dioxaborinane (465 mg, 1.82 mmol), potassium carbonate (420 mg, 3.04 mmol) and dry acetonitrile (20 cm^3) the reaction afforded the title compound **135**(anthracene) as a yellow powder (283 mg, 56%); Found: C, 75.7; H, 7.1; N, 4.3. $C_{42}H_{46}B_2N_2O_4$ requires C, 75.9; H, 7.0; N, 4.2%; mp 163-166 °C; δ_H (300 MHz, $CDCl_3$ with a few drop of MeOD) 1.26-1.46 (8H, m, $NHCH_2(CH_2)_4CH_2NH$), 2.26-2.35 (2H, m, phenyl $ArNHCH_2$), 2.43-2.49 (2H, m, anthryl $ArCH_2NHCH_2$), 3.55-4.19 (8H, m, $ArCH_2$), 7.12-7.47 (16H, m, Ar*H*), 7.80-8.14 (5H, m, Ar*H*), 8.42 (1H, s, Ar*H*); δ_C (75 MHz, $CDCl_3$ with a few drop of MeOD) 24.8, 25.9, 27.2, 27.4, 29.5, 50.0, 52.2, 54.6, 61.6, 124.9, 125.3, 125.8, 126.3, 127.7, 128.0, 128.4, 128.7, 128.9, 129.0, 129.5, 130.0, 130.6, 11.3, 131.7, 131.8, 136.5, 136.5, 136.7, 142.2; *m/z* (FAB with NBA as the matrix liquid) 1205 (8%, $[2(M - H) - C_6H_5B(OH)_2 - H]^+$), 388 (100, $[C_6H_5CH_2N(CH_2)CH_2C_6H_4B(OH)O\text{-}NBA - H]^+$).

N-benzyl-N',N-bis- (2-borono-benzyl)-N-naphthalen-1-ylmethyl-hexamethylene-1,6-diamine

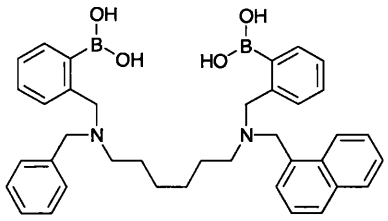

136(1-naphthalene)

Following the protocol laid out in the general procedure (page 230) and utilising: diamine **142**$_{(1\text{-naphthalene})}$ (250 mg, 0.721 mmol), 2-(2-bromobenzyl)-1,3,2-dioxaborinane (422 mg, 1.66 mmol), potassium carbonate (381 mg, 2.76 mmol) and dry acetonitrile (15 cm^3) the reaction afforded the title compound **136**$_{(1\text{-naphthalene})}$ as a yellow powder (207 mg, 47%); Found: C, 75.1; H, 7.3; N, 4.4. $C_{38}H_{44}B_2N_2O_4$ requires C, 74.3; H, 7.2; N, 4.6%; δ_H (300 MHz, $CDCl_3$ with a few drop of MeOD) 1.22-1.54 (8H, m, $NHCH_2(CH_2)_4CH_2NH$), 2.31-2.49 (4H, m, $NCH_2(CH_2)_2CH_2NH$), 3.56-3.97 (8H, m, $ArCH_2$), 7.24-7.45 (15H, m, Ar*H*), 7.74-7.90 (5H, m, Ar*H*); δ_C (75 MHz, $CDCl_3$ with a few drop of MeOD) 24.5, 24.6, 27.0, 27.1, 51.8, 53.3, 54.1, 57.1, 61.2, 61.8, 123.6, 125.0, 125.5, 125.7, 127.1, 127.27, 127.32, 128.0, 128.1, 128.2, 128.4, 129.4, 129.7, 129.8, 130.6, 131.0, 132.0, 132.5, 133.6, 135.7, 135.9, 136.2, 141.4.

_N_-Benzyl-_N'_,_N_-bis-(2-borono-benzyl)-_N_-naphthalen-2-ylmethyl-hexamethylene-1,6-diamine

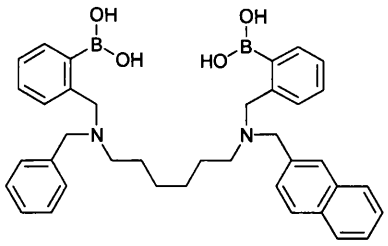

137$_{(2\text{-naphthalene})}$

Following the protocol laid out in the general procedure (page 230) and utilising: diamine **143**$_{(2\text{-naphthalene})}$ (400 mg, 1.15 mmol), 2-(2-bromobenzyl)-1,3,2-dioxaborinane (704 mg, 2.76 mmol), potassium carbonate (636 mg, 4.60 mmol) and dry acetonitrile (25 cm^3) the reaction afforded the title compound **137**$_{(2\text{-naphthalene})}$ as a yellow powder (390 mg, 55%); Found: C, 74.4; H, 7.1; N, 4.7. $C_{38}H_{44}B_2N_2O_4$ requires C, 74.3; H, 7.2; N, 4.6%; δ_H (300 MHz, $CDCl_3$ with a few drop of MeOD) 1.23-1.55 (8H, m, $NHCH_2(CH_2)_4CH_2NH$), 2.32-2.50 (4H, m, $NCH_2(CH_2)_4CH_2NH$), 3.53-3.82 (8H, m, $ArCH_2$), 7.14-7.49 (15H, m, Ar*H*), 7.68 (1H, s, Ar*H*), 7.79-7.89 (4H, m, Ar*H*); δ_C (75 MHz, $CDCl_3$ with a few drop of MeOD) 23.0, 24.8, 27.5, 31.9, 52.2, 52.4, 57.4, 57.8, 61.6, 61.7, 126.3, 126.5, 127.6, 127.7, 127.8, 128.0, 128.1, 128.6, 128.8, 128.9, 129.9, 130.27, 130.32, 131.18, 131.23, 136.8, 142.0; *m/z* (FAB) 1156 (100%, $[2(M + H) - C_6H_4 + H]^+$).

4.4 MOLECULAR TWEEZERS

4.4.1 Additional Intermediates *157-159* and *161*

N,*N*'-Bis(tert-butyl 6-aminohexylcarbamate)isophthalamide

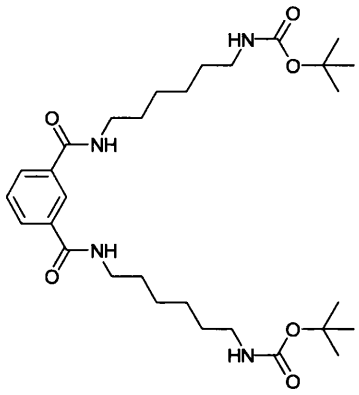

157

To a solution of *tert*-butyl 6-aminohexylcarbamate **3** (651 mg, 3.01 mmol) and triethylamine (0.40 cm^3, 2.85 mmol) in dry dichloromethane (50 cm^3) was added dropwise a solution of isophthaloyl dichloride (292 mg, 1.44 mmol) in dry dichloromethane (50 cm^3) at room temperature under an nitrogen atmosphere. The system was allowed to stir at room temperature for 4 hours and was then condensed under reduced pressure. The resulting powder was dissolved in dichloromethane (75 cm^3) and washed with water (3 × 30 cm^3). The organic phase was dried *in vacuo* to afford the title compound **157** as a cream powder (780 mg, 96%); mp 119 °C (dec); ν (KBr) 3353, 2976, 2937, 2868, 1683, 1634, 1520; δ_H (300 MHz, $CDCl_3$) 1.34 (26 H, s, $(CH_3)_2(CH_2)_2NHCOOC(CH_3)_3$), 1.37-1.46 (4H, m, $CH_2CH_2NHCOOC$), 1.54 (4H, tt, $^3J_{HH}$ 6.9, $^3J_{HH}$ 6.9, $CONHCH_2CH_2$), 3.06 (4H, t, $^3J_{HH}$ 6.5, $CH_2NHCOOC$), 3.37 (4H, dt, $^3J_{HH}$ 6.3, $^3J_{HH}$ 6.3, $CONHCH_2$), 4.62 (2H, br s, NHCOOC), 6.82 (2H, br s, CONH), 7.44 (1H, app t, $^3J_{HH}$ 7.7, ArH-5), 7.94 (2H, app dd, $^3J_{HH}$ 7.7, $^4J_{HH}$ 1.7, ArH-4/6), 8.21 (1H, app t, $^4J_{HH}$ 1.5 ArH-2); δ_H (300 MHz, MeOD) 1.32 (26 H, s, $(CH_3)_2(CH_2)_2NHCOO C(CH_3)_3$), 1.37-1.44 (4H, m, $CH_2CH_2NHCOOC$), 1.54 (4H, tt, $^3J_{HH}$ 7.2, $^3J_{HH}$ 7.2, $CONHCH_2CH_2$), 2.94 (4H, t, $^3J_{HH}$ 6.9, $CH_2NHCOOC$), 3.29 (4H, t, $^3J_{HH}$ 7.2, $CONHCH_2$), 7.45 (1H, app t, $^3J_{HH}$ 7.7, ArH-5), 7.85 (2H, app dd, $^3J_{HH}$ 7.7, $^4J_{HH}$ 1.7, ArH-4/6), 8.15 (1H, app t, $^4J_{HH}$ 1.5 ArH-2); δ_C PENDANT (75 MHz, $CDCl_3$) 26.0 (+), 26.3 (+), 28.8 (-), 29.6 (+), 30.4 (+), 39.9 (+), 40.3 (+), 79.6 (+), 125.3 (-), 129.3 (-),

130.7 (-), 135.1 (+), 156.8 (+), 167.1 (+); *m/z* (ES+) 563.3808 ($[M + H]^+$. $C_{30}H_{51}O_6N_4$ requires 563.3803), (ES+) 563 (100%, $[M + H]^+$).

N^2,N^3-Bis(6-aminohexyl)isophthalamide dihydrochloride

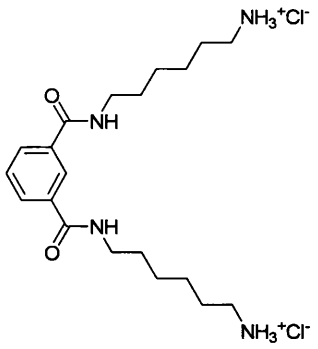

158

N^2,N^3-Bis(*tert*-butyl 6-aminohexylcarbamate)isophthalamide **157** (5.41 g, 9.61 mmol) was dissolved in a solution of hydrochloric acid (10 cm^3, S.G. 1.16, 32%), ethyl acetate (100 cm^3) and methanol (10 cm^3). The system was then stirred at room temperature for 30 minutes. The solution was condensed under reduced pressure using ethanol and then methanol to aid the removal of solvents azeotropically before drying the resulting product *in vacuo* to yield the title compound **158** as a cream powder (4.20 g, 100%); mp 241 °C (dec); ν (KBr) 3324, 2967, 2921, 2862, 1634, 1601, 1582, 1535; δ_H (300 MHz, MeOD) 1.43-1.51 (8H, m, $(CH_2)_2(CH_2)_2NH_2HCl$), 1.62-1.75 (8H, m, $CH_2(CH_2)_2CH_2$ CH_2NH_2HCl), 2.94 (4H, t, $^3J_{HH}$ 7.5, CH_2NH_2HCl), 3.42 (4H, t, $^3J_{HH}$ 7.2, $CONHCH_2$), 7.57 (1H, app t, $^3J_{HH}$ 7.8, Ar*H*-5), 7.97 (2H, app dd, $^3J_{HH}$ 7.8, $^4J_{HH}$ 1.8, Ar*H*-4/6), 8.31 (1H, app t, $^4J_{HH}$ 1.6 Ar*H*-2); δ_C PENDANT (75 MHz, MeOD) 27.4 (+), 27.8 (+), 28.9 (+), 30.6 (+), 41.1 (+), 41.2 (+), 127.7 (-), 130.3 (-), 131.6 (-), 136.6 (+), 169.8 (+); *m/z* (ES+) 363.2755 ($[M + H - 2HCl]^+$. $C_{20}H_{35}O_2N_4$ requires 363.2755), (ES+) 363 (100%, $[M + H - 2HCl]^+$).

N^1,N^1-bis[6-[(pyren-1-yl)methylamino]hexyl]isophthalamide dihydrochloride

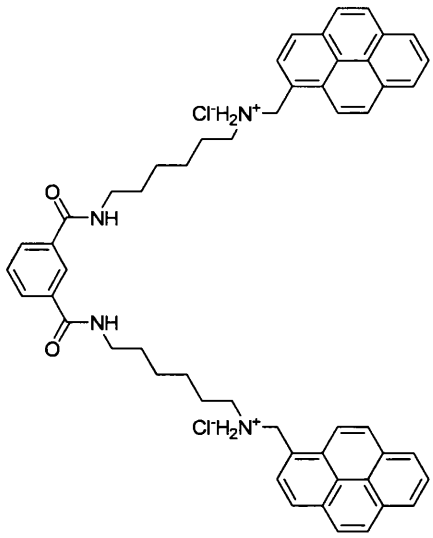

161

To a solution of N^2,N^3-bis(6-aminohexyl)isophthalamide dihydrochloride **158** (271 mg, 0.622 mmol) and caesium carbonate (192 mg, 0.589 mmol) in dry tetrahydrofuran (100 cm^3) and methanol (100 cm^3), pyrene-1-carboxaldehyde (328 mg, 1.43 mmol) was added and the system heated under reflux for 7 hours. The reaction mixture was cooled to 0 °C in an ice bath and sodium borohydride (165 mg, 4.36 mmol) added in portions. Stirring continued at room temperature for 2 hours before the careful addition of 1 M hydrochloric acid (10 cm^3). The solvents were removed under reduced pressure, prior to the extraction of the intermediate in dichloromethane (3 × 100 cm^3) from 0.5 M sodium hydroxide (100 cm^3), ensuring that any precipitate at the water/dichloromethane interface was drawn into the organic layer. To the recombined organic phases methanol (100 cm^3) was added. This was stirred to afford a clear solution, before being dried over magnesium sulfate, filtered and condensed under reduced pressure. The residue was dissolved in a solution of hydrochloric acid (10 cm^3, S.G. 1.16, 32%), methanol (50 cm^3) and dichloromethane (50 cm^3), then stirred for 30 minutes at room temperature. The solution was condensed under reduced pressure using ethanol and then methanol to aid the removal of solvents azeotropically before being dried *in vacuo*. The resulting salt was dissolved in the minimum amount of boiling, dry dichloromethane and then heated under reflux for 1 hour before allowing the system to cool to room temperature. The resulting suspension was slurried over a glass sinter, vacuum filtered and washed with dry dichloromethane (250 cm^3) prior to the removal of all solvent from the resulting

product *in vacuo* to afford the title compound **161** as a yellow powder (365 mg, 68%); mp 181 °C (onset, dec); ν (KBr) 2931, 2782, 1634, 1540, 847; δ_H (300 MHz, MeOD) 1.35-1.53 (8H, br m, (C*H*$_2$)$_2$(CH$_2$)$_2$NHCH$_2$), 1.59-1.71 (4H, br m, C*H*$_2$CH$_2$NHCH$_2$), 1.75-1.87 (4H, br m, CONHCH$_2$C*H*$_2$), 3.23 (4H, br t, $^3J_{HH}$ 8.0, C*H*$_2$NHCH$_2$Ar), 3.40 (4H, br t, $^3J_{HH}$ 7.0, CONHC*H*$_2$), expected signal at approximately 4.9 ppm masked by the residual water in the MeOD, 7.55 (1H, app t, $^3J_{HH}$ 7.8, isophthalamido Ar*H*-5), 7.96 (2H, app dd, $^3J_{HH}$ 7.7, $^4J_{HH}$ 1.7, isophthalamido Ar*H*-4/6), 8.01-8.31 (16H, m, pyrenyl Ar*H*), 8.32-8.34 (1H, m, isophthalamido Ar*H*-2), 8.36-8.43 (2H, m, pyrenyl Ar*H*); δ_H (300 MHz, DMSO) 1.26-1.41 (8H, br m, (C*H*$_2$)$_2$(CH$_2$)$_2$NHCH$_2$), 1.48-1.59 (4H, br m, C*H*$_2$CH$_2$NHCH$_2$), 1.67-1.79 (4H, br m, CONHCH$_2$C*H*$_2$), 3.04-3.14 (4H, br m, C*H*$_2$NHCH$_2$Ar), 3.20-3.29 (4H, br m, CONHC*H*$_2$), 4.90 (4H, br s, NHC*H*$_2$Ar) 7.52 (1H, app t, $^3J_{HH}$ 7.7, isophthalamido Ar*H*-5), 7.96 (2H, app dd, $^3J_{HH}$ 7.7, $^4J_{HH}$ 1.7, isophthalamido Ar*H*-4/6), 8.07-8.56 (18H, m, pyrenyl Ar*H*), 8.69 (1H, br app t, $^4J_{HH}$ 5.6, isophthalamido Ar*H*-2), 9.28 (2H, br s, CON*H*); δ_C (75 MHz, DMSO) 25.7, 26.2, 26.3, 29.2, expected signal at approximately 40 ppm masked by DMSO, 47.3, 47.5, 123.6, 124.0, 124.2, 125.1, 126.0, 126.05, 126.10, 126.2, 126.5, 126.9, 127.6, 128.5, 128.6, 129.5, 129.7, 130.0, 130.5, 131.0, 131.7, 135.1, 166.1; *m/z* (ES+) 791.4327 ([M + H - 2HCl]$^+$. $C_{54}H_{55}O_2N_4$ requires 791.4320), (ES+) 792 (100%, [M + H - 2HCl]$^+$).

***N*,*N*'-bis[6-{[(pyren-1-yl)methylamino]hexyl}isophthalamide**

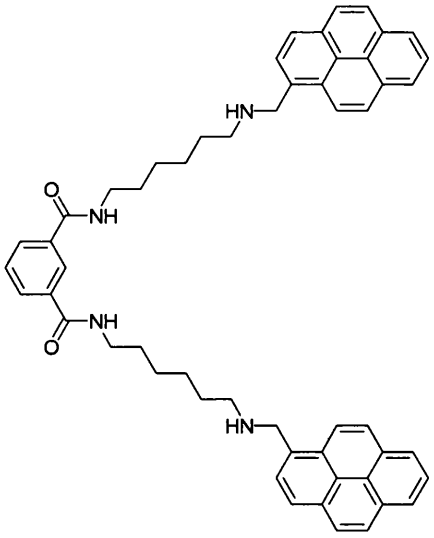

159

To confirm formation of compound **161** the intermediate amine base **159** was isolated as a cream powder and characterised; R_f (10:90 MeOH/DCM) 0.25; ν (KBr) 3285, 3037, 2925, 2852, 1634, 1538, 841; δ_H (300 MHz, $CDCl_3$) 1.13-1.24 (8H, br m, $CONH(CH_2)_2(CH_2)_2(CH_2)_2NHCH_2$), 1.34-1.46 (8H, br m, $CONHCH_2CH_2(CH_2)_2CH_2CH_2NHCH_2$), 2.07 (2H, br s, $NHCH_2Ar$), 2.62 (4H, t, $^3J_{HH}$ 7.2, CH_2NHCH_2Ar), 3.24 (4H, dt, $^3J_{HH}$ 6.7, $^3J_{HH}$ 6.7, $CONHCH_2$), 4.33 (4H, s, $NHCH_2Ar$), 6.56 (2H, t, $^3J_{HH}$ 5.7, $CONHCH_2$), 7.26 (1H, app t, $^3J_{HH}$ 7.7, isophthalamido Ar*H*-5), 7.72 (2H, app dd, $^3J_{HH}$ 7.8, $^4J_{HH}$ 1.8, isophthalamido Ar*H*-4/6), 7.84-7.92 (8H, m, pyrenyl Ar*H*), 7.96-8.07 (8H, m, pyrenyl Ar*H*), 8.11 (1H, app t, $^4J_{HH}$ 1.6 isophthalamido Ar*H*-2), 8.16-8.22 (2H, m, pyrenyl Ar*H*); δ_C PENDANT (75 MHz, $CDCl_3$) 27.1 (-), 27.2 (-), 29.75 (-), 29.76 (-), 30.1 (-), 40.3 (-), 40.4 (-), 50.0 (-), 51.9 (-), 123.4 (+), 125.1 (+), 125.2 (-), 125.35 (-), 125.42 (+), 125.5 (+), 125.6 (+), 126.3 (+), 127.4 (+), 127.5 (+), 127.8 (+), 128.1 (+), 129.1 (+), 129.4 (-), 130.3 (+), 131.1 (-), 131.2 (-), 131.7 (-), 133.8 (-), 135.16 (-), 135.18 (-), 167.06 (-), 167.13 (-); *m/z* (ES+) 791.4321 ($[M + H]^+$. $C_{54}H_{55}O_2N_4$ requires 791.4320), (ES+) 792 (100%, $[M + H]^+$).

4.4.2 Molecular Tweezers **162**

N,N'-bis[6-[N,N'-[2-boronobenzyl]- N,N'-[[pyren-1- yl]methyl]amino]hexyl]iso-phthalamide

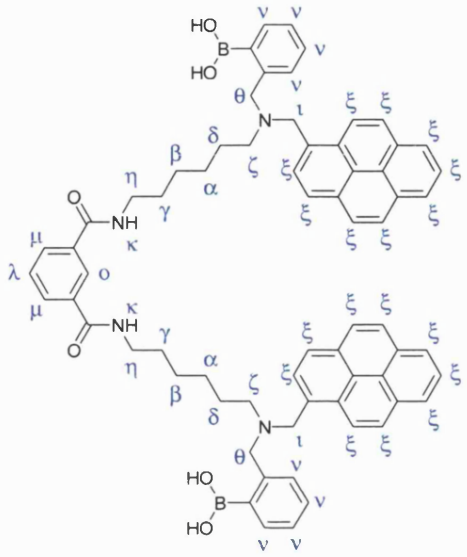

162

To a solution of the ammonium hydrochloride salt **161** (157 mg, 0.181 mmol) in tetrahydrofuran (100 cm^3) and acetonitrile (100 cm^3) was added an excess of potassium carbonate (494 mg, 3.57 mmol). The solution was stirred for 10 minutes before 2-(2-(bromomethyl)phenyl)-5,5-dimethyl-1,3,2-dioxaborinane (175 mg, 0.618 mmol) was added and the system heated under reflux for 2 days. The solvent was removed under reduced pressure. To the residue was added water (50 cm^3) which was adjusted to, and maintained at, pH ~ 7 with hydrochloric acid (1 M). From this aqueous layer the required intermediate was extracted into dichloromethane (3 × 50 cm^3). The organic phases were recombined and the solvent removed under reduced pressure. The resulting oil was purified by flash column chromatography on silica gel (methanol/dichloromethane, gradient elution: loading with a 3:97 ratio and incrementing the percentage methanol until a 90:10 ratio was obtained). The desired fractions were re-condensed and dried *in vacuo* to afford the title compound **162** as a yellow powder (27.2 mg, 14%). δ_H (400 MHz, $CDCl_3$ with a few drops of MeOD) 1.00 (4H, tt, $^3J_{HH}$ 7.1, $^3J_{HH}$ 7.1, $CH_2(\alpha)$), 1.10 (4H, tt, $^3J_{HH}$ 7.4, $^3J_{HH}$ 7.4, $CH_2(\beta)$), 1.31 (4H, tt, $^3J_{HH}$ 7.3, $^3J_{HH}$ 7.3, $CH_2(\gamma)$), 1.47 (4H, tt, $^3J_{HH}$ 7.7, $^3J_{HH}$ 7.7, $CH_2(\delta)$), 2.46 (4H, t, $^3J_{HH}$ 7.9,

$CH_2CH_2N(\zeta)$), 3.16 (4H, t, $^3J_{HH}$ 7.2, $CONHCH_2(\eta)$), 3.82 (4H, s, $NHCH_2Ar(\theta)$), 4.16 (4H, s, $NHCH_2Ar(\iota)$), 7.22-7.38 (9H, m, phenyl Ar*H*(ν) and isophthalamido Ar*H*-5(λ)), 7.75 (2H, app dd, $^3J_{HH}$ 7.7, $^4J_{HH}$ 1.7, isophthalamido Ar*H*-4/6(μ)), 7.87-8.08 (19H, m, pyrenyl Ar*H*(ξ) and isophthalamido Ar*H*-2(o)); δ_C PENDANT (100 MHz, $CDCl_3$ with a few drops of MeOD) 24.8 (-, $CH_2(\delta)$), 26.4 (-, $CH_2(\beta)$), 26.9 (-, $CH_2(\alpha)$), 29.1(-, $CH_2(\gamma)$), 39.8 (-, $CH_2(\eta)$), 39.9 (-, $CH_2(\eta)$), 53.1 (-, $CH_2(\zeta)$), 54.3 (-, $CH_2(\iota)$), 62.0 (-, $CH_2(\theta)$), 123.1 (+), 124.5 (+), 124.6 (-), 124.8 (-), 125.0 (+), 125.16 (+), 125.23 (+), 125.8 (+), 127.29 (+), 127.34 (+), 127.4 (+), 128.5 (+), 128.7 (+), 129.7 (+), 129.8 (-), 130.0 (+), 130.4 (-), 130.6 (-), 130.8 (-), 131.1 (+), 134.8 (-), 136.0 (+), 141.6 (-), 166.77 (-, *C*O), 166.84 (-, *C*O); *m/z* (ES+ in MeOH/DCM following exposure to MeOD/$CDCl_3$) 1063.5132 ($[M - 4H + 4D + H]^+$. $C_{68}H_{65}D_4O_6N_4B_2$ requires 1063.5649), (ES+ in MeOH/DCM following exposure to MeOD/$CDCl_3$) 1077 (100%, $[M + MeOH - H_2O + 3D - 3H]^+$), 1023 (85%, $[M - 2H_2O]$), 1091 (69%, $[M + 2MeOH - 2H_2O + 2D - 2H]$), 1063 (68%, $[M + 4D - 4H]$).

4.5 FLUORESCENCE MEASUREMENTS

Buffer and Solvents

The fluorescence titrations of the diboronic acid sensors **133**$_{(pyrene)}$ - **137**$_{(2\text{-naphthalene})}$ and monoboronic acid reference compounds **128**$_{(pyrene)}$ - **132**$_{(2\text{-naphthalene})}$ with different saccharides were carried out in a pH 8.21 aqueous methanolic buffer. The buffer was prepared according to the literature method of Perrin and Dempsey[193] and contained: 52.1wt% HPLC grade methanol in deionised water with KCl, 0.01000 mol dm^{-3}, KH_2PO_4, 0.002752 mol dm^{-3} and Na_2HPO_4, 0.002757 mol dm^{-3}. When not in use the buffer was stored in the dark at 4 °C, with the solution being allowed time to return to room temperature before each use.

Fluorescence Titrations

In each instance the required sensor was weighed out in a small volumetric flask. The sample was then made up to the required volume with HPLC grade methanol to generate a stock solution of known molarity. 50 μL of the stock solution were then transferred *via* microsyringe to a beaker containing a known volume of the stirred pH 8.21 aqueous methanolic buffer (the buffer was transferred by pipette). This method therefore generated a solution of known molarity (with a typical volume of 50 cm^3 or 100 cm^3).*****

The concentrations used for each particular diboronic acid sensor **133**$_{(pyrene)}$ - **137**$_{(2\text{-naphthalene})}$ in solution were matched when evaluating the analogous monoboronic acid reference compound **128**$_{(pyrene)}$ - **132**$_{(2\text{-naphthalene})}$ bearing the same fluorophore. For clarity the concentrations used and emission and excitation wavelengths used in these studies are reported in Table 10.

***** Worked example: 9.2 mg (15 μmol) of the diboronic acid sensor **137**$_{(2\text{-naphthalene})}$ was weighed out and made up to 3 cm^3 in HPLC grade methanol to generate a 5 mM stock solution. 50 μL (250 nmol) of this stock solution were then syringed into 100 cm^3 of stirred pH 8.21 aqueous methanolic buffer. This procedure therefore afforded a 2.5 μM solution of the diboronic acid sensor **137**$_{(2\text{-naphthalene})}$ in pH 8.21 aqueous methanolic buffer.

Table 10. Fluorescence measurement conditions

fluorophore	concentration / mol dm^{-3}	λ_{ex} / nm	λ_{em} / nm
pyrene	$1.0\ 10^{-6}$	342	397
phenanthrene	5.0×10^{-6}	299	369
anthracene	1.0×10^{-6}	370	420
1-naphthalene	2.5×10^{-6}	275	335
2-naphthalene	2.5×10^{-6}	274	335

Fluorescence spectra were recorded as increasing amounts of solid saccharide (D-glucose, D-galactose, D-fructose and D-mannose) were added to the stirred sensor solutions. Typically the fluorescence response was evaluated over a saccharide concentration range from 0 to 0.1 mol dm^{-3}.

Data Analysis

Data was collected *via* the Perkin-Elmer FL Winlab software package on a PC running a Microsoft Windows graphical user interface. The observed stability constants (K_{obs}) with coefficient of determination (r^2) were calculated by the fitting of emission intensity *versus* saccharide concentration using custom written non-linear (Levenberg-Marquardt algorithm) curve fitting.[182] The data collected for the diboronic acids **133**$_{(pyrene)}$ - **137**$_{(2\text{-}naphthalene)}$ and monoboronic acid reference compounds **128**$_{(pyrene)}$ - **132**$_{(2\text{-}naphthalene)}$ tabulated above, Section 3.5.1, see page 158.

CHAPTER FIVE: Conclusions

All we have to decide is what to do with the time that is given us.

John R. R. Tolkein

The Lord of the Rings: The Fellowship of the Ring

5 Conclusions

It remains the case that many of the finer details regarding the precise mode of action by which boronic acid based fluorescent PET sensors function have not been fully elucidated. The nature of the nitrogen – boron interaction for instance, or the rate determining step and transition state involved in boronate anion – diol complexation are still unknown. Nevertheless, since the first publication on glucose selective diboronic acid based PET sensors a decade ago, these systems have proved their worth and have come to find application at the cutting edge of medical care.

Despite the proven importance of these sensors and the burgeoning potential they currently hold, the organic synthesis of these compounds appears to have relied heavily on a piecemeal approach with most researchers in the field developing their own individual purification methods to find ways around the obtuse handling properties of these compounds on a case-by-case basis.

In this thesis, following an introduction of the contemporary scientific understanding of these systems and a selective literature review on published sensors, we have documented the development of a generally applicable and readily accessible synthetic strategy to allow boronic acid based fluorescent PET sensors to be isolated with exacting levels of purity.

The design strategy implemented takes advantage of protecting group chemistry to afford intermediate amines functionalised to suit the needs of the researcher. With this approach the ammonium hydrochloride salts of the penultimate compounds in the reaction sequence can be generated, permitting formation of boronic acid sensors to occur from scrupulously purified and entirely stable precursors.

The design strategy discussed was developed during the synthesis of a library of di-boronic acid based fluorescent PET sensors **133**$_{(pyrene)}$ - **137**$_{(2\text{-naphthalene})}$ with varied fluorophore sub-units and their respective monoboronic acid reference compounds **128**$_{(pyrene)}$ - **132**$_{(2\text{-naphthalene})}$. Having established both a design strategy and a practical laboratory protocol for the construction of these compounds the applicability of the approach to other boronic acid based fluorescent PET sensors was evaluated.

The structure of a desired boronic acid based fluorescent PET sensor with carefully considered dimensions and containing specific functionality was drafted. Using the design strategy and synthetic protocols established, the synthesis of the molecular tweezers **162** was undertaken.

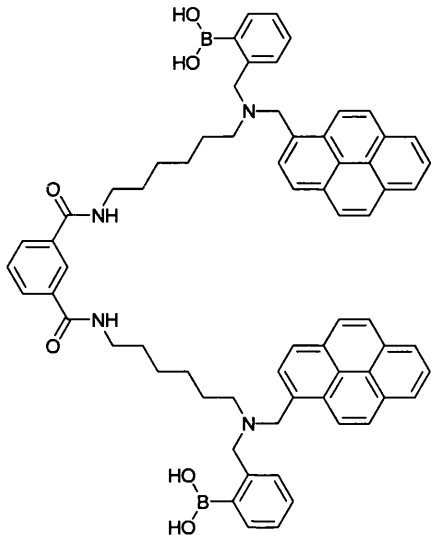

162

The direct isolation of compound **162** confirmed the versatility of our approach. The methodology permitted synthetic routes to be rationally designed and the synthetic assembly to proceed through robust and readily accessible synthetic procedures. The approach afforded target molecules with high levels of purity *via* efficient hierarchical routes and as such has been shown to provide an effective and generally applicable method for the construction of fluorescent PET sensors containing the *N*-methyl-*o*-(aminomethyl)phenylboronic acid fragment.

Future Work: Modular Sensors

From the fluorescence evaluation of the modular diboronic acid sensors **133**$_{(pyrene)}$ - **137**$_{(2\text{-naphthalene})}$ and their analogous monoboronic acid reference compounds **128**$_{(pyrene)}$ - **132**$_{(2\text{-naphthalene})}$ it has became apparent that D-galactose selectivity can be obtained with the use of 1- and 2- naphthalene. It is also the case, from the studies undertaken on linker length dependence, that D-galactose selectivity can be introduced into these modular systems through the use of heptamethylene and octamethylene linkers. In view of these observations the logical course of action is to combine the moieties from the

two most promising results (2-naphthalene and octamethylene diamine) and construct a modular sensor containing both. Such a system could be readily constructed utilising our synthetic approach (as could any other analogous species) and would provide further valuable information on differentiating between D-glucose and D-galactose in these systems.

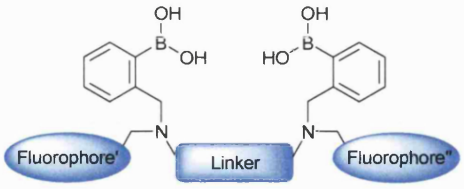

Figure 71. *Generic template of the diboronic acid modular sensors with a variable linker unit and one or two fluorophore units.*

Future Work: Diboronic Acid Molecular Tweezers

With the synthesis of molecular tweezers **162** complete, the fluorescence evaluation of these species must be undertaken. These tweezers were designed, and have the potential to be D-glucose selective, however, selectivity is an attribute which will be empirically determined and the conformational flexibility introduced by the two arms of the tweezers may provide some interesting results. Whilst the arms may provide an enlarged binding pocket it should be recalled from our previous results that only the terminal saccharide ring appears to participate significantly in the complexation of di-boronic acids with di- and higher saccharides. Nonetheless, the selectivity demonstrated by the sensor Figure 41 (**f**), page 112, for particular tetrasaccharides means that a broad range of possible guest molecules should be screened.

If the conformationally flexible binding pocket of these molecular tweezers proves to be successful then the ability to further tune saccharide specificity can be readily undertaken. The energy transfer process between phenanthrene and pyrene in sensor $\mathbf{117}_{(\text{phenanthrene-pyrene})}$, page 106, proved particularly effective in refining the recognition event and the use of non-equivalent fluorophores can be readily envisaged in the modified molecular tweezers **164**.

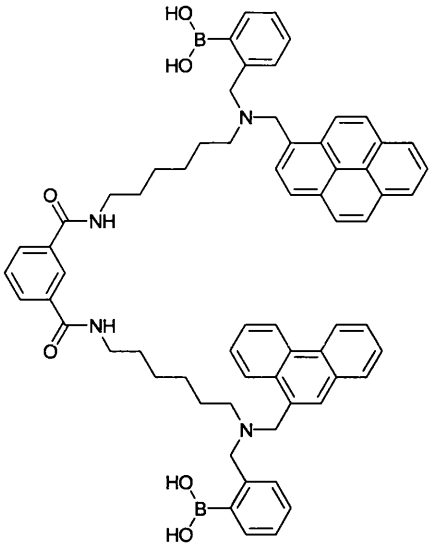

164

Derivatised Systems

The molecular tweezers **162** were developed around the isophthalamide core with a number of future studies in mind. Functionality introduced at the isophthalamido Ar*H*-5 position could see the attachment of a chiral group or the placement of the sensor on to a polymer support. With the recent acquisition of a flow cytometer by the T. D. James research group, the use of polymer supported sensors could lead to the mass screening of sensors against vast arrays of potential guest species.

Under conditions of increased concentration the possibility of intermolecular interactions occurring between the isophthalamide cores of compound **162** has the potential to interdigitate two molecular tweezers. As reported by Leigh and co-workers rotation of one of the tweezers' amide carbonyl groups such that it lies within the binding pocket of a second pair of tweezers would see it interact with the host's amide NH groups (it should be recalled that the presence of *trans*/*trans* and *cis*/*trans* amide rotamers has been confirmed in the ^{13}C NMR spectra of the molecular tweezers **162**). If this interdigitated conformation were to be adopted, it is possible that ring closure could be mediated under saccharide control to afford mechanically interlinked catenane rings.

CHAPTER SIX:
Bibliography

I must go down to the seas again to the lonely sea and the sky,
And all I ask is a tall ship and a star to steer her by

John Masefield

Sea Fever

6 Bibliography

1 G. R. Desiraju, *Nature*, 2001, **412**, 397-400.

2 T. Frängsmyr and B. G. Malmström, 'Nobel Lectures in Chemistry (1981-1990)', Nobel Lectures, World Scientific, 1992.

3 A. P. de Silva, H. Q. N. Gunaratne, T. Gunnlaugsson, A. J. M. Huxley, C. P. McCoy, J. T. Rademacher, and T. E. Rice, *Chem. Rev.*, 1997, **97**, 1515-1566.

4 A. W. Czarnik, 'Fluorescent Chemosensors for Ion and Molecule Recognition', Acs Symposium Series 538, American Chemical Society Books, 1993.

5 M. D. Phillips and T. D. James, *J. Fluorescence*, 2004, **14**, 549-559.

6 A. P. Davis and R. S. Wareham, *Angew. Chem., Int. Ed.*, 1999, **38**, 2978-2996.

7 R. Jelinek and S. Kolusheva, *Chem. Rev.*, 2004, **104**, 5987-6015.

8 T. D. James and S. Shinkai, 'Artificial Receptors as Chemosensors for Carbohydrates' in 'Host-Guest Chemistry. Mimetic Approaches to Study Carbohydrate Recognition', p 159-200, ed. S. Penadés, Springer-Verlag GmbH, 2002.

9 A. P. Davis and T. D. James, 'Carbohydrate Receptors' in 'Functional Synthetic Receptors', p 45-110, ed. T. Schrader and A. D. Hamilton, Wiley-VCH, 2005.

10 T. D. James, 'Boronic Acids Based Receptors and Sensors for Saccharides' in 'Boronic Acids in Organic Synthesis and Chemical Biology', p 441-480, ed. D. G. Hall, Wiley-VCH, 2005.

11 P. M. Collins and R. J. Ferrier, 'Monosaccharides: Their Chemistry and Their Roles in Natural Products', John Wiley & Sons Ltd, 1995.

12 R. H. Garrett and C. M. Grisham, 'Biochemistry', 2nd edition, Saunders College Publishing, 1999.

13 R. A. Dwek and T. D. Butters, *Chem. Rev.*, 2002, **102**, 283-284 (and succeeding articles).

14 T. Yamamoto, Y. Seino, H. Fukumoto, G. Koh, H. Yano, N. Inagaki, Y. Yamada, K. Inoue, T. Manabe, and H. Imura, *Biochem. Biophys. Res. Commun.*, 1990, **170**, 223-230.

15 P. Baxter, J. Goldhill, P. T. Hardcastle, and C. J. Taylor, *Gut.*, 1990, **31**, 817-820.

16 S. de Marchi, E. Cecchin, A. Basil, G. Proto, W. Donadon, A. Jengo, D. Schinella, A. Jus, D. Villalta, P. De Paoli, G. Santini, and F. Tesio, *J. Nephrol.*, 1984, **4**, 280-286.

17 L. J. Elsas and L. E. Rosenberg, *J. Clinic. Invest.*, 1969, **48**, 1845-1854.

18 S. Wild, G. Roglic, A. Green, R. Sicree, and H. King, *Diabetes Care*, 2004, **27**, 1047-1053.

19 S. P. Marso (Editor), 'The Handbook of Diabetes Mellitus and Cardiovascular Disease', Remidica Publishing, 2003.

20 T. Barnett, 'The Insulin Treatment of Diabetes: A Practical Guide', EMAP Healthcare, 1998.

21 The British Diabetic Association Cohort Study, *Diabet. Med.*, 1999, **16**, 459-465.

22 I. M. Stratton, E. M. Kohner, S. J. Aldington, R. C. Turner, R. R. Holman, S. E. Manley, and D. R. Matthews, *Diabetologia*, 2001, **44**, 156-163.

23 J. S. Cameron and S. Challah, *Lancet*, 1986, **2**, 962-966.

24 D. S. Bell, *Diabetes Care*, 1994, **17**, 213-219.

25 D. E. Bild, J. V. Selby, P. Sinnock, W. S. Browner, P. Braveman, and J. A. Showstack, *Diabetes Care*, 1989, **12**, 24-31.

26 Department of Health: London, 'National Service Framework for Diabetes: One Year On', 2004.

27 W. Gatling, R. Hill, and M. Kirby, 'Shared Care for Diabetes', Isis Medical Media, 1997.

28 Collaborative Atorvastatin Diabetes Study, *Lancet*, 2004, **364**, 685-696.

29 The Epidemiology of Diabetes Interventions and Complications Study, *J. Am. Med. Assoc.*, 2003, **290**, 2159-2167.

30 The Diabetes Control and Complications Trial Research Group, *N. Engl. J. Med.*, 1993, **329**, 977-986.

31 P. M. Collins, 'Carbohydrates', Chapman and Hall, 1987.

32 S. J. Angyal, *Adv. Carbohydr. Chem. Biochem.*, 1991, **49**, 19-35.

33 N. K. Vyas, M. N. Vyas, and F. A. Quiocho, *Science*, 1988, **242**, 1290-1295.

34 D. C. Harris, 'Quantitative Chemical Analysis', 6th edition, Freeman, 2003.

35 R. W. Cattrall, 'Chemical Sensors', Oxford Chemistry Primers, Oxford University Press, 1997.

36 A. P. F. Turner, B. N. Chen, and S. A. Piletsky, *Clin. Chem.*, 1999, **45**, 1596-1601.

37 S. Striegler, *Curr. Org. Chem.*, 2003, **7**, 81-102.

38 Y. Aoyama, Y. Tanaka, H. Toi, and H. Ogoshi, *J. Am. Chem. Soc.*, 1988, **110**, 634-635.

39 A. P. Davis and R. S. Wareham, *Angew. Chem., Int. Ed.*, 1998, **37**, 2270-2273.

40 G. Das and A. D. Hamilton, *Tetrahedron Lett.*, 1997, **38**, 3675-3678.

41 S. Anderson, U. Neidlein, V. Gramlich, and F. Diederich, *Angew. Chem.-Int. Edit. Engl.*, 1995, **34**, 1596-1600.

42 U. Neidlein and F. Diederich, *Chem. Commun.*, 1996, 1493-1494.

43 A. S. Droz, U. Neidlein, S. Anderson, P. Seiler, and F. Diederich, *Helv. Chem. Acta*, 2001, **84**, 2243-2289.

44 E. Frankland and B. F. Duppa, *Justus Liebigs Ann. Chem.*, 1860, **115**, 319-322.

45 A. Michaelis and P. Becker, *Ber. Dtsch. Chem. Ges.*, 1880, **13**, 58-61.

46 A. Michaelis and P. Becker, *Ber. Dtsch. Chem. Ges.*, 1882, **15**, 180-185.

47 E. Khotinsky and M. Melamed, *Ber. Dtsch. Chem. Ges.*, 1909, **42**, 3090-3096.

48 J. Böeseken, *Adv. Carbohydr. Chem.*, 1949, **4**, 189-210.

49 J. Böeseken, *Ber.*, 1913, **46**, 2612-2628.

50 H. G. Kuivila, A. H. Keough, and E. J. Soboczenski, *J. Org. Chem.*, 1954, **19**, 780-783.

51 M. I. Wolfrom and J. Solms, *J. Org. Chem.*, 1956, **21**, 815 - 816.

52 M. F. Lappert, *Chem. Rev.*, 1956, **56**, 959-1064.

53 K. Torssel, *Arkiv. Kemi.*, 1957, **10**, 473.

54 J. P. Lorand and J. O. Edwards, *J. Org. Chem.*, 1959, **24**, 769-774.

55 J. H. Hartley, M. D. Phillips, and T. D. James, *New J. Chem.*, 2002, **26**, 1228-1237.

56 S. Soundararajan, M. Badawi, C. M. Kohlrust, and J. H. Hageman, *Anal. Biochem.*, 1989, **178**, 125-134.

57 G. Springsteen and B. H. Wang, *Tetrahedron*, 2002, **58**, 5291-5300.

58 A. Yuchi, A. Tatebe, S. Kani, and T. D. James, *Bull. Chem. Soc. Jpn.*, 2001, **74**, 509-510.

59 J. Juillard and N. Gueguen, *Comp. Rend. Acad. Sci. C*, 1967, **264**, 259-261.

60 S. Friedman, B. Pace, and R. Pizer, *J. Am. Chem. Soc.*, 1974, **96**, 5381-5384.

61 J. O. Edwards and R. J. Sederstrom, *J. Phys. Chem.*, 1961, **65**, 862-862.

62 L. I. Bosch, T. M. Fyles, and T. D. James, *Tetrahedron*, 2004, **60**, 11175-11190.

63 A. E. Martell and R. M. Smith, 'Critical Stability Constants', Plenum Press, 1976.

64 N. DiCesare and J. R. Lakowicz, *Anal. Biochem.*, 2001, **294**, 154-160.

65 S. Friedman and R. Pizer, *J. Am. Chem. Soc.*, 1975, **97**, 6059-6062.

66 R. Pizer and R. Selzer, *Inorg. Chem.*, 1983, **23**, 3023.

67 K. Kustin and R. Pizer, *J. Am. Chem. Soc.*, 1969, **91**, 317-322.

68 L. Babcock and R. Pizer, *Inorg. Chem.*, 1980, **19**, 56-61.

69 R. Pizer and C. Tihal, *Inorg. Chem.*, 1992, **31**, 3243-3247.

70 R. J. Ferrier, *Adv. Carbohydr. Chem. Biochem.*, 1978, **35**, 31-80.

71 S. J. Rettig and J. Trotter, *Can. J. Chem.*, 1977, **55**, 3071-3075.

72 P. Rodriguez-Cuamatzi, G. Vargas-Diaz, T. Maris, J. D. Wuest, and H. Hoepfl, *Acta Cryst.*, 2004, **E60**, o1316-o1318.

73 J. H. Fournier, T. Maris, J. D. Wuest, W. Z. Guo, and E. Galoppini, *J. Am. Chem. Soc.*, 2003, **125**, 1002-1006.

74 P. Rodriguez-Cuamatzi, G. Vargas-Diaz, and H. Hopfl, *Angew. Chem., Int. Ed.*, 2004, **43**, 3041-3044.

75 R. R. Shuvalov and P. C. Burns, *Acta Cryst.*, 2003, **C59**, i47-i49.

76 S. P. Draffin, P. J. Duggan, and G. D. Fallon, *Acta Cryst.*, 2004, **E60**, o1520-o1522.

77 C. C. Freyhardt, M. Wiebcke, and J. Felsche, *Acta Cryst.*, 2000, **C56**, 276-278.

78 T. D. James and S. Shinkai, *Top. Curr. Chem.*, 2002, **218**, 159-200.

79 K. L. Bhat, S. Hayik, and C. W. Bock, *J. Mol. Struct.*, 2003, **638**, 107-117.

80 K. L. Bhat, S. Hayik, J. N. Corvo, D. M. Marycz, and C. W. Bock, *J. Mol. Struct.*, 2004, **673**, 145-154.

81 S. Hayik, K. L. Bhat, and C. W. Bock, *Struct. Chem.*, 2004, **15**, 133-147.

82 R. D. Pizer and C. A. Tihal, *Polyhedron*, 1996, **15**, 3411-3416.

83 J. Clayden, N. Greeves, S. Warren, and P. Wothers, 'Organic Chemistry', Oxford University Press, 2001.

84 G. Lorber and R. Pizer, *Inorg. Chem.*, 1976, **15**, 978-980.

85 P. J. Duggan and E. M. Tyndall, *J. Chem. Soc., Perkin Trans. 1*, 2002, 1325-1339.

86 G. E. K. Branch, D. L. Yabroff, and B. Bettman, *J. Am. Chem. Soc.*, 1934, **56**, 937-941.

87 K. Ishihara, Y. Mouri, S. Funahashi, and M. Tanaka, *Inorg. Chem.*, 1991, **30**, 2356-2360.

88 C. Y. Shao, S. Matsuoka, Y. Miyazaki, K. Yoshimura, T. M. Suzuki, and D. A. P. Tanaka, *J. Chem. Soc., Dalton Trans.*, 2000, 3136-3142.

89 S. Kagawa, K.-I. Sugimoto, and S. Funahashi, *Inorg. Chim. Acta*, 1995, **231**, 115-119.

90 H. Ito, Y. Kono, A. Machida, Y. Mitsumoto, K. Omori, N. Nakamura, Y. Kondo, and K. Ishihara, *Inorg. Chim. Acta*, 2003, **344**, 28-36.

91 R. Pizer and P. J. Ricatto, *Inorg. Chem.*, 1994, **33**, 2402-2406.

92 S. Toyota, T. Futawaka, H. Ikeda, and M. Oki, *J. Chem. Soc., Chem. Commun.*, 1995, **24**, 2499-2500.

93 J. Grotewold, E. A. Lissi, and A. E. Villa, *J. Chem. Soc. A*, 1966, 1034-1037.

94 J. Grotewold, E. A. Lissi, and A. E. Villa, *J. Chem. Soc. A*, 1966, 1038-1041.

95 M. M. Kreevoy and J. E. C. Hutchins, *J. Am. Chem. Soc.*, 1972, **94**, 6371-6376.

96 I. M. Pepperberg, T. A. Halgren, and W. N. Lipscomb, *J. Am. Chem. Soc.*, 1976, **98**, 3442-3451.

97 D. Y. Lee and J. C. Martin, *J. Am. Chem. Soc.*, 1984, **106**, 5745-5746.

98 M. Yamashita, Y. Yamamoto, K. Akiba, and S. Nagase, *Angew. Chem., Int. Ed.*, 2000, **39**, 4055-4058.

99 W. H. Zachariasen, *Acta Cryst.*, 1963, **16**, 385-389.

100 S. Shinkai, K. Tsukagoshi, Y. Ishikawa, and T. Kunitake, *J. Chem. Soc., Chem. Commun.*, 1991, 1039-1041.

101 A. Finch, P. J. Gardner, P. M. McNamara, and G. R. Wellum, *J. Chem. Soc. A*, 1970, 3339-3345.

102 K. Tsukagoshi and S. Shinkai, *J. Org. Chem.*, 1991, 4089-4091.

103 K. Kondo, Y. Shiomi, M. Saisho, T. Harada, and S. Shinkai, *Tetrahedron*, 1992, 8239-8252.

104 G. Springsteen and B. Wang, *Tetrahedron*, 2002, **58**, 5291-5300.

105 R. A. Bissell, A. P. Desilva, H. Q. N. Gunaratne, P. L. M. Lynch, G. E. M. Maguire, and K. Sandanayake, *Chem. Soc. Rev.*, 1992, **21**, 187-195.

106 M. Böhmer and J. Enderlein, *ChemPhysChem*, 2003, **4**, 793-808.

107 W. E. Moerner and D. P. Fromm, *Rev. Sci. Instrum.*, 2003, **74**, 3597-3619.

108 W. P. Ambrose, P. M. Goodwin, J. H. Jett, A. Van Orden, J. H. Werner, and R. A. Keller, *Chem. Rev.*, 1999, **99**, 2929-2956.

109 M. Sauer, *Angew. Chem., Int. Ed.*, 2003, **42**, 1790-1793.

110 J. R. Epstein and D. R. Walt, *Chem. Soc. Rev.*, 2003, **32**, 203-214.

111 M. Fehr, S. Lalonde, D. W. Ehrhardt, and W. B. Frommer, *J. Fluorescence*, 2004, **14**, 603-609.

112 A. P. deSilva, H. Q. N. Gunaratne, T. Gunnlaugsson, and M. Nieuwenhuizen, *Chem. Commun.*, 1996, 1967-1968.

113 H. R. He, M. A. Mortellaro, M. J. P. Leiner, S. T. Young, R. J. Fraatz, and J. K. Tusa, *Anal. Chem.*, 2003, **75**, 549-555.

114 A. J. Tudos, G. A. J. Besselink, and R. B. M. Schasfoort, *Lab Chip*, 2001, **1**, 83-95.

115 H. Schlebusch, I. Paffenholz, R. Zerback, and R. Leinberger, *Clin. Chim. Acta*, 2001, **307**, 107-112.

116 R. Badugu, J. R. Lakowicz, and C. D. Geddes, *Biorg. Med. Chem.*, 2005, **13**, 113-119.

117 J. Yoon and A. W. Czarnik, *J. Am. Chem. Soc.*, 1992, **114**, 5874-5875.

118 T. D. James, K. Sandanayake, and S. Shinkai, *Angew. Chem., Int. Ed. Engl.*, 1994, **33**, 2207-2209.

119 T. D. James, K. R. A. S. Sandanayake, and S. Shinkai, *Nature*, 1995, **374**, 345-347.

120 J. R. Lakowicz, 'Principles of Fluorescence Spectroscopy', 2nd edition, Plenum, 1999.

121 M. Kasha, *Discussions of the Faraday Society*, 1950, **9**, 14-19.

122 E. Lippert, W. Lueder, F. Moll, W. Naegele, H. Boos, H. Prigge, and I. Seibold-Blankenstein, *Angew. Chem.*, 1961, **73**, 695-706.

123 E. Lippert, W. Lüder, and H. Boos, 'Advances in Molecular Spectroscopy', ed. A. Mangini, Pergamon Press, 1962.

124 W. Rettig, *Angew. Chem., Int. Ed. Engl.*, 1986, **25**, 971-988.

125 Z. R. Grabowski, K. Rotkiewicz, and W. Rettig, *Chem. Rev.*, 2003, **103**, 3899-4031.

126 K. Rotkiewicz, K. H. Grellmann, and Z. R. Grabowski, *Chem. Phys. Lett.*, 1973, **19**, 315-318.

127 K. Rotkiewicz, K. H. Grellmann, and Z. R. Grabowski, *Chem. Phys. Lett.*, 1973, **21**, 212 (Errata).

128 A. Siemiarczuk, Z. R. Grabowski, A. Krowczynski, M. Asher, and M. Ottolenghi, *Chem. Phys. Lett.*, 1977, **51**, 315-320.

129 J. Yoon and Czarnik, Anthony W., *Biorg. Med. Chem.*, 1993, **1**, 267-271.

130 M. W. G. de Bolster, *Pure Appl. Chem.*, 1997, **69**, 1251-1303.

131 Y. Nagai, K. Kobayashi, H. Toi, and Y. Aoyama, *Bull. Chem. Soc. Jpn.*, 1993, **66**, 2965-2971.

132 H. Shinmori, M. Takeuchi, and S. Shinkai, *Tetrahedron*, 1995, **51**, 1893-1902.

133 N. DiCesare and J. R. Lakowicz, *J. Phys. Chem. A*, 2001, **105**, 6834-6840.

134 N. DiCesare and J. R. Lakowicz, *J. Photochem. Photobiol., A*, 2001, **143**, 39-47.

135 K. R. A. S. Sandanayake, S. Imazu, T. D. James, M. Mikami, and S. Shinkai, *Chem. Lett.*, 1995, 139-140.

136 S. Arimori, L. I. Bosch, C. J. Ward, and T. D. James, *Tetrahedron Lett.*, 2001, **42**, 4553-4555.

137 L. I. Bosch, M. F. Mahon, and T. D. James, *Tetrahedron Lett.*, 2004, **45**, 2859-2862.

138 P. F. Barbara, T. J. Meyer, and M. A. Ratner, *J. Phys. Chem.*, 1996, **100**, 13148-13168.

139 S. Fukuzumi, *Org. Biomol. Chem.*, 2003, **1**, 609-620.

140 H. Kurreck and M. Huber, *Angew. Chem., Int. Ed. Engl.*, 1995, **34**, 849-866.

141 M. R. Wasielewski, *Chem. Rev.*, 1992, **92**, 435-461.

142 M. B. Zimmt and D. H. Waldeck, *J. Phys. Chem. A*, 2003, **107**, 3580-3597.

143 H. Oevering, M. N. Paddonrow, M. Heppener, A. M. Oliver, E. Cotsaris, J. W. Verhoeven, and N. S. Hush, *J. Am. Chem. Soc.*, 1987, **109**, 3258-3269.

144 G. L. Closs and J. R. Miller, *Science*, 1988, **240**, 440-447.

145 H. Knibbe, D. Rehm, and A. Weller, *Ber. Bunsen-Ges. Phys. Chem.*, 1968, **72**, 257-263.

146 A. P. de Silva and R. Rupasinghe, *J. Chem. Soc., Chem. Commun.*, 1985, 1669-1670.

147 J. D. Jackson, 'Classical Electrodynamics', 2nd edition, John Wiley & Sons, 1975.

148 M. C. Beard, G. M. Turner, and C. A. Schmuttenmaer, *J. Am. Chem. Soc.*, 2000, **122**, 11541-11542.

149 M. C. Beard, G. M. Turner, and C. A. Schmuttenmaer, *J. Phys. Chem. A*, 2002, **106**, 878-883.

150 V. Balzani and F. Scandola, 'Supramolecular Photochemistry', ed. T. J. Kemp, Ellis Horwood Limited, 1991.

151 M. D. Ward, *Chem. Soc. Rev.*, 1997, **26**, 365-376.

152 B. G. Malmström, 'Nobel Lectures in Chemistry (1991-1995)', Nobel Lectures, World Scientific, 1997.

153 L. Flamigni, A. M. Talarico, S. Serroni, F. Puntoriero, M. J. Gunter, M. R. Johnston, and T. P. Jeynes, *Chem. Eur. J.*, 2003, **9**, 2649-2659.

154 J. W. Verhoeven, *Pure Appl. Chem.*, 1996, **68**, 2223-2286.

155 R. C. Dorfman, Y. Lin, and M. D. Fayer, *J. Phys. Chem.*, 1990, **94**, 8007-8009.

156 G. Wulff, *Pure Appl. Chem.*, 1982, **54**, 2093-2102.

157 T. D. James, K. Sandanayake, and S. Shinkai, *J. Chem. Soc., Chem. Commun.*, 1994, 477-478.

158 T. D. James, K. R. A. S. Sandanayake, R. Iguchi, and S. Shinkai, *J. Am. Chem. Soc.*, 1995, **117**, 8982-8987.

159 J. Z. Zhao, T. M. Fyles, and T. D. James, *Angew. Chem., Int. Ed.*, 2004, **43**, 3461-3464.

160 C. W. Gray and T. A. Houston, *J. Org. Chem.*, 2002, **67**, 5426-5428.

161 T. D. James, H. Shinmori, M. Takeuchi, and S. Shinkai, *Chem. Commun.*, 1996, 705-706.

162 B. Kukrer and E. U. Akkaya, *Tetrahedron Lett.*, 1999, **40**, 9125-9128.

163 R. R. Anderson and J. A. Parrish, *J. Invest. Dermatol.*, 1981, **77**, 13-19.

164 R. M. P. Doornbos, R. Lang, M. C. Aalders, F. W. Cross, and H. Sterenborg, *Phys. Med. Biol.*, 1999, **44**, 967-981.

165 J. V. Frangioni, *Curr. Opin. Chem. Biol.*, 2003, **7**, 626-634.

166 J. Zhao, M. G. Davidson, M. F. Mahon, G. Kociok-Köhn, and T. D. James, *J. Am. Chem. Soc.*, 2004, **126**, 16179-16186.

167 H. Höpfl, *J. Organomet. Chem.*, 1999, **581**, 129-149.

168 S. L. Wiskur, J. J. Lavigne, H. Ait-Haddou, V. Lynch, Y. Hung Chiu, J. W. Canary, and E. V. Anslyn, *Org. Lett.*, 2001, **3**, 1311-1314.

169 W. J. Ni, G. Kaur, G. Springsteen, B. H. Wang, and S. Franzen, *Bioorg. Chem.*, 2004, **32**, 571-581.

170 K. L. Bhat, V. Braz, E. Laverty, and C. W. Bock, *Theochem-J. Mol. Struct.*, 2004, **712**, 9-19.

171 K. L. Bhat, N. J. Howard, H. Rostami, J. H. Lai, and C. W. Bock, *Prepress*, 2005.

172 J. D. Morrison and R. L. Letsinger, *J. Org. Chem.*, 1964, **29**, 3405-3407.

173 M. Bielecki, H. Eggert, and J. C. Norrild, *J. Chem. Soc., Perkin Trans. 2*, 1999, 449-455.

174 J. C. Norrild and H. Eggert, *J. Am. Chem. Soc.*, 1995, **117**, 1479-1484.

175 M. P. Nicholls and P. K. C. Paul, *Org. Biomol. Chem.*, 2004, **2**, 1434-1441.

176 S. J. Angyal, *Adv. Carbohydr. Chem. Biochem.*, 1984, **42**, 15-68.

177 J. C. Norrild and H. Eggert, *J. Chem. Soc., Perkin Trans. 2*, 1996, 2583-2588.

178 C. R. Cooper and T. D. James, *Chem. Lett.*, 1998, 883-884.

179 H. Eggert, J. Frederiksen, C. Morin, and J. C. Norrild, *J. Org. Chem.*, 1999, **64**, 3846-3852.

180 W. Yang, H. He, and D. G. Drueckhammer, *Angew. Chem., Int. Ed.*, 2001, **40**, 1714-1718.

181 C. R. Cooper and T. D. James, *Chem. Commun.*, 1997, 1419-1420.

182 C. R. Cooper and T. D. James, *J. Chem. Soc., Perkin Trans. 1*, 2000, 963-969.

183 L. A. Cabell, M. K. Monahan, and E. V. Anslyn, *Tetrahedron Lett.*, 1999, **40**, 7753-7756.

184 K. Sandanayake, T. D. James, and S. Shinkai, *Chem. Lett.*, 1995, 503-504.

185 B. Appleton and T. D. Gibson, *Sens. Actuators, B*, 2000, **65**, 302-304.

186 M. E. Huston, E. U. Akkaya, and A. W. Czarnik, *J. Am. Chem. Soc.*, 1989, **111**, 8735-8737.

187 T. P. Wunz, R. T. Dorr, D. S. Alberts, C. L. Tunget, J. Einspahr, S. Milton, and W. A. Remers, *J. Med. Chem.*, 1987, **30**, 1313-1321.

188 M. D. Phillips, 'Fluorescent Phosphate Sensors', M.NatSc(Chem) Dissertation, The University of Birmingham, Birmingham, 2000.

189 H. K. Hall, *J. Am. Chem. Soc.*, 1957, **78**, 5441-5444.

190 W. H. Carothers, C. F. Bickford, and G. J. Hurwitz, *J. Am. Chem. Soc.*, 1927, **49**, 2908-2914.

191 S. Arimori, M. L. Bell, C. S. Oh, K. A. Frimat, and T. D. James, *Chem. Commun.*, 2001, 1836-1837.

192 S. Arimori, M. L. Bell, C. S. Oh, K. A. Frimat, and T. D. James, *J. Chem. Soc., Perkin Trans. 1*, 2002, 803-808.

193 D. D. Perrin and B. Dempsey, 'Buffers for Ph and Metal Ion Control', Chapman & Hall, 1974.

194 G. Lecollinet, A. P. Dominey, T. Velasco, and A. P. Davis, *Angew. Chem., Int. Ed.*, 2002, **41**, 4093-4096.

195 K. Sandanayake, K. Nakashima, and S. Shinkai, *J. Chem. Soc., Chem. Commun.*, 1994, 1621-1622.

196 H. Kijima, M. Takeuchi, and S. Shinkai, *Chem. Lett.*, 1998, 781-782.

197 Z. Zhong and E. V. Anslyn, *J. Am. Chem. Soc.*, 2002, **124**, 9014-9015.

198 A. Sugasaki, K. Sugiyasu, M. Ikeda, M. Takeuchi, and S. Shinkai, *J. Am. Chem. Soc.*, 2001, **123**, 10239-10244.

199 A. Sugasaki, M. Ikeda, M. Takeuchi, and S. Shinkai, *Angew. Chem., Int. Ed.*, 2000, **39**, 3839-3842.

200 M. Yamamoto, M. Takeuchi, and S. Shinkai, *Tetrahedron*, 2002, **58**, 7251-7258.

201 M. Ikeda, S. Shinkai, and A. Osuka, *Chem. Commun.*, 2000, 1047-1048.

202 W. Yang, S. Gao, X. Gao, V. V. R. Karnati, W. Ni, B. Wang, W. B. Hooks, J. Carson, and B. Weston, *Bioorg. Med. Chem. Lett.*, 2002, **12**, 2175-2177.

203 S. Patterson, B. D. Smith, and R. E. Taylor, *Tetrahedron Lett.*, 1998, **39**, 3111-3114.

204 T. Nagase, E. Nakata, S. Shinkai, and I. Hamachi, *Chem. Eur. J.*, 2003, **9**, 3660-3669.

205 S. Arimori, M. D. Phillips, and T. D. James, *Tetrahedron Lett.*, 2004, **45**, 1539-1542.

206 The *K* values were analysed in KaleidaGraph using nonlinear (Levenberg-Marquardt algorithm) curve fitting. The errors reported are the standard errors obtained from the best fit.

207 S. Arimori, M. L. Bell, C. S. Oh, and T. D. James, *Org. Lett.*, 2002, **4**, 4249-4251.

208 T. Jin, *Chem. Commun.*, 1999, 2491-2492.

209 V. V. Karnati, X. Gao, S. Gao, W. Yang, W. Ni, S. Sankar, and B. Wang, *Bioorg. Med. Chem. Lett.*, 2002, **12**, 3373-3377.

210 D. Stones, S. Manku, X. S. Lu, and D. G. Hall, *Chem. Eur. J.*, 2004, **10**, 92-100.

211 F. A. Carey and R. J. Sundberg, 'Advanced Organic Chemistry', 4th edition, Kluwer Academic/Plenum Publishers, 2000.

212 S. Arimori, G. A. Consiglio, M. D. Phillips, and T. D. James, *Tetrahedron Lett.*, 2003, **44**, 4789-4792.

213 K. A. Frimat, 'Synthesis and Evaluation of Novel Modular Fluorescent Diboronic Acid Sensors', PhD Thesis, University of Bath, Bath, 2002.

214 S. J. M. Koskela, 'Molecular Logic Gates', PhD Thesis, University of Bath, Bath, 2003.

215 W. Seaman and J. R. Johnson, *J. Am. Chem. Soc.*, 1931, **53**, 711.

216 D. M. Schubert, *Struct. Bonding*, 2003, **105**, 1-40.

217 V. Kuksa, R. Buchan, and P. K. T. Lin, *Synthesis*, 2000, 1189-1207.

218 P. J. Kocienski, 'Protecting Groups', Thieme Foundations of Organic Chemistry Series, ed. D. Enders, R. Noyori, and B. M. Trost, Georg Thieme Verlag, 1994.

219 T. W. Greene and P. G. M. Wuts, 'Protective Groups in Organic Synthesis', John Wiley & Sons, Inc, 1999.

220 A. P. Krapcho and C. S. Kuell, *Synth. Commun.*, 1990, **20**, 2559-2564.

221 A. P. Krapcho, M. J. Maresch, and J. Lunn, *Synth. Commun.*, 1993, **23**, 2443-2449.

222 M. Pittelkow, R. Lewinsky, and J. B. Christensen, *Synthesis*, 2002, 2195-2202.

223 C. S. Dean, D. S. Tarbell, and A. W. Friederang, *J. Org. Chem.*, 1970, **35**, 3393-3397.

224 The Chemicals (Hazard Information and Packaging for Supply) Regulations, 2002, Statutory Instrument 2002/1689.

225 T. Apelqvist and D. Wensbo, *Tetrahedron Lett.*, 1996, **37**, 1471-1472.

226 P. E. Broutin, P. Hilty, and A. W. Thomas, *Tetrahedron Lett.*, 2003, **44**, 6429-6432.

227 D. H. Williams and I. Fleming, 'Spectroscopic Methods in Organic Chemistry', 5th edition, McGraw-Hill, 1995.

228 D. D. Perrin and B. Dempsey, 'Buffer for Ph and Metal Ion Control', Chapman and Hall, 1974.

229 M. Barboiu, C. T. Supuran, A. Scozzafava, F. Briganti, C. Luca, G. Popescu, L. Cot, and N. Hovnanian, *Liebigs Ann. Chem.*, 1997, 1853-1859.

230 S. A. Galema, M. J. Blandamer, and J. Engberts, *J. Am. Chem. Soc.*, 1990, **112**, 9665-9666.

231 D. Fabri, M. A. K. Williams, and T. K. Halstead, *Carbohydr. Res.*, 2005, **340**, 889-905.

232 S. A. Galema, M. J. Blandamer, and J. Engberts, *J. Org. Chem.*, 1992, **57**, 1995-2001.

233 M. Janado and Y. Yano, *Bull. Chem. Soc. Jpn.*, 1985, **58**, 1913-1917.

234 Y. Yano, K. Tanaka, Y. Doi, and M. Janado, *Bull. Chem. Soc. Jpn.*, 1988, **61**, 2963-2964.

235 E. Fischer, *Ber. Dtsch. Chem. Ges.*, 1894, **27**, 2985-2993.

236 R. U. Lemieux and U. Spohr, *Adv. Carbohydr. Chem. Biochem.*, 1994, **50**, 1-20.

237 D. T. Warner, *Nature*, 1962, **196**, 1055-1058.

238 M. D. Walkinshaw, *J. Chem. Soc., Perkin Trans. 2*, 1987, 1903-1905.

239 R. U. Lemieux, *Acc. Chem. Res.*, 1996, **29**, 373-380.

240 P. R. Westmark and B. D. Smith, *J. Am. Chem. Soc.*, 1994, **116**, 9343-9344.

241 S. P. Draffin, P. J. Duggan, and S. A. M. Duggan, *Org. Lett.*, 2001, **3**, 917-920.

242 S. J. Gardiner, B. D. Smith, P. J. Duggan, M. J. Karpa, and G. J. Griffin, *Tetrahedron*, 1999, **55**, 2857-2864.

243 P. R. Westmark, S. J. Gardiner, and B. D. Smith, *J. Am. Chem. Soc.*, 1996, **118**, 11093-11100.

244 J. A. Riggs, R. K. Litchfield, and B. D. Smith, *J. Org. Chem.*, 1996, **61**, 1148-1150.

245 G. T. Morin, M. P. Hughes, M. F. Paugam, and B. D. Smith, *J. Am. Chem. Soc.*, 1994, **116**, 8895-8901.

246 J. McKenna, J. M. McKenna, and D. W. Thornthwaite, *J. Chem. Soc., Chem. Commun.*, 1977, **22**, 809-811.

247 C.-W. Chen and H. W. Whitlock Jr., *J. Am. Chem. Soc.*, 1978, **100**, 4921-4922.

248 S. C. Zimmerman, Z. J. Zeng, W. M. Wu, and D. E. Reichert, *J. Am. Chem. Soc.*, 1991, **113**, 183-196.

249 S. C. Zimmerman, W. M. Wu, and Z. J. Zeng, *J. Am. Chem. Soc.*, 1991, **113**, 196-201.

250 S. C. Zimmerman and W. M. Wu, *J. Am. Chem. Soc.*, 1989, **111**, 8054-8055.

251 F. G. Gatti, D. A. Leigh, S. A. Nepogodiev, A. M. Z. Slawin, S. J. Teat, and J. K. Y. Wong, *J. Am. Chem. Soc.*, 2001, **123**, 5983-5989.

252 R. W. Hoffmann, *Angew. Chem., Int. Ed. Engl.*, 1992, **31**, 1540-1540.

253 S. C. Zimmerman and C. M. Vanzyl, *J. Am. Chem. Soc.*, 1987, **109**, 7894-7896.

254 S. C. Zimmerman, *Top. Curr. Chem.*, 1993, **165**, 71-102.

255 R. Leppkes and F. Vögtle, *Angew. Chem., Int. Ed. Engl.*, 1981, **20**, 396-397.

256 C. A. Schalley, C. Verhaelen, F. G. Klarner, U. Hahn, and F. Vögtle, *Angew. Chem., Int. Ed.*, 2005, **44**, 477-480.

257 R. Güther, M. Nieger, and F. Vögtle, *Angew. Chem., Int. Ed. Engl.*, 1993, **32**, 601-603.

258 J. Rebek, *Angew. Chem., Int. Ed. Engl.*, 1990, **29**, 245-255.

259 M. Irie and M. Kato, *J. Am. Chem. Soc.*, 1985, **107**, 1024-1028.

260 F. G. Klärner, J. Benkhoff, R. Boese, U. Burkert, M. Kamieth, and U. Naatz, *Angew. Chem., Int. Ed. Engl.*, 1996, **35**, 1130-1133.

261 F. G. Klärner, U. Burkert, M. Kamieth, R. Boese, and J. Benet-Buchholz, *Chem. Eur. J.*, 1999, **5**, 1700-1707.

262 S. P. Brown, T. Schaller, U. P. Seelbach, F. Koziol, C. Ochsenfeld, F. G. Klarner, and H. W. Spiess, *Angew. Chem., Int. Ed.*, 2001, **40**, 717-720.

263 F. G. Klärner and B. Kahlert, *Acc. Chem. Res.*, 2003, **36**, 919-932.

264 M. Takeuchi, T. Imada, and S. Shinkai, *J. Am. Chem. Soc.*, 1996, **118**, 10658-10659.

265 M. Harmata, C. L. Barnes, S. R. Karra, and S. Elahmad, *J. Am. Chem. Soc.*, 1994, **116**, 8392-8393.

266 M. Harmata, *Acc. Chem. Res.*, 2004, **37**, 862-873.

267 V. V. Borovkov, J. M. Lintuluoto, M. Sugiura, Y. Inoue, and R. Kuroda, *J. Am. Chem. Soc.*, 2002, **124**, 11282-11283.

268 N. C. Gianneschi, S. H. Cho, S. T. Nguyen, and C. A. Mirkin, *Angew. Chem., Int. Ed.*, 2004, **43**, 5503-5507.

269 S. K. Chang, D. Vanengen, E. Fan, and A. D. Hamilton, *J. Am. Chem. Soc.*, 1991, **113**, 7640-7645.

270 F. J. Carver, C. A. Hunter, P. S. Jones, D. J. Livingstone, J. F. McCabe, E. M. Seward, P. Tiger, and S. E. Spey, *Chem. Eur. J.*, 2001, **7**, 4854-4862.

271 S. R. Collinson, T. Gelbrich, M. B. Hursthouse, and J. H. R. Tucker, *Chem. Commun.*, 2001, 555-556.

272 J. M. Mahoney, A. M. Beatty, and B. D. Smith, *J. Am. Chem. Soc.*, 2001, **123**, 5847-5848.

273 H. M. Colquhoun, Z. X. Zhu, and D. J. Williams, *Org. Lett.*, 2003, **5**, 4353-4356.

274 S. K. Chang and A. D. Hamilton, *J. Am. Chem. Soc.*, 1988, **110**, 1318-1319.

275 S. J. Cantrill, D. A. Fulton, A. M. Heiss, A. R. Pease, J. F. Stoddart, A. J. P. White, and D. J. Williams, *Chem. Eur. J.*, 2000, **6**, 2274-2287.

276 L. M. Greig and D. Philp, *Chem. Soc. Rev.*, 2001, **30**, 287-302.

277 M. S. Cubberley and B. L. Iverson, *J. Am. Chem. Soc.*, 2001, **123**, 7560-7563.

278 A. G. Johnston, D. A. Leigh, R. J. Pritchard, and M. D. Deegan, *Angew. Chem., Int. Ed. Engl.*, 1995, **34**, 1209-1212.

279 A. G. Johnston, D. A. Leigh, L. Nezhat, J. P. Smart, and M. D. Deegan, *Angew. Chem., Int. Ed. Engl.*, 1995, **34**, 1212-1216.

280 D. A. Leigh, A. Murphy, J. P. Smart, M. S. Deleuze, and F. Zerbetto, *J. Am. Chem. Soc.*, 1998, **120**, 6458-6467.

281 T. J. Kidd, D. A. Leigh, and A. J. Wilson, *J. Am. Chem. Soc.*, 1999, **121**, 1599-1600.

282 M. S. Deleuze, D. A. Leigh, and F. Zerbetto, *J. Am. Chem. Soc.*, 1999, **121**, 2364-2379.

283 D. A. Leigh, K. Moody, J. P. Smart, K. J. Watson, and A. M. Z. Slawin, *Angew. Chem., Int. Ed. Engl.*, 1996, **35**, 306-310.

284 D. A. Leigh, A. Murphy, J. P. Smart, and A. M. Z. Slawin, *Angew. Chem., Int. Ed. Engl.*, 1997, **36**, 728-732.

285 J. V. Hernandez, E. R. Kay, and D. A. Leigh, *Science*, 2004, **306**, 1532-1537.

286 A. G. Johnston, D. A. Leigh, A. Murphy, J. P. Smart, and M. D. Deegan, *J. Am. Chem. Soc.*, 1996, **118**, 10662-10663.

287 A. S. Lane, D. A. Leigh, and A. Murphy, *J. Am. Chem. Soc.*, 1997, **119**, 11092-11093.

288 A. M. Brouwer, C. Frochot, F. G. Gatti, D. A. Leigh, L. Mottier, F. Paolucci, S. Roffia, and G. W. H. Wurpel, *Science*, 2001, **291**, 2124-2128.

289 M. Cavallini, F. Biscarini, S. Leon, F. Zerbetto, G. Bottari, and D. A. Leigh, *Science*, 2003, **299**, 531-531.

290 D. A. Leigh, M. Á. F. Morales, E. M. Pérez, J. K. Y. Wong, C. G. Saiz, A. M. Z. Slawin, A. J. Carmichael, D. M. Haddleton, A. M. Brouwer, W. J. Buma, G. W. H. Wurpel, S. León, and F. Zerbetto, *Angew. Chem., Int. Ed.*, 2005, **44**, 3062-3067.

291 G. W. H. Wurpel, A. M. Brouwer, I. H. M. van Stokkum, A. Farran, and D. A. Leigh, *J. Am. Chem. Soc.*, 2001, **123**, 11327-11328.

292 J. March, 'Advanced Organic Chemistry: Reactions Mechanisms, and Structures', 4th Edition, Wiley-Interscience, 1992.

293 J. Jones, 'Core Carbonyl Chemistry', Oxford Chemistry Primers, Oxford University Press, 1997.

294 'The Merck Index: An Encyclopedia of Chemicals and Drugs', 9th edition, ed. M. Windholz, Merck & Co., Inc., 1976.

295 H. E. Gottlieb, V. Kotlyar, and A. Nudelman, *J. Org. Chem.*, 1997, **62**, 7512-7515.

296 J. Homer and M. C. Perry, *J. Chem. Soc., Perkin Trans. 2*, 1995, 533-536.

297 K. N. Carter and K. N. Carter Jr., *J. Chem. Educ.*, 1995, **72**, 647-648.

298 A. Gehenot, R. C. Rao, G. Maire, and M. Gachon, *Int. J. Pharm.*, 1988, **45**, 13-17.

299 A. D. Ainley and F. Challenger, *J. Chem. Soc.*, 1930, 2171-2180.

300 E. F. Elslager, J. L. Johnson, and L. M. Werbel, *J. Med. Chem.*, 1981, **24**, 140-145.

301 R. E. Lutz, P. S. Bailey, R. J. Rowlett, J. W. Wilson, R. K. Allison, M. T. Clark, N. H. Leake, R. H. Jordan, R. J. Keller, and K. C. Nicodemus, *J. Org. Chem.*, 1947, **12**, 760-766.

302 H. Dahn and P. Zoller, *Helv. Chem. Acta*, 1952, **35**, 1348-1358.

303 T. D. James and S. Shinkai, *J. Chem. Soc., Chem. Commun.*, 1995, 1483-1485.

304 M. Takeuchi, M. Yamamoto, and S. Shinkai, *Chem. Commun.*, 1997, 1731-1732.

305 M. Yamamoto, M. Takeuchi, and S. Shinkai, *Tetrahedron*, 1998, **54**, 3125-3140.

306 W. Yang, J. Yan, H. Fang, and B. Wang, *Chem. Commun.*, 2003, 792-793.

307 S. J. M. Koskela, T. M. Fyles, and T. D. James, *Chem. Commun.*, 2005, 945-947.

308 C. R. Cooper, N. Spencer, and T. D. James, *Chem. Commun.*, 1998, 1365-1366.

309 S. Arimori, M. G. Davidson, T. M. Fyles, T. G. Hibbert, T. D. James, and G. I. Kociok-Köhn, *Chem. Commun.*, 2004, 1640-1641.

CHAPTER SEVEN: Appendices

Perfect as the wing of a bird may be, it will never enable the bird to fly if unsupported by the air. Facts are the air of science. Without them a man of science can never rise.

Ivan Pavlov

7 Appendices

7.1 APPENDIX 1: DITOPIC SENSORS

Boronic acid based fluorescent PET sensors developed for the recognition of simple monosaccharides have been extended to include ditopic recognition sites and so introduce selectivity for a diverse range of guest species.

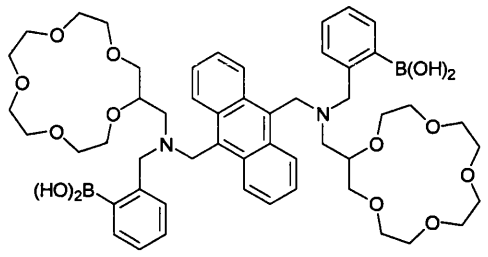

165

Developed around the D-glucose sensor **68** (page 60) the allosteric diboronic acid biscrown ether **165** displayed a fluorescence increase upon binding D-glucose.[303] Addition of metal cations with a similar ionic diameter to potassium favour a 1:1 (metal ion/sensor) binding motif, causing the 15-crown-5-ether receptors to sandwich the metal ion. The metal induced conformational change disrupts the 1:1 (saccharide: sensor) complex with D-glucose, restoring PET and thus quenching fluorescence.

The observed stability constants (K_{obs}), (and ionic diameters) for the metal cations were 19 M^{-1} (2.04 Å) with Na^+, 35 M^{-1} (2.36 Å) with Sr^{2+}, 63 M^{-1} (2.76 Å) with K^+ and 2 500 M^{-1} (2.70 Å) with Ba^{2+} in 33.3 wt% methanol in water in the presence of 0.03 mol dm^{-3} D-glucose. The fluorescence changes for Li^+ (1.52 Å) and Cs^+ (3.40 Å) were so small that observed stability constants (K_{obs}) could not be determined.

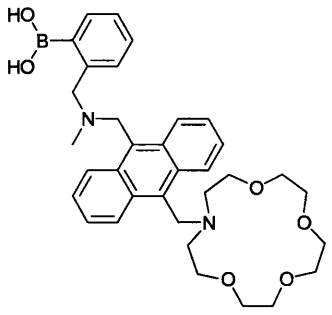

166

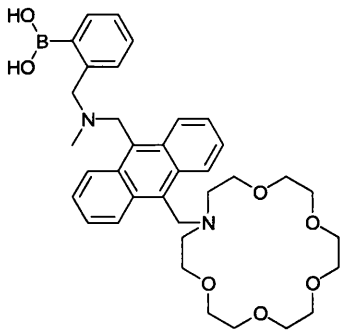

167

The fluorescent PET sensors **166** and **167** demonstrated selectivity for an ammonium terminus at the monoaza-crown ether receptor and selectivity for saccharides at the boronic acid receptor. This dual targeted approach induced D-glucosamine hydrochloride selectivity within the system.[181,182]

Curiously the azacrown ether imparts little if any additional stability to the complex on binding. Nevertheless binding at the azacrown ether is a prerequisite of generating a fluorescent response as it directly participates in PET, the system requiring both recognition units to complex for fluorescence to be restored. The observed stability constants (K_{obs}) for sensors **166** and **167** with D-glucosamine were 18 M^{-1} and 17 M^{-1} respectively, in 33.2 wt% ethanol/water at pH 7.18 (triethanolamine buffer).

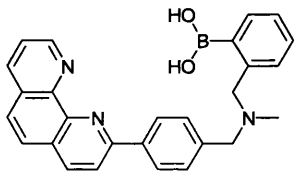

168

Designed by Shinkai and co-workers **168** also takes advantage of two distinct recognition moieties.[304,305] The monoboronic acid receptor allows selectivity towards saccharides to be introduced to the sensor and modulated through PET. When Zn(II) is coordinated with the two phenanthroline nitrogen atoms the selectivity for saccharides remains unchanged. However, the interaction of the metal centre with carboxylate groups on guest species significantly enhances the selectivity for sialic and uronic acids. In keeping with the expected trends for monoboronic acids the observed stability constants (K_{obs}) for sensor **168** were 79 M^{-1} for D-galacturonic acid, 50 M^{-1} for D-galactose and 320 M^{-1} for D-fructose. With the introduction of Zn(II) the values

increased to 2 510 M^{-1} for D-glucuronic acid, 1 260 M^{-1} for D-galacturonic acid, 200 M^{-1} for sialic acid, whilst remaining nearly constant for the monosaccharides, 20 M^{-1} for D-galactose and 250 M^{-1} for D-fructose.

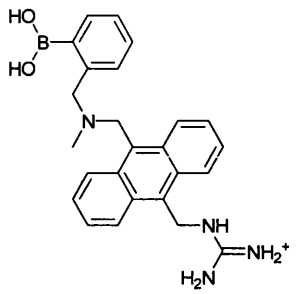

169

The boronic acid, guanidinium appended fluorescent PET sensor **169** developed by Wang and co-workers displayed selectivity for D-glucarate.[306] As with other ditopic sensors both receptor units must be occupied for fluorescence to be restored. In this instance the boronic acid participates in diol complexation and the guanidinium participates in carboxylate complexation.

The observed stability constants (K_{obs}) for sensor **169** were 5 140 M^{-1} with D-glucarate, 1 450 M^{-1} with D-gluconate, 1 300 M^{-1} with D-sorbitol, 62 M^{-1} with D-glucose and 46 M^{-1} with D-glucuronic acid in 50% methanol in 0.1 M aqueous HEPES buffer at pH 7.4.

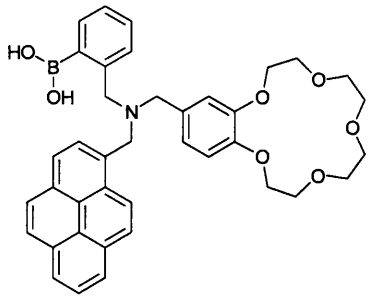

170

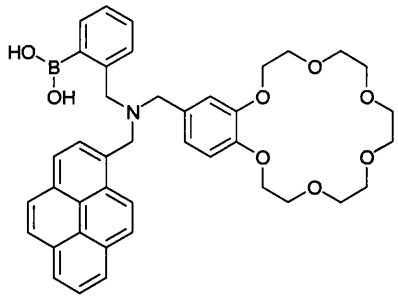

171

The ditopic fluorescent sensors **170** and **171** have been developed as reversible AND logic gates with selectivity for potassium fluoride.[307] The binding of fluoride with boronic acids is well documented.[308,309] In this case the sp^2 hybridised boronic acid, which is a hard Lewis acid, interacts strongly with the fluoride anion, which is a hard

Lewis base, to become sp^3 hybridised. The potassium cation is held *in situ* partly by the crown ether and partly by the electrostatic interaction with the fluoride anion. This co-operative complexation allows the cationic and anionic guests to be bound to the host as an ion pair, whilst allowing the host to discriminate between potassium fluoride and other similar ion pairs such as potassium chloride and potassium bromide.

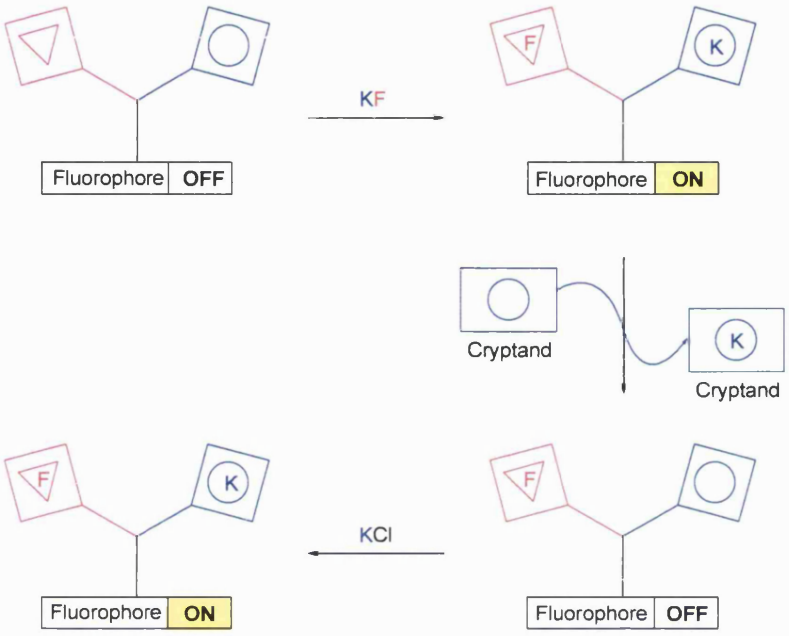

Scheme 90. *Schematic representation of the ditopic fluorescent PET sensors **170** and **171**, demonstrating selective and reversible binding of potassium fluoride with concurrent modulation of fluorescence intensity. The initial unbound complex is "off", addition of KF generates a large increase in fluorescence intensity turning the system "on", removal of potassium by addition of [2.2.2]-cryptand (4,7,13,16,21,24-hexaoxa-1,10-diazabicyclo[8.8.8]-hexacosane) quenches fluorescence returning the sensor to an "off" state, subsequent addition of potassium chloride re-introduces potassium to the system and restores fluorescence to the "on" state.*

The dynamic characteristics of this sensor are particularly attractive. Not only are both guests required at the binding sites to generate a fluorescence response but it is possible to add and remove individual guests producing a controlled and reversible read-out signal derived from the AND logic functionality inherent to the sensor. This example is illustrated in Scheme 90 and provides an elegant representation of the dynamic and versatile disposition of these recognition systems, permitting selective and reversible binding to be designed into sensors and switches alike.

The observed stability constants (K_{obs}) for sensor **170** were 10 000 M^{-1} with potassium and 320 M^{-1} with fluoride. Those for sensor **171** were 50 000 M^{-1} with potassium and 250 M^{-1} with fluoride in methanol.

7.2 APPENDIX 2: SELECTED NMR SPECTRA

N'-benzylhexane-1,6-diamine (138)

^{1}H NMR spectrum (300 MHz, $CDCl_3$)

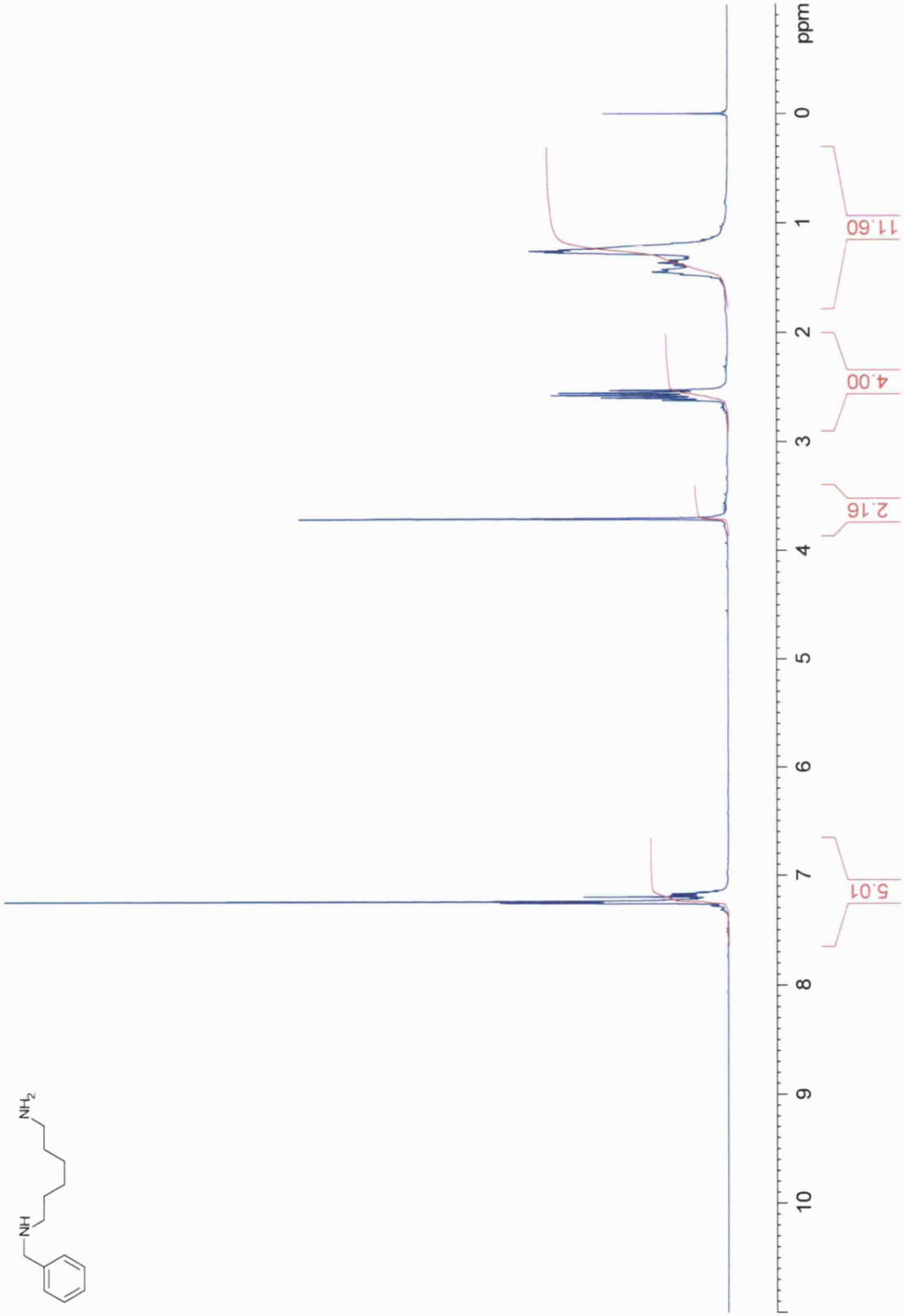

N'-Pyren-1-ylmethyl-hexane-1,6-diamine (144)

^{1}H NMR spectrum (300 MHz, $CDCl_3$)

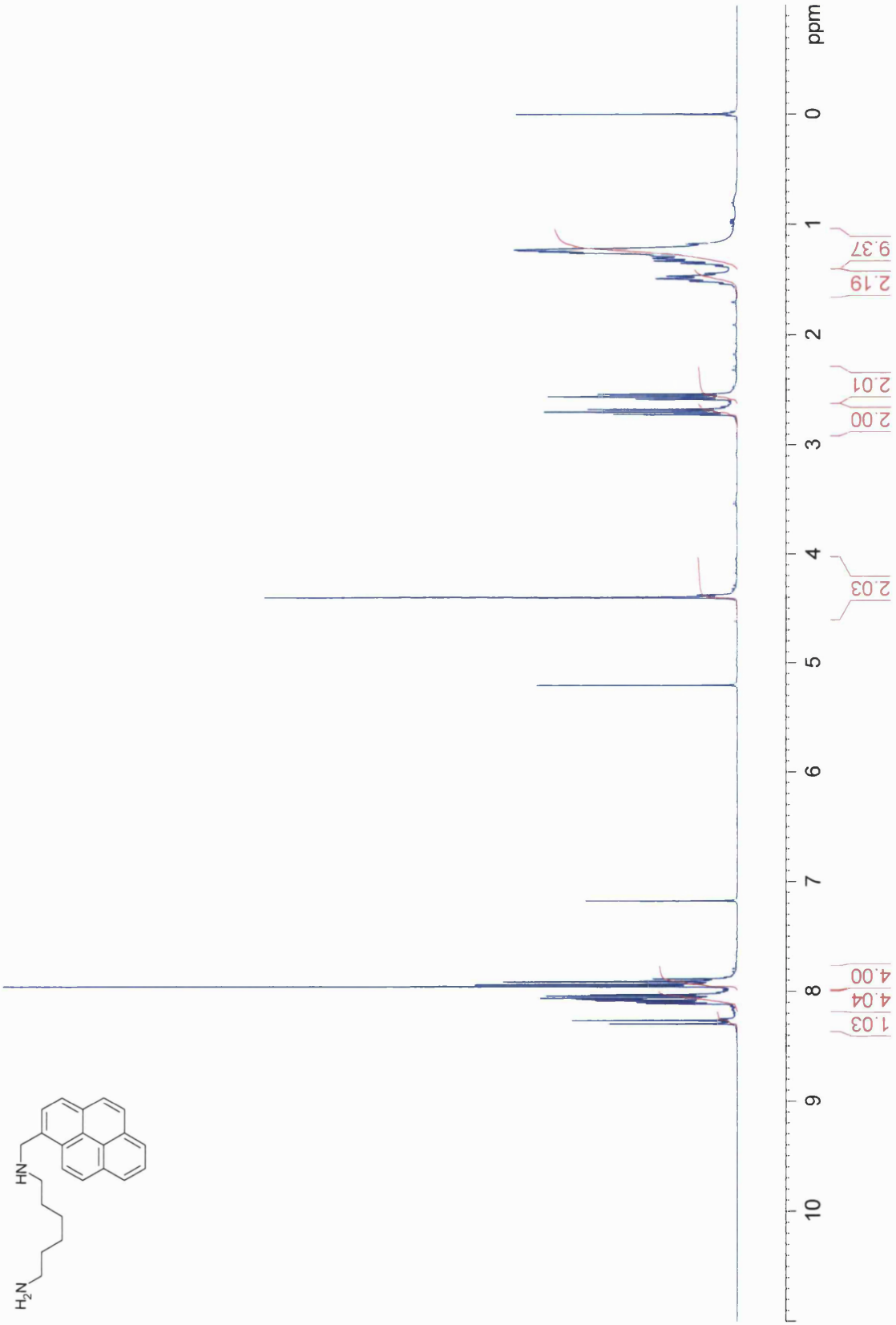

2-*o*-Tolyl-1,3,2-dioxaborinane (125)

^{1}H NMR spectrum (300 MHz, $CDCl_3$)

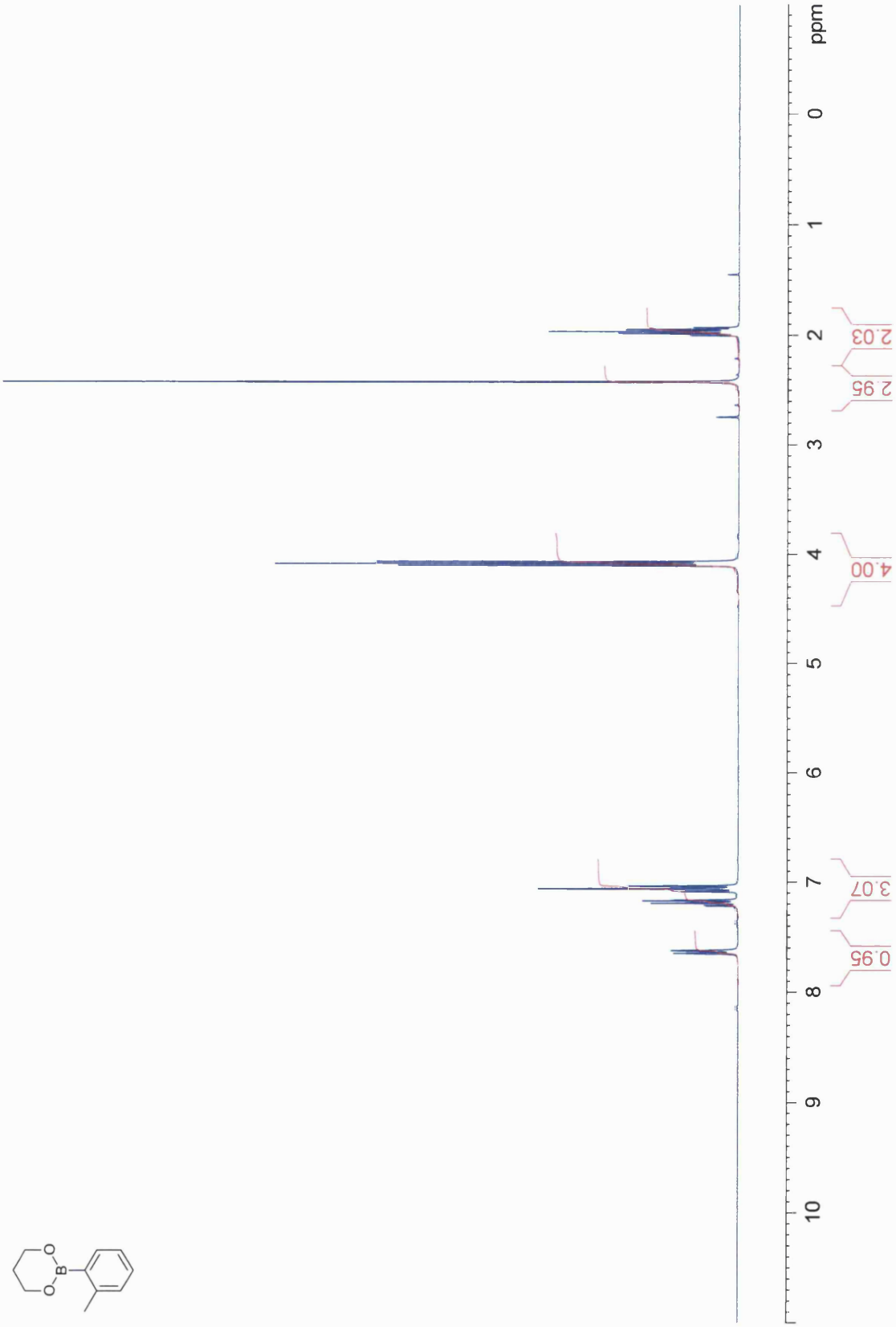

5,5-dimethyl-2-*o*-tolyl-1,3,2-dioxaborinane (126)

^{1}H NMR spectrum (300 MHz, $CDCl_3$)

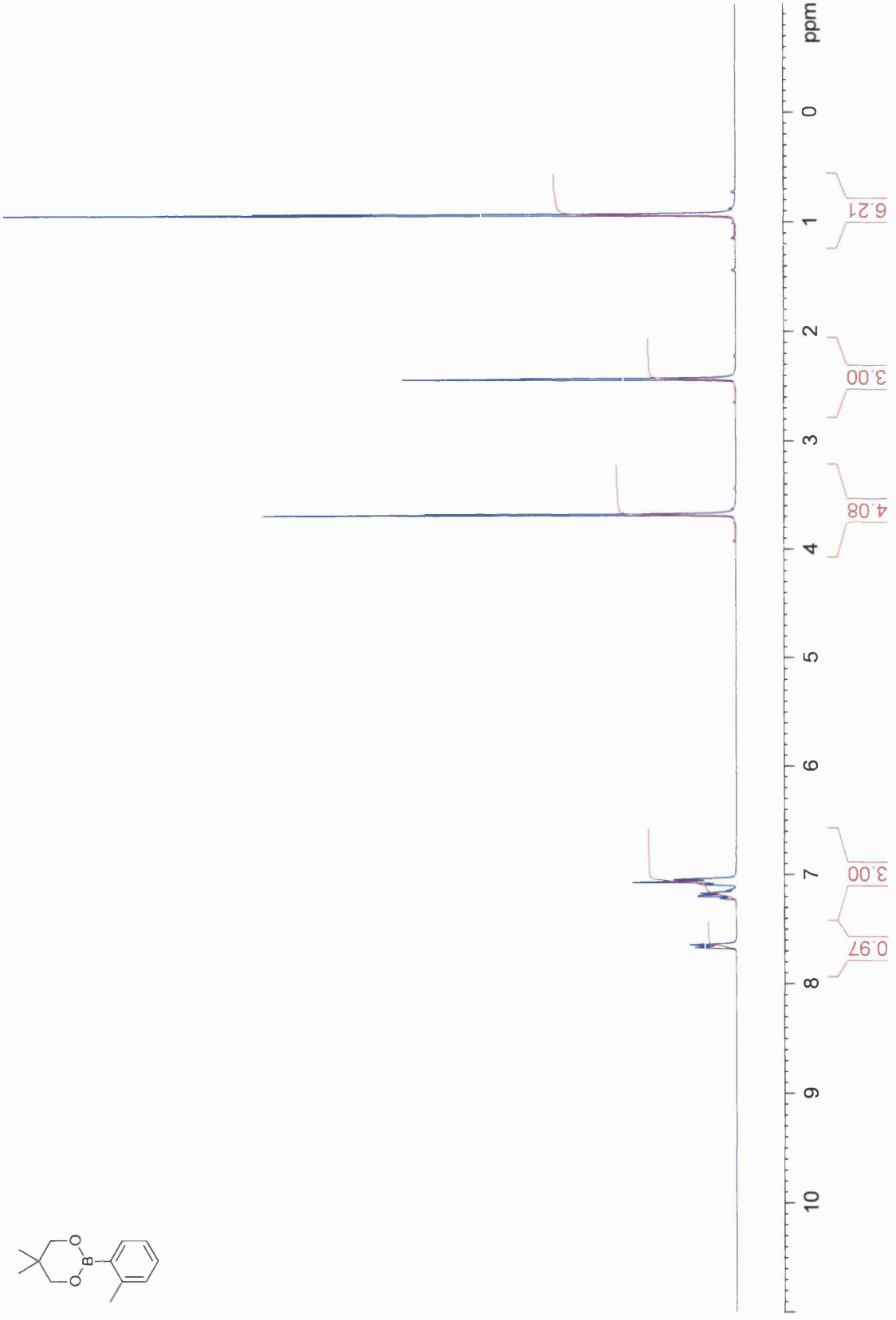

2-(2-(bromomethyl)phenyl)-5,5-dimethyl-1,3,2-dioxaborinane (127)

^{1}H NMR spectrum (300 MHz, $CDCl_3$)

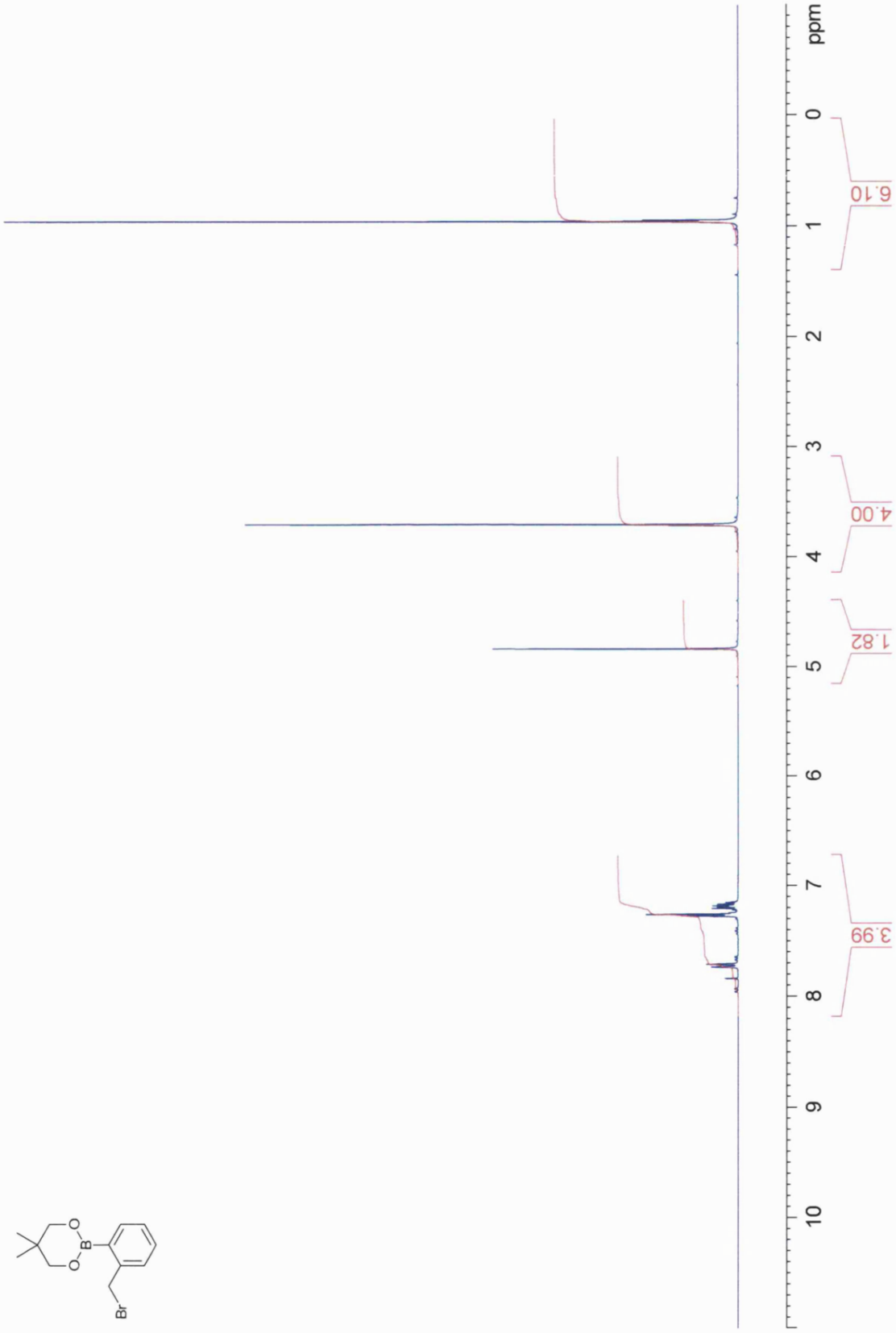

Methyl-pyren-1-ylmethyl-ammonium chloride (119$_{(pyrene)}$)

^{1}H NMR spectrum (300 MHz, MeOD)

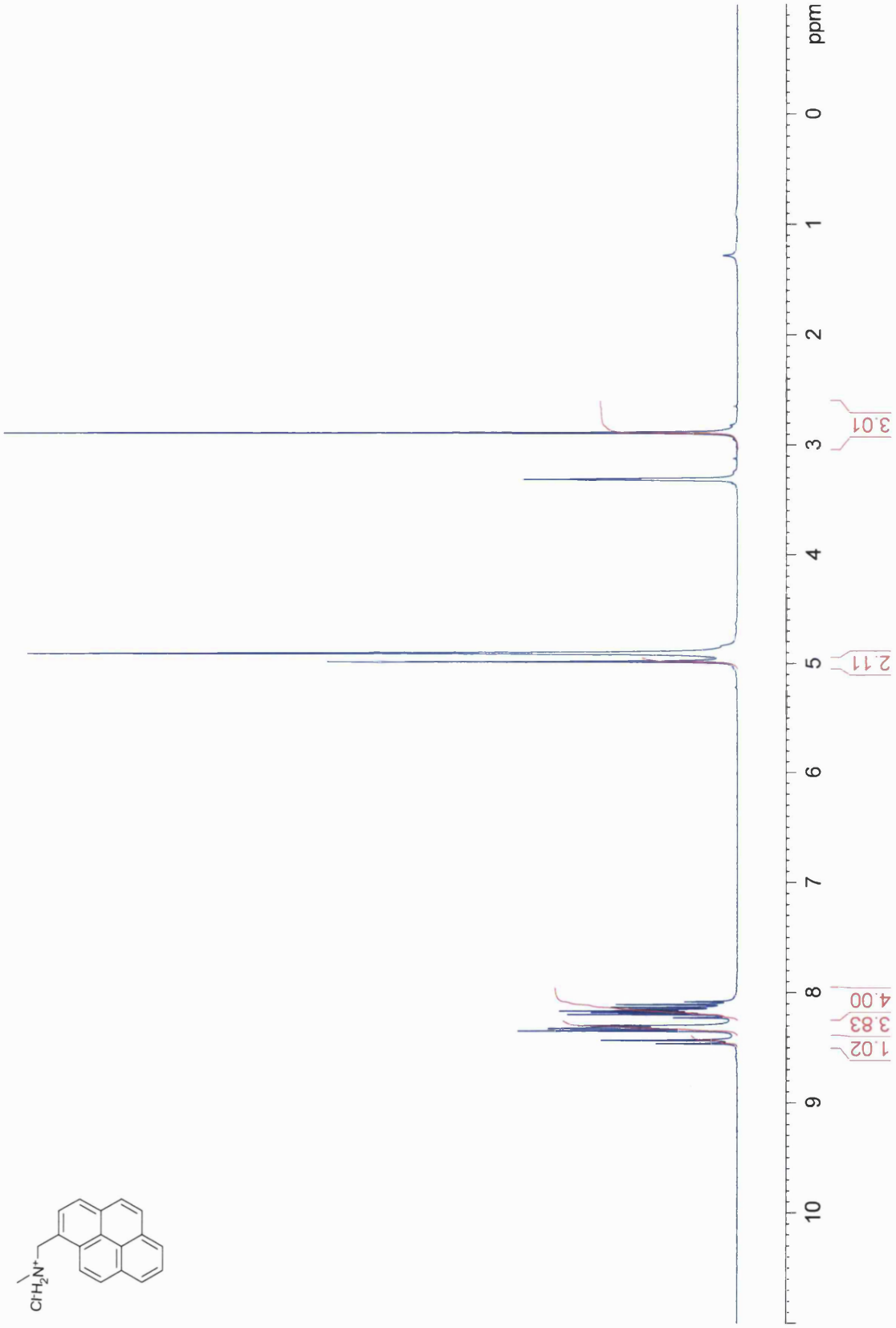

Methyl-phenanthren-9-ylmethyl-ammonium chloride (120$_{(phenanthrene)}$)

^{1}H NMR spectrum (300 MHz, MeOD)

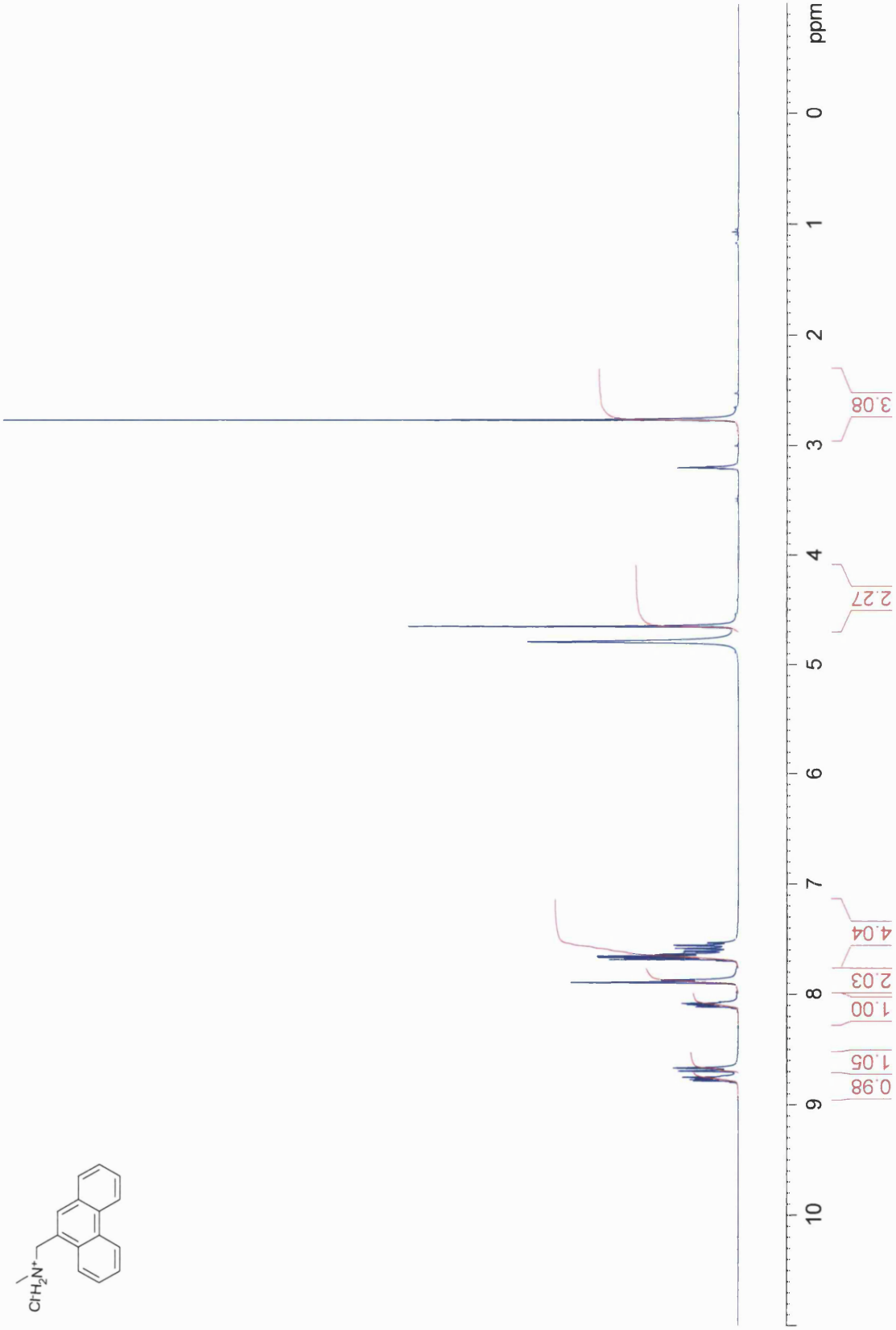

Anthracen-9-ylmethyl-methyl-ammonium chloride (121 [anthracene])

^{1}H NMR spectrum (300 MHz, MeOD)

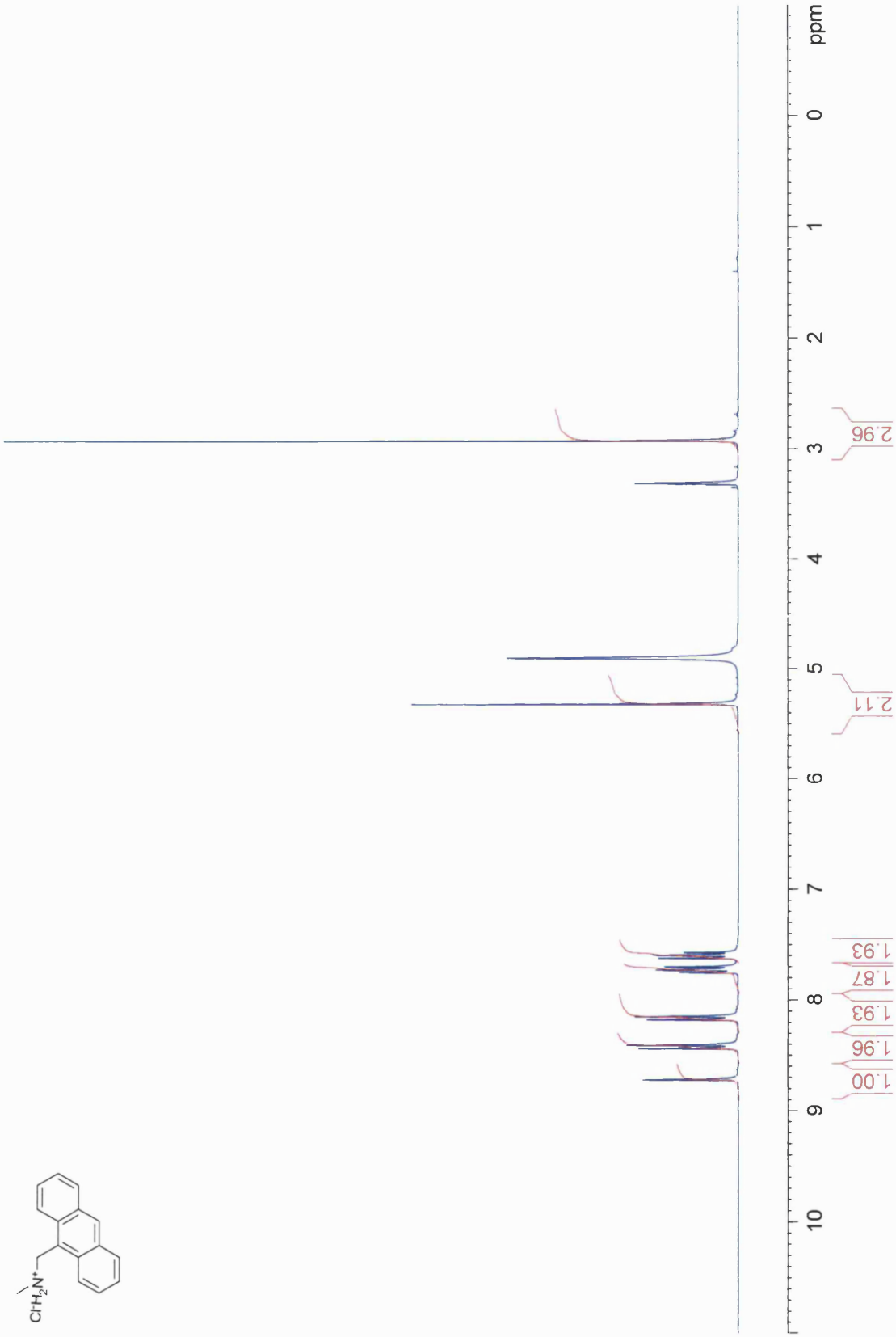

Methyl-naphthalen-1-ylmethyl-ammonium chloride (122$_{(1\text{-naphthalene})}$)

^{1}H NMR spectrum (300 MHz, MeOD)

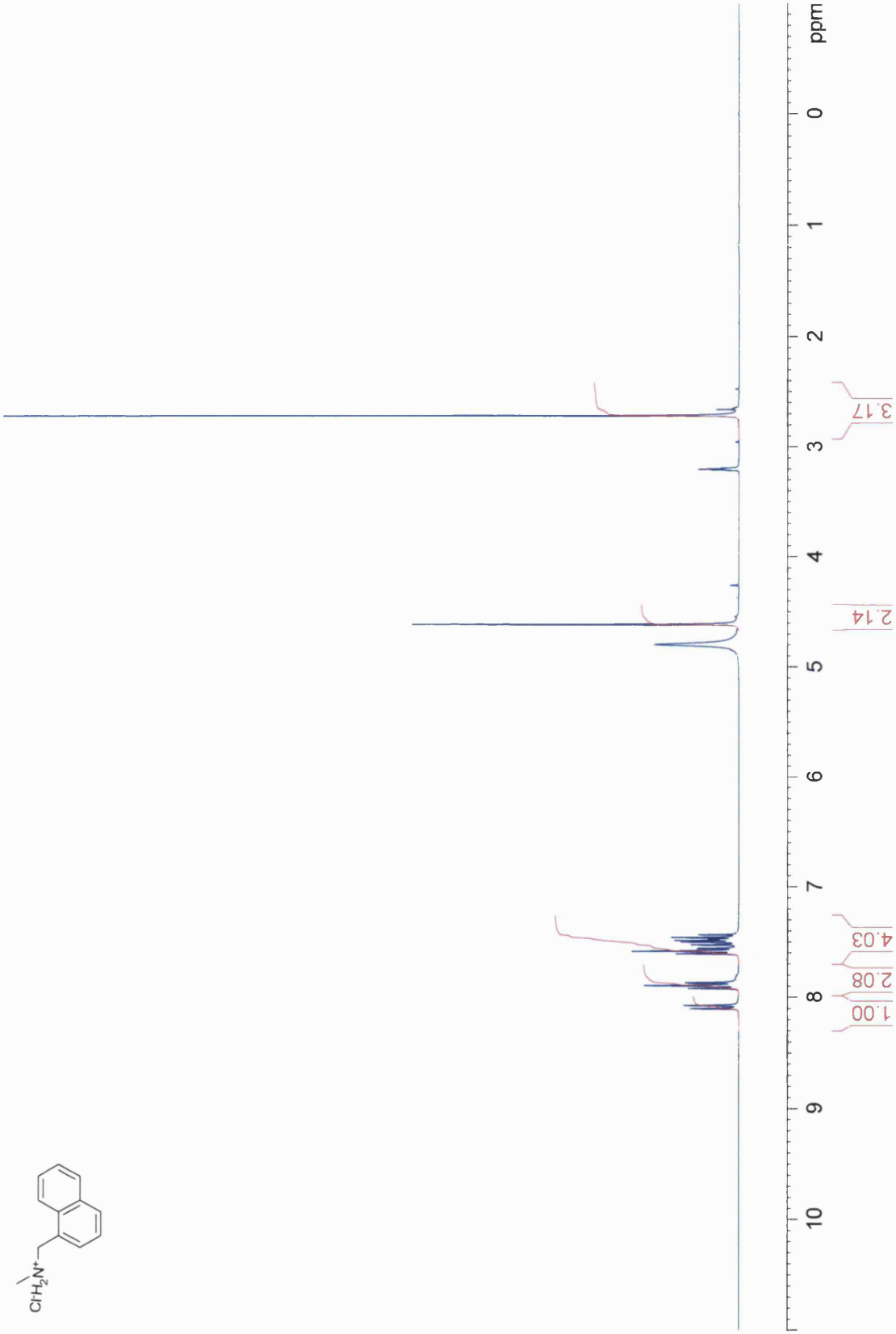

Methyl-naphthalen-2-ylmethyl-ammonium chloride (123$_{(2\text{-naphthalene})}$)

^{1}H NMR spectrum (300 MHz, MeOD)

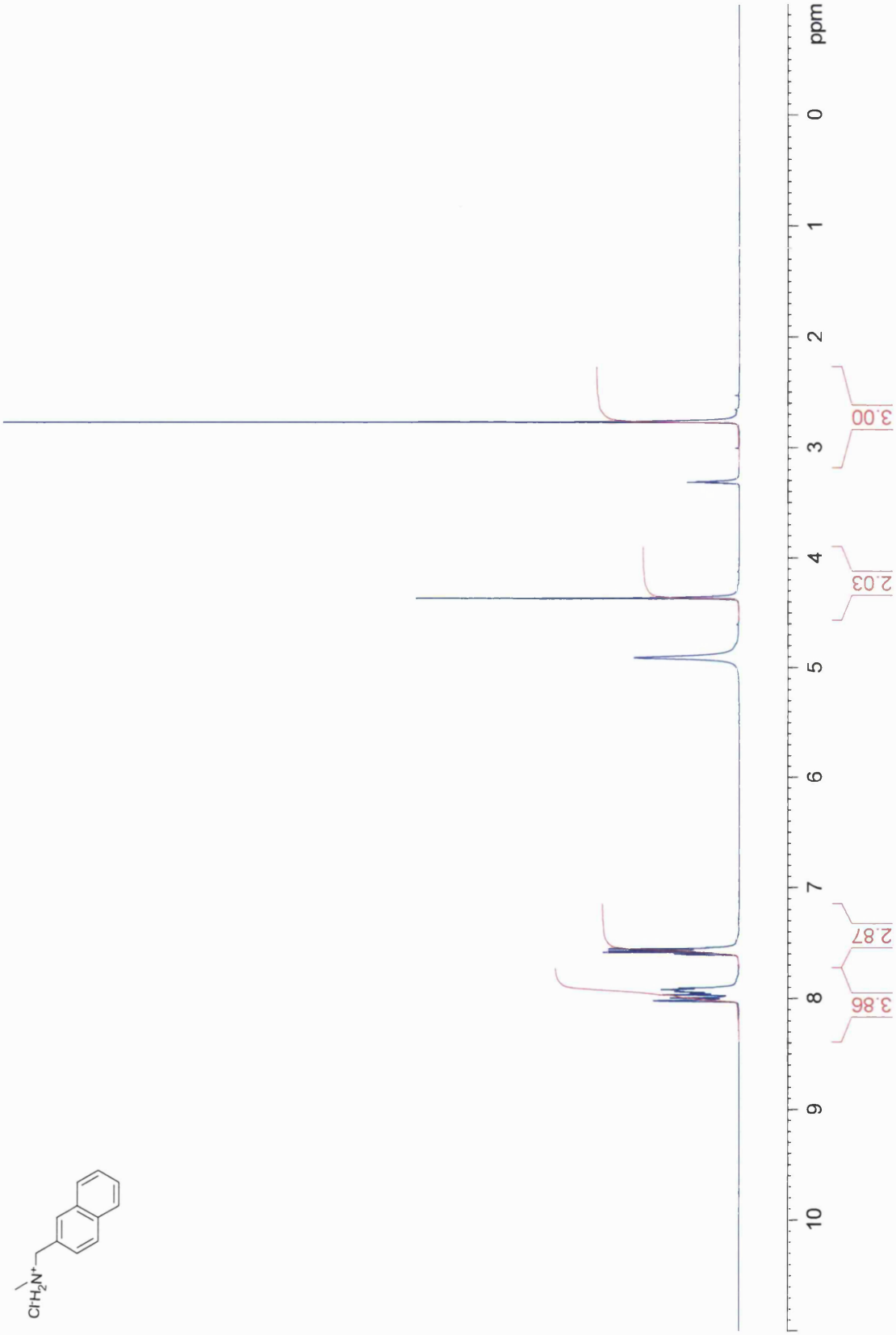

(2-Borono-benzyl)-methyl-pyren-1-ylmethyl-amine (128$_{(pyrene)}$)

^{1}H NMR spectrum (300 MHz, $CDCl_3$ with a few drops of MeOD)

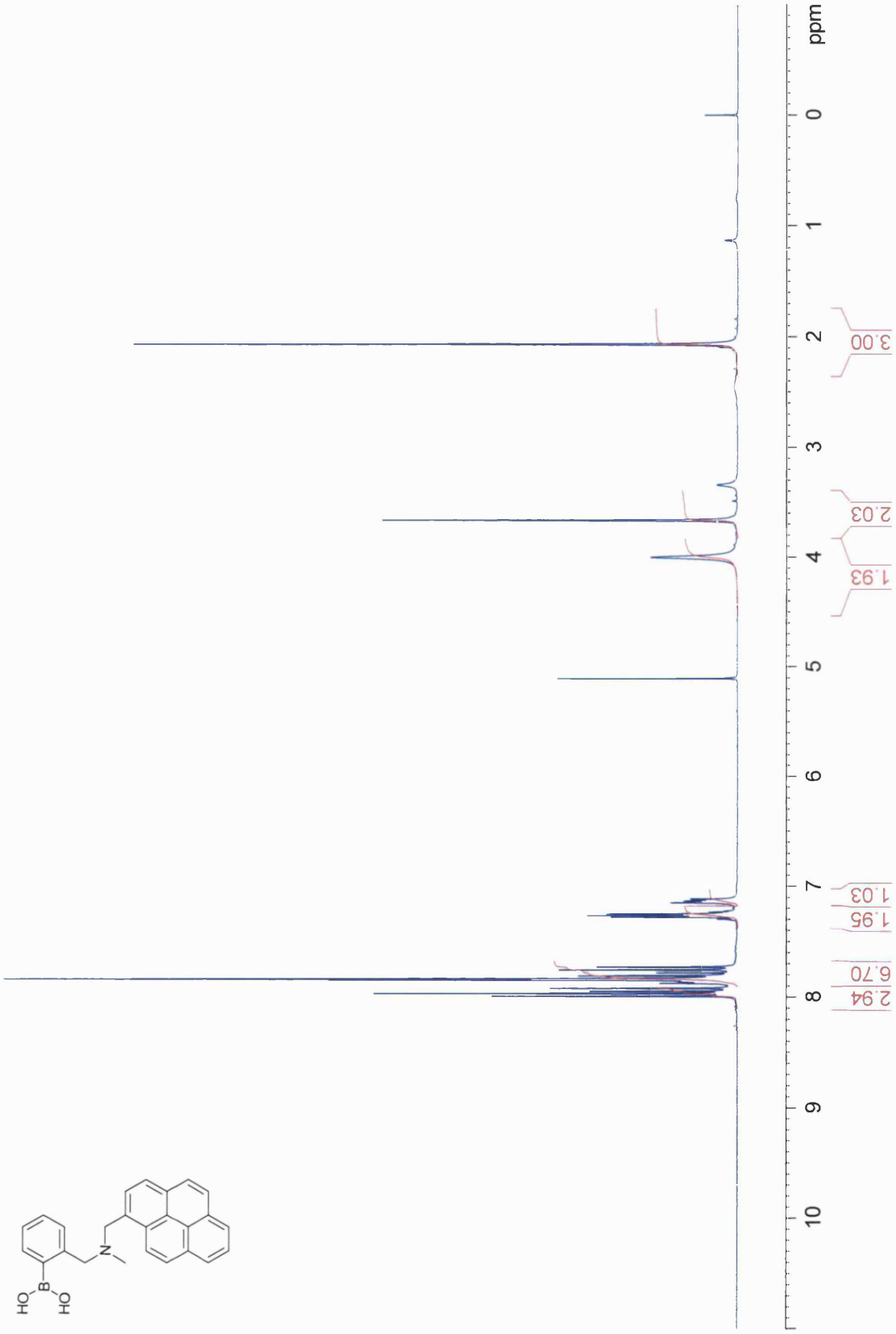

(2-Borono-benzyl)-methyl-phenanthren-1-ylmethyl-amine (129$_{(phenanthrene)}$)

^{1}H NMR spectrum (300 MHz, $CDCl_3$ with a few drops of MeOD)

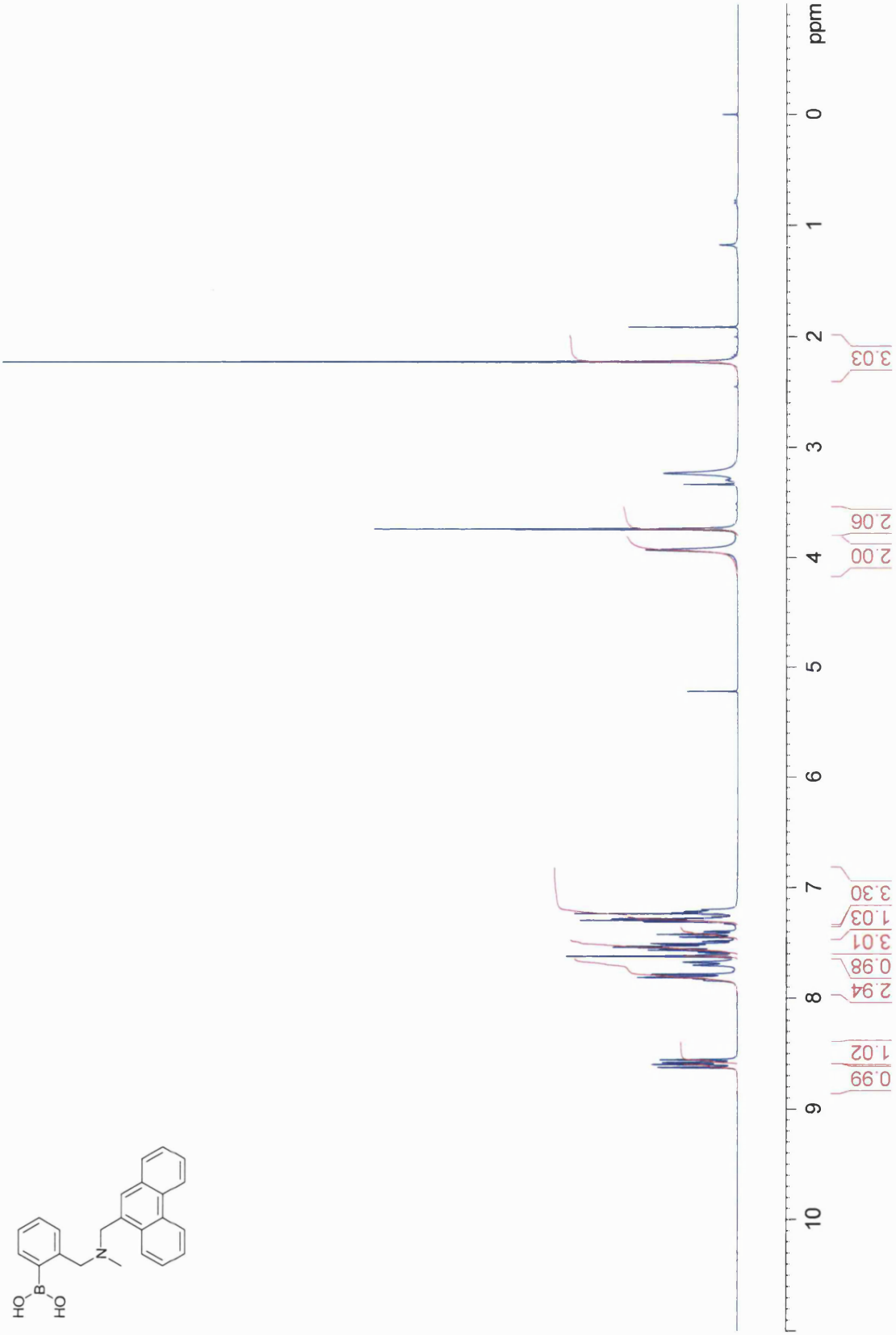

Anthracen-9-ylmethyl-(2-borono-benzyl)-methyl-amine (130$_{(anthracene)}$)

^{1}H NMR spectrum (300 MHz, $CDCl_3$ with a few drops of MeOD)

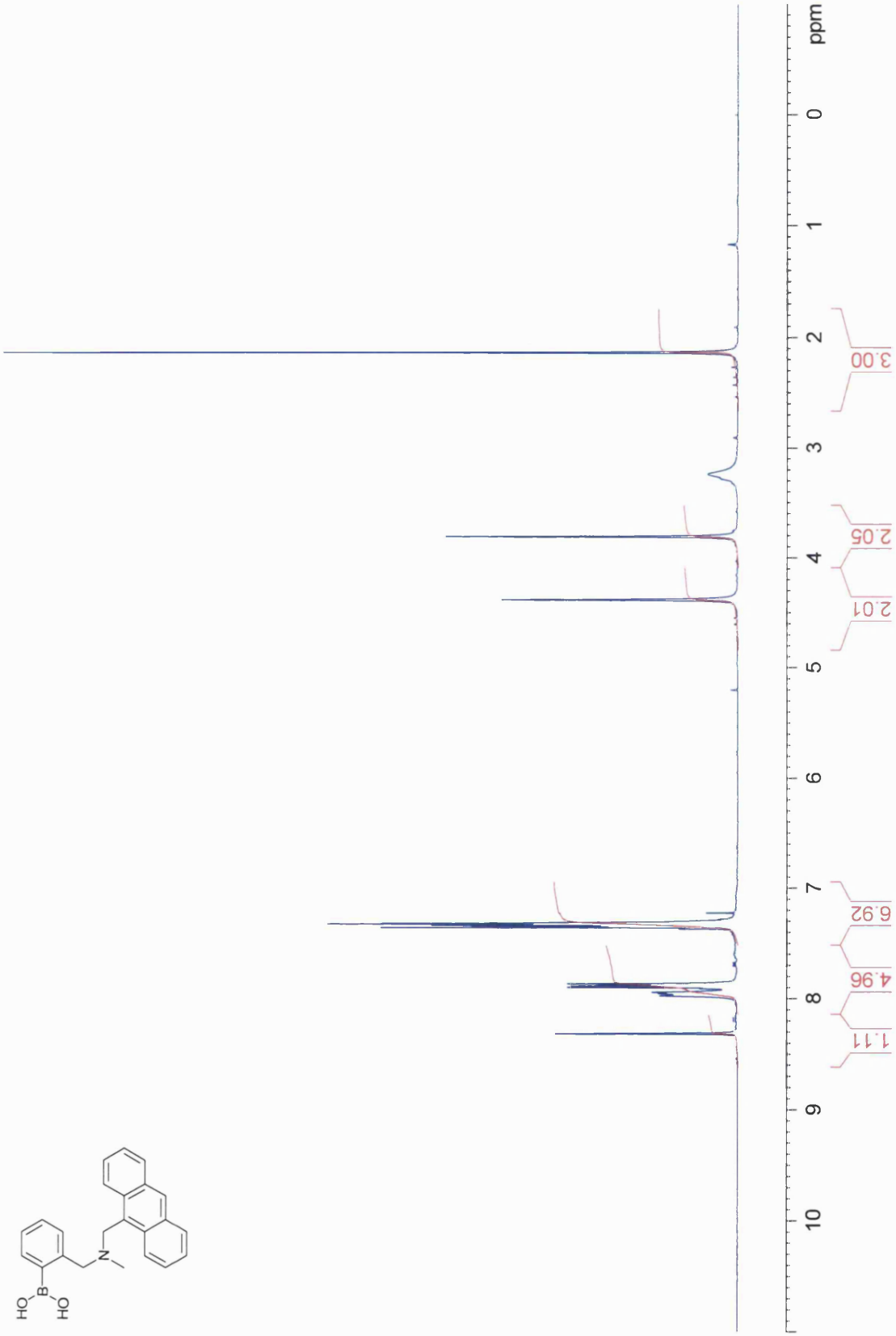

Anthracen-9-ylmethyl-(2-borono-benzyl)-methyl-amine (130$_{(anthracene)}$)

HMQC NMR spectrum (300 MHz, $CDCl_3$ with a few drops of MeOD)

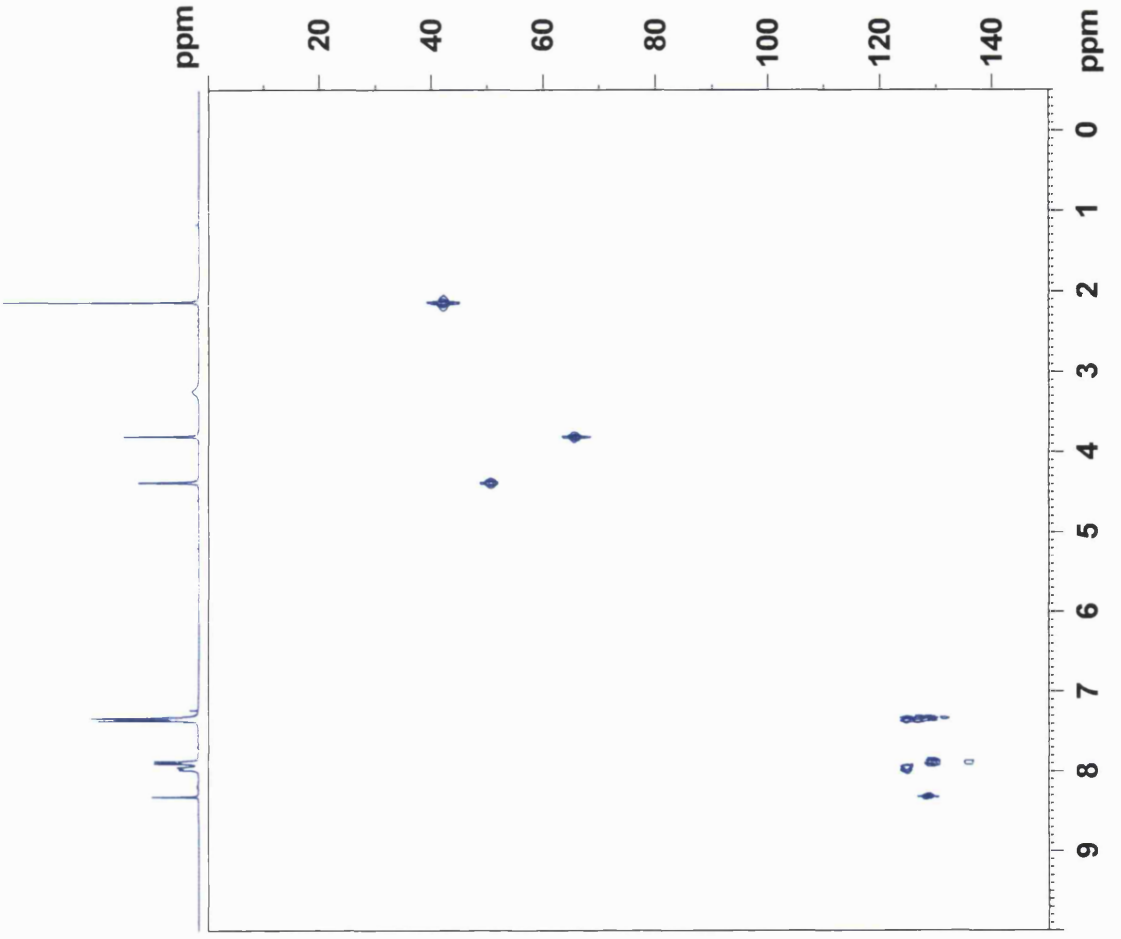

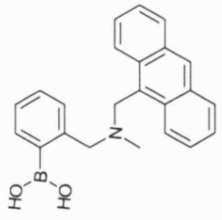

Anthracen-9-ylmethyl-(2-borono-benzyl)-methyl-amine (130$_{(anthracene)}$)

HMBC NMR spectrum (300 MHz, $CDCl_3$ with a few drops of MeOD)

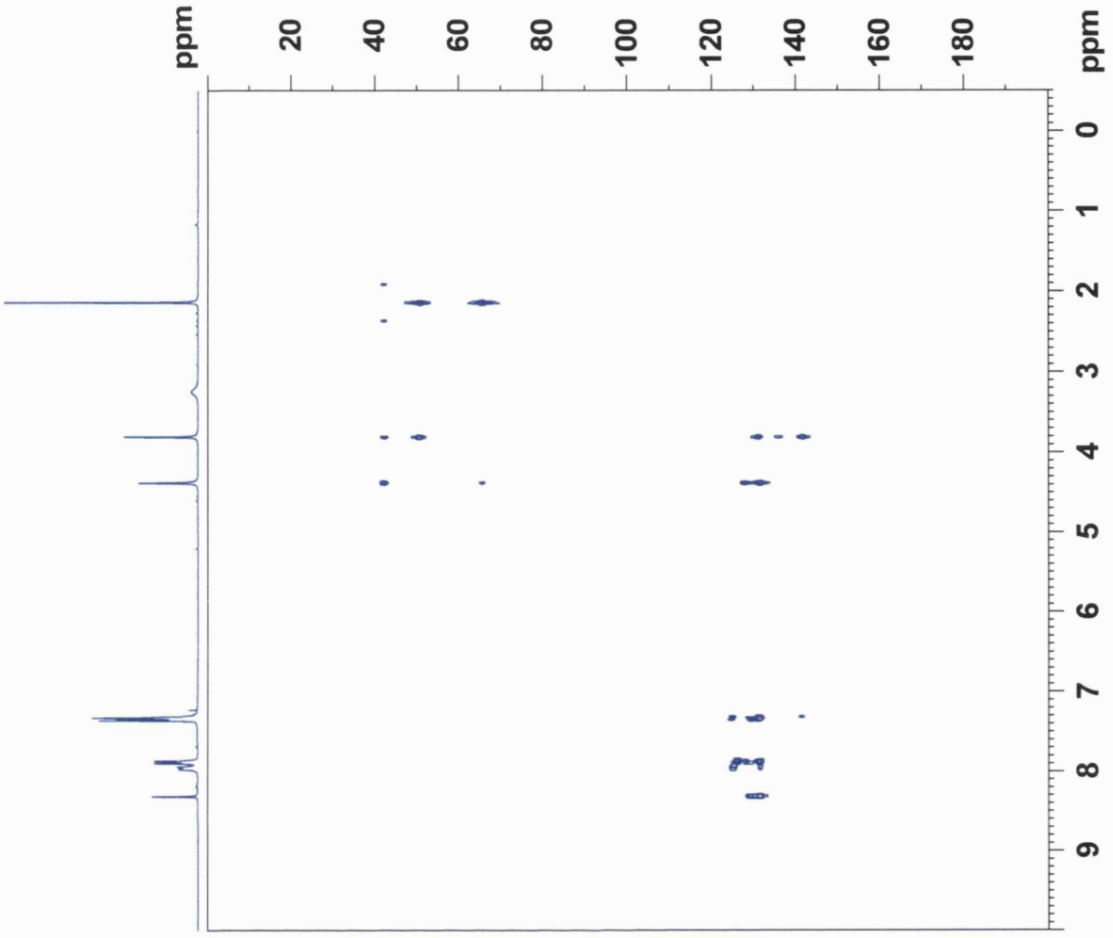

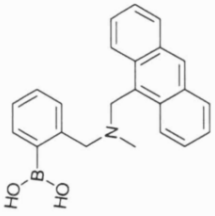

(2-Borono-benzyl)-methyl-naphthalen-1-ylmethyl-amine (131$_{(1\text{-naphthalene})}$)

^{1}H NMR spectrum (300 MHz, $CDCl_3$ with a few drops of MeOD)

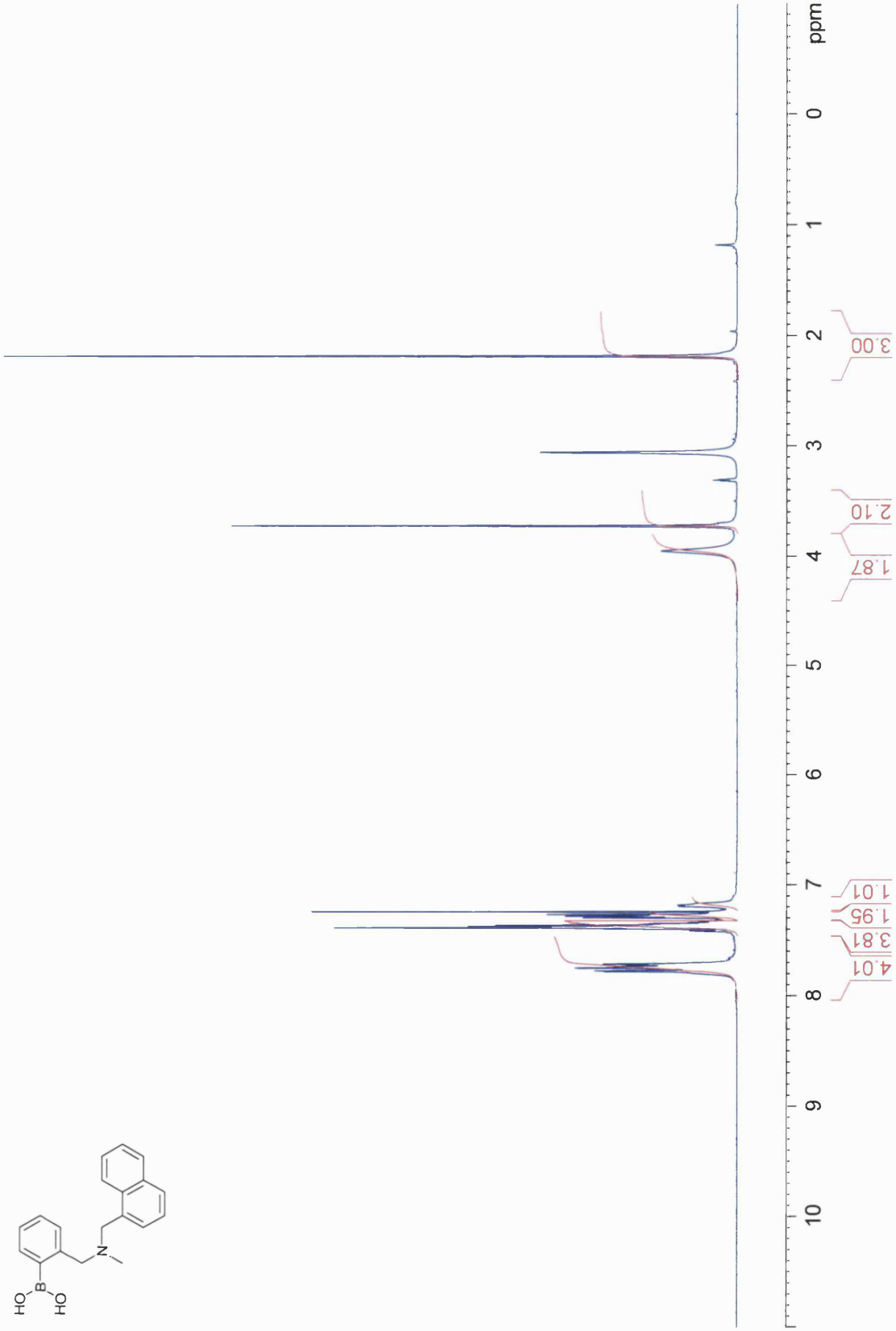

(2-Borono-benzyl)-methyl-naphthalen-2-ylmethyl-amine (132$_{(2\text{-naphthalene})}$)

^{1}H NMR spectrum (300 MHz, $CDCl_3$ with a few drops of MeOD)

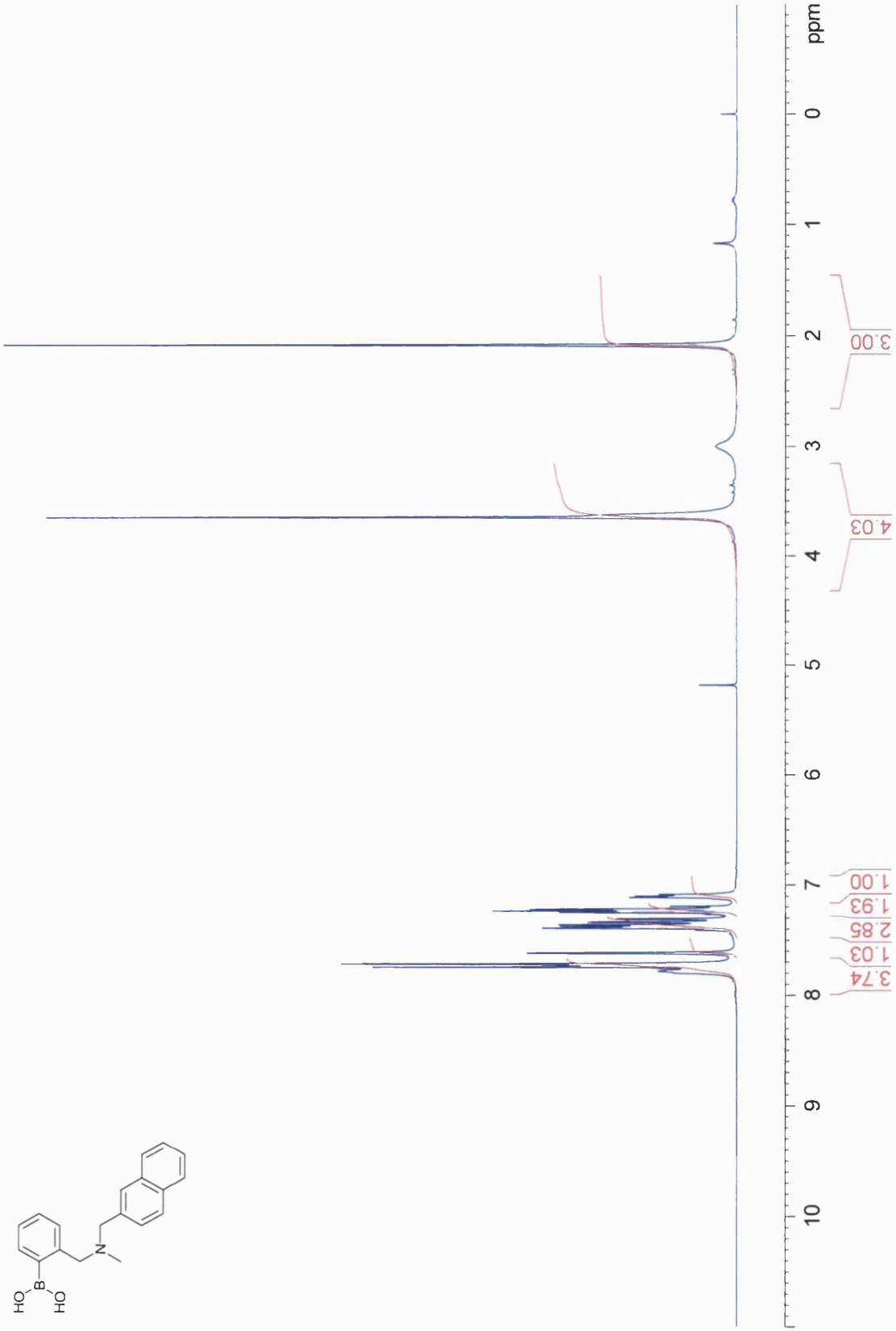

tert-Butyl 6-aminohexylcarbamate (147)

^{1}H NMR spectrum (300 MHz, $CDCl_3$)

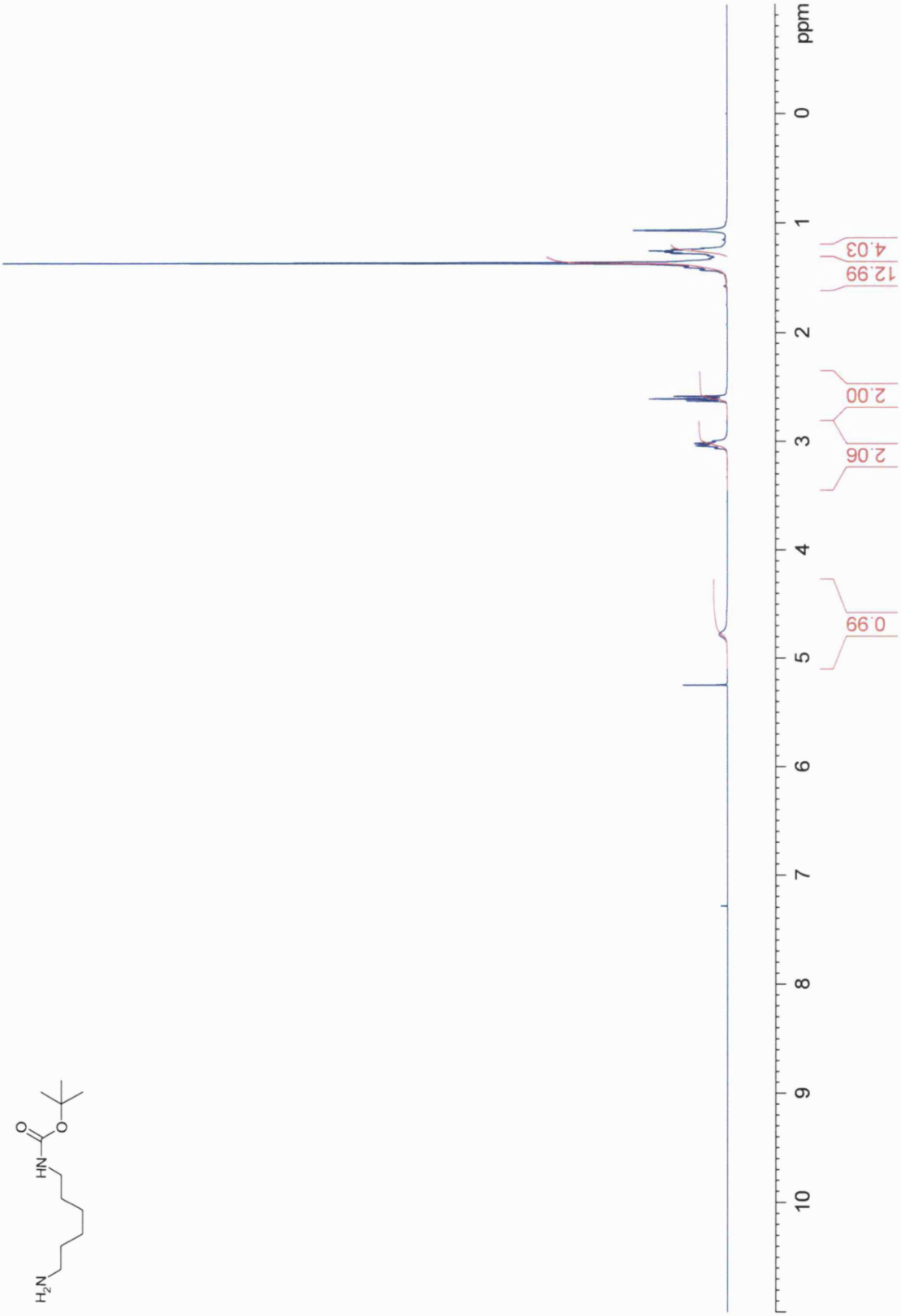

tert-Butyl 6-(benzylamino)hexylcarbamate (148)

^{1}H NMR spectrum (300 MHz, $CDCl_3$)

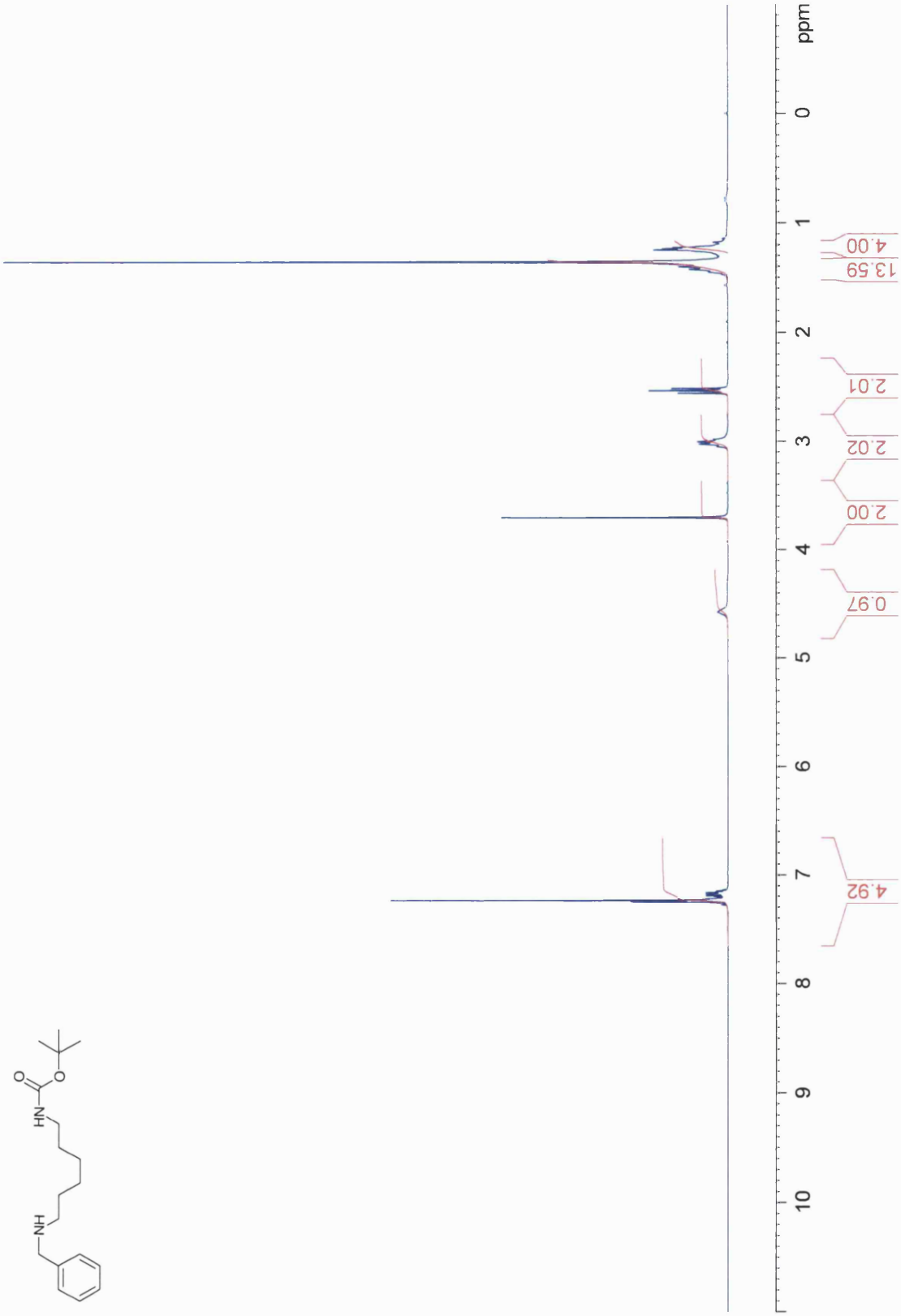

N^1-benzylhexane-1,6-diammonium dichloride (149)

^{1}H NMR spectrum (300 MHz, MeOD)

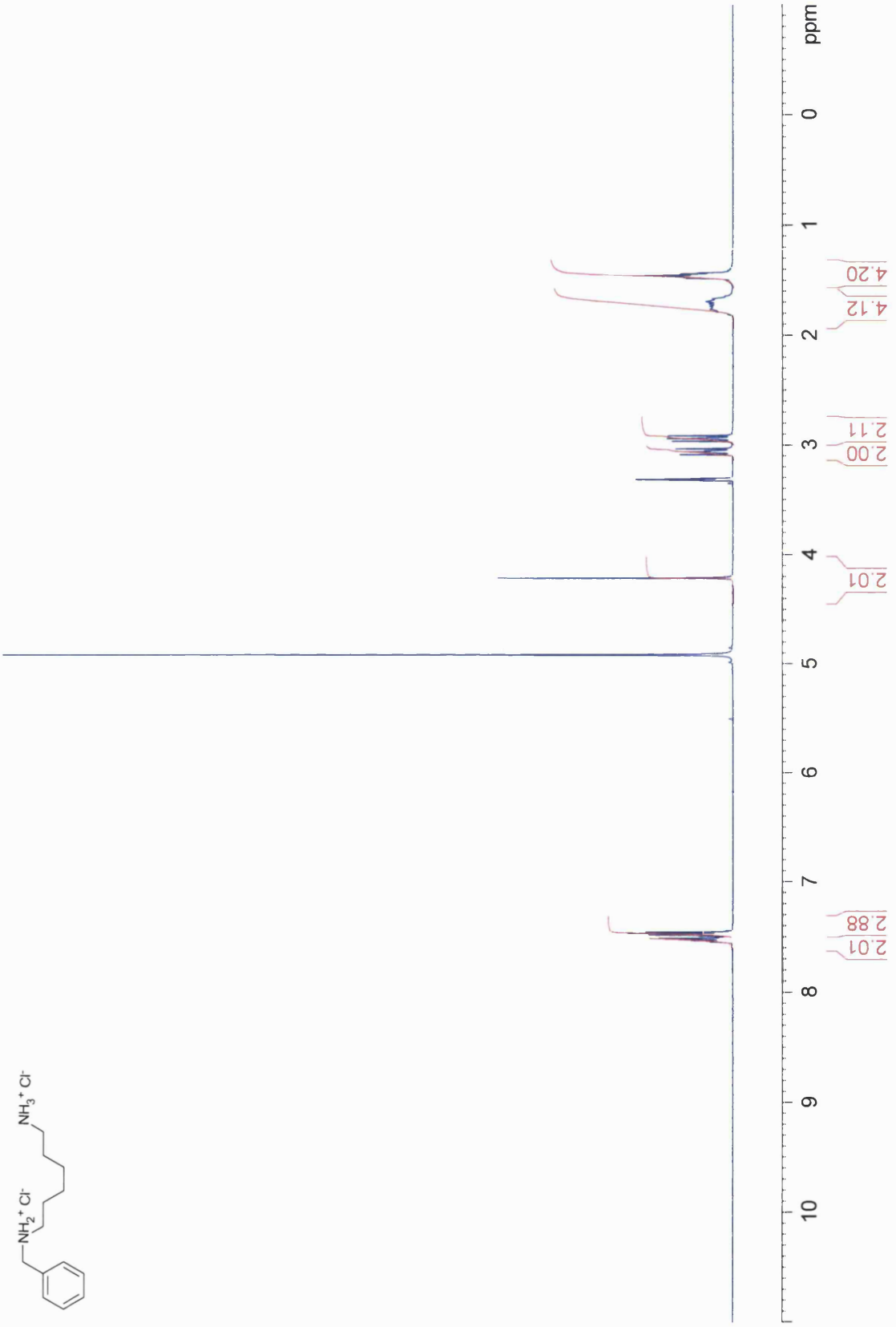

_N_'-[(anthracen-9-yl)methyl]-_N_'-benzylhexane-1,6-diammonium dichloride [151$_{(anthracene)}$]

^{1}H NMR spectrum (300 MHz, MeOD)

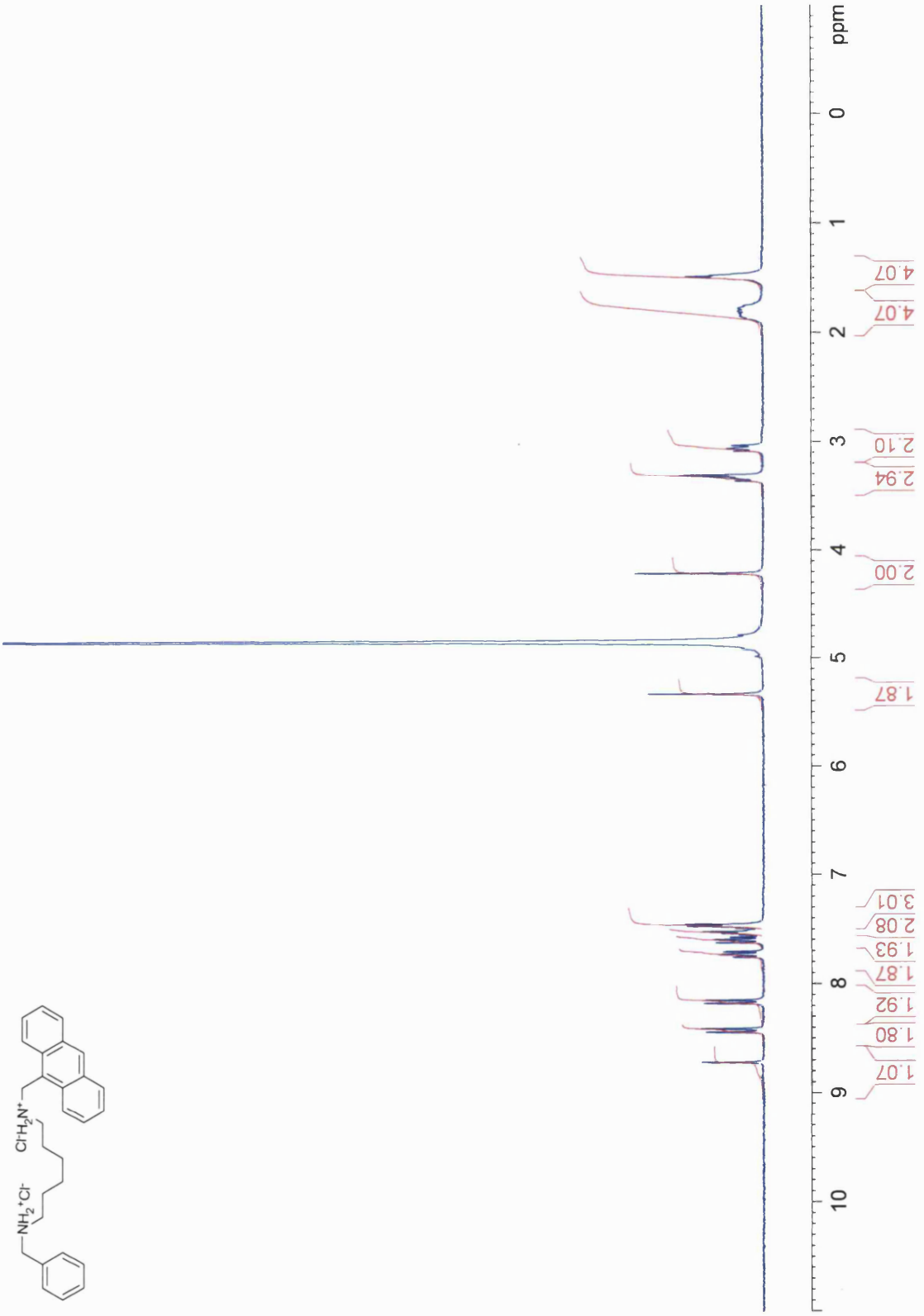

N',N'-Bis(tert-butyl 6-aminohexylcarbamate)isophthalamide (157)

^{1}H NMR spectrum (300 MHz, $CDCl_3$)

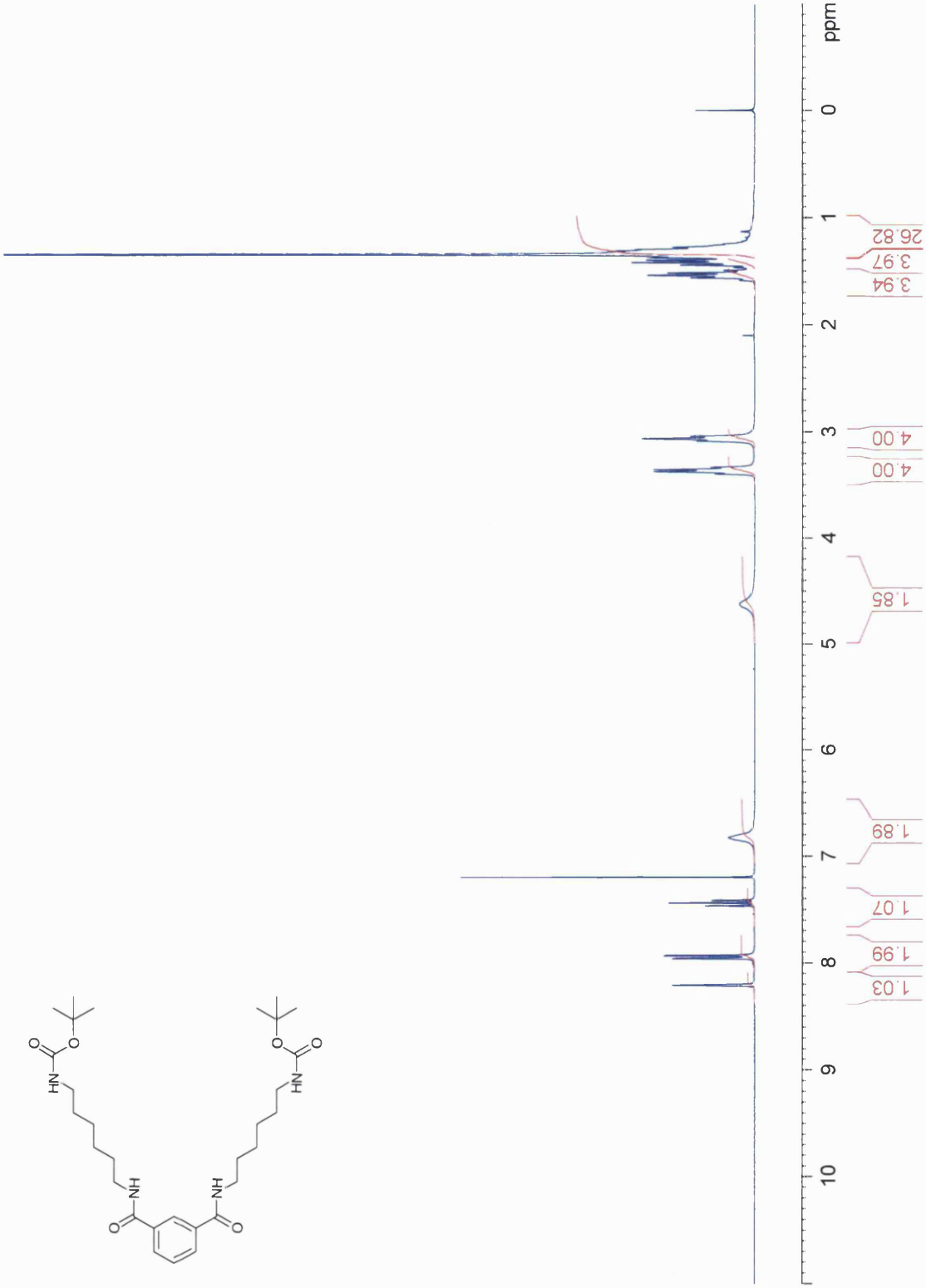

N',N'-Bis(6-aminohexyl)isophthalamide dihydrochloride (158)

^{1}H NMR spectrum (300 MHz, MeOD)

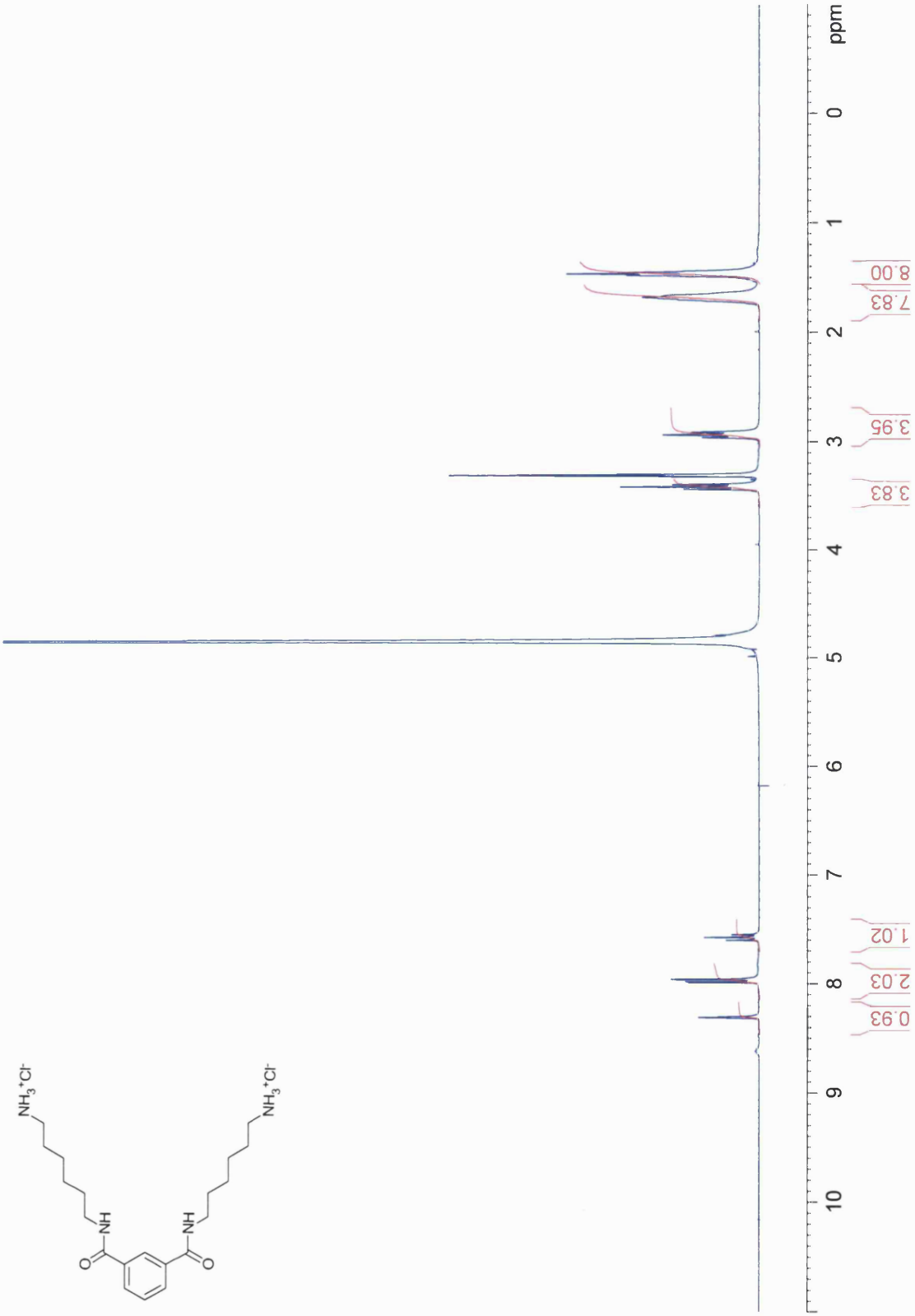

N',N'-bis[6-[[pyren-1-yl]methylamino]hexyl]isophthalamide dihydrochloride (161)

^{1}H NMR spectrum (300 MHz, DMSO)

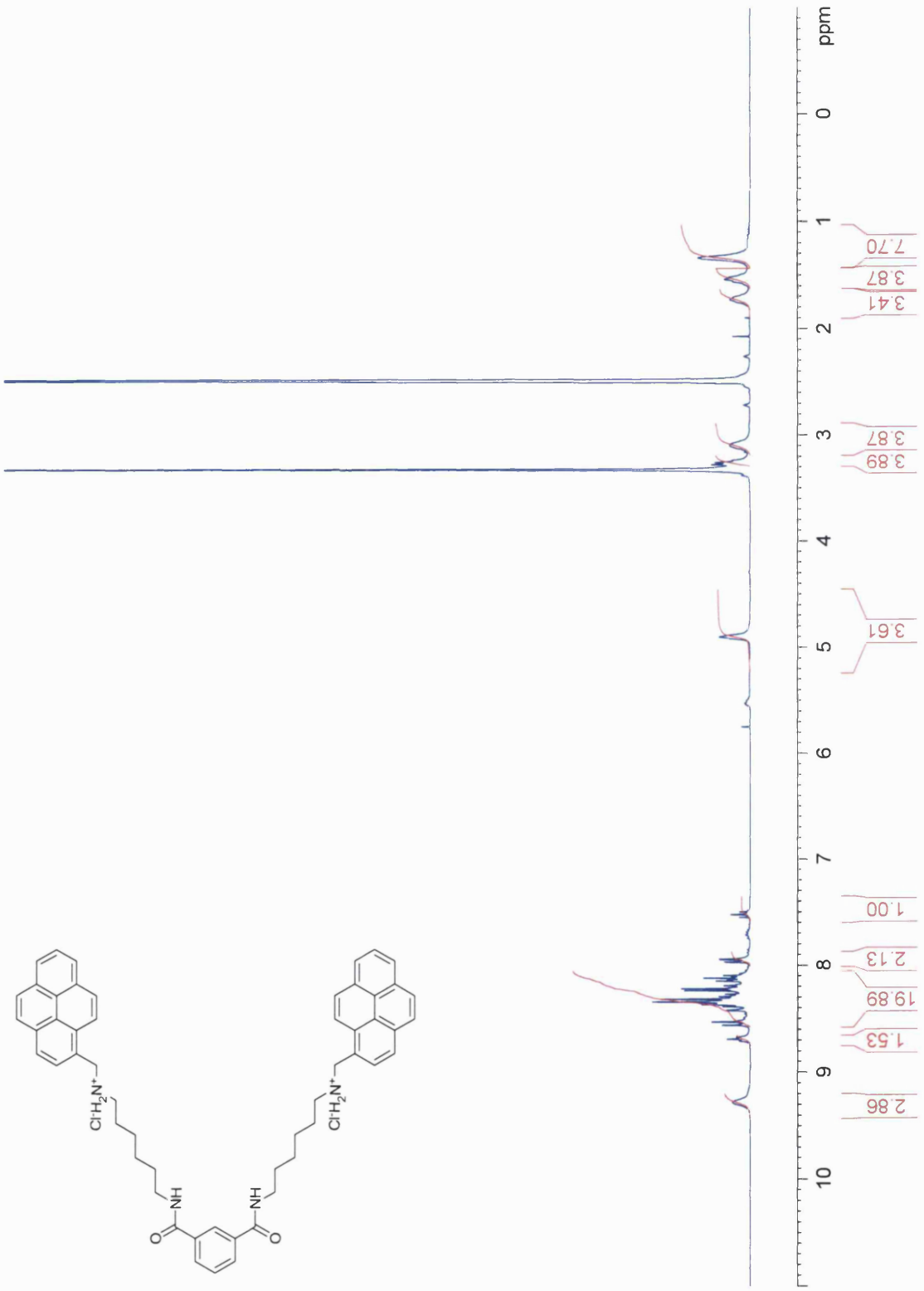

N',N'-bis(6-{(pyren-1-yl)methylamino}hexyl)isophthalamide dihydrochloride (161)

^{1}H NMR spectrum (300 MHz, MeOD)

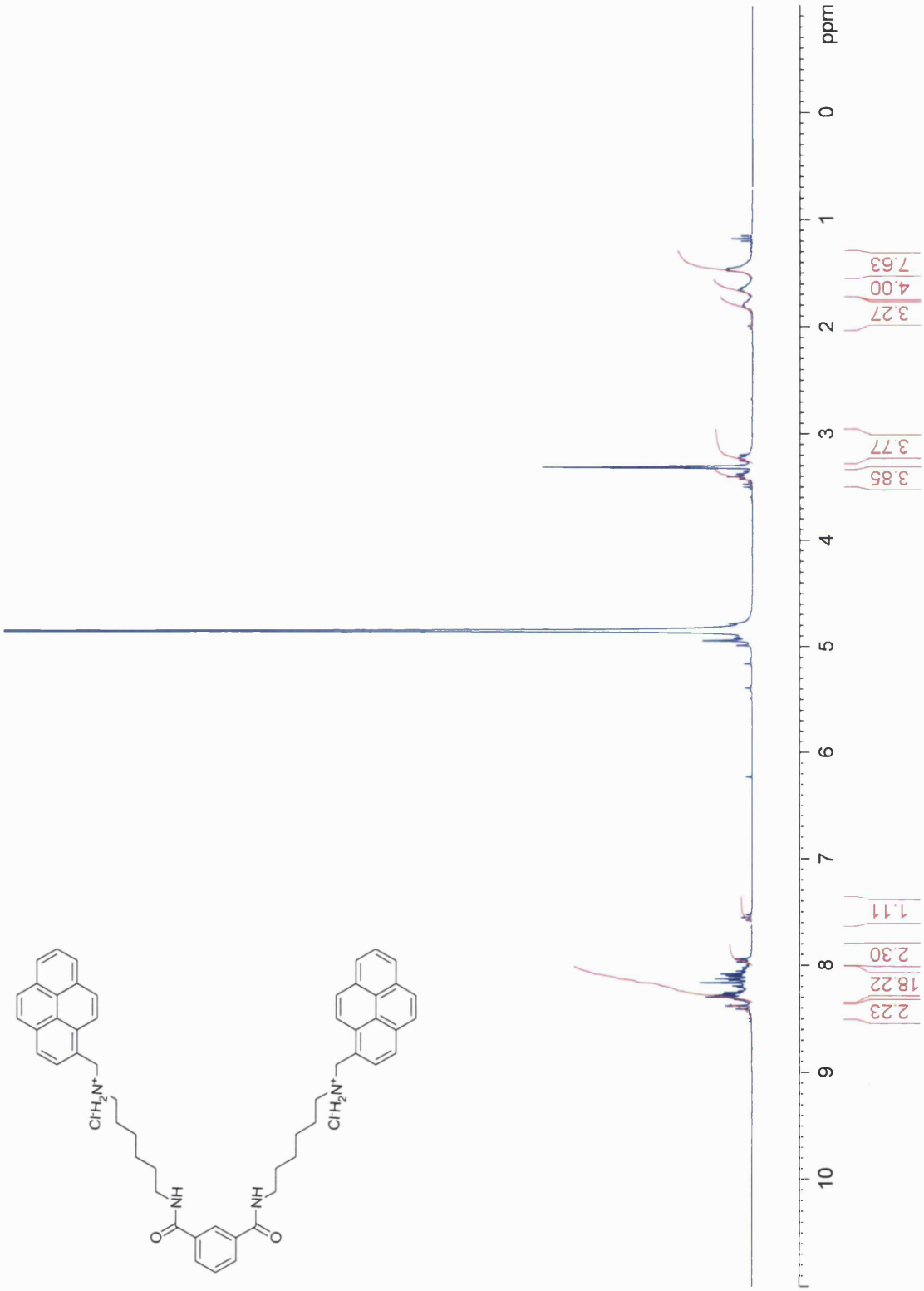

N⁶,N²-bis(6-((pyren-1-yl)methylamino)hexyl)isophthalamide (159)

^{1}H NMR spectrum (300 MHz, $CDCl_3$)

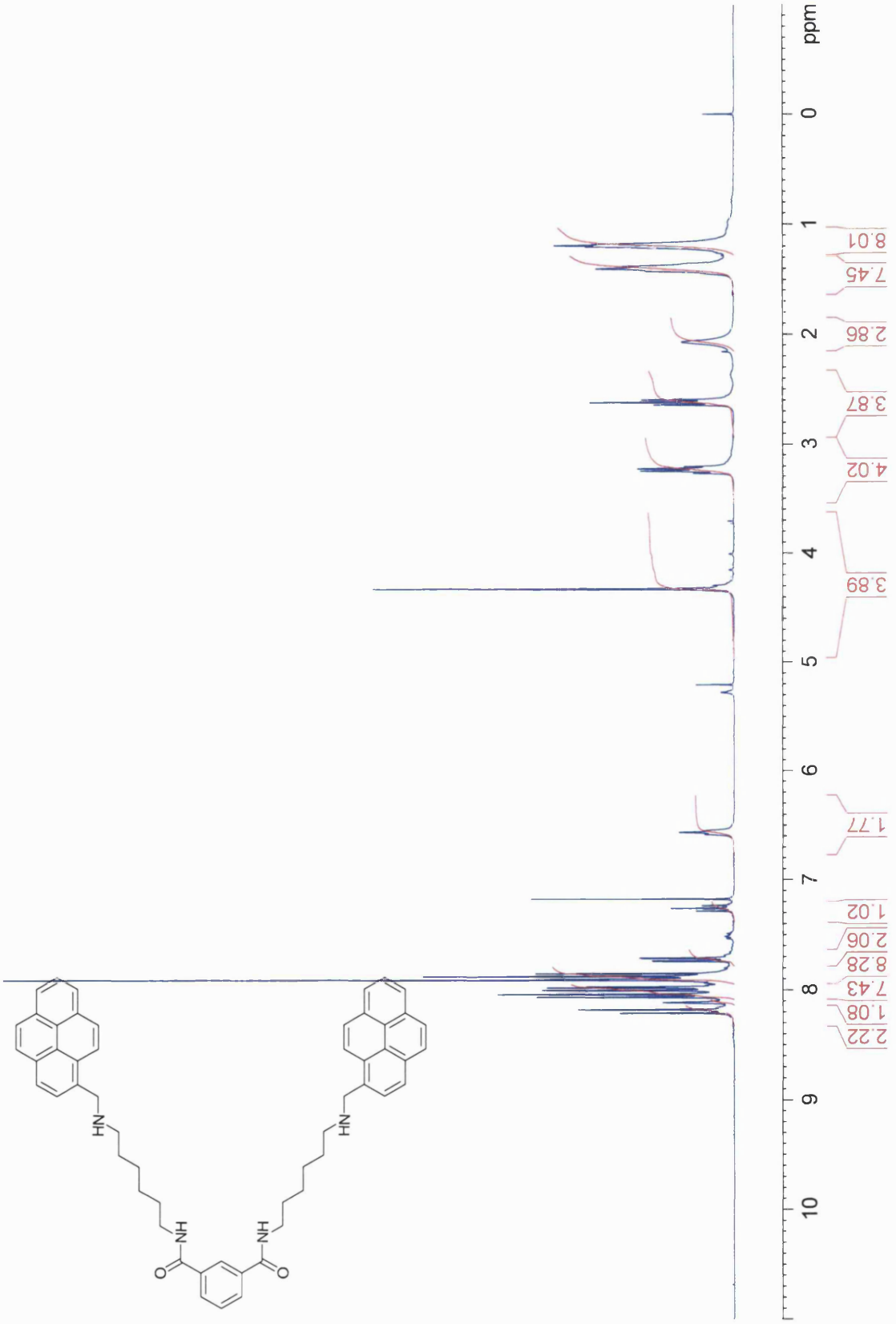

N',N'-bis[6-[N',N'-(2-boronobenzyl)- N',N'-((pyren-1- yl)methyl)amino)hexyl]isophthalamide (162)

^{1}H NMR spectrum (400 MHz, $CDCl_3$ with a few drops of MeOD)

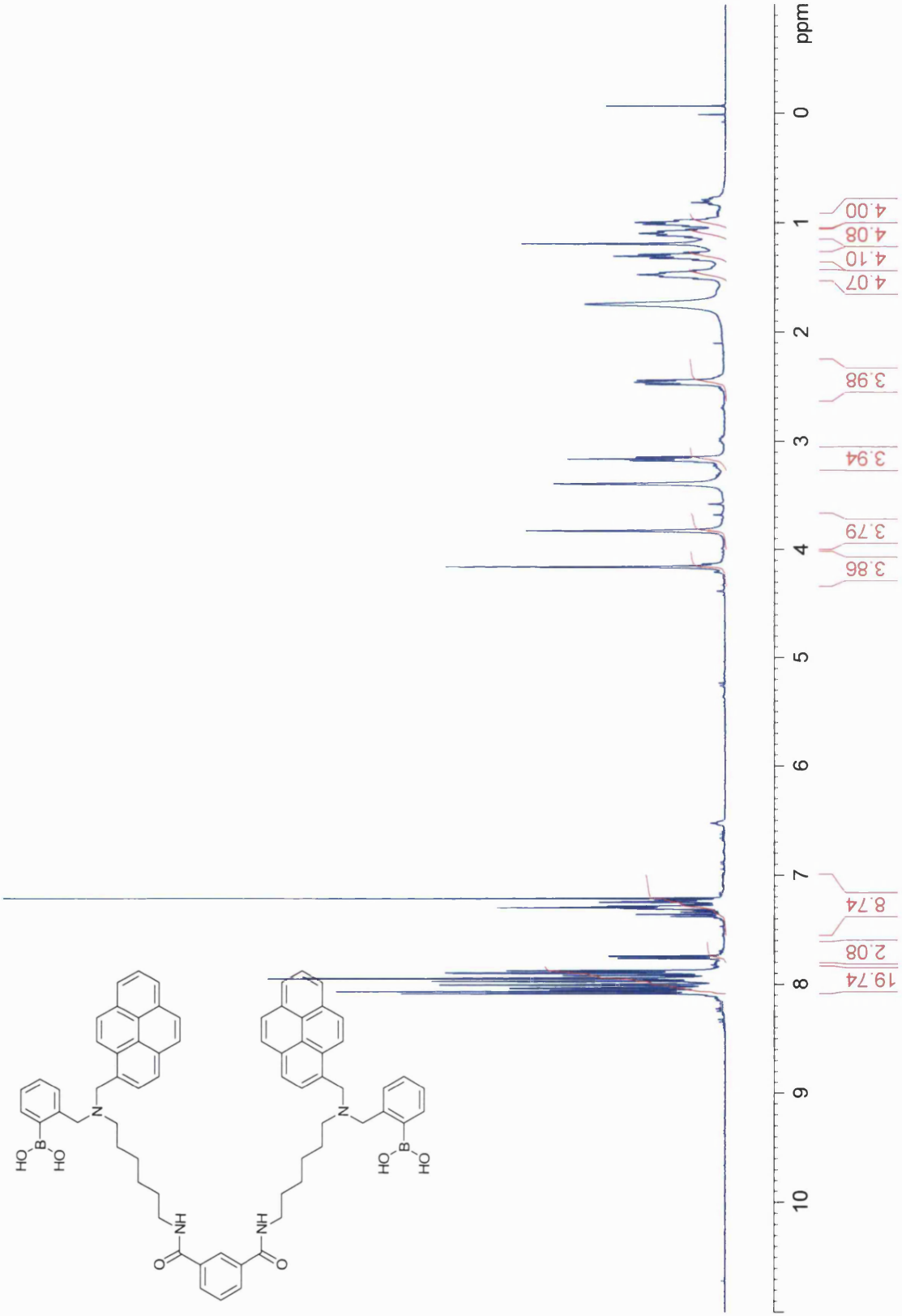

_N_,_N'_-bis[6-[_N_,_N'_-[2-boronobenzyl]- _N_,_N'_-[[pyren-1- yl]methyl]amino]hexyl]iso-phthalamide (162)

COSY NMR spectrum (300 MHz, $CDCl_3$ with a few drops of MeOD)

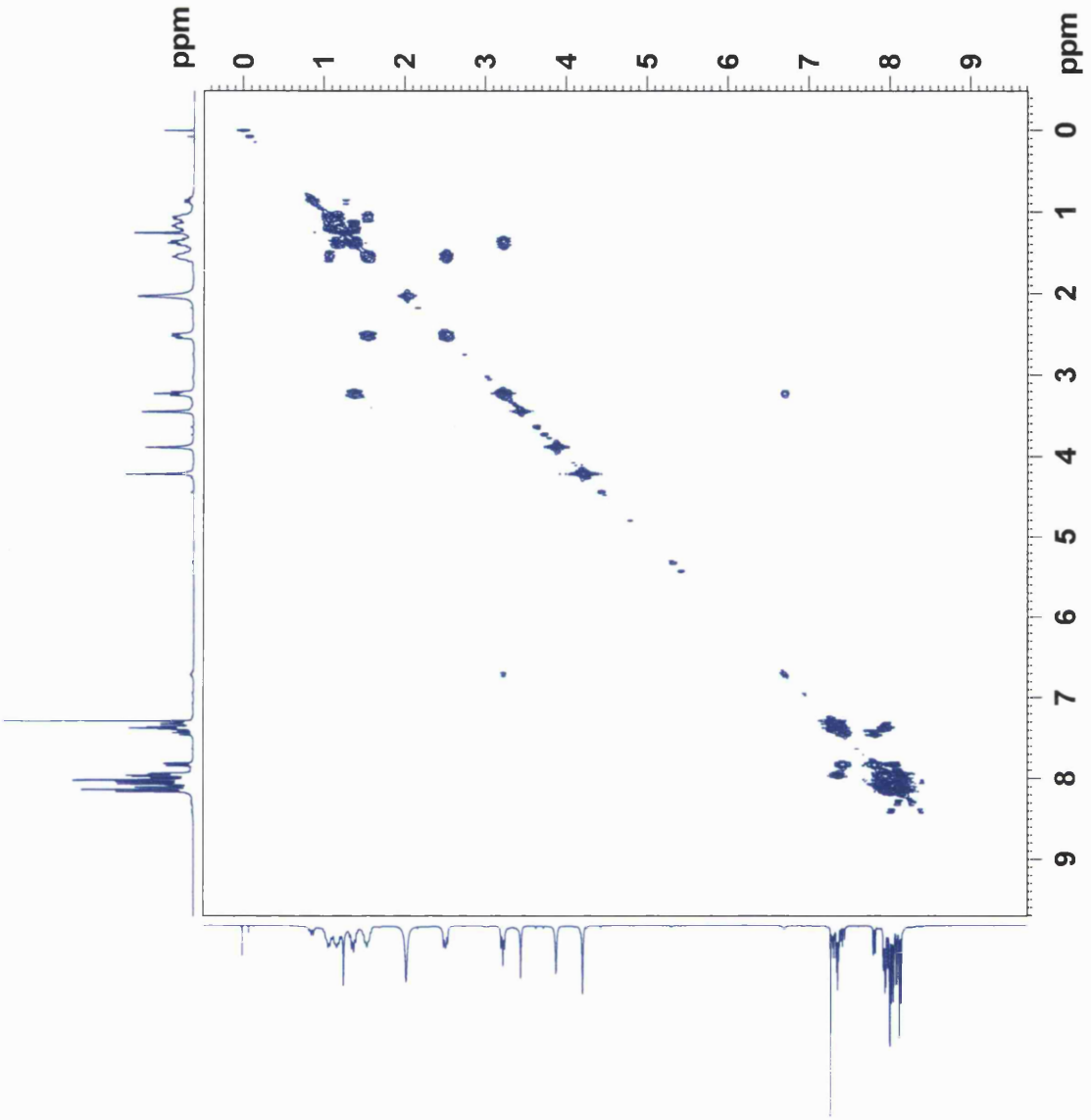

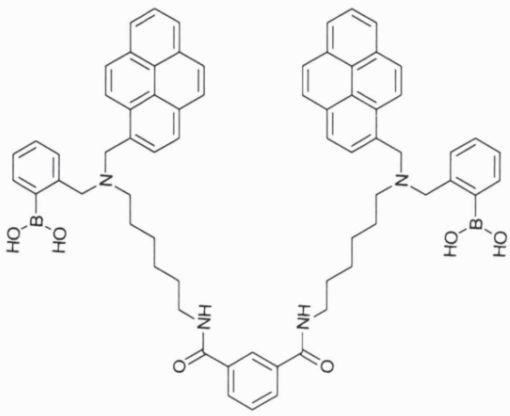

N',N'-bis[6-(N',N'-(2-boronobenzyl)- N',N'-((pyren-1- yl)methyl)amino)hexyl]isophthalamide (162)

HMQC NMR spectrum (300 MHz, $CDCl_3$ with a few drops of MeOD)